



Phytochemical studies on natural products and their biological activities against Trypanosoma

By

Naif Alenzi

A Thesis Submitted in Fulfillment of the Requirements for the Award of Degree of Doctor of Philosophy in Strathclyde Institute of Pharmacy and Biomedical Sciences at the University of Strathclyde

2018

Declaration

'I declare that, except where specifically indicated, all the work presented in this report is my own and I am the sole author of all parts.'

The copyright of this thesis belongs to the author under the terms of the United Kingdom Copyright Acts as qualified by University of Strathclyde Regulation 3.50. Due acknowledgement must always be made of the use of any material contained in, or derived from, this thesis.'

Signed: _____

Date: _____

Abstract

The therapeutic properties of plants have been recognised since the earliest human communities. One plant considered to have biological effects is Holy Basil (*Ocimum sanctum L.*), with pre-clinical screening uncovering many compounds with effects against bacteria, anaphylaxis, histamines, and diabetes as well as with wound healing and radio-protective effects, including eugenol, euginal, ursolic acid, carvacrol, linalool, limatrol, and caryophyllene. The phytochemistry of this plant is studied in the first section of this thesis.

Propolis is also receiving ample attention in the context of initiatives to discover novel drugs, thanks to its biological and pharmacological qualities. A resinous substance, propolis is produced by honeybees from different plant materials. Different biological effects have been allocated to propolis extracts by earlier studies and their phytoconstituents have been extensively characterised, especially flavonoids, polyphenols, phenolic aldehydes, sesquiterpene quinines, coumarins, amino acids, steroids and inorganic compounds.

The present study employed high-resolution LC-MS, HPLC-ELSD and NMR profiling to analyse the chemical composition of Holy Basil (*Ocimum sanctum L.*) and a range of types of propolis from various geographical areas. Subsequently, suitable methods of extraction, fractionation and identification were employed to isolate and identify compounds. Furthermore, one-dimensional and two-dimensional NMR as well as LC-MS will be applied to elucidate the structures of the isolated compounds.

A range of compounds were isolated from Holy Basil extracts and different types of propolis by employing various phytochemical methods, including VLC, CC, SEC, preparative TLC.

All crudes extracts, fractions as well as 12 isolated compounds then were subjected for biological testing against *Trypanosoma*, *T. brucei* S427 WT, and their cytotoxicity

against mammalian cells was also determined. The Holy Basil MeOH extract yielded three pure compounds which were tested against *Trypanosoma, T. brucei* S427 WT for the first time and scored relatively moderate to weak activity. While the ethanolic extracts of different types of propolis yielded nine pure compounds. Three of them were isolated for the first time from Philippine propolis and yielded against *Trypanosoma, T. brucei* S427 WT relatively moderate activity. The other pure compounds were isolated from Saudi, red Nigerian and red Brazilian, two pures per each sample, gave as well relatively moderate activity. Red Nigerian and red Brazilian showed a high degree of similarity in pures obtained from them.

Acknowledgments

I am greatly thankful to Allah who keeps me healthy, committed through my entire PhD study.

My deepest thanks will go to my principle supervisor Dr David G Watson for his guidance, encouragement and help during the project. I would like also to extend my thanks to my second supervisor Professor Sandy Gray who's thankfully supervised me in my first year.

It is a pleasure as well to thank members of both Dr Watson's labs and Professor Sandy Gray's lab for their help and support through my PhD. Special thanks also go to my colleague Sameah for her help in testing the biological activities of samples.

I would like to express the deepest appreciation to my wife Dr. Samyah for her support, understanding and motivation through my entire life. Thanks to my children Rayan, Reema and Rakan for carrying this journey with me. Lastly but most importantly I would like to express my gratitude to my father, mother, brothers and sisters for their love, support and understanding during my educational life.

Thanks to The Saudi FDA in the Kingdom of Saudi Arabia for funding my PhD study.

List of contents

Declaration	i
Abstract	ii

Aknowledgments	iv
Table of contents	v
List of Abbreviations	ix
List of Figures	xi
List of Table	xvi
Chapter 1 : General introduction	1
1 Introduction	2
1.1 Natural products	2
1.1.1 Definition of natural products	2
1.1.2 The history of natural products	2
1.2 Herbal medicines	5
1.2.1 General background to the use of herbal medicines	5
1.2.2 The biological effects of herbal medicines	7
1.2.3 The correlation between plants and human healthcare	9
1.3 Ocimum sanctum Linn	10
1.3.1 Characterisation and distribution of Ocimum sanctum Linn	10
1.3.2 Pharmacological properties and phytochemical components	11
1.4 Propolis	14
1.4.1 Introduction	14
1.4.2 Use of propolis throughout history	17
1.4.3 Physical properties of propolis	18
1.4.4 The chemical composition of propolis and correlation with geographic area	18
1.4.4.1 Flavonoids	22
1.4.4.2 Terpenoids	29
1.4.4.3 Phenolics and acids	30
1.4.4.4 Sugars	32
1.4.4.5 Hydrocarbons	32
1.4.4.6 Mineral elements	32
1.4.4.7 Overview	32
1.4.5 Species of bees and propolis	33
1.4.6 Biological effects of propolis	34
1.4.7 Antiprotozoal Activity of Propolis	36
1.4.7.1 Trypanosomiasis	37
1.4.7.2 African trypanosomiasis	38
1.4.7.3 American trypanosomiasis	38
1.4.7.4 Treatments for Trypanosomiasis	39
1.5 Extraction and bulk extraction methods	41
1.5.1 Plant material extraction	41
1.5.2 Soxhlet extraction	41
1.6 Instrumental methods	41
1.6.1 Introduction	41
1.6.2 High-resolution mass spectrometry	43
1.6.2.1 Different ionisation methods are compatible with LC-MS	44
1.6.2.1.1 Ionisation methods	44
1.6.2.1.2 Separation of ions and mass analysis	45

1.6.3 HPLC with evaporative light scattering detection	45
1.6.4 Nuclear magnetic resonance techniques	48
1.6.4.1 ¹ H NMR	50
1.6.4.2 ¹³ C NMR	50
1.6.4.3 Correlation spectroscopy	51
1.6.4.4 Heteronuclear single quantum correlation	51
1.6.4.5 Heteronuclear multiple bond correlation	52
1.7 Aims and Objectives	53
Chapter 2 : Materials and methods	54
2.1 Chemical and reagents	55
2.2 Laboratory equipment and instruments	55
2.3 Plant material	56
2.4 Collection and preparation of the propolis sample	56
2.5 Methods	56
2.5.1 Extraction of <i>Ocimum sanctum</i>	56
2.5.2 Propolis sample extraction	57
2.5.2.1 Propolis extraction for LC-MS profiling	57
2.5.2.2 Propolis extraction for fractionation and purification	57
2.6 Plant and propolis purification procedures	58
2.6.1 Analytical and chromatographic methods	58
2.6.1.1 Thin layer chromatography	58
2.6.1.1.1 UV light-based detection	59
2.6.1.1.2 Spray reagent-based detection	59
2.6.1.1.2 Modified anisaldehyde-sulphuric acid reagent	59
2.6.1.1.3 Vanillin-sulphuric acid reagent	59
2.6.1.2 Vacuum liquid chromatography	60
2.6.1.2.1 The method of vacuum liquid chromatography employed for plant	60
2.6.1.3 Column chromatography	60
2.6.1.3.1 The CC method employed for plant	60
2.6.1.3.2 The CC method employed for propolis	61
2.6.1.4 Size-exclusion chromatography	62
2.6.1.5 Preparative thin layer chromatography	62
2.7 Structure elucidation	63
2.7.1 Nuclear magnetic resonance	63
2.7.1.1 One-dimensional NMR experiments	64
2.7.1.2 Two-dimensional NMR experiments	64
2.7.2 Mass spectrometry	65
2.7.3 HPLC-UV-ELSD	66
2.7.4 Optical rotation	66
2.8 Cell culture and medium preparation	67
2.8.1 Cell viability assay	67
2.8.2 Anti-trypanosomal assay in-vitro	68
3.Results	70

Chapter 3: Chemical profiling, extraction, purification, isolation and elucidation of Ocimum sanctum Labiatae	71
3 Phytochemical results for Ocimum sanctum Labiatae	72
3.1 Introduction	72
3.2 Solvent Extraction and Yields	72
3.3 Characterisation of M-3-21 as rosmarinic acid	78
3.4 Characterization of M-3-9 as luteolin-7-O-glucuronide	84
3.5 Characterisation of M-1-1 as ursolic acid	91
3.6 Biological activities of Ocimum sanctum Linn against trypanosome (T.brucei S427 strain)	98
3.7 Discussion	100
Chapter 4: Chemical profiling, extraction, purification, isolation and elucidation of different types of propolis from various geographical areas	102
4 Phytochemical results for Saudi propolis	103
4.1 Introduction	103
4.1.1 Extraction of sample of Saudi raw propolis	103
4.1.2 Characterisation of S-6-7 as fisetinidol	111
4.1.3 Characterization of S-6-13 as ferulic acid	119
4.1.4 Biological activities of Saudi propolis sample against trypanosome (T.brucei S427 strain)	125
4.2 Phytochemical results for Philippine propolis	127
4.2.1 Introduction	127
4.2.2 Extraction of sample of Philippine raw propolis	127
4.2.3 Characterisation of Ph-2-14 as 27-hydroxymangiferonic acid	134
4.2.4 Characterisation of Ph-2-11 as 27-hydroxyisomangiferolic acid	143
4.2.5 Characterisation of Ph-2-20 as isomangiferolic acid	150
4.2.6 Biological activities of Philippines propolis sample against trypanosome (T.brucei S427 strain)	158
4.3 Phytochemical results for Red Nigerian propolis	160
4.3.1 Introduction	160
4.3.2 Extraction of sample of Red Nigerian raw propolis	160
4.3.3 Characterisation of RN-6-16 as isosativan	166
4.3.4 Characterisation of RN-6-24 as medicarpin	173
4.3.5 Biological activities of Red Nigerian propolis sample against trypanosome (T.brucei S427 strain)	178
4.4 Phytochemical results for red Brazilian propolis	180
4.4.1 Introduction	180
4.4.2 Extraction of sample of red Brazilian raw propolis	180
4.4.3 Characterisation of FB-3-10 as calycosin	187
4.4.4 Characterisation of FB-3-14 as liquiritigenin	192
4.4.5 Biological activities of Red Brazilian propolis sample against trypanosome (T.brucei S427 strain)	197
4.5 Discussion	199
Chapter 5: General conclusion and future work	205
5.1 Conclusion and further research	206

5.2 Future Work	210
6. Bibliography	212

List of Abbreviations

Liquid chromatography mass spectrometry	LC-MS
2, 2-dimethyl-6-carboxyethenyl-2H-1-benzopyran	DCBEN

3, 5-diprenyl-4-hydroxycinnamic acid 4	DHCA4
50% Effective Concentration	EC50
Alongside photodiode array	PDA
Artemisinin-based combined therapy	ACT
Atmospheric pressure chemical ionisation	APCI
Atmospheric pressure ionisation	API
Carbon	C
Chemical ionisation	CI
Collision-induced dissociation	CID
Column chromatography	CC
Column chromatography	CC
Correlation spectroscopy	COSY
Desorption electrospray ionisation	DESI
Distortionless Enhancement by Polarisation Transfer	DEPT
Electron impact	EI
Electrospray ionisation	ESI
Ethyl Acetate	EtOA
Evaporative light scattering detector	ELSD
Fast atom bombardment	FAB
Fourier transform ion cyclotron resonance	FT-ICR
Gel filtration chromatography	GF
heteronuclear multiple bond correlation	HMBC
Heteronuclear Single Quantum Coherence	HSQC
Hexane	HE
High-performance liquid chromatography	HPLC
High-resolution mass spectrometry	HRMS
High-resolution mass spectrometry	HRMS
High-throughput screening	HTS
Mass spectrometry	MS
Mass to charge	m/z
Matrix-assisted laser desorption/ionisation	MALDI
Mobile phase	MP
Nuclear magnetic resonance spectroscopy	NMR
Optical rotation	OR
Partial least squares	PLS
Preparative thin layer chromatography	PTLC
Principle component analysis	PCA
Size-exclusion chromatography	SEC
Stationary phase	SP
Tetramethylsilane	TMS
Thin layer chromatography	TLC
Time-of-flight	TOF
Traditional and complementary medicine	T&CM
Traditional medicine	TM
Ultraviolet	UV
Ultraviolet/visible	UV/VIS

Vanillin-sulphuric acid
Vacuum liquid chromatography

VAS
VLC

List of Figures

Figure 1: <i>Ocimum sanctum</i> Linn.	11
Figure 2: A wide range of chemical compounds are found in <i>Ocimum sanctum</i> Linn	13

Figure 3: The structures of some flavonoids and phenolics identified in propolis	16
Figure 4: The structures of some flavonoids, isoflavonoids and benzofurans isolated from African propolis	21
Figure 5: The general structures of flavonoids and other classes of compounds found in propolis.	24
Figure 6: The general structures of the principle flavonoids described in propolis	25
Figure 7: Main flavonols described in propolis	25
Figure 8: Main flavones described in propolis	26
Figure 9: Isoflavones described in propolis	26
Figure 10: Main isoflavones described in propolis	26
Figure 11: The structures of some prenylated flavonoids isolated from Nigerian red propolis	27
Figure 12: The structures of some classes of terpenes	29
Figure 13: The structures of the principle phenolic acids described in propolis	31
Figure 14: Schematic of the basic components of a mass spectrometer	44
Figure 15: High Performance Liquid Chromatography System	47
Figure 16: Commercial Evaporative light Scattering Detector	48
Figure 17: Nuclear magnetic resonance Spectroscopy	50
Figure 18: ¹ H (400 MHz) NMR spectrum of MeOH extract in DMSO-d ₆	73
Figure 19: Chromatogram view of MeOH extract on the LC-MS negative ion mode (-ve ESI)	75
Figure 20: Structure of rosmarinic acid	79
Figure 21: ¹ H NMR spectrum (400 MHz) of rosmarinic acid (M-3-21) in DMSO-d ₆	80
Figure 22: Selected ¹ H expansion for the aromatic region of rosmarinic acid (M-3-21)	80
Figure 23: ¹³ C NMR spectrum (100 MHz) of rosmarinic acid (M-3-21) in DMSO-d ₆	81
Figure 24: COSY spectrum (400 MHz) of rosmarinic acid (M-3-21) in DMSO-d ₆	81
Figure 25: HSQC spectrum (400 MHz) of rosmarinic acid (M-3-21) in DMSO-d ₆	82
Figure 26: HMBC spectrum (400 MHz) of rosmarinic acid (M-3-21) in DMSO-d ₆	82
Figure 27: Selected HMBC expansion for the aromatic region of rosmarinic acid (M-3-21)	83
Figure 28: (A) refers to the chromatogram correspond to the mass of rosmarinic acid in the negative ion mode (ve ESI) whereas (B) shows the spectrum corresponding to the rosmarinic acid chromatogram	83
Figure 29: Structure of luteolin-7-O-glucuronide	85
Figure 30: ¹ H NMR spectrum (400 MHz) of luteolin-7-O-glucuronide (M-3-9) in DMSO-d ₆	87
Figure 31: Selected ¹ H expansion for the aromatic region of luteolin-7-O-glucuronide (M-3-9)	87
Figure 32: ¹³ C NMR spectrum (100 MHz) of luteolin-7-O-glucuronide (M-3-9) in DMSO-d ₆	88

Figure 33: COSY spectrum (400 MHz) of luteolin-7-O-glucuronide (M-3-9) in DMSO-d6	88
Figure 34: HSQC spectrum (400 MHz) of luteolin-7-O-glucuronide (M-3-9) in DMSO-6	89
Figure 35: HMBC spectrum (400 MHz) of luteolin-7-O-glucuronide (M-3-9) in DMSO-d6	89
Figure 36: Selected HMBC expansion for the aromatic region of luteolin-7-O-glucuronide (M-3-9)	90
Figure 37: (A) Extracted ion chromatogram (EIC) corresponding to the mass of luteolin-7-O-glucuronide in the negative ion mode (-ve ESI) whereas (B) The mass spectrum corresponding to luteolin-7-O-glucuronide chromatogram	90
Figure 38: Separation of ursolic acid by PTLC after developing with the mobile phase HE: EtOAc (80:20%) and spraying with p-anisaldehyde-sulphuric acid and heating	91
Figure 39: Structure of ursolic acid	92
Figure 40: 1H NMR spectrum (400 MHz) of ursolic acid (M-1-1) in DMSO-d6	94
Figure 41: Selected 1H expansion for the aliphatic region of ursolic acid (M-1-1)	94
Figure 42: Full DEPTq 135 13C NMR spectrum (100 MHz) of ursolic acid (M-1-1) in DMSO-d6	95
Figure 43: COSY spectrum (400 MHz) of ursolic acid (M-1-1) in DMSO-d6	95
Figure 44: HSQC spectrum (400 MHz) of ursolic acid (M-1-1) in DMSO-d6	96
Figure 45: HMBC spectrum (400 MHz) of ursolic acid(M-1-1) in DMSO-d6	96
Figure 46: (A) TIC corresponding to the mass of ursolic acid in the negative ion mode (-ve ESI) whereas (B) shows the mass spectrum corresponding to the ursolic acid chromatogram	97
Figure 47: 1H (400 MHz) NMR spectra of ethanolic Saudi extract in CDCl3	105
Figure 48: Chromatogram view of ethanolic Saudi crude in LC-MS negative ion mode (-ve ESI)	107
Figure 49: Chromatogram of ethanolic Saudi crude obtained by using HPLC with the ELSD. (Black traces ELSD while blue trace UV at 290 nm and pink trace UV at 320 nm)	107
Figure 50: Chromatogram view of Saudi's fraction (S-6) using the LC-MS in negative ion mode (-ve ESI)	110
Figure 51: Chromatogram view of Saudi's fraction (S-6) on the ELSD	111
Figure 52: Structure of fisetinidol	113
Figure 53: 1H NMR spectrum (400 MHz) of fisetinidol (S-6-7) in DMSO-d6	114
Figure 54: Selected 1H expansion for the aliphatic region for fisetinidol (S-6-7)	114
Figure 55: Selected 1H expansion for the aromatic region for fisetinidol (S-6-7)	115
Figure 56: Full DEPTq 135 13C NMR spectrum (100 MHz) of fisetinidol (S-6-7) in DMSO-d6	115
Figure 57: COSY spectrum (400 MHz) of fisetinidol (S-6-7) in DMSO-d6	116

Figure 58: COSY correlations NMR spectra of fisetinidol in DMSO-d6. The coloured arrows show the correlations corresponding COSY correlations in (figure 57)	116
Figure 59: HSQC spectrum (400 MHz) of fisetinidol (S-6-7) in DMSO-d6	117
Figure 60: HMBC spectrum (400 MHz) of fisetinidol (S-6-7) in DMSO-d6	117
Figure 61: Selected HMBC expansion for the aromatic region for fisetinidol (S-6-7)	118
Figure 62: (A) is refers to the chromatogram correspond to mass of fisetinidol in the negative ion mode (-ve ESI) whereas (B) shows the spectrum corresponding to the fisetinidol chromatogram.	118
Figure 63: LC-UV-ELSD chromatogram of fisetinidol purified from SEC (Black traces ELSD and blue trace UV at 290 nm)	119
Figure 64: Structure of ferulic acid	120
Figure 65: 1H NMR spectrum (400 MHz) of ferulic acid (S-6-13) in DMSO-d6	121
Figure 66: 13C NMR spectrum (100 MHz) of ferulic acid (S-6-13) in DMSO-d6	122
Figure 67: COSY spectrum (400 MHz) of ferulic acid (S-6-13) in DMSO-d6	122
Figure 68: HSQC spectrum (400 MHz) of ferulic acid (S-6-13) in DMSO-d6	123
Figure 69: HSQC correlations NMR spectra of ferulic acid. The coloured arrows show the correlations corresponding HSQC correlations in figure (68)	123
Figure 70: HMBC spectrum (400 MHz) of ferulic acid (S-6-13) in DMSO-d6	124
Figure 71: (A) is refers to the chromatogram correspond to mass of ferulic acid in the negative ion mode (-ve ESI) whereas (B) showed the spectra corresponding to ferulic acid chromatogram	124
Figure 72: LC-UV-ELSD chromatogram of ferulic acid purified from SEC. (Black traces ELSD and blue trace UV at 290 nm)	125
Figure 73: Chromatogram of the ethanolic extract of Philippine popolis with the ELSD (red) and UV detection (green).	128
Figure 74: 1H (400 MHz) NMR spectra of ethanolic Philippine extract in CDCl3	129
Figure 75: Chromatogram view of ethanolic Philippine crude on the LC-MS negative ion mode (-ve ESI)	131
Figure 76: Chromatogram view of Philippine's fraction (Ph-2) analysed by LC-MS negative ion mode	133
Figure 77: Chromatogram of the Philippine fraction (Ph-2) on the ELSD	134
Figure 78: Structure of 27-hydroxymangiferonic acid	136
Figure 79: 1H NMR spectrum (400 MHz) of 27-hydroxymangiferonic acid(Ph-2-14) in DMSO-d6	138
Figure 80: Selected 1H NMR spectrum expansion for the aliphatic region of 27 hydroxymangiferonic acid (Ph-2-14)	138
Figure 81: Full DEPTq 135 13C NMR spectrum (100 MHz) of 27-hydroxymangiferonic acid (Ph-2-14) in DMSO-d6	139
Figure 82: Selected 13C NMR spectrum expansion for the aliphatic region of 27-hydroxymangiferonic acid (Ph-2-14)	139

Figure 83: COSY spectrum (400 MHz) of 27-hydroxymangiferonic acid (Ph-2-14) in DMSO-d6	140
Figure 84: HSQC spectrum (400 MHz) of 27-hydroxymangiferonic acid (Ph-2-14) in DMSO-d6	140
Figure 85: Selected HSQC spectrum expansion for the aliphatic region of 27-hydroxymangiferonic acid (Ph-2-14)	141
Figure 86: HMBC spectrum (400 MHz) of 27-hydroxymangiferonic acid (Ph-2-14) in DMSO-d6	140
Figure 87: (A) is refers to the chromatogram correspond to mass of 27-hydroxymangiferonic acid in the negative ion mode (-ve ESI) whereas (B) shows the spectrum corresponding to the 27-hydroxymangiferonic acid chromatogram	142
Figure 88: LC-UV-ELSD chromatogram of 27-hydroxymangiferonic acid purified from SEC	142
Figure 89: Structure of 27-hydroxyisomangiferolic acid	143
Figure 90: 1H NMR spectrum (400 MHz) of 27-hydroxyisomangiferolic acid (Ph-2-11) in DMSO-d6	145
Figure 91: Selected 1H NMR spectrum expansion for 27-hydroxyisomangiferolic acid (Ph-2-11) in the aliphatic region	145
Figure 92: Full DEPTq 135 13C NMR spectrum (100 MHz) of 27-hydroxyisomangiferolic acid (Ph-2-11) in DMSO-d6	146
Figure 93: Selected 13C NMR spectrum expansion for the aliphatic region of 27-hydroxyisomangiferolic acid (Ph-2-11)	146
Figure 94: COSY spectrum (400 MHz) of 27-hydroxyisomangiferolic acid (Ph-2-11) in DMSO-d6	147
Figure 95: Selected COSY spectrum expansion for the aliphatic region of 27-hydroxyisomangiferolic acid (Ph-2-11)	147
Figure 96: HSQC spectrum (400 MHz) of 27-hydroxyisomangiferolic acid (Ph-2-11) in DMSO-d6	148
Figure 97: Selected HSQC spectrum expansion for the aliphatic region of 27-hydroxyisomangiferolic acid (Ph-2-11)	148
Figure 98: HMBC spectrum (400 MHz) of 27-hydroxyisomangiferolic acid (Ph-2-11) in DMSO-d6	149
Figure 99: (A) is refers to the chromatogram corresponding to the mass of 27-hydroxyisomangiferolic acid in the negative ion mode (-ve ESI) whereas (B) showed the spectra corresponding to 27-hydroxyisomangiferolic acid chromatogram	149
Figure 100: LC-UV-ELSD chromatogram of 27-hydroxyisomangiferolic acid purified from SEC	150
Figure 101: Structure of isomangiferolic acid	151
Figure 102: 1H NMR spectrum (400 MHz) of isomangiferolic acid (Ph-2-20) in CDCl3	153
Figure 103: Selected 1H NMR spectrum expansion of isomangiferolic acid (Ph-2-20) for the aliphatic region	153
Figure 104: Full DEPTq 135 13C NMR spectrum (100 MHz) of isomangiferolic acid (Ph-2-20) in CDCl3	154
Figure 105: Selected 13C NMR spectrum expansion for the aliphatic region of isomangiferolic acid (Ph-2-20)	154
Figure 106: COSY spectrum (400 MHz) of isomangiferolic acid (Ph-2-20) in CDCl3	155

Figure 107: HSQC spectrum (400 MHz) of isomangiferolic acid (Ph-2-20) in CDCl ₃	155
Figure 108: HMBC spectrum (400 MHz) of isomangiferolic acid (Ph-2-20) in CDCl ₃	156
Figure 109: Selected HMBC spectrum expansion for the aliphatic region of isomangiferolic acid (Ph-2-20)	156
Figure 110: (A) refers to the chromatogram corresponding to the mass of isomangiferolic acid in the negative ion mode (-ve ESI) whereas (B) shows the spectrum corresponding to isomangiferolic acid chromatogram	157
Figure 111: LC-UV-ELSD chromatogram of isomangiferolic acid purified from SEC	157
Figure 112: Chromatogram of ethanolic extract of red Nigerian on the HPLC UV (red)-ELSD (blue)	161
Figure 113: ¹ H (400 MHz) NMR spectra of ethanolic extract of red Nigerian propolis in DMSO-d	161
Figure 114: Chromatogram view of ethanolic extract of red Nigerian propolis by LC-MS in negative ion mode (-ve ESI)	163
Figure 115: Chromatogram view of red Nigerian propolis fraction RN-6 on the LC-MS negative ion mode (-ve ESI)	165
Figure 116: Chromatogram of the red Nigerian propolis fraction RN-6 HPLC UV/ ELSD	166
Figure 117: Structure of isosativan	167
Figure 118: ¹ H NMR spectrum (400 MHz) of isosativan (RN-6-16) in CDCl ₃	169
Figure 119: Selected ¹ H expansion for the aromatic region of isosativan (RN-6-16)	169
Figure 120: Full DEPTq ¹³⁵ ¹³ C NMR spectrum (100 MHz) of isosativan (RN-6-16) in CDCl ₃	170
Figure 121: COSY spectrum (400 MHz) of isosativan (RN-6-16) in CDCl ₃	170
Figure 122: HSQC spectrum (400 MHz) of isosativan (RN-6-16) in CDCl ₃	171
Figure 123: HSQC correlations NMR spectra of isosativan	171
Figure 124: HMBC spectrum (400 MHz) of isosativan (RN-6-16) in CDCl ₃	172
Figure 125: (A) refers to the chromatogram corresponding to the mass of isosativan in the negative ion mode (-ve ESI) whereas (B) showed the spectrum corresponding to isosativan chromatogram	172
Figure 126: Structure of medicarpin	174
Figure 127: ¹ H NMR spectrum (400 MHz) of medicarpin (RN-6-24) in CDCl ₃	175
Figure 128: ¹³ C NMR spectrum (100 MHz) of medicarpin (RN-6-24) in CDCl ₃	175
Figure 129: COSY spectrum (400 MHz) of medicarpin (RN-6-24) in CDCl ₃	176
Figure 130: HSQC spectrum (400 MHz) of medicarpin (RN-6-24) in CDCl ₃	176
Figure 131: HMBC spectrum (400 MHz) of medicarpin (RN-6-24) in CDCl ₃	177
Figure 132: Selected HMBC expansion for the aromatic region of medicarpin (RN-6-24)	177

Figure 133: (A) is refers to the chromatogram corresponding to the mass of medicarpin in the negative ion mode (-ve ESI) whereas (B) showed the spectrum corresponding to the medicarpin chromatogram	178
Figure 134: Chromatogram of ethanolic extract of Brazilian red propolis by using ELSD-UV	181
Figure 135: ¹ H (400 MHz) NMR spectra of the ethanolic extract of red Brazilian propolis in DMSO-d ₆	182
Figure 136: Chromatogram view of ethanolic extract of red Brazilian propolis by LC-MS in negative ion mode (-ve ESI)	183
Figure 137: Chromatogram view of red Brazilian fraction FB-3 on the LC-MS in negative ion mode	186
Figure 138: Chromatogram of the red Brazilian fraction (FB-3) on the ELSD-UV system	187
Figure 139: Structure of calycosin	188
Figure 140: ¹ H NMR spectrum (400 MHz) of calycosin (FB-3-10) in DMSO-d ₆	189
Figure 141: ¹³ C NMR spectrum (100 MHz) of calycosin (FB-3-10) in DMSO-d ₆	190
Figure 142: COSY spectrum (400 MHz) of calycosin (FB-3-10) in DMSO-d ₆	190
Figure 143: HSQC spectrum (400 MHz) of calycosin (FB-3-10) in DMSO-d ₆	191
Figure 144: HMBC spectrum (400 MHz) of calycosin (FB-3-10) in DMSO-d ₆	191
Figure 145: (A) refers to the chromatogram corresponding to the mass of calycosin in the negative ion mode (-ve ESI) whereas (B) shows the spectrum corresponding to the calycosin chromatogram	192
Figure 146: Structure of liquiritigenin	193
Figure 147: ¹ H NMR spectrum (400 MHz) of liquiritigenin (FB-3-14) in CDCl ₃	194
Figure 148: ¹³ C NMR spectrum (100 MHz) of liquiritigenin (FB-3-14) in CDCl ₃	195
Figure 149: COSY spectrum (400 MHz) of liquiritigenin (FB-3-14) in CDCl ₃	195
Figure 150: HSQC spectrum (400 MHz) of liquiritigenin (FB-3-14) in CDCl ₃	196
Figure 151: HMBC spectrum (400 MHz) of liquiritigenin (FB-3-14) in CDCl ₃	196
Figure 152: (A) refers to the chromatogram corresponding to the mass of liquiritigenin in the negative ion mode (-ve ESI) whereas (B) shows the spectrum corresponding to the liquiritigenin chromatogram	197

List of Tables

Table 1: A brief summary of history of natural products medicine	4
--	---

Table 2: The available of trypanocidal drugs	40
Table 3: Deuterated solvents used for NMR analysis	63
Table 4: Mobile phase system used in Mass spectroscopy experiments	66
Table 5: Result weighing of <i>Ocimum sanctum</i> L. extracts	72
Table 6: The LC-MS profiling for MeOH extract when analysed by reversed phase LC-MS in negative ion mode	74
Table 7: A step gradient elution technique used for separation of the MeOH extract by VLC	76
Table 8: Sequence of Column Chromatography Solvent Systems and fractions collected	77
Table 9: ¹ H (400 MHz) and ¹³ C (100 MHz) NMR data of rosmarinic acid (M-3-21) in DMSO-d ₆	79
Table 10: ¹ H (400 MHz) and ¹³ C (100 MHz) NMR data of luteolin-7-O-glucuronide(M-3-9) in DMSO-d ₆	86
Table 11: ¹ H (400 MHz) and ¹³ C (100 MHz) NMR data of ursolic acid (M-1-1) in DMSO-d ₆	93
Table 12 a: Drug Sensitivity assay of plant sample and its fractions on <i>T. brucei</i> S427 WT	99
Table 12 b: Cytotoxicity assay of plant sample and its fractions on U937 cells	99
Table 13: Result of weighing of ethanolic extract of Saudi propolis	104
Table 14: The LC-MS profiling for ethanolic Saudi extract when analysed by reversed phase LC-MS in negative ion mode	106
Table 15: Sequence of Column Chromatography Solvent Systems and fractions collected	109
Table 16: The most abundant in the Saudi's fraction (S-6) when analysed by reversed phase LC-MS in negative ion mode	110
Table 17: ¹ H (400 MHz) and ¹³ C (100 MHz) NMR data of fisetinidol (S-6-7) in DMSO-d ₆	113
Table 18: ¹ H (400 MHz) and ¹³ C (100 MHz) NMR data of ferulic acid (S-6-13) in DMSO-d ₆	121
Table 19 a: Drug Sensitivity assay of Saudi propolis sample and its fractions on <i>T. brucei</i> S427 WT	126
Table 19 b: Cytotoxicity assay of Saudi propolis sample and its fractions on U937 cells	126
Table 20: Result weighing of ethanolic Philippine propolis extract	128
Table 21: The LC-MS profiling for ethanolic Philippine extract when analysed by reversed phase LC-MS in negative ion mode	130
Table 22: Sequence of Column Chromatography Solvent Systems and fractions collected	132
Table 23: The most abundant components in the Philippine propolis fraction (PH-2) when analysed by reversed phase LC-MS in negative ion mode	133
Table 24: ¹ H (400 MHz) and ¹³ C (100 MHz) NMR data of 27-hydroxymangiferonic acid (Ph-2-14) in DMSO-d ₆	137
Table 25: ¹ H (400 MHz) and ¹³ C (100 MHz) NMR data of 27-hydroxyisomangiferolic acid (Ph-2-11) in DMSO-d ₆	144
Table 26: ¹ H (400 MHz) and ¹³ C (100 MHz) NMR data of isomangiferolic acid (Ph-2-200 in CDCl ₃)	152
Table 26 a: Drug Sensitivity assay of Philippines propolis sample and its fractions on <i>T. brucei</i> S427 WT	159

Table 26 b: Cytotoxicity assay of Philippines propolis sample and its fractions on U937 cells	159
Table 27: Results of weighing of ethanolic red Nigerian propolis extract	160
Table 28: The LC-MS profiling for ethanolic extract of red Nigerian propolis when analysed by reversed phase LC-MS in negative ion mode	162
Table 29: Sequence of Column Chromatography Solvent Systems and fractions collected	164
Table 30: The most abundant components in RN-6 when analysed by reversed phase LC-MS in negative ion mode	165
Table 31: ¹ H (400 MHz) and ¹³ C (100 MHz) NMR data of isosativan (RN-6-16) in CDCl ₃	168
Table 32: ¹ H (400 MHz) and ¹³ C (100 MHz) NMR data of medicarpin (RN-6-24) in CDCl ₃	174
Table 33 a: Drug Sensitivity assay of red Nigerian propolis sample and its fractions on <i>T. brucei</i> S427 WT	179
Table 33 b: Cytotoxicity assay of red Nigerian propolis sample and its fractions on U937 cells	179
Table 34: Result weighing of ethanolic red Brazilian propolis extract	181
Table 35: The LC-MS profiling for the ethanolic extract of red Brazilian propolis when analysed by reversed phase LC-MS in negative ion mode	183
Table 36: Sequence of Column Chromatography Solvent Systems and fractions collected	185
Table 37: The most abundant compounds in red Brazilian's fraction FB-3 when analysed by reversed phase LC-MS in negative ion mode	186
Table 38: ¹ H (400 MHz) and ¹³ C (100 MHz) NMR data of calycosin (FB-3-10) in DMSO-d ₆	189
Table 39: ¹ H (400 MHz) and ¹³ C (100 MHz) NMR data of liquiritigenin (FB-3-14) in CDCl ₃	194
Table 40 a: Drug Sensitivity assay of Red Brazilian propolis sample and its fractions on <i>T. brucei</i> S427 WT	198
Table 40 b: Cytotoxicity assay of red Brazilian propolis sample and its fractions on U937 cells	198

Chapter 1

General introduction

1 Introduction

1.1 Natural products

1.1.1 Definition of natural products

Natural products are products derived from a natural source that has not been processed or treated in any way besides straightforward preservation such as by drying. They may take the form of a whole or part of an organism such as a marine or terrestrial plant (e.g. paclitaxel from *Taxus brevifolia*), animal (e.g. vitamin A and D from cod liver oil) or microorganism (e.g. penicillin G from *Penicillium notatum*). They may be obtained from sources such as plant leaves or flowers, a specific organ from an animal, organism extracts or exudates, or may be pure compounds, including alkaloids, coumarins, flavonoids, glycosides, iridoids, lignans, steroids and terpenoids of plant, animal or microorganism origin (Samuelson, 1999). Nonetheless, natural products are usually understood to represent secondary metabolites in the shape of small molecules with a molecular weight of less than 2,000 amu that a living organism produces but does not rely on them to survive, grow, develop or reproduce. Frequently restricted to just a few species in a phylogenetic group, secondary metabolites comprise overflow metabolism products due to inadequate nutrition or shunt metabolism associated with the idiophase, defence mechanism or are regulator molecules (Sarker et al., 2005). It is believed that secondary metabolites are centrally involved in protecting plants against herbivores and other species.

1.1.2 The history of natural products

Humans have always resorted to natural products, particularly from terrestrial higher plants, for their curative properties. Mesopotamian clay tablets from 2600 BC are the earliest record of the use of a number of popular plant species, including liquorice (*Glycyrrhiza glabra*), myrrh (*Commiphora* species), and poppy capsule latex (*Papaver somniferum*) (Newman et al., 2000). Indeed, Sumer is one of the earliest

places where plants are known to have been used for therapeutic purposes, while the variety of plant species that Hippocrates is recorded as using in 400 BC comprised around 400 species (Sarker et al., 2005). Many ancient civilisations, including those of China and Egypt, employed natural products within traditional medicine and many of those products continue to be used nowadays to treat a range of conditions. A brief summary of the history of natural products medicine is illustrated in table 1.

In fact, in underdeveloped or developing countries, the primary healthcare available to more than 75% of the population is dependent on plant-based traditional medicine, as revealed by statistics from the World Health Organisation (WHO) (Sarker et al., 2005).

Table 1: A brief summary of the history of natural products medicine

Period	Type	Description
>3000 BC	Ayurveda and Chinese Traditional Medicine	Introduced medicinal properties of plants and other natural products
1550 BC	Ebers Papyrus	Presents a large number of crude drugs from natural sources (e.g., castor seeds and gum Arabic)
460–377 BC	Hippocrates "The Father of Medicine"	Described several plants and animals that can be the sources of medicine
370–287 BC	Theophrastus	Described several plants and animals that can be the sources of medicine
23–79 AD	Pliny the Elder	Described several plants and animals that can be the sources of medicine
60–80 AD	Dioscorides	Wrote, "De Materia Medica" which described more than 600 medicinal plants
131–200 AD	Galen	Developed botanical medicines (Galenicals) and made them popular in the west
Fifteenth century	Kräuterbuch (herbals)	Presented information and pictures of medicinal plants

(Sarker and Nahar, 2012).

Throughout history, humans have tapped into the rich source of products with curative properties that is nature, which is still the source of numerous drugs used today, the development of which was inspired by uses in traditional medicine. One major outcome of the use of plants for treatment purposes has been the isolation of chemical compounds that are therapeutically valuable in contemporary medicine (Chin et al., 2006). In fact, in the first days of drug research, the foremost medicine source employed was plants, and in particular plants exhibiting ethnomedicinal properties, which are believed to have accounted for the development of 80% of 122 plant-based drugs (Chin et al., 2006). Furthermore, natural products were either the basis or the inspiration for over 80% of drug substances prior to the introduction of high-throughput screening (HTS) and the post-genomic era (Harvey, 2008).

Vincristine (*Vinca rosea*), morphine (*P. somniferum*), and Taxol® (*T. brevifolia*) are examples of popular drugs derived from natural products in the past one hundred years. Indeed, natural products represent the basis of around 40% of drugs available nowadays. As reported by Cragg et al., 1997, during the period 1983-1994, a

proportion of 39% of 520 new approved drugs and 60-80% of drugs against bacteria and cancers were from natural products. Furthermore, more than half of drugs being clinically trialled in the year 2000 for different types of cancers had a natural origin, while in the following year, natural products were the basis or inspiration for eight out of the 30 most popular drugs (e.g. simvastatin, pravastatin, amoxicillin, clavulanic acid, clarithromycin, azithromycin, ceftriaxone, cyclosporin, and paclitaxel) that generated an overall revenue of US\$16 billion. Moreover, natural products constitute the basis of nearly half of all drugs that have received approval since 1994 (Harvey, 2008). Additionally, the 23 novel drugs that became available during 2001-2005 to treat bacterial and fungal infections, cancer, diabetes, dyslipidaemia, atopic dermatitis, Alzheimer's disease, and genetic diseases (e.g. tyrosinemia and Gaucher's disease) were of natural origin (Lam, 2007).

During 2005-2007, approval was granted to 13 drugs based on natural products, five of which laid the foundation for new categories of drugs e.g. exenatide, ziconotide, ixabepilone, retapamulin, and trabectedin (Harvey, 2008).

1.2 Herbal medicines

1.2.1 General background to the use of herbal medicines

Ever since they started walking the earth, humans have had a close bond with nature, taking advantage of the wide variety of natural products to feed, clothe, protect and treat themselves. According to fossil records, plants first began to be used by humans for their medicinal properties around 60,000 years ago, during the Middle Palaeolithic (Solecki, 1975), and their use in traditional medicine (TM) evolved ever since. In developing Asian, African and Latin American countries, native healers have employed plants to treat a range of conditions, particularly in rural areas, where other forms of healthcare are either too expensive or unavailable. The Organization (WHO), 2002 recorded that TM was used by up to 80% of people in African countries and by about 40% of the population of China.

Malaria is recorded as being treated with the bark of various *Cinchona* species from South America in 1630 (Evans, 2009), while congestive heart failure was treated with the leaves of *Digitalis purpurea* since medieval times (Bessen, 1986). Furthermore, Chinese TM and Japanese Kampo medicine have treated respiratory conditions, including asthma, coughs, nasal congestion and influenza, with mixtures of various herbal formulae, including species of *Ephedra* (e.g. *E. sinica* and *E. equisetina*), for a very long time (Kitani et al., 2009). Indeed, countless plants exhibiting anti-inflammatory, hypotensive, hypoglycaemic, amoebicidal, antifertility, and antiprotozoal effects are employed for therapeutic purposes around the world.

TM has begun to be increasingly used in developed countries alongside synthetic drug preparations, thanks to the marked changes in mentality towards herbal medicines that have occurred over the past three decades among both the general population and researchers. In Europe, the number of people employing traditional and complementary medicine (T&CM) has increased to more than 100 million and one-fifth of them employ T&CM on a regular basis or express a preference for healthcare that encompasses T&CM (WHO). The main group of commercially available drugs during the period 1981-2006 consisted of 24 compounds of natural origin, of which 19 were derived from soil microbes and 5 from plants. Examples of the latter are Taxol® (Paclitaxel) from *Taxus brevifolia* and Artemisinin from *Artemisia annua*, respectively used for their properties against cancer and malaria (Ganesan, 2008). Moreover, more than half of the top 150 brands prescribed in the US in 1993 were natural products with biological activity derived from plants and their analogues (Newman and Cragg, 2012).

The current known number of flowering plant species exceeds a quarter of a million, and of these species, no more than 10% have been extensively exploited for their

therapeutic properties. Thus, nature as a source of therapeutic products is nowhere near exhaustion (Reid and Sarker, 2006).

1.2.2 The biological effects of herbal medicines

The extensive testing conducted on different substances extracted from plants has had promising outcomes regarding the antibacterial, antifungal, antiviral and antiparasitic effects of those substances. The biological activity for which plant products are most commonly used is for chemotherapeutic activity against microorganisms or cancer. Unlike in earlier periods of history, when knowledge of microorganisms was poor or lacking, nowadays a battery of tests is available to assess the antibacterial properties of active plant compounds (Karou et al., 2005). For instance, a range of techniques and antibacterial bioassays were adopted by (Akinsulire et al., 2007) to measure the minimum inhibitory concentration and minimum bactericidal concentration, and thus determine the antimicrobial effects of crude extracts of the plants *Kalanchoe crenata* and *Bryophyllum pinnatum*. According to the findings obtained, although both plants exhibited antibacterial effects, the potency of those effects differed depending on the bacterial strain and the techniques employed to obtain the extracts. Likewise, the antibacterial effect of *Pterospermum diversifolium* was analysed by (Hidayathulla et al., 2011) by using varying extract concentrations on different bacterial strains. The disc diffusion technique involved the use of Gram –ve *E. coli* and *Pseudomonas aeruginosa* and Gram +ve *Bacillus subtilis* and *S. aureus*, revealing that the most intense activity was against Gram +ve, whereas the highest minimum inhibitory concentration was associated with Gram -ve.

Recent evidence suggests that compounds from numerous plant products commonly employed to treat gastrointestinal diseases (e.g. diarrhoea and vomiting) manifest

cytotoxic effects and therefore may be potential therapeutic agents in cancer treatment (Bisi-Johnson et al., 2011). The isolation of vinca alkaloids and production of vinblastine and vincristine during the 1950s constituted the starting point of research into the anti-cancer activity of plant compounds. At the same time, additional cytotoxic chemotypes of plant products were uncovered, driving the development of new methods for identifying, isolating, and examining plant-based anti-cancer agents (Cragg and Newman, 2005). The growing attention paid to plant-based agents with potential anti-cancer effects is due to the ever-expanding cancer-related morbidity rate in both developing and developed countries (Shoeb, 2006). Particularly good anti-cancer potential has been exhibited by epipodophyllotoxin-derived compounds such as topotecan, etoposide and taxol.

In numerous parts of the world and in particular in African countries, trypanosomes and other protozoa constitute a key public health issue due to the range of conditions they cause, so plant products with effects against these parasites have attracted a great deal of interest. For instance, *Azadiracta indica* extract was investigated by (Ngure et al., 2009) in terms of its potency against *Trypanosoma brucei rhodesiense* by employing infected mice and various parameters compared against a water control. It was found that, by comparison to a water-treated control, treatment with extract slowed down packed cell reduction, deferred parasitaemia and helped the mice live longer. Likewise, both the *in vivo* and *in vitro* assays undertaken by (Maikai, 2010) indicated that the flavonoids of *Ximenia Americana* had potent action against *Trypanosoma congolense*.

Immunotherapy and metabolism improvement or normal maintenance also benefit from the biological activity of plant products. As explained by (Blaylock and Maroon, 2012), the foremost cause of neurological conditions is excessive activation of immune cells, leading to the production of an abundance of glutamate, which displays toxicity if it is not secreted at the right moment. Plant products have been effective in

inhibiting excessive microglial activation and inflammatory agents, as well as contributing to the repair of the nervous system through stimulation of the release of neurotrophic agents. In addition, metabolic disorders like obesity and diabetes have been effectively regulated with plant products.

Furthermore, the compound berberine, which is present in several plants, has been reported to have marked effects in diabetes and obesity associated with insulin resistance, inducing weight loss and improved glucose tolerance in mouse models with no impact on food assimilation (Lee et al., 2006). Moreover, mice given a diet rich in fat exhibited better insulin sensitivity and lower levels of plasma triglycerides, as well as losing weight. Additionally, berberine downregulated lipogenesis genes and upregulated muscle and adipose tissue genes participating in energy consumption.

1.2.3 The correlation between plants and human healthcare

From the early days of human communities and up to the present day, a number of natural products have been shown to be effective for treating and managing numerous different conditions, including conditions caused by microbes, parasites, as well as inflammation and cancer. Besides their effectiveness, natural products are also affordable and sustainable due to their natural growth and straightforward extraction facilitated by innovations in methods and tools. Throughout the world, one significant health issue associated with poor quality of life and systemic and chronic disorders is oral disease, including periodontal disease and dental caries. The growing prevalence of this disease has been worsened by the fact that synthetic antibiotics are becoming increasingly ineffective and treatment is becoming more and more expensive. Under these circumstances, plant extracts provide an affordable, safe and sustainable approach to managing oral disease without the necessity of synthetic drugs (Palombo, 2011). Meanwhile, with regard to the management of malaria, a plant extract of high effectiveness is Artemisinin, which is mixed with a

base to develop the Artemisinin-based combined therapy (ACT), which is suitable for treating not only infection with *Plasmodium falciparum* like previous approaches, but also infection with *Plasmodium vivax* (Douglas et al., 2010).

1.3 *Ocimum sanctum* Linn

1.3.1 Characterisation and distribution of *Ocimum sanctum* Linn

The plant species called *Ocimum tenuiflorum* or *Ocimum sanctum* belongs to the genus *Ocimum*, family *Lamiaceae*, order *Lamiales*, class *Magnoliopsida*, division *Magnoliophyta* and kingdom *Plantae* (Pattanayak et al., 2010). Plants with medicinal properties that show particularly high promise as therapeutic agents are the plants of the genus *Ocimum* and family *Labiatae*. Called Holy Basil, Tulsi or Tulasi, *Ocimum sanctum* L. (*Labiatae*) is an annual herb with a powerful scent, growing as a low bush that can reach 18 inches in height (Pattanayak et al., 2010) (figure 1). Among the plants of the genus *Ocimum* that are medicinally valuable and can be found in various regions around the world are *Ocimum sanctum* L. (Tulsi), *Ocimum gratissimum* (Ram Tulsi), *Ocimum canum* (Dulal Tulsi), *Ocimum basilicum* (Ban Tulsi), *Ocimum kilimandscharicum*, *Ocimum ammericanum*, *Ocimum camphora* and *Ocimum micranthum* (Satyavati et al., 1987, Gupta et al., 2002, Sen, 1993, Prakash and Gupta, 2005). In the Indian subcontinent, the two types of *Ocimum sanctum* L. that are usually planted in gardens are Tulsi plants with green leaves called Sri Tulsi and Krishna Tulsi.



Figure 1: *Ocimum sanctum* Linn.

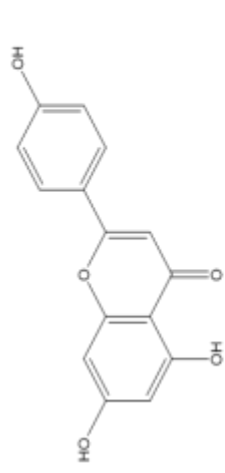
1.3.2 Pharmacological properties and phytochemical components

Traditionally, *Ocimum sanctum* L. has a range of different pharmacological attributes, depending on which part of the plant is used, such as leaves, flowers, stem, root or seeds, which have been employed for different purposes in traditional medicine, including for the treatment of coughs, pain, cancer, asthma, vomiting, diabetes, stress, fever, bronchitis, arthritis, and convulsions, as well as to induce perspiration, to prevent conception, to protect the liver, and to lower blood tension and levels of fats.

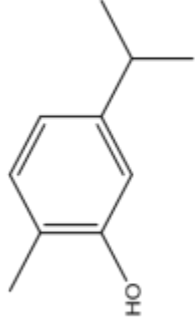
Ocimum sanctum L. displays a chemical composition of high complexity, with varieties and even plants in the same field having different concentrations of the various nutrients and compounds with biological activity. Moreover, processes such as growth, harvest, processing and storage have a considerable impact on the abundance of the different components, but knowledge about this impact is still limited (Pattanayak et al., 2010).

The various different active phytochemicals interact with each other synergistically, giving rise to the nutritional and pharmacological attributes of the plant that have been exploited in traditional medicine. For example, figure 2, the compounds present in the leaves are volatile oil eugenol, euginal or eugenic acid, urosolic acid, carvacrol, linalool, limatrol, caryophyllene, and methyl carvicol or estragol. Furthermore, the volatile oil in the seeds contains fatty acids and sitosterol, while different amounts of sugars are present in the seed mucilage which is made up of xylose and polysaccharides, and the green leaves contain anthocyanins (Kelm et al., 2000; Pattanayak et al., 2010; Shishodia et al., 2003).

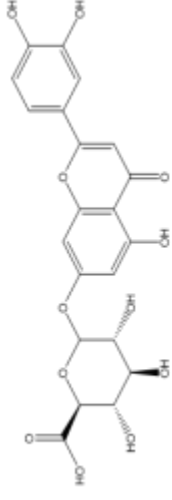
Despite lacking caffeine or other stimulants, *Ocimum sanctum* L. is considered to be a general vitaliser and improves physical endurance. Numerous potentially biologically active compounds are present in the stem and leaves, such as saponins, flavonoids, triterpenoids and tannins (Jaggi et al., 2003). Furthermore, rosmarinic acid, apigenin, cirsimaritin, isothymusin and isothymonin are among the phenolic compounds that have been proven to have effects against oxidants and inflammation. Moreover, it has been shown that chromosomal damage triggered by radiation in human blood lymphocytes was prevented by two flavonoids from *Ocimum sanctum* with solubility in water, namely, orientin and vicerin (Pattanayak et al., 2010).



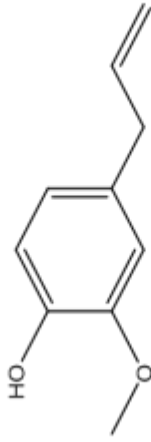
Apigenin



Carvacrol



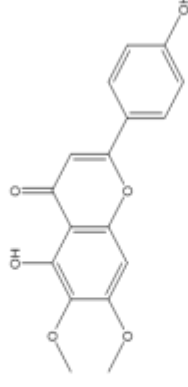
Luteolon-7-o-Glucuronide



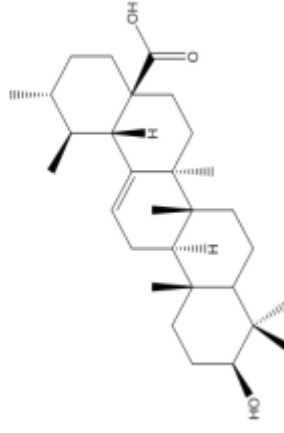
Eugenol



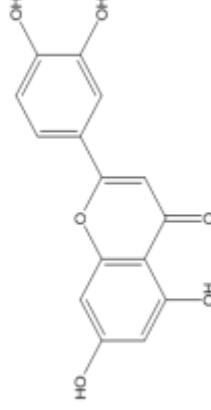
Linalool



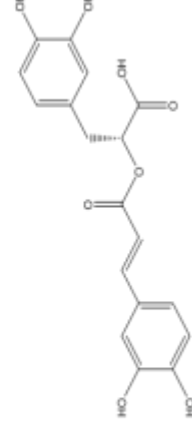
Cirsimaritin



Ursolic acid



Luteolin



Rosmarinic acid

Figure 2: A wide range of chemical compounds are found in *Ocimum sanctum* Linn

1.4 Propolis

1.4.1 Introduction

A resinous substance with a complex and diverse composition but comprising mainly beeswax and secondary metabolites from plants, propolis or bee glue is produced by honeybees from materials derived from plants, with the purpose of sterilising the hive environment (Krell, 1996), thus ensuring the health of the bee community. The propolis production process involves partial digestion or mixing with saliva of the materials gathered from plant bark, buds and flowers (Wagh, 2013). Studies have shown that colonies of bees that produce substantial quantities of propolis were more sanitary, achieved greater honey production, the brood was more viable and worker bees lived longer (Nicodemo et al., 2013; Nicodemo et al., 2014).

In numerous countries, traditional medicine relies greatly on propolis (Popova et al., 2010), which in recent times it has also started to be used in health foods and alternative medicine. Propolis differs in its chemical composition depending on geographical location, botanical source and bee species. For instance, geranyl flavanones are the main compounds found in propolis produced in the area around the Pacific and in Africa while diterpenes are abundant in propolis from Southern Europe and North Africa.

Although the value of propolis has begun to be widely acknowledged, bee farmers or honey collectors mostly ignore it, leaving it in the hive once the honey is collected. Thus, farmers need to be made aware of the great economic and medicinal values of propolis so that they start gathering it and can make significant profit. Propolis is extensively employed in the prevention and treatment of colds, wounds and ulcers, rheumatism, sprains, heart disease, diabetes and dental caries due to its biological effects against cancer (Marcucci, 1995), inflammation and oxidants (Siripatrawan et al., 2013), microbes (Bankova, 2009) and cell growth (Shubharani et al., 2014).

Propolis exhibits softness, malleability, and stickiness at high temperatures, but hardness and brittleness when exposed to low temperatures less than zero. When it is subjected to low temperatures, it no longer becomes flexible at high temperatures, maintaining its brittleness. In its raw state, the composition of propolis is 50% plant resins, 30% waxes, 10% essential and aromatic oils, 5% pollens and 5% other organic substances (Pietta et al., 2002). Furthermore, it varies according to the plant source of the component materials, when the materials are collected and where the hive is located. The substance can be coloured in various ways, such as yellow, red, green and brown (Fearnley, 2001, Wagh, 2013). The chemical composition of propolis has attracted interest due to the broad usage of this substance in modern herbal medicine, with extensive evidence pointing to the fact that the visible effects might arise from the complex components interacting synergistically. Figure 3 shows some of the components of temperate propolis which was collected from poplar buds.

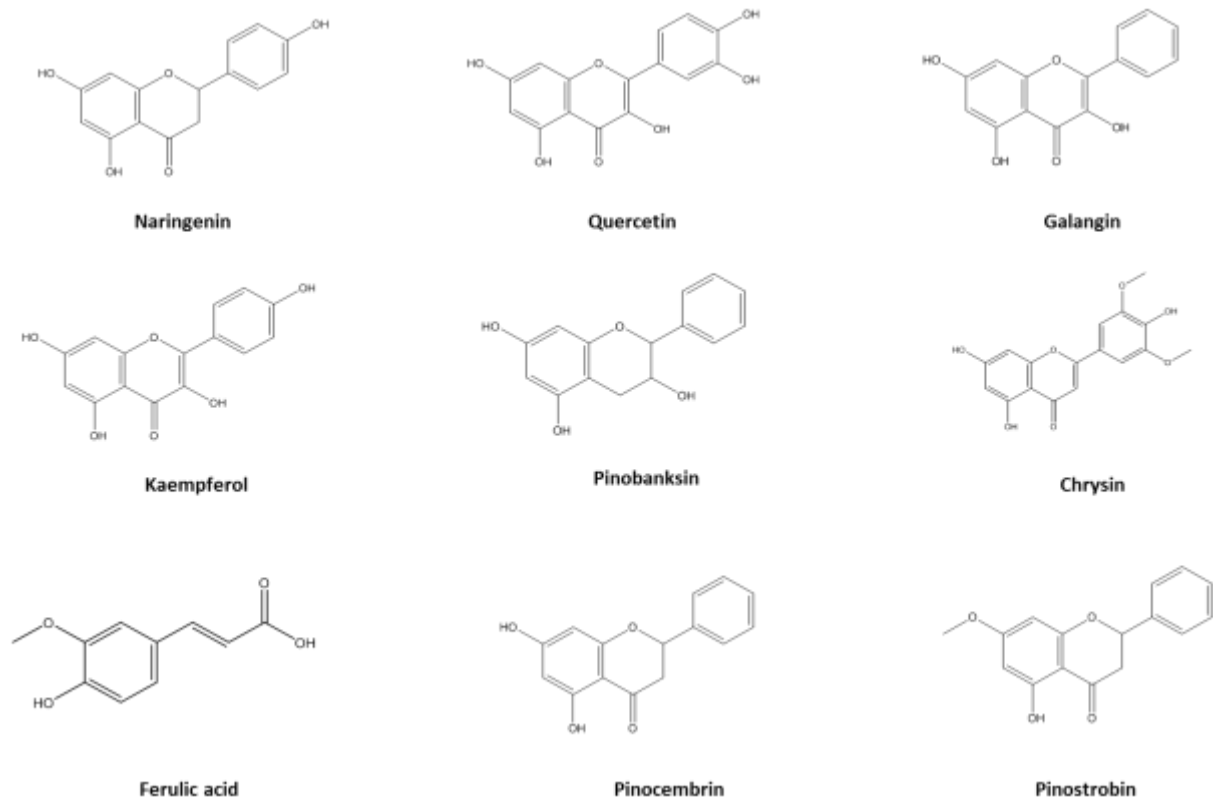


Figure 3: The structures of some flavonoids and other phenolics identified in propolis

1.4.2 Use of propolis throughout history

The term “propolis” comes from the ancient Greek word for suburb, which in turn comes from the verb “promalasso” (Liddell and Scott, 1897). Alongside honey, propolis has been used from the earliest civilisations, including the civilisations of Egypt, Persia and Rome (Houghton, 1998). In ancient Egypt, bee production of propolis was illustrated in paintings and on various objects, being employed not only to treat a range of conditions (Langenheim, 2003), but also in the process of embalming. Indeed, the whole process might have been inspired by the bees, as they use propolis to coat the bodies of dead invaders that cannot be removed from the hive (Nicolas, 1947), thus containing the infection caused by the decaying bodies. (Derevici et al., 1965) and colleagues were the first to observe in the 1960s that propolis reduced the incidence of bacteria in hives.

Called *tzori* in Hebrew, propolis was deemed to be medicine by the ancient Jews, and its properties were even highlighted in several Holy Books, being most likely the biblical Balm of Gilead (*tzori Gilead*), which occurred in the area of the Dead Sea for around 1,500 years and became famous for its aromatic and therapeutic attributes. Its composition was resin from a range of poplars, such as *P. balsamifera*, *P. nigra*, and *P. gileadensis* (Broadhurst, 1996). The Balm was among the constituents of the incense employed in religious rituals. Furthermore, through names such as *Afarsemon*, *kataf*, *nataf*, and *tzori Gilead*, the Balm of Gilead can be directly associated with a number of sages, such as Shimon Ben-Gamliel, Rambam (Maimonides), Saadia Gaon, and the modern biblical botanist Yehuda Feliks (Ben-Yehoshua et al., 2012).

Meanwhile, in ancient Greece, the perfume *polyanthus* was made primarily of propolis, alongside olibanum, styrax, and aromatic herbs (Bogdanov, 2012). Considered the third natural product of bees, after honey and wax, propolis was

discussed in terms of how it was prepared and used by over fifteen Greek and Roman authors. In later times, the Renaissance theory of *ad fontes* returned the spotlight on ancient teaching and medicine, making propolis popular again in Europe. The well-known herbal book, *The History of Plants*, indicated that healing ointments were based on the resin or clammy substance derived from the buds of the black poplar, being used to treat inflammation, bruises, sprains and falls. In England, pharmacopoeias began to incorporate propolis as a key component of healing ointments from the 1600s.

1.4.3 Physical properties of propolis

According to where it is from and how old it is, propolis can display different colours, such as yellow, dark brown or even transparent (Coggshall and Morse, 1984). At temperatures in the range of 25-45°C, propolis typically begins to soften, becoming malleable and highly sticky. Conversely, at temperatures below 15°C, propolis acquires a hardness and brittleness, and after it is frozen, it maintains its brittleness even at high temperatures. The usual melting point for propolis is 60-70°C, although it may be up to 100°C for certain samples. Ethanol, ether, glycerol and water are the main solvents employed for extracting propolis for commercial purposes. A wider range of solvents is available for extracting fractions to chemically analyse different targeted compounds (Krell, 1996).

1.4.4 The chemical composition of propolis and correlation with geographic area

In recent times, propolis has attracted a great deal of attention within pharmacological and chemical research, leading to the isolation of over 300 compounds and significant advancement of knowledge (Huang et al., 2014). It must be highlighted that there has been a significant shift in the paradigm regarding the chemical composition of propolis. The assumption dominant in the 1960s that,

despite its high complexity, the chemical composition of propolis was fairly homogeneous was turned on its head by investigations of a wide range of samples from various geographic areas, which showed the high variability and complexity of propolis chemistry (Bankova, 2005).

The phylogeographic features of the collection site, the bee species and the collection season are just some of the variables determining the chemical composition of propolis (Bankova et al., 2000). Processing can involve production of a propolis tincture through elimination of the wax and organic residue (Burdock, 1998).

To shed light on the determinants of the significant heterogeneity of propolis chemistry, (Bankova, 2005) analysed samples of propolis based on the knowledge that bees employ materials from more than one plant part, which are the outcomes of different botanical processes and are produced either through active secretion or exudation from plant wounds. For instance, lipophilic materials are derived from leaves, leaf buds, gums, resins, and lattices (Crane, 1988). Based on the analysis conducted, two major categories of propolis were identified by (Bankova, 2005) depending on whether the area of origin was tropical and subtropical or temperate.

The resinous substances exuded from poplar trees, and especially the black poplar *Populus nigra*, is the key source of propolis in areas with a temperate climate, including Europe, North America, New Zealand and Western Asia (Toreti et al., 2013). Consequently, this kind of propolis is composed mainly of phenolics, including flavonoid aglycones, phenolic acids and their esters, which are the major compounds present in poplar buds (Bankova et al., 2000). However, the buds of the birch tree *Betula verrucosa* are the main source of propolis in northern areas of Russia (Bankova et al., 2000).

In tropical and subtropical areas, bees collect materials for propolis production from plants other than poplars and birch, as these are not to be found in such areas. Hence, in tropical zones, a range of plant species serve as sources of propolis, including exudate from the leaves of certain *Cistus* species in the case of propolis from Tunisia (Martos et al., 1997) and *Ambrosia deltoidea* and *Encelia farinose* in the case of propolis from the Sonoran Desert (Wollenweber and Buchmann, 1997). As regards propolis from Australia, it was found to derive from *Xanthorrhoea* spp., which can only be found in Australia.

When tropical samples from Venezuela were subjected to chromatographic comparison, it was found that isolated polyprenylated benzophenones from propolis were identical to the major constituents of resin exudates from the flowers of *Clusia major* and *Clusia minor* (Guttiferae). However, more research is needed to determine the sources of fatty acids, terpenoids, and flavonoids (e.g. pinocembrin) in the case of African propolis. The results of chemical profiling and chemometric analysis on samples from South Africa revealed that phenolic acids and flavonols were abundant in most South African samples and there were close similarities between the chemical profile of most samples and that of propolis from temperate areas (Kasote et al., 2014). Figure 4 shows some of the phenolic compounds isolated from South African propolis.

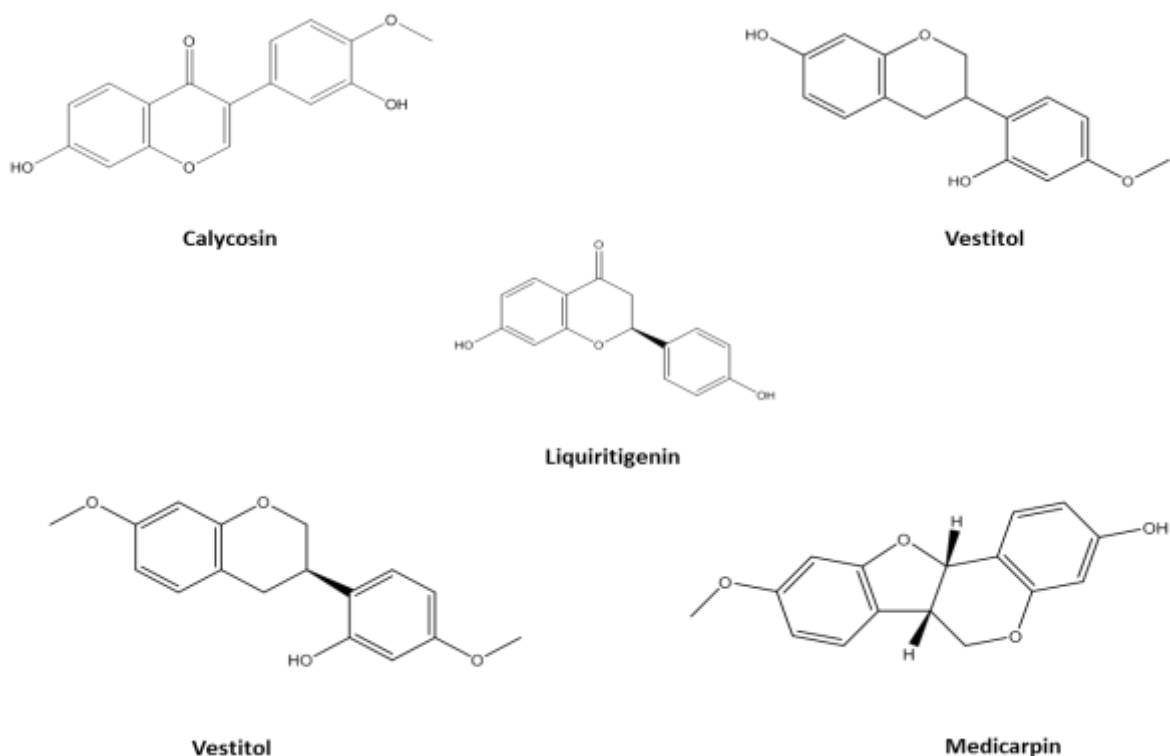


Figure 4: The structures of some flavonoids, isoflavonoids and benzofurans isolated from African propolis

A growing amount of attention is currently paid to propolis from Brazil, which eloquently illustrates how variation in chemical composition is possible even in the same region. Due to the large size of the country and the diversity of climate zones and vegetation types, a physicochemical classification of Brazilian propolis into twelve distinct types has been created, with differences due to botanical source and chemical composition. (Banskota et al., 1998) conducted chemometric profiling and found that tropical Brazilian propolis derived mainly from *Baccharis* spp., alongside *Clusia minor*, *Clusia major*, and *Araucaria heterophylla*. Propolis has been established to be chemically constituted primarily of flavonoids, terpenoids, phenolic acids and their esters, and to a lesser extent, of aldehydes, ketones, fatty acids,

sugars and mineral elements. On the other hand, propolis has not been so far found to contain typical phytochemicals like alkaloids and iridoids (Kasote et al., 2014).

1.4.4.1 Flavonoids

It is believed that the biological effects of propolis are largely underpinned by flavonoids, which dominate the chemical composition of propolis in temperate areas, occurring without B-ring substitution, such as chrysin, galangin, pinocembrin, pinobanksin. Such flavonoids serve as markers for standardisation and assessment of the quality of propolis in temperate regions. Four distinct types of flavonoid action mechanisms have been identified, namely, binding to biological polymers, binding to heavy metal ions, electron transport catalysis, and scavenging of free radicals (Havsteen, 1983, Burdock, 1998). The typical types of flavonoids shown in figure 5 include flavones, flavonols, flavanones, flavanonols, chalcones, dihydrochalcones, isoflavones, isodihydroflavones, flavans, isoflavans and neoflavonoids. Furthermore, some samples of propolis have revealed flavonoid glycosides like isorhamnetin-3-O-rutinoside (Popova et al., 2009) and narigenin-8-C-hexoside, the first flavone C-glycoside that was extracted from Brazilian red propolis (Righi et al., 2011). Samples of propolis from the Solomon Islands and Kenya yielded geranylated flavonols such as 2'-Geranylquercetin, 8-(8"-Hydroxy-3", 8"-dimethyl-Oct-2"-enyl)-quercetin and macarangin, indicating that propolis originated primarily from the genus *Macaranga*. Awale et al. employed singular open-chain neoflavonoids from Nepalese propolis as markers to determine where the propolis had originated from (Awale et al., 2005). Meanwhile, Pacific propolis from Japan, Thailand and the Solomon Islands was observed to contain numerous prenylated and geranylated flavonones (e.g. propolins A to E), which had potent effects against bacteria because they contained the lipophilic prenyl group that quickly causes destruction of the membrane of bacterial cells (Raghukumar et al., 2010). Novel propolis types, red Brazilian propolis and Cuban propolis are garnering significant interest because of the variety of flavonoids

with different biological effects that they contain. Their primary source of origin is the resinous exudate of the leguminous plant *Dalbergia ecastophyllum*, which consists of flavanones like liquiritigenin, naringenin, dihydroroxylin A, garbanzol and alnustinol. In addition, the exudate was found to contain isoflavones (e.g. calycosin), isodihydroflavones (e.g. daidzein, formononetin, xenognosin B, biochanin A, (3S)-vestitone and violanone), chalcones (e.g. isoliquiritigenin), dihydrochalcones (e.g. 2', 4'-Dihydroxychalcone), and pterocarpins (e.g. medicarpin). Red propolis was observed to comprise homopterocarpin and 6a-ethoxymedicarpin as well (Li et al., 2008). Figures 6-11 show the different types of flavonoids found in propolis.

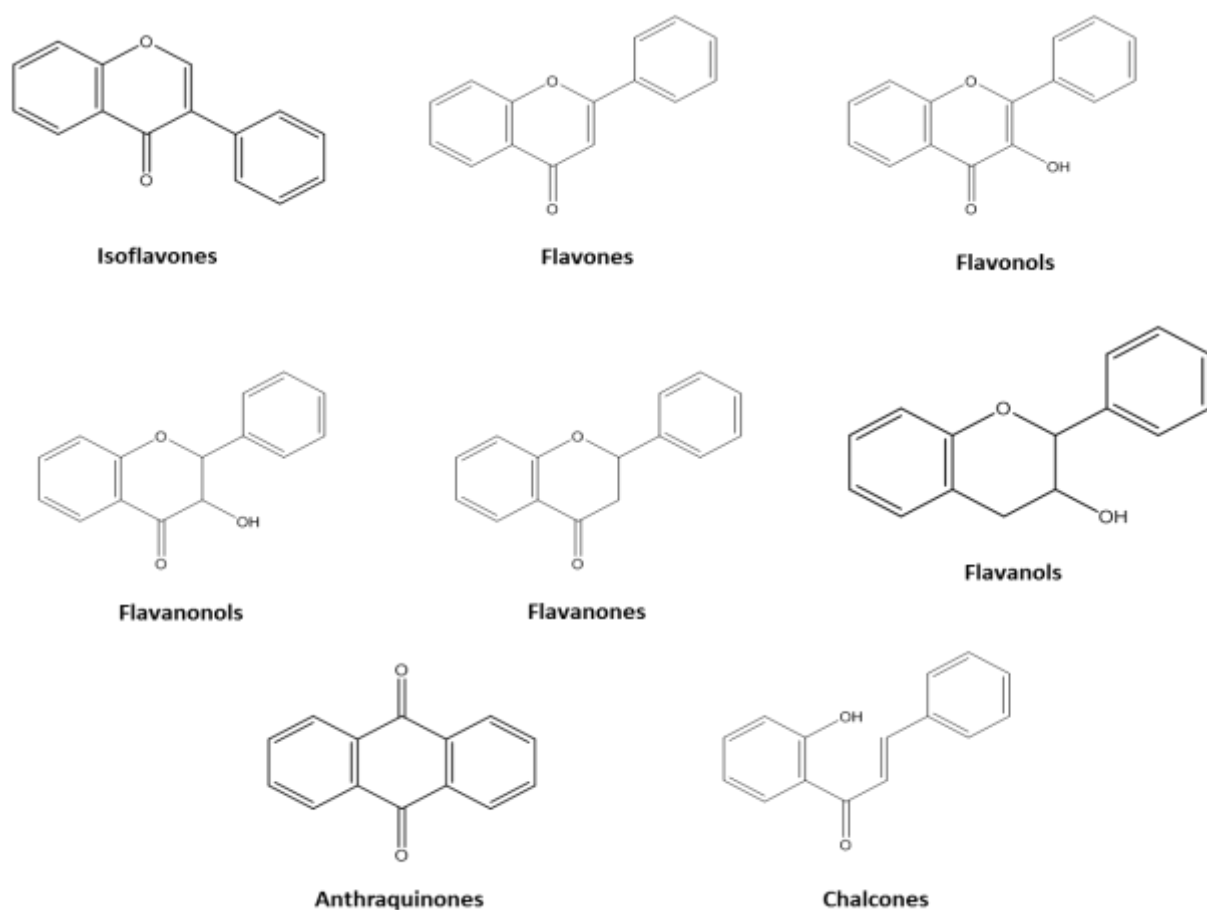
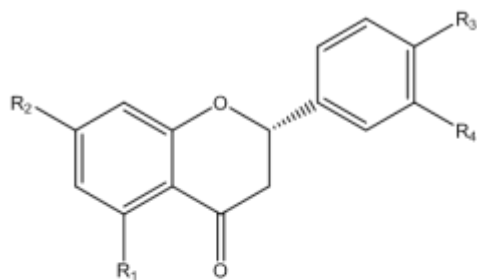
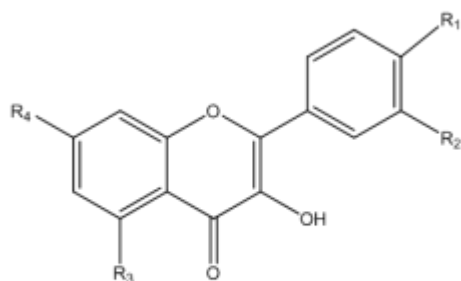


Figure 5: The general structures of flavonoids and other classes of compounds found in propolis.



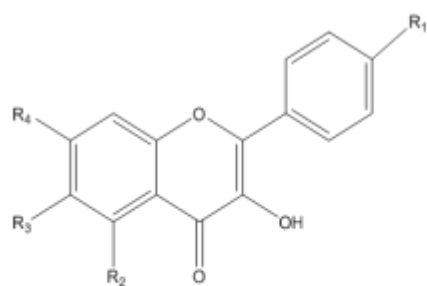
	R1	R2	R3	R4
Pinocembrin	OH	OH	H	H
Pinostrobin	OCH3	OH	H	H
Naringenin	OH	OH	OH	H
Sakuranetin	OCH3	OH	OH	H
Isosakuranetin	OH	OH	OCH3	OH
Liquiritigenin	H	OH	OH	H

Figure 6: Structure of the principal flavanones described in propolis



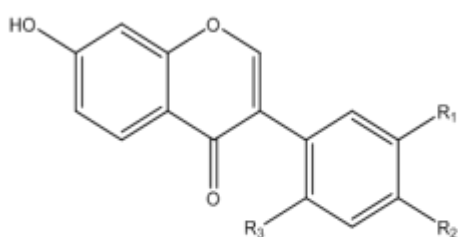
	R1	R2	R3	R4
Galangin	H	H	OH	OH
Kaempferol	OH	H	OH	OH
Quercetin	H	OH	OH	OH
Fisetin	H	H	H	OH
Izalpinin	H	H	OH	OCH3

Figure 7: Main flavonols described in propolis



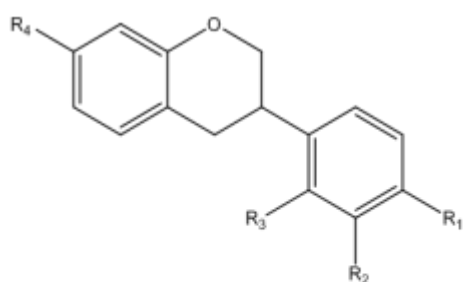
	R1	R2	R3	R4
Chrysin	H	OH	H	OH
Tectochrysin	H	OH	H	OCH3
Apigenin	OH	OH	H	OH
Acacetin	OCH3	OH	H	OH
Pectolinarigenin	OCH3	OH	OCH3	OH

Figure 8: Main Flavones described in propolis



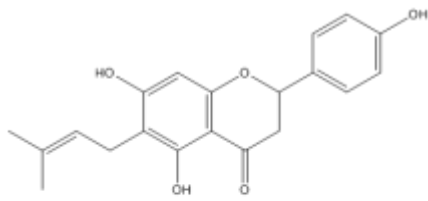
	R1	R2	R3
Daidzein	H	OH	H
Formononetin	H	OCH3	H
Calycosin	OH	OCH3	H
Xenognosin B	H	OCH3	OH

Figure 9: Isoflavones described in propolis

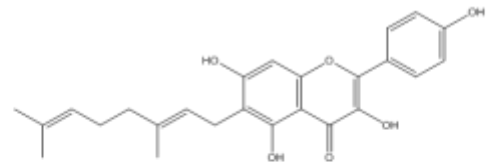


	R1	R2	R3	R4
Vestitol	OCH3	H	OH	OH
Neovestitol	OH	H	OH	OCH3
Mucronulatol	OCH3	OH	OCH3	OH

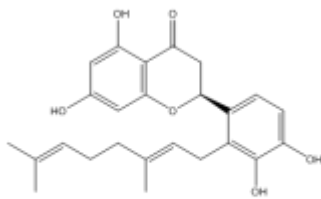
Figure 10: Main isoflavans described in propolis



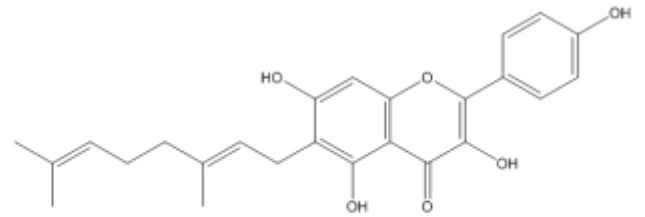
6-prenylnaringenin



8-prenylnaringenin



Propolin D



Macarangin

Figure 11: The structures of some prenylated flavonoids isolated from Nigerian red propolis (Omar et al, 2017)

1.4.4.2 Terpenoids

Propolis is made up of volatile terpenoids in a proportion of 10%. These compounds give propolis its characteristic resinous scent and help to differentiate real propolis from fake samples. The biological effects of propolis may owe much to terpenoids, which are categorised into monoterpenes (C₁₀), sesquiterpenes (C₁₅), diterpenes (C₂₀), and tetracyclic triterpenes (C₃₀). Monoterpenes consist of the subcategories of acyclic, monocyclic, bicyclic monoterpenes, and their derivatives. Sesquiterpenes are the dominant propolis compounds and are divided into acyclic, monocyclic, bicyclic and tricyclic, depending on how many rings they have.

The main diterpenes in propolis are cembrane, labdane, abietane, pimarane, and totarane structures, with evidence existing that some of these possess numerous pharmacological qualities. Last but not least, propolis contains the tetracyclic triterpenes lanostanes and cycloartane, and the pentacyclic triterpenes oleanane, ursane and lupane. Furthermore, Popova et al. reported that Egyptian and Brazilian propolis samples consisted of various diterpenes and triterpenes, including pimaric and abietic acids, oleanane and ursane, lupeol and cycloartenol (Popova et al., 2009). The above mentioned terpenes and others are illustrated in figure 12.

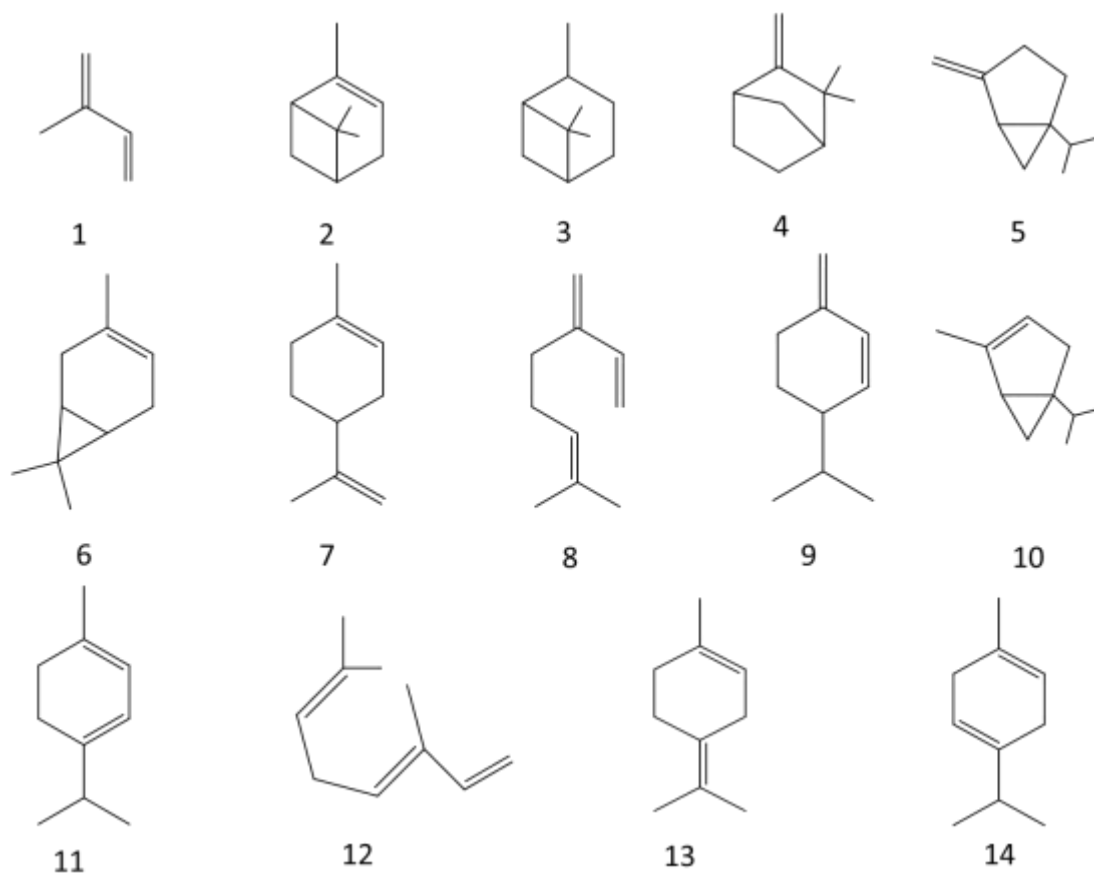


Figure 12: The structures of some classes of terpenes. 1 isoprene, 2 α -pinene, 3 β -pinene, 4 camphene, 5 sabinene, 6 δ -3-carene, 7 d-limonene, 8 myrcene, 9 β -phellandrene, 10 α -thujene, 11 α -terpinene, 12 ocimene, 13 terpinolene and 14 γ -terpinene

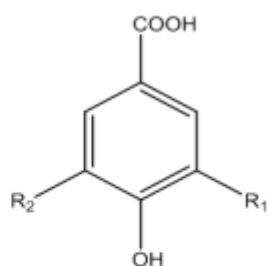
1.4.4.3 Phenolics and acids

Green propolis from Brazil was found to contain phenolics and acids such as cinnamic acid, p-coumaric acid, caffeic acid, ferulic acid and their derivatives, which manifest different biological effects (Salatino et al., 2005).

Plants rarely contain stilbenes, and in particular geranylated stilbenes. However, these were found to be present in propolis from Kenya and the Solomon Islands owing to the occurrence of *Macaranga* Sp. resins in it. Propolis from the Australian Kangaroo Island was found to contain prenylated stilbenes as well (Abu-Mellal et al., 2012).

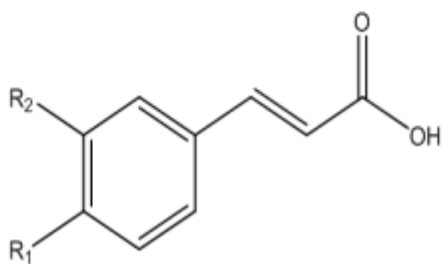
Propolis from tropical areas contain abundant lignans, which are categorised as phenolics. Present in propolis from Kenya and Brazil, lignans consist of compounds including phyllamricin C, tetrahydrojusticidin, and 6-methoxydiphyllin (Petrova et al., 2010).

It is of note that a discovery was made in 1997 that brown propolis from Cuba contained four additional distinctive polyisoprenylatedbenzophenone compounds, namely, propolone A, nemorosone, guttiferone E, and xanthochymol. A couple of years later, in 2005, further compounds from the same family were identified, namely, propolones B-D, alongside garcinielliptone I and hyperibone B. The resin from the flowers of *Clusia rosea* was identified as the origin of these compounds (Hernández et al., 2005). Some phenolics and acids are represented in figure 13.



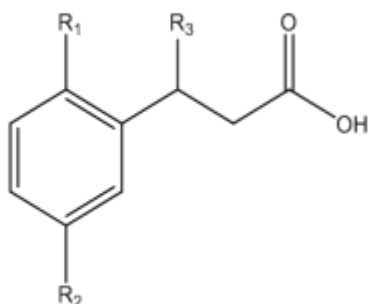
Benzoic acids

Acid	R1	R2
4-hydroxybenzoic	H	H
Protocatechuic	H	OH
Gallic	OH	OH
Vanillic	H	OCH3
Syringic	OCH3	OCH3



Cinnamic acids

Acid	R1	R2
Cinnamic acid	H	H
<i>p</i> -Coumaric acid	OH	H
Caffeic acid	OH	OH
Ferulic acid	OH	OCH3



Other acids

Acid	R1	R2	R3
Phenylacetic	H	H	H
Mandelic	H	H	OH
Homogentisic	OH	OH	H

Figure13: The Structures of the principal phenolic acids described in propolis

1.4.4.4 Sugars

Propolis was found to contain glucose, fructose and sucrose, but the source of these sugars (e.g. nectar and honey or hydrolysis of flavonoid glycosides) remains unknown. Propolis produced in the Canary Islands, Malta and Egypt was reported to contain numerous sugars, sugar alcohols and uronic acids, of which galactitol, gluconic acid, galacturonic acid and 2-O-glycerylgalactose were established for the first time to be present in propolis from Egypt (El Hady and Hegazi, 2002).

1.4.4.5 Hydrocarbons

A wide range of types of propolis, including propolis from Egypt, Brazil and Anatolia, were found to contain alkanes, alkenes, alkadienes, monoesters, diesters, aromatic esters, fatty acids and steroids. Furthermore, (Negri et al., 1998) provided evidence that the secretion of propolis waxes by bees was determined not by the plant source, but by the genetic structure of the bees.

1.4.4.6 Mineral elements

Propolis from Croatia and Argentina was reported to contain the elements calcium, potassium, magnesium, sodium, aluminium, boron, barium, chromium, iron, manganese, nickel, strontium, and zinc, as well as the toxic elements arsenic, cadmium, mercury, and lead. Cantarelli et al. suggested that these elements could serve as markers for profiling and classifying propolis based on where they are produced (Cantarelli et al., 2011).

1.4.4.7 Overview

There is significant variation in propolis chemistry, even in the same geographical area. However, in order to standardise propolis samples, it is not possible to rely solely on chemical composition; the quality of propolis also depends significantly on

biological properties. Although propolis was found to contain over 300 compounds, not all compounds are associated with biological effects. Hence, standardisation of propolis samples from different geographical areas with varying biological effects has not been achieved. To permit correlation between a specific chemical type of propolis and a specific biological effect and to put forth suggestions, further research is needed to attain standardisation of propolis types. One approach for matching chemical composition and biological effect is principle component analysis (PCA) or other statistical tools. A precise chemical standardisation that can confirm the quality, safety and efficacy of propolis is an unavoidable prerequisite for propolis to be approved for widespread use within healthcare.

1.4.5 Species of bees and propolis

Propolis chemistry and quality depend significantly on bee species, subspecies and varieties. There are ten species making up the genus *Apis*, and of these, the species most extensively researched and encountered throughout Europe, Africa and Asia is *Apis mellifera* (honeybee). The other species are found in Asia. There are around 25 subspecies of *A. mellifera*, differing morphometrically, behaviourally and biogeographically (Arias and Sheppard, 2005).

Meliponinae (Brazilian stingless bee) is also a key species that is found solely in tropical areas. *Melipona scutellaris* is the producer of propolis, which does not have as potent an antibacterial effect as the propolis produced by *A. mellifera* because it is abundant in benzophenones yet lacks flavonoids. Meanwhile, the propolis produced by *Melipona fasciculata* is rich in polyphenols, flavonoids, triterpenoids, saponins, as well as tannins (Dutra et al., 2014).

Different honeybee species do not have the same plant preferences, and even within the same species, propolis may have a different chemical profile. To give an example,

there are considerable differences between Brazilian green and red propolis, despite being both produced by Africanised *A. mellifera*; they respectively have an abundance of prenylated phenylpropanoids and isoflavonoids. The reason for the differences is that the materials for green propolis are derived from the *Baccharis dracunculifolia* plant, while the materials for red propolis are derived from the *Dalbergia ecastophyllum* plant. Hence, the plants preferred by the bees and the bee species and varieties are the main factors determining the propolis chemistry.

1.4.6 Biological effects of propolis

The medicinal properties of propolis have been exploited for a very long time. Around 300 BC, propolis began to be incorporated in traditional medicine, being used as an anti-inflammatory, for cosmetic reasons or to heal injuries (Banskota et al., 2001). Its purported antifungal, antibacterial, antiviral, anti-ulcer, anti-inflammatory and anaesthetic qualities have made it popular for both internal and external use (Banskota et al., 2001, Lotfy, 2006). Furthermore, propolis boosts immunity and is a hypotensive. There is also a long tradition of employing propolis products to stimulate body energy and support health (Rai et al., 2012). For over two millennia, Asian, Middle Eastern and European cultures have relied on propolis to destroy microbes and heal festering wounds like diabetic ulcers and bedsores.

Although there is evidence that propolis has effects against a number of Gram-positive and cocci rods, such as the human tubercle Bacillus (Lu et al., 2005), its effects against Gram -ve bacilli are not as strong (Lu et al., 2005, Banskota et al., 2001). *Escherichia coli*, *Salmonella enteric* and *Pseudomonas aeruginosa* are the most widely encountered Gram -ve bacteria, while the species *aureus* figures among the Gram +ve bacteria, the one with the highest sensitivity to propolis being *Staphylococcus aureus* (Rai et al., 2012). Propolis can help treat infections acquired in hospitals and within the community due to the mechanisms present in resins that

suppress bacterial growth. (Wojtyczka et al., 2013) highlighted that the different constituents of propolis interacting synergistically may be the basis for the demonstrated effects against bacteria. Furthermore, propolis has been proven to be useful in the prevention of oral ulcers and tooth decay, whilst also supporting the health of damaged teeth, which is why it has been used in dental and oral products (Wagh, 2013).

Evidence was provided by Salomao et al., (2008) that the chemical composition of propolis compounds was positively correlated with trypanocidal activity, and in particular some phenolic and prenylated derivatives, such as 3, 5-diprenyl-4-hydroxycinnamic acid 4 (DHCA4) and 2, 2-dimethyl-6-carboxyethenyl-2H-1-benzopyran (DCBEN). The compounds were deemed to be the propolis components with the most potent anti-trypanosomal effect. As revealed by findings of investigations on propolis effects on trypanosomes, parasitaemia was diminished by the trypanocidal active compounds (Salomao et al., 2008).

There is also evidence that tumour cells and tumours were prevented from growing in animals due to the cytotoxic effect of propolis and its components, with terpenes, flavonoids, and caffeic acid phenethyl esters being among the major active compounds (Lu et al., 2005, Wagh, 2013). Furthermore, (Banskota et al., 2001) indicated that cancer treatment could be made more cost-effective through the use of propolis extracts. Meanwhile, (Lu et al., 2005) reported that the tumour effects of cancer cells could be minimised through application of propolis components capable of eradicating such cells. Research has explored a wide range of phenolic compounds for their potential as chemopreventive substances, with current research focusing on the actual mechanisms underpinning the anti-cancer activity of these substances.

Propolis has also been shown to have activity against fungi, oxidants and parasites. Antioxidants are molecules that prevent radicals from damaging other molecules via oxidation. Propolis has significant promise as a preservative because it possesses such antioxidant activity, safeguarding other compounds from damage (Banskota et al., 2001). Furthermore, propolis can target fungi like *Candida albicans* owing to the antifungal activity of compounds such as caffeic acid, ferulic acid and cinnamic acid. In addition, propolis can serve as an effective treatment of parasitic diseases like leishmaniasis. However, propolis may irritate the mucous and skin membranes, resulting in allergic reactions (Shaw et al., 1997, Lotfy, 2006).

1.4.7 Antiprotozoal Activity of Propolis

Recent research has been primarily concerned with propolis's antiparasitic properties. This is due to the need to improve existing treatments for tropical diseases caused by protozoa. The effects of both raw propolis and of compounds isolated from propolis have been studied by means of various *in vivo* and *in vitro* experiments. The findings of these experiments suggest that propolis is effective against a number of parasitic species, including *Cholomonas paramecium*, *Eimeria magna*, *Media perforans*, *Giardia lamblia*, *Giardia duodenalis*, *Trichomonas vaginalis*, *Trypanosoma cruzi* and *Trypanosoma evansi* (Freitas et al., 2006, Falcão et al., 2014, Bogdanov and Bankova, 2012, Parreira et al., 2010). The effects of both propolis and its components have been demonstrated against a variety of protozoan parasites responsible for human diseases such as *Trypanosoma brucei*, responsible for sleeping sickness and *Trypanosoma cruzi*, responsible for Chagas disease (Higashi and De Castro, 1994, De Castro and Higashi, 1995, Marcucci et al., 2001, Dantas et al., 2006a, Dantas et al., 2006b, Salomão et al., 2010, Falcão et al., 2014).

1.4.7.1 Trypanosomiasis

Trypanosomiasis is an infectious, parasitic disease caused by protozoa. It is found primarily in the regions of Africa and South America. This is an insect-borne disease, with its protozoa, which belong to the trypanosoma genus, infecting humans via bites. Multiple types of trypanosomes exist, however, according to (Barrett et al., 2003), the only diseases of this type known to infect humans are sleeping sickness and Chagas disease. Furthermore, both of these diseases fall into the WHO's neglected tropical disease's category (Fairlamb, 2003). Three kinds of trypanosomiasis exist, of which two are sleeping sicknesses found in Africa. The infected tsetse fly, belonging to the Glusina genus, spreads the disease by biting humans. There are two stages to the development of the disease's symptoms in an infected patient. The first stage, known as the haemolympathic phase, occurs after infection. Symptoms such as fever, rashes, joint pain, fatigue and severe headaches are caused by the multiplication of the protozoa in the blood and lymphatic tissue. These symptoms may or may not present immediately after infection. The second stage is known as the neurological stage. Patients progress to this stage when the protozoa cross the blood-brain barrier and reach the patient's organs, including the central nervous system and heart. The symptoms produced by this include apathy, convulsions, loss of mental acuity, severe fatigue, tremors and eventually coma (Barrett et al., 2003).

1.4.7.2 African trypanosomiasis

According to (Lee and Maurice (1983) there are two types of sleeping sickness in Africa. The first is a chronic variant found in West Africa caused by *Trypanosoma brucei gambiense*. The second is an acute variant found in East Africa caused by *Trypanosoma brucei rhodesiense*.

1.4.7.3 American trypanosomiasis

According to (Rassi and de Rezende, 2012), Chagas disease, caused by *Trypanosomiasis cruzi*, is found in twenty-one countries in South America including Mexico and Argentina. It is spread by Reduviid bugs, which includes Assassin Bugs and Rhodnius. The initial symptoms of Chagas disease can appear quickly after infection, often within several hours. Lesions (chagomas) begin to appear at around the insect bite through which the infection was transmitted. Acute infections often lead to fever, vomiting, severe anaemia, muscle pain and loss of appetite, while chronic infections lead to megacolon, megaesophagus, neurological problems such as dementia and heart muscle damage (Rassi and de Rezende, 2012).

1.4.7.4 Treatments for Trypanosomiasis

Sleeping sickness is almost uniformly fatal regardless of its stage, in fact, in the past forty years, very few treatments have been attempted (Bouteille et al., 2003; Hoet et al., 2004). The treatment approach employed depends on its cause and on the stage the disease has progressed to; whether it is in the first, haemolympathic stage or the second, neurological stage (Barrett et al., 2007). Different drugs are used during the two stages of the disease. It is preferable for treatment to begin in the first stage as the drugs used are less harmful and less difficult to administer. According to the WHO (2013), if the disease has progressed to the second stage, only drugs that can cross the blood-brain barrier stand any chance of treating the disease. These drugs are therefore more toxic and administering them presents more difficulty. In terms of chemotherapy, treatment options are limited. Table 2 shows the two compounds that can be employed against sleeping sickness regardless of its stage. Pentamidine and Suramin can be used in the first stage of the disease. In the second stage of the disease, several drugs can be used. These are Eflornithine, which can only be used to treat *Trypanosoma brucei gambiense*, Melarsoprol, which can be used to treat *Trypanosoma brucei rhodesiense* and *Trypanosoma brucei gambiense*. Nifurtimox is

used to treat both Chagas disease and American Trypanosomiasis. It can be used in monotherapy or in combination with other drugs such as Eflornithine (Barrett et al., 2007).

Table 2: The available of trypanocidal drugs (Bouteille et al., 2003, Legros et al., 2002).

Drug	Activity	Stage of Disease	Route	First Marketed	Comments
Suramin	<i>T.b. rhodesiense</i> <i>T.b. gambiense</i>	Stage 1	I.V.	1922	Not recommended for <i>T. b. gambiense</i>
Pentamidine	<i>T. b. gambiense</i>	Stage 1	I.M.	1937	Treatment failures
Diminazene aceturate	<i>T. b. gambiense</i>	Stage 1	I.V.	1960	Veterinary use
Melarsoprol	<i>T. b. gambiense</i> <i>T.b. rhodesiense</i>	Stage 2	I.V.	1949	2 to 12% mortality rates, reactive encephalopathy, treatment failures
Eflornithine	<i>T. b. gambiense</i>	Stage 2	I.V.	1981	Difficult to administer Not effective against <i>T.b. rhodesiense</i>
Nifurtimox	<i>T. b. gambiense</i>	Stage 2	Per os (orally)	1960	Not approved for sleeping sickness Effects on <i>T. b. rhodesiense</i> unknown

1.5 Extraction and bulk extraction methods

Extraction or release of the natural products from the natural material must be undertaken before the products are isolated and purified. The purpose of the initial extraction is to acquire a primary extract from a small quantity of material within the context of a pharmacological research or to obtain insight into the chemical composition of the metabolites in the material. After identification of particular metabolites in the primary extract, a bulk extraction may be carried out to identify more metabolites (Seidel, 2012).

1.5.1 Plant material extraction

As matrices of great complexity, plants generate a multitude of secondary metabolites that differ in terms of functional groups and polarities. In conventional procedures, the extractant employed is water, but in more sophisticated extraction techniques, organic solvents with different polarities are usually employed in order to take advantage of the different solubilities of plant components. Plant metabolites are subjected to a range of processes of solvent extraction, such as maceration, solvent extraction facilitated by ultrasound, percolation, soxhlet extraction, pressurised solvent extraction, extraction under reflux, steam distillation, and acid-base extraction. The characteristics and quantity of material intended for extraction determines which technique is used. The challenges involved in transferring from initial to bulk scale must be taken into account if the quantities intended for extraction are sizable. Nevertheless, with every technique, organic solvent evaporation or freeze-drying in the case of water-based solution is necessary to derive dried crude extracts (Seidel, 2012).

1.5.2 Soxhlet extraction

Both initial and bulk extraction are regularly conducted via soxhlet extraction (Mulholland et al., 2010, Pfundstein et al., 2010), which is useful primarily due to the ongoing extraction of the material, meaning that the solvent containing solubilised

metabolites drains into the flask, new recondensed solvent is used, followed by re-extraction of the material in the thimble. Compared to maceration or percolation, soxhlet extraction is quicker and requires a smaller amount of solvent. On the downside, thermolabile compounds may be adversely affected and/or artefacts may form because of the continuous heating of the extract at the boiling point of the employed solvent (Seidel, 2012). The steps of the Soxhlet extraction are as follows: introduction of the plant material in powdered form into a cellulose thimble is carried out, followed covering it with cotton wool. The thimble is introduced into the thimble in the Soxhlet extraction chamber above a collecting flask with a round bottom and a small quantity of anti-bumping granules is added. Addition of an appropriate solvent into the Soxhlet chamber is carried out and following accumulation of a certain amount of solvent in the thimble, the solvent is siphoned to the flask below. A reflux condenser is connected to the soxhlet chamber and the collecting flask is placed in a heating mantle, followed by heating the setup under reflux.

1.6 Instrumental methods

1.6.1 Introduction

As previously mentioned, the complexity and variability of the composition of extracts of propolis and other natural products (plant) make it impossible to achieve the highest effectiveness from the raw material. Thus, separate compounds must be isolated through several processes, namely, elimination of inert materials through extraction with appropriate solvents, preservation of active compounds in fractions, and purified compound detection and biological assessment. Extracts of propolis and other natural products (plant) can be analysed and purified through a range of analytical methods, including simple conventional phytochemical methods (e.g. column chromatography), and more sophisticated spectrometric methods, such as high-performance liquid chromatography (HPLC) in association with various detectors like evaporative light scattering detector (ELSD), ultraviolet (UV), and high-

resolution mass spectrometry (HRMS) for constituent fractionation and isolation. Another popular method is nuclear magnetic resonance spectroscopy (NMR), which helps to gain insight into the structure of the isolated constituents.

The general purpose of all chromatographic methods is separation of compounds according to size, form or charge and their interaction with either a surface or stationary phase (Heftmann, 2004). The interplay between the analyte and the mobile and stationary phases (MP and SP, respectively) is the basis of the separation process, which is underpinned by component polarity and the manner in which the components are partitioned among the active sites on the two phases (Salituro and Dufresne, 1998). The physicochemical attributes of the compounds intended for separation (e.g. solubility, volatilities and ionizability) typically dictates the method selection. To achieve selectivity, either MP or SP or both are varied. The present study approached the detection or separation of compounds in the raw propolis extracts via a range of chromatographic methods.

1.6.2 High-resolution mass spectrometry

Natural products mixtures are usually dereplicated via the method of high-resolution mass spectrometry (HRMS) because it is widely available, precise, and highly sensitive, as well as allowing characterisation according to molecular weight, elemental composition and/or fragmentation patterns. The elements of LC-MS are an ion source, mass analyser, detector and computer (figure 14). After dissolution in a solvent with polar volatility, the sample is transported via a needle of high potential. The warm nitrogen flow causes evaporation of the MP, followed by production and transfer of the ions to the high vacuum area of the mass analyser, where they are separated according to their ratio of mass to charge (m/z). The detector gathers the generated data and transforms them into signals for display on a computer monitor.

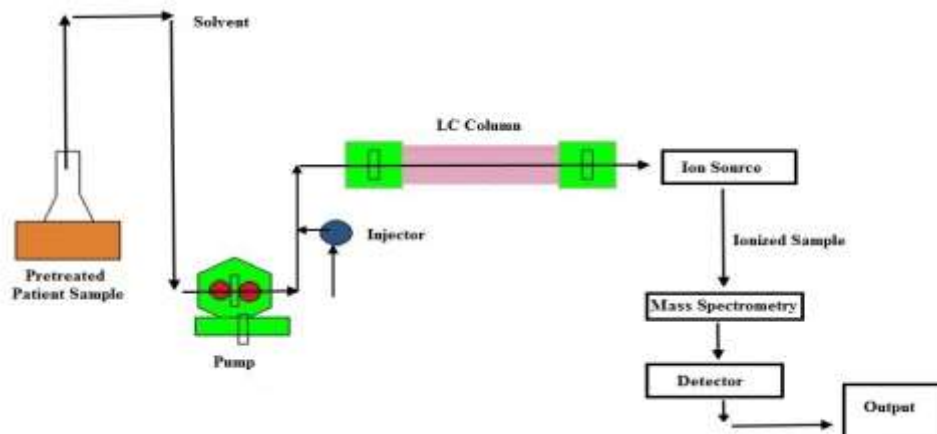


Figure 14: Schematic of the basic components of a mass spectrometer

www.thyrocare.com

1.6.2.1 Different ionisation methods are compatible with LC-MS:

1.6.2.1.1 Ionisation methods

There are two basic functioning mechanisms of the various ionisation methods. The first one is ionisation of a neutral molecule via electron ejection, electron capture, protonation, cationization, or deprotonation. The second one is transfer of a charged molecule from a condensed phase to the gas phase (Watson and Sparkman, 2007). There are a number of types of ionisation methods. Small molecules are usually profiled via atmospheric pressure ionisation (API) methods like electrospray ionisation (ESI) (Wilm, 2011), desorption electrospray ionisation (DESI), as well as atmospheric pressure chemical ionisation (APCI) (Matysiak et al., 2011) and atmospheric pressure photo ionisation (APPI). Fragmentation is minimal or completely absent in APCI and APPI, which exhibit such properties as robustness, tolerance to high buffer concentration, and compatibility with compounds that lack polarity and exhibit thermal stability, like lipids. Matrix-assisted laser

desorption/ionisation (MALDI), chemical ionisation (CI), and fast atom bombardment (FAB) are additional ionisation methods available for particular applications (Matysiak et al., 2011). Every one of the methods cited above is classified as a soft ionisation method, as opposed to electron ionisation (EI) (Watson, 2015), which can achieve analyte fragmentation and is therefore classified as a hard ionisation method.

Electrospray (ESI) can achieve ionisation of compounds across a broad mass range, which is why it is the preferred soft ionisation method. Its sensitivity varies between the picomole (10^{-12}) to the zeptomole (10^{-21}) level and it is compatible with compounds with higher polarity and molecular weight and lacking volatility. Furthermore, it is usable in both positive and negative mode, unlike other ionisation methods, like electron impact (EI) and chemical ionisation (CI). On the downside, ESI might cause signal inhibition due to its sensitivity to matrix effects like pH, solvent composition and salt concentration. The pattern of fragmentation is of great significance when determining structure and, post-ESI, fragmentation patterns are frequently produced via collision-induced dissociation (CID) MS/MS (Banerjee and Mazumdar, 2012).

1.6.2.1.2 Separation of ions and mass analysis

Various types of mass analysers are currently available commercially and include: magnetic sector instruments, single and triple quadrupoles (El-Aneed et al., 2009), time-of-flight (ToF) instruments (Watson, 2015), ion traps, Fourier transform ion cyclotron resonance (FT-ICR) spectrometers (Scigelova et al., 2011) and Orbitraps (Makarov and Scigelova, 2010).

1.6.3 HPLC with evaporative light scattering detection

The preferred detectors in modern HPLC (figure 15) are ultraviolet/visible (UV/VIS), which, alongside photodiode array (PDA), have facilitated the acquisition of spectra

for a natural product that is not known. Exhibiting extremely high sensitivity, UV/VIS detectors are capable of detecting various compounds, although they lack high specificity and are limited to compounds that contain chromophores. By contrast, a detector deemed to be universal is the evaporative light scattering detector (ELSD) (figure 16) (Young and Dolan, 2003; 2004), which can detect compounds without chromophores and with low UV absorption, including terpenoids, fatty acids and glycosides. Furthermore, the solvent has no impact on ELSD response, but it still should exhibit volatility and not contain any additives without volatility. ELSD is also advantageous because it can use mobile phases assimilating light at an identical wavelength with the compound(s) in question. Moreover, the linear response of ELSD allows its quantitative use across a broad spectrum of analyte concentrations, due to the direct proportionality between the amount of scattered light and the concentration of the compounds of interest in a sample.

ELSD has several limitations, such as the fact that it is a destructive method and sensitivity may diminish as the analyte becomes more volatile. The mechanism underpinning ELSD is MP evaporation and subsequent measurement of the light disseminated from analyte particles. Suspension of non-volatile analyte particles is achieved after nebulisation of the column effluent under a nitrogen gas flow and MP evaporation in a drift tube (Young and Dolan, 2003; 2004).

A photodetector placed at a constant angle in relation to the incident beam detects the light diffused by the particles.

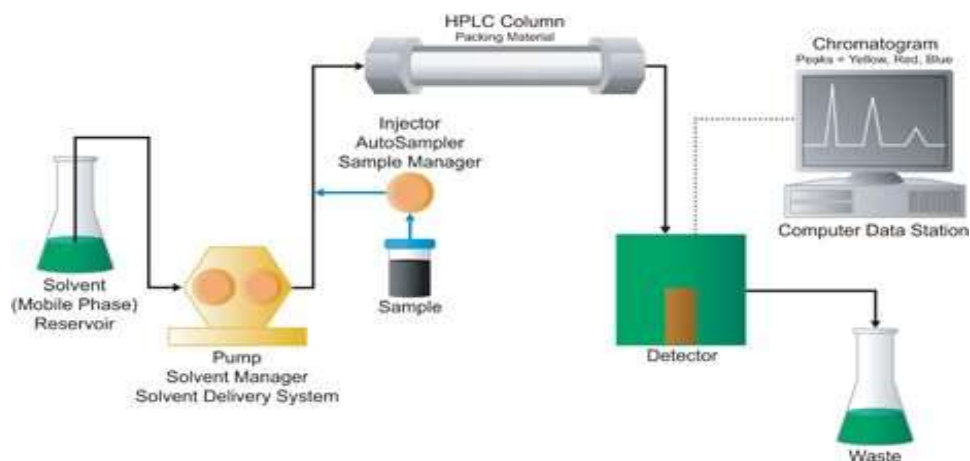


Figure 15: High Performance Liquid Chromatography System

www.waters.com

To enable detection of the majority of compounds irrespective of their nature, the HPLC system employed in this study was linked not only to UV (five channels) but also to an ELSD. It also aided assessment of purity and formulation of a strategy to purify raw extracts or fractions gathered from the open column chromatography prior to transfer to additional purifications (Young and Dolan, 2003).

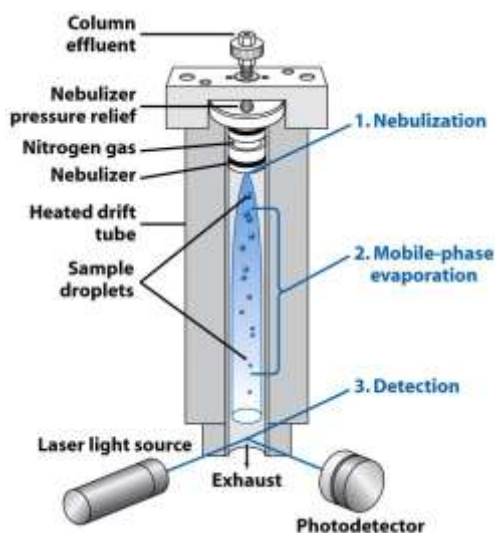


Figure 16: Commercial Evaporative Light Scattering Detector

www.quimica.udea.edu.co

1.6.4 Nuclear magnetic resonance techniques

The physical phenomenon of nuclear magnetic resonance (NMR) involves excitation of nuclei by a magnetic field, followed by measurement of the re-emitted electromagnetic radiation. The magnetic field strength and the magnetic attributes of the atom isotope determine the resonance frequency of the energy. Intrinsic magnetic moment, angular momentum and non-zero spin characterise every isotope consisting of an odd number of protons and/or neutrons. Meanwhile, zero spin characterises every nucleotide with even number of protons and neutrons (figure 17). ^1H and ^{13}C are the nuclei that have been the focus of most investigations.

No other method capable of concomitantly identifying compounds from different types of natural product has greater efficacy than NMR. The detectable compounds

comprise waxes, terpenoids and phenolics of varying polarity and with no restrictions associated with ionizability and chromophore specification. Besides identifying all compounds that contain spin-active nuclei, NMR also makes it easy to analyse organic compounds. Although it presents shortcomings in terms of resolution and sensitivity, where magnet power enhancement helps to address these. Phytochemical analysis relies greatly on NMR, especially for determining how chemical compounds are structured based on comparison between the attained NMR spectra and the spectra of standard samples or spectra from earlier studies. However, it is challenging to interpret the data generated from NMR, particularly in the case of non-pure propolis extracts and extracts of other natural materials. Hence, in order to produce relevant data for profiling and establishing a connection between propolis chemical composition and biological effects or geographical distribution, chemometric methods like principal component analysis (PCA) and partial least squares (PLS) have been recently employed (Stoyanova and Brown, 2001, Gavaghan et al., 2002).

One-dimensional ^1H and ^{13}C NMR spectroscopy were the methods employed in this study to identify pure compounds, which in turn permitted the obtained spectra to be compared with spectra reported in earlier studies. Furthermore, to ensure that proton and carbon chemical shifts were allocated correctly to new compounds or compounds that had not been characterised before, additional two-dimensional experiments were conducted when required.

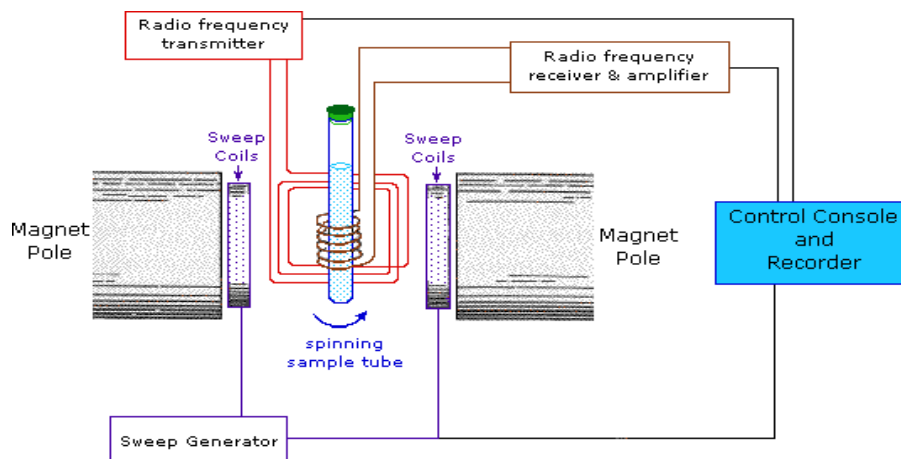


Figure 17: Nuclear magnetic resonance Spectroscopy

www2.chemistry.msu.edu

1.6.4.1 ^1H NMR

^1H NMR is informative about the chemical shifts of the protons existent in the molecule, their multiplicity (coupling information), as well as approximated numbers of protons from the integration. The method was conducted not only for every isolated compound, but also for raw extracts and fractions to help determine their structure. Furthermore, the acquired spectra were indicative of how pure the isolated compounds were (Breitmaier and Sinnema, 1993).

1.6.4.2 ^{13}C NMR

To determine how many and what kinds of carbons occur in an isolated compound, ^{13}C NMR can be carried out. Two types of spectra were derived by conducting this method in the present study, namely, broad band-decoupled or J -modulated. The former type involves irradiation of the ^1H nuclei during the ^{13}C acquisition, leading to complete decoupling of every proton from the ^{13}C nuclei. As a result, an individual singlet signal is generated by every ^{13}C environment in the molecule.

J-modulated spectra provide a differentiation between carbons based on the extent of their proton attachments (C, CH, CH₂ and CH₃). The information of CH signal multiplicity and spin–spin coupling is converted into a phase relationship by the pulse sequenced experiment of DEPT (Distortionless Enhancement by Polarisation Transfer) spectrum. Within a DEPT 135 spectrum, the direction of CH₃ and CH is towards the positive phase of the spectrum, whereas the direction of CH₂ is towards the negative phase. Compared to a traditional broad band-decoupled carbon spectrum, the DEPT 135 spectrum is more useful because it permits differentiation between C/CH₂ carbons and CH/CH₃ in a single experiment, as well as because its sensitivity is four times higher due to employing ¹H -¹³C polarisation transfer (Friebolin and Beconsall, 1993, Breitmaier and Sinnema, 1993).

1.6.4.3 Correlation spectroscopy

Correlation spectroscopy (COSY) is a two-dimensional experiment that is indicative of ¹H -¹H coupling in a molecule, enabling the determination of all coupling relationships in a single experiment based on an appropriate pulse sequence. The plotting of the proton shifts is done on both axes and the contour plot is along the square diagonal, with cross peaks indicating the relationships and the diagonal being equivalent to the ordinary ¹H spectrum. Hence, the cross peaks denote the spin-spin coupled protons. Germinal (²*J*) and vicinal (³*J*) protons make the relationships visible. Furthermore, a COSY spectrum reveals ⁴*J* and ⁵*J* couplings or allylic couplings as well (Breitmaier and Sinnema, 1993).

1.6.4.4 Heteronuclear single quantum correlation

One-bond (¹*J*) direct correlations are revealed by the two-dimensional ¹H -¹³C experiment of heteronuclear single quantum correlation (HSQC). Within an HSQC spectrum, the plotting of ¹H is along the abscissa, while ¹³C (or DEPT) is along the

ordinate, or the other way around. Protons and carbons with direct correlations between one another are denoted by cross peaks (Claridge, 2016).

1.6.4.5 Heteronuclear multiple bond correlation

Heteronuclear shift correlations based on long-range couplings ($^2J_{CH}$ and $^3J_{CH}$) are indicated by the spectra produced by heteronuclear multiple bond correlation (HMBC). The proton and carbon spectra are plotted along the two axes and the cross peaks indicate the correlations (Claridge, 2016, Breitmaier and Sinnema, 1993).

1.7 Aims and Objectives

The present study seeks to:

1-Employ high-resolution LC-MS, HPLC-ELSD and NMR profiling to analyse the chemical composition of Holy Basil (*Ocimum sanctum* L.) and a range of types of propolis from various geographical areas.

2-Applying suitable methods of extraction, purification and identification to isolate and identify compounds.

3-Elucidate the structures of the isolated compounds using one-dimensional and two-dimensional NMR as well as LC-MS.

4- Testing obtained compounds i.e. crudes, fractions and pures against trypanosome (*T. brucei* S427 WT strains) for a possible anti-parasitic activity.

5- Testing the concentrations that showed inhibitory activities for their possible toxic effects.

Chapter 2

Materials and General methods

2.1 Chemical and reagents

Sigma-Aldrich (Dorset, UK) was the provider of Davisil grade 633 amorphous precipitated silica pore size 60 A, mesh size 200–425 μm , Sephadex LH-20, *p*-Anisaldehyde, vanillin, sulphuric acid and deuterated solvents chloroform-d (CDCl_3) and dimethyl sulfoxide-d₆ (DMSO-d_6). Merck (Germany) was the provider of Davisil grade 636 column grade silica gel pore size 60 A, mesh size 35–60 μm , TLC grade silica gel (60H) and TLC silica gel 60 F254 pre-coated aluminium sheet. Fisher Scientific (Loughborough, UK) was the provider of anti-bumping granules and the HPLC grade solvents ethyl acetate, methanol, acetonitrile, n-hexane, and absolute ethanol. A MilliQ water filter was employed to obtain the water in-house. Other materials were obtained as following: Alamar blue® BUF 012B (AbD Serotec®, UK). HMI-9 medium (Invitrogen, UK). RPMI-1640 (Lonza, Verviers, Belgium), L-glutamine (Life Tech, Paisley, UK), Penicillin/Streptomycin (Life Tech, Paisley, UK), Foetal bovine serum (FBS) (Sigma-Aldrich, Dorset, UK), U937 cell cultures (obtained from ECACC, Porton Down, Salisbury), 96-well plates (Corning®, Sigma-Aldrich), Plate reader (Perkin Elmer-Wallac).

2.2 Laboratory equipment and instruments

Fisher Scientific (Loughborough, UK) provided of the syringes and Acrodisc filters, rotary evaporator (Buchi, Switzerland), ultrasonic Bath, Erlenmeyer flasks, beakers, and vials (Scientific Laboratory Supplies, Ltd), while Sigma-Aldrich (Dorset, UK) was the provider of the Gilson automatic pipettes (Anachem, UK) and NMR tubes (5mm, 300 MHz, 187 mm L) (Norell, USA). Rotaflo (UK) provided the glass columns for column chromatography, while Quickfit (UK) provided the Soxhlet apparatus. UVP (US) was the provider of the UV-Lamp 254 nm and 364 nm UVGL-58, and IKA® Werke GmbH & Co. KG (Staufen im Breisgau, Germany) provided the IKA® Grinder.

2.3 Plant material

Professor Alexander Gray from the Strathclyde Institute of Pharmacy and Biomedical Sciences at Strathclyde University supplied the plant material *Ocimum sanctum* Labiatae in June 2015. To prevent chemical deterioration of heat-labile compounds, drying of the material was conducted at under 30°C and without exposure to sunlight.

2.4 Collection and preparation of the propolis sample

Once the approval of Dr Sultan Almutairi was obtained, the sample of Saudi propolis was collected in the summer of 2016 from the Rihal Alma'a village in the Assir region in the south-west of Saudi Arabia. Mr James Fearnley undertook the collection of red propolis samples from Nigeria and Brazil, and a sample from the Philippines was provided by Nicola Bradbear from Bees for Development. The storage of the samples was at room temperature, away from light and humidity, until the research process was commenced. Apart from the samples from Nigeria and Brazil, which were red coloured, the other samples were dark brown in colour and sticky.

2.5 Methods

2.5.1 Extraction of *Ocimum sanctum*

Powdered *Ocimum sanctum* was placed in a soxhlet extraction apparatus and solvents of increasing polarity (n-hexane, ethyl acetate, and methanol) were used to extract *Ocimum sanctum* L. over a period of 2-4 days with every solvent or until the solvents became transparent in the Soxhlet chamber.

Filter paper was used for the filtration of the extracts, and a rotary evaporator was then used to concentrate the extracts by evaporation under reduced pressure at 40°C. Various chemical analyses were carried out on the three distinct crude sample extracts.

2.5.2 Propolis sample extraction

In the context of the processing of raw propolis samples, the key procedure is effective extraction. In a scientific study of propolis, Sforcin and Bankova suggested that the raw propolis sample should be macroscopically observed as a first step for removal of impurities (e.g. pollen, wood, dead bees) from the sample prior to extract preparation (Sforcin and Bankova, 2011).

2.5.2.1 Propolis extraction for LC-MS profiling

A mortar and pestle were employed to fragment the samples of propolis. For profiling, 5 ml of ethanol was used for extraction of 50 mg of every sample thrice via sonication for 180 minutes. A syringe filter (Acrodisc 0.45 μm) was employed for filtering the samples, and a nitrogen flow was used for drying the filtered solution. The weight of the empty vial was subtracted from the overall weight to determine the residue quantity.

2.5.2.2 Propolis extraction for fractionation and purification

An appropriate quantity of absolute ethanol (100 ml/g) was used for extraction of a particular quantity of every raw propolis sample via sonication for one hour. An appropriate quantity of ethanol was subsequently used to filter and re-extract the extract two times, with subsequent filtering every time. After the extracts were merged together, a rotary evaporator was used to evaporate and dry the solvent, followed by weighing. A small quantity of ethyl acetate was employed to re-dissolve the residue in the flask, followed by sonication to stimulate the dissolution of the residue. The extracted solution was poured into empty weighed vials with suitable labelling, which were then stored in the fridge. Various chemical analyses were conducted on ethanolic extracts of each crude propolis samples.

2.6 Plant and propolis purification procedures

2.6.1 Analytical and chromatographic methods

Isolation and purification of compounds from the crude extracts were achieved in the present study by employing several traditional and modern chromatographic methods, as described below.

2.6.1.1 Thin layer chromatography

Selection of a suitable solvent system for additional chromatographic techniques, including column chromatography (CC), gel filtration chromatography (GF) and preparative thin layer chromatography (PTLC), was based on thin layer chromatography (TLC). For purposes of identification and monitoring of compounds via the separation processes, TLC was applied on normal phase pre-coated silica gel 60 aluminium plates. A suitable solvent was used for dissolution of every sample (crude extract, fractions, and pure compounds), which was then applied as a spot or thin line on the silica, around 1-2 cm on top of the plate base (origin). The plate was introduced in a tank made of glass and containing an adequate solvent mixture at such a level to wet only the inferior plate margin. Furthermore, to help saturate the TLC chamber with solvent vapours, a filter paper was earlier inserted into the tank. The plate was taken out when the solvent was around 1 cm underneath the plate top, and a pencil line was made to mark the solvent front. After air-drying the developed TLC plate, detection of the spots was undertaken in the following way:

2.6.1.1.1 UV light-based detection

A non-destructive ultraviolet detection was employed for the initial inspection of the plates. Observation of the spots was done under UV light at λ 254 nm or at λ 366 nm. In the first case, the quenching fluorescence of a fluorescent indicator in the silica gel made the spots appear as dark bands on a green background, while in the other

case, the spots manifested as coloured bands. A pencil outline was made to indicate the visible bands.

2.6.1.1.2 Spray reagent-based detection

Chemical reagents like *p*-anisaldehyde-sulphuric acid or vanillin-sulphuric acid (VAS) were used to spray the TLC plates, which were subsequently heated at 120°C with a hand-held heater to stimulate the colours to develop. This was followed by determination of the R_f values, which made it possible to aggregate fractions with comparable profiles for spectroscopic analysis.

2.6.1.1.2 Modified anisaldehyde-sulphuric acid reagent

0.5 ml of *p*-anisaldehyde was combined with a mixture of glacial acetic acid (10 ml) and methanol (85 ml), followed by slow addition of 5 ml of concentrated (97%) sulphuric acid (Waldi, 1965).

2.6.1.1.3 Vanillin-sulphuric acid reagent

80 ml of absolute ethanol was used to dissolve 1 g of vanillin, after which 20 ml of concentrated (97%) sulphuric acid was added slowly (Waldi, 1965).

2.6.1.2 Vacuum liquid chromatography

2.6.1.2.1 The method of vacuum liquid chromatography employed for plant samples

To quickly fractionate the crude extracts (Reid and Sarker, 2006) the chromatographic method employed involved dry-packing of a straight-sided sintered glass Büchner funnel (13 × 10 cm) with TLC grade silica (silica gel 60H) under vacuum applied through a water vacuum pump. A non-polar solvent was permitted to go through the column under vacuum in order to assess the column consistency.

A small quantity of a suitable solvent was used for the dissolution of plant samples, followed by their adsorption on a small quantity of silica gel 60 (CC-grade silica gel). After drying, the silica gel with the adsorbed sample was moved to the top of the column bed in the form of a narrow layer. Solvents in ascending order of polarity (n-hexane, n-hexane/EtOAc and EtOAc/MeOH) were used to perform elution. Every time during vacuum application, every solvent system was added in a particular quantity until column drying was achieved. A vacuum flask was used to manually collect the fractions and a rotary evaporator was used to evaporate them until dry. TLC was conducted to inspect the fractions so that they could be combined based on their similarities (Coll and Bowden, 1986).

2.6.1.3 Column chromatography

A widely employed and effective purification technique that enables isolation and collection of compounds from a crude extract or fractions separately is the traditional system of column chromatography (CC).

2.6.1.3.1 The CC method employed for plant samples

Compounds from crude extracts or simpler mixtures/fractions can be separated through CC, the underlying procedure consisting of the following steps: plugging of a glass column of varying size with cotton wool and packing it by two-thirds with a slurry of silica gel 60 in the system with lowest polarity, which is typically n-hexane; permitting the solvent to pass through the column to leave a packed silica gel bed; dissolving the sample in the smallest quantity possible of an appropriate solvent, followed by pre-adsorption on silica gel 60 and drying in a fume cupboard prior to being loaded on the column top; preventing distortion by applying a cotton plug to the top; performing elution with different mobile phases consisting of polar/non-polar solvents of different ratios of growing polarity (addition of a particular amount of each

solvent system every time); and analysing the acquired fractions through TLC to combine them based on chemical profile similarities (Megalla, 1983).

2.6.1.3.2 The CC method employed for propolis

Silica gel 60 with a mesh size of 200–425 μm was used for performance of CC. The wet packing method was adopted for packing the column, with approximately 50 g of silica slurry and the solvent with the lowest polarity (i.e. hexane) being mixed before pouring and packing in a suitably sized glass column e.g. (55 x 3 cm). Air bubbles were eliminated by tapping the column. Excess solvent was permitted to pass through and the column was allowed to settle down. The smallest amount of solvent (ethyl acetate) was used to dissolve an amount of propolis extract, which was then mixed with coarse silica and dried under a vacuum hood. This was followed by the loading of the dried extract on the column top. Disruption of interface between the sample and solvent during solvent application was avoided by covering the sample with a small quantity of coarse silica or cotton wool (Haddad, 1996). This was followed by sequential performance of elution with each solvent system consisting of polar and non-polar solvents in different proportions, with addition of a particular amount of each solvent system every time. A rotatory evaporator was used to collect and concentrate the fractions, which were then aggregated via HPLC-UV-ELSD analysis based on similar chemical profiles.

2.6.1.4 Size-exclusion chromatography

Size-exclusion chromatography (SEC) or gel filtration chromatography divides molecules based on their size and form as the solute phase and the stationary phase interact minimally or not at all. Initially, the molecules of largest size undergo elution from the column, after which the molecules of smaller size undergo elution and usually spread into the porous gel particles. Preparation of a slurry of Sephadex LH-

20 involved overnight suspension of the stationary phase in 50:50 dichloromethane/methanol for non-polar fractions and in 100% methanol for polar fractions. This slurry was then used to pack a 2 x 100 cm glass column covered with cotton wool. After the settling of the packed bed and the solvent level exceeded the top of the bed, a Pasteur pipette was used for cautious application of the sample intended for fractionation following dissolution in the minimal quantity possible of the solvent employed for column packing. Elution was commenced and completed with 100 % MeOH in an isocratic manner and small vials of around 1 ml were used for collection of the fractions (Kremmer and Boross, 1979).

2.6.1.5 Preparative thin layer chromatography

Separation and purification of fractions with simple mixtures can be achieved via preparative thin layer chromatography (PTLC). To establish the ideal solvent system for effectively conducting separation. A larger sample amount was subsequently separated with larger TLC plates (20 x 20 cm). The smallest amount possible of a suitable solvent was used for dissolution of the samples and a Pasteur pipette was afterwards used to apply the dissolved samples 2 cm from the bottom as a thin band over the whole plate width. The development of the plates was carried out as described in the section on TLC. UV light permitted visualisation of the plates, with the invisible ones being sprayed at one side with an appropriate reagent, and the notable bands were cut into strips together with the absorbent. To enhance recovery as much as possible, the strips associated with each individual constituent were cut into small fragments and the sample was desorbed with a polar solvent overnight.

2.7 Structure elucidation

2.7.1 Nuclear magnetic resonance

To determine the structure, the method that is usually adopted is nuclear magnetic resonance (NMR). To identify what compounds were present in the fractions and

determine how pure compounds were structured, both one- and two-dimensional experiments were carried out. The acquisition of the NMR data was made possible by a JEOL (JNM LA400) spectrometer (400 MHz) at SIPBS and by Bruker Avance 300 (400MHz) spectrometer at the Department of Pure and Applied Chemistry, with the internal standard being tetramethylsilane (TMS). According to how soluble the compounds were, preparation of the sample solutions involved the use of deuterated solvents like CDCl₃ and DMSO- d₆ which have residual proton shifts and carbon shifts shown in table 3.

Table 3: Deuterated solvents used for NMR analysis

Solvent	Chemical Formula	¹ H shift(s) in ppm	¹³ C shift(s) in ppm
Deuterated chloroform	CDCl ₃	7.27	77.2
Deuterated dimethyl sulfoxide- d ₆	(CD ₃) ₂ SO	2.5	39.5

(Gottlieb et al., 1997).

500-600 µl of a suitable solvent was used for the dissolution of 10 mg of every sample, which was then poured into a typical 5 x 178 mm NMR tube to a depth of around 4 cm. MestReNova software 8.1.2 (Mestrelab Research, A Coruña, Spain) was employed for the processing of the NMR spectroscopic data, while the structures of the compounds were illustrated with ChemBioDraw Ultra, Version 14 (PerkinElmer, Yokohama, Japan).

2.7.1.1 One-dimensional NMR experiments

To determine what kind of constituents were present in a sample or to determine how pure a sample was, a one-dimensional (1D) ¹H NMR experiment was conducted. This experiment is indicative not only about how many and what kind of protons occur in a molecule, based on chemical shifts and integration, but also about proton

multiplicity (coupling constant) to provide some information about neighbouring protons. Furthermore, the relative molar ratio of the constituents of a mixture can be established via ^1H NMR as well. Meanwhile, the 1D ^{13}C NMR experiment is indicative of what type and how many carbon atoms are in a molecule. Types of carbon atoms can be distinguished based on their proton attachment via the experiment of Distortionless Enhancement through Polarisation Transfer (DEPTq-135). The CH_3 and CH carbon atoms issue signals in one direction, whereas the CH_2 and quaternary carbons issue signals in the opposite direction.

2.7.1.2 Two-dimensional NMR experiments

To ensure that the allocations of the proton and carbon chemical shifts were precise and to determine the relative stereochemistry, additional two-dimensional (2D) experiments were conducted. In order to find out how adjacent protons were correlated, the correlation spectroscopy (COSY) experiment was carried out, with cross peaks with a symmetrical arrangement along the diagonal being indicative of the ^1H - ^1H correlations associated with germinal (2J) and vicinal (3J) coupling. Furthermore, the 1J ^1H - ^{13}C correlations were determined via the ^1H -detected Heteronuclear Single Quantum Coherence (HSQC) experiment, and the ^1H - ^{13}C correlations were identified based on the Heteronuclear Multiple Bond Coherence (HMBC) experiment through long-range couplings ($^3J_{\text{CH}}$ and $^2J_{\text{CH}}$).

2.7.2 Mass spectrometry

Mass spectrometry (MS) supplies useful structural data, including the molecular weight and molecular formula of the examined compounds, and thus it is complementary to NMR spectroscopy. In this study, crude samples and purified compounds were prepared at 1 mg/ml in HPLC grade methanol before conducting analysis with LC-MS. A reverse phase $5\mu\text{m}$ C18 column (4.6 x 150 mm) (Hypersil,

Thermo) was used and the performance of elution was carried out by using the gradient shown in table 4 at a flow rate of 0.3 ml/min, with 0.1% v/v formic acid in water and 0.1% v/v formic acid in acetonitrile being the two solvents (A and B) making up the mobile phase.

The ESI interface in negative ionisation permitted identification of [M-1]⁻. The spray voltage for the capillary and cone was respectively -4.0 kV and 35 V. The flow rate of the sheath gas and auxiliary gas was respectively 50 and 15 arbitrary units. Ion transfer capillary had a temperature of 275°C and m/z 100-1500 provided the full-scan data. The sample data were acquired and processed with the Xcalibur software (Thermo Fisher Corporation, Hemel Hempstead, UK).

Table 4: Mobile phase system used in mass spectroscopy experiments

No.	Time (min)	A (%) aqueous phase (0.1% v/v formic acid in water)	B (%) organic phase (0.1% v/v formic acid in acetonitrile)	Flow ml/min
1	0	75	25	0.3
2	10	50	50	0.3
3	20	50	50	0.3
4	35	20	80	0.3
5	45	20	80	0.3
6	46	0	100	0.3
7	60	0	100	0.3
8	61	75	25	0.3
9	70	75	25	0.3
		100	0	0.3

2.7.3 HPLC-UV-ELSD

A 1 mg/ml solution was produced for every sample dried under nitrogen in 1 ml of the initial composition of the mobile phase LC gradient. A reverse phase 5 μ m C18 column (4.6 x 150 mm) (Hypersil, Thermo) was employed for separation purposes, with water and acetonitrile being the two solvents (A and B) in the mobile phase. The gradient elution programme was the same as that shown in table 4. An Agilent 1100 system (Agilent Technologies, Germany) consisting of a quaternary pump, a diode array UV detector (set to monitor 290 and 320 nm wavelengths), and an ELSD (SEDEX75 SEDERE, France) constituted the used HPLC-UV-ELSD equipment. Data were collected and processed with the Clarity software (Data Apex).

2.7.4 Optical rotation

Mr Gavin Bain undertook the measurement of the optical rotation (OR) of certain isolated compounds with a 341 polarimeter at the Department of Pure and Applied Chemistry of Strathclyde University. Methanol was the solvent used to dissolve the compounds and prepare different concentrations to generate 2 ml test solutions in volumetric flasks. An average of ten machine readings was created and the equation applied to determine the OR was

$$[\alpha]_D^T = \frac{100 \times \alpha}{l \times c}$$

with the average of the measured rotation (α) and the path length (dm) respectively denoted by α and l , the solution concentration (g/100 ml) and the measurement temperature (20°C) respectively denoted by c and T , and the wavelength ($D = 589$ nm) given by λ .

2.8 Cell culture and medium preparation

The U937 cells (a human monocytes cell line), were cultured in the RPMI 1640 medium (500 ml) which was supplemented with 1% penicillin and streptomycin (v/v), 1% L-glutamine (v/v) and 5% FCS (v/v). Cells were sub-cultured every 2-4 days and maintained at 37 °C in a humidified atmosphere of 5% CO₂.

2.8.1 Cell viability assay

U937 cells were seeded at 1×10^5 cells/ml in 96-well plates, cells were counted manually using a haemocytometer under a microscope. 100 µl/well of the cells were added and the plate incubated for 24 hours at 37°C, 5% CO₂, 100% humidity. The samples (the crude, fractions and the purified compounds) were prepared in 8 different concentrations in another 96 well plate for the purpose of not disturbing the cells during mixing since U937 are a suspension cell line. The highest concentration started from 200 µg/ml and a serial 1:2 dilution was carried out reduced by half until 1.56 µg/ml (n = 3). The samples were then transferred (100 µl) to the cultured cells using a multichannel pipette and left in the incubator for 24 h. 10% (v/v) DMSO were added to serve as a positive control (to kill the cells completely). While cells with medium were used as a negative control and 0.5% (v/v) DMSO (the solvent concentration in the samples) were tested as well.

The plate was then incubated at 37 °C and 5% CO₂ in a humidified atmosphere for 24 hrs. After incubation, the resazurin indicator (Alamar blue) was added at a final concentration of 10% and the plate incubated for a further 24 hours. Fluorescence readings of the plate were taken using a Wallac Victor 2 microplate reader (λEx/EM: 560/590 nm). Cell viability was then calculated for each well as a percentage of fluorescence readings in the presence of test sample relative to the value of the

negative controls. The resulting data were analyzed with GraphPad Prism 5 to obtain dose-response curves for each sample and their corresponding mean inhibitory concentration (IC₅₀) values.

2.8.2 Anti-trypanosomal assay in-vitro

Crude extracts, fractions, and isolated compounds were testing against the blood stream form of wild-type *Trypanosoma brucei brucei* (S427) in vitro. *Trypanosoma brucei brucei*, type strain Lister 427 were cultured as described by (Yang et al., 2015). Anti-trypanosomal tests were carried out by using an Alamar blue assay according to a standard protocol, as described in (Ráz *et al.*, 1997). This assay is based on viable cells metabolizing the blue resazurin dye to resorufin, which is pink and fluorescent. It was performed using stock solutions of the samples prepared with a concentration of 20 mg/ml in 100% DMSO and *Trypanosoma brucei* S427 at the seeding density of 2×10^5 cells. The assays were performed using (1:1) serial dilution of test compounds in Hirumi's Modified Iscove's medium 9 (HMI-9), where, 100 μ L of each compound or fraction was doubling diluted over one row in the 96-wells plate, (starting from 200 μ g/ml as the top concentration until 0.19 μ g/ml) ensuring an optimally defined 50% Effective Concentration (EC₅₀) after plotting of the reading to a sigmoid curve with variable slope by using GraphPad Prism software. A 100 μ L of trypanosome suspension was eventually added to each well plate followed by an incubation period of 48 hours at 37 °C in a 5% CO₂ humidified incubator, before the addition of the resazurin dye and a further incubation of 24 hours under the same conditions. Fluorescence was determined in a FLUOstar Optima (BMG Labtech) at wavelengths of 544 nm and 620 nm for excitation and emission, respectively.

Results and discussion

Chapter 3

Chemical profiling, extraction, purification, isolation and elucidation

of *Ocimum sanctum Labiatae*

3 Phytochemical results for *Ocimum sanctum Labiatae*

3.1 Introduction

Ocimum sanctum L. belongs to family Labiatae. It is an odoriferous small annual herb growing into a low shrub of about 18 inches in height. It is commonly known as Holy Basil, Tulsi or Tulasi (Pattanayak et al., 2010). *Ocimum sanctum* L. (Tulsi), *Ocimum gratissimum* (Ram Tulsi), *Ocimum canum* (Dulal Tulsi), *Ocimum basilicum* (Ban Tulsi), *Ocimum kilimandscharicum*, *Ocimum ammericanum*, *Ocimum camphora* and *Ocimum micranthum* are important species of the genus *Ocimum* and they grow in various places around the world and are known to have medicinal properties (Gupta et al., 2002, Sen, 1993, Prakash and Gupta, 2005).

3.2 Solvent Extraction and Yields

A Soxhlet apparatus was employed to sequentially apply solvents of growing polarity (n-hexane, ethyl acetate, and methanol) to ground dried *Ocimum sanctum* L. Table 5 indicates what was obtained from the crude extracts.

Table 5: weights of *Ocimum sanctum* L. extracts

Weight of plant material (g)	n-Hexane extract g	EtOAc extract g	MeOH extract g
402 g	13.65 g	6.78 g	42.84 g

The methods employed to undertake chemical profiling included NMR and high-performance liquid chromatography (HPLC) together with high-resolution mass spectrometry (HRMS). An understanding of the composition of the crude extracts was thus gained. In order to establish the major features of the constituents, 10 mg extract sample was subjected to preliminary NMR analysis (figure 18), followed by implementation of LC-MS for performance of LCMS profiling (table 6, figure 19).

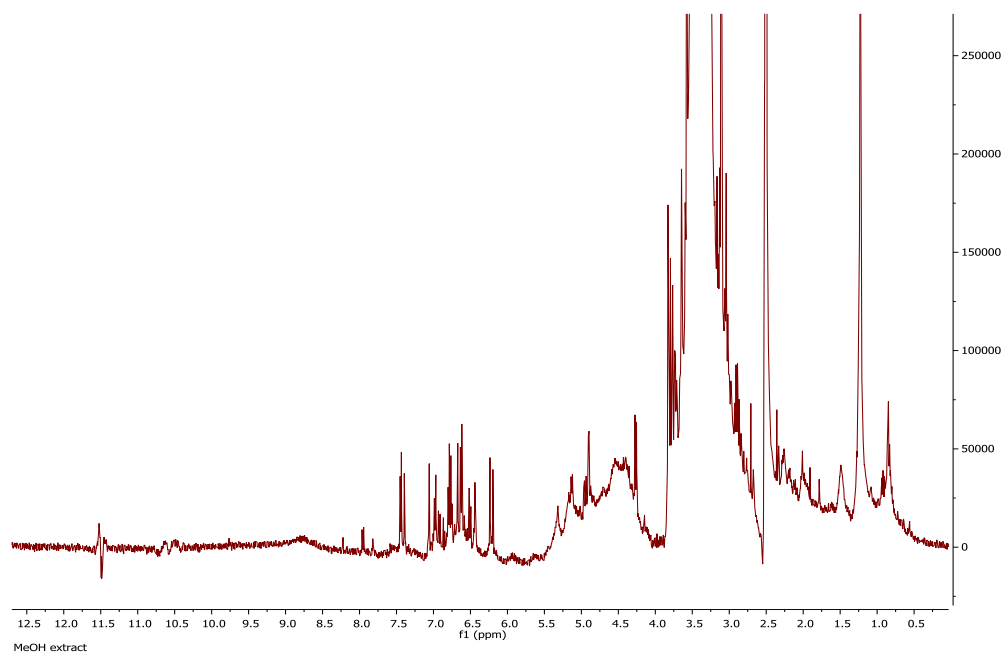


Figure 18: ^1H (400 MHz) NMR spectrum of MeOH extract in DMSO-d_6 . The main constituents highlighted by ^1H NMR spectrum were flavonoids and phenolics, while terpenoids and fatty acids of lesser intensity compared to flavonoids and phenolics were detected as well. MeOH extract was observed to contain aromatic compounds, this was shown by several signals from 6 to 8 ppm as well as phenolic hydroxyl group between 10-13 ppm.

Table 6: The LC-MS profiling for MeOH extract when analysed by reversed phase LC-MS in negative ion mode

Peak NO	Retention time (min)	[M-1]	Chemical formula	Delta (ppm)	Intensity
1	4.91	290.08	C ₈ H ₁₈ O ₁₁	-4.997	E 7
2	6.85	461.07	C ₂₈ H ₁₃ O ₇	-1.119	E 6
3	9.24	359.07	C ₂₅ H ₁₁ O ₃	1.483	E 7
4	11.44	232.08	C ₆ H ₁₆ O ₉	-3.922	E 6
5	11.44	408.11	C ₁₉ H ₂₀ O ₁₀	1.213	E 6
6	14.14	316.94	C ₉ HO ₁₃	3.555	E 6
7	14.14	459.09	C ₂₉ H ₁₅ O ₆	-1.158	E 6
8	17.21	373.09	C ₂₆ H ₁₃ O ₃	0.784	E 7
9	18.94	327.22	C ₁₈ H ₃₁ O ₅	-0.145	E 6
10	19.43	285.04	C ₁₅ H ₁₉ O ₆	-0.32	E 7
11	19.43	577.27	C ₃₀ H ₄₁ O ₁₁	4.876	E 7
12	20.44	269.04	C ₁₅ H ₉ O ₅	-2.106	E 6
13	20.44	329.23	C ₁₈ H ₃₃ O ₅	-1.602	E 6
14	21.14	461.07	C ₂₁ H ₁₇ O ₁₂	-3.1885	E 5
15	21.45	555.28	C ₂₈ H ₄₃ O ₁₁	3.268	E 7
16	25.23	313.07	C ₁₇ H ₁₃ O ₆	-1.122	E 6
17	25.23	359.08	C ₁₈ H ₁₅ O ₈	0.754	E 6
18	35.86	285.04	C ₁₅ H ₉ O ₆	-0.952	E 6
19	41.49	325.14	C ₂₀ H ₂₁ O ₄	-1.514	E 6
20	41.49	559.31	C ₂₈ H ₄₇ O ₁₁	-1.762	E 6
21	58.51	455.35	C ₃₀ H ₄₇ O ₃	-1.029	E 5

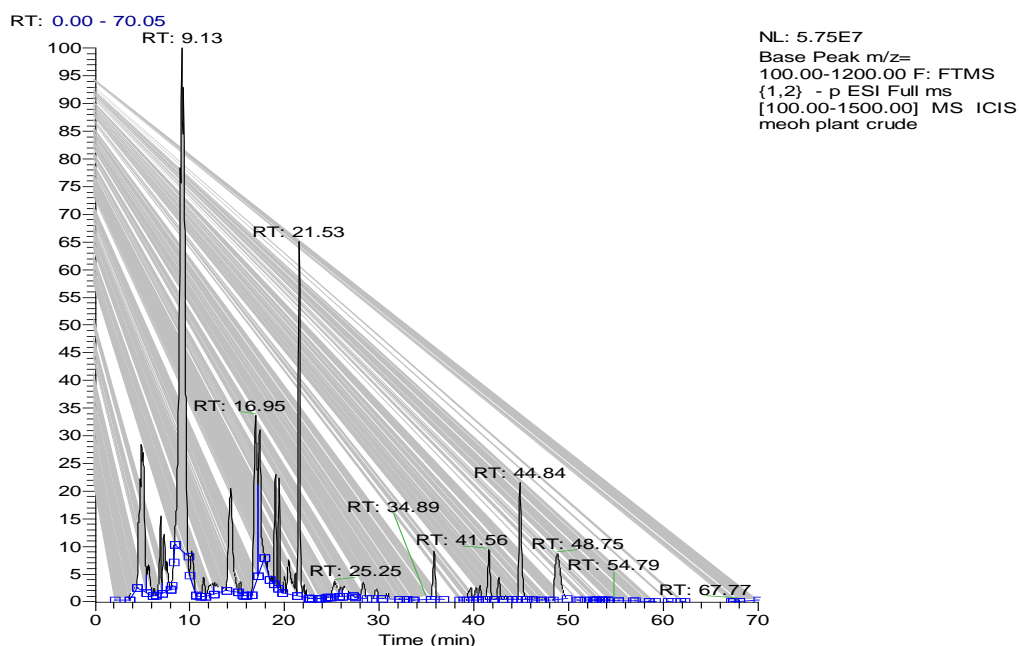


Figure 19: Chromatogram view of MeOH extract on the LC-MS negative ion mode (-ve ESI)

Multiple peaks of greater or lesser intensity showed up on the complex LC-MS chromatogram of the crude sample. Table (6) and figure (19) indicate that terpenoids and flavonoids were distinguished by LC-MS analysis as the key constituents of the crude MeOH extract. Meanwhile, the main constituents highlighted by the ^1H NMR spectra were flavonoids and other phenolics (figure 18). Furthermore, terpenoids and fatty acid compounds of lesser intensity compared to flavonoids and other phenolics were identified based on several signals produced by carrying out NMR analysis on the crude sample.

Since the mixture in a crude plant extract is complex, more than one separation method may be necessary to obtain one pure compound from the crude extract. As such, the crude extract frequently has to be fractionated into multiple separate fractions that contain compounds with comparable polarities or molecular sizes. To

this end, the fractions produced should not be too many, as it may lead to the excessive stretching of the compound in question across numerous fractions so that the compound may not be identified in those fractions if its concentration is not high enough or bioassays in isolation procedures based on bioassay may not pick up any activity (Sarker and Nahar, 2012). Given these considerations, VLC was used to originally fractionate 23.10 g of MeOH extract. Gradient solvent systems were used for elution of the column (table 7), followed by performance of TLC and ¹H NMR experiments to examine the acquired and combined fractions.

Table 7: A step gradient elution technique used for separation of the MeOH extract by VLC

Fraction	1	2	3	4	5	6	7	8	9	10
He (ml)	100	80	60	40	20	0	0	0	0	0
EtOAc (ml)	0	20	40	60	80	100	80	60	40	20
MeOH (ml)	0	0	0	0	0	0	20	40	60	80

Note: the minimum quantity of the mobile phase used in each step is 500ml

To be able to conduct additional chromatographic analysis, the chemical constituent must be available in a quantity that is large enough, due to the fact that chemical analysis relies significantly on the mass of a fraction. Hence, column chromatography was performed on 5.5 g of fraction four He: EtOAc (40:60) and elution was sequentially performed based on a gradient profile (table 8). The total number of acquired fractions was 145, and these were inserted in 15-30 ml vials. Chromatographic characteristics were distinguished via TLC, in combination with a suitable solvent system. Furthermore, performance of LC-MS and NMR permitted

identification of the different components and combined fractions. Eventually, eight fractions were left after combining similar fractions.

Table 8: Sequence of Column Chromatography Solvent Systems and fractions collected

No.	He %	EtOAc %	MeOH %	M.P (ml)	Fractions obtained	Weight (mg)
1	80	20	0	500-1000	1 to18 fraction (M-1)	90 mg
2	60	40	0	500-1000	19 to 33 fraction (M-2)	215 mg
3	40	60	0	500-1000	34 to 65 fraction (M-3)	450 mg
4	20	80	0	500-1000	66 to 84 fraction (M-4)	170 mg
5	0	100	0	500-1000	85 to 102 fraction (M-5)	90 mg
6	0	70	30	500-1000	103 to 115 fraction (M-6)	55 mg
7	0	50	50	500-1000	116 to 131 fraction (M-7)	75 mg
8	0	30	70	500-1000	132 to 145 fraction (M-8)	40 mg

Given that isolation is like extraction, the aspect that must be taken into account prior to selection of the isolation procedure is the nature of the compound(s) of interest occurring in the crude extracts or fractions, especially with regard to solubility (hydrophobicity or hydrophilicity), acid–base properties, charge, stability, and molecular size (Sarker et al., 2005). In this study, 450 mg of fraction (M-3) from CC was subjected to size-exclusion chromatography, yielding 35 sub-fractions (M-3-1 to M-3-35) and two pure compounds (M-3-9 and M-3-21). Furthermore, given that two compounds occurred in fraction (M-1), separation and purification was undertaken with PTLC based on a suitable mobile phase Hexane: EtOAc (80:20). A single pure compound was derived from this process (M-1-1).

3.3 Characterisation of M-3-21 as rosmarinic acid

Following several chromatographic methods, including VLC and CC, SEC was applied and yielded M-3-21 from the MeOH extract of *Ocimum sanctum* L., taking the form of a red-orange solid. Spraying with *p*-anisaldehyde-sulphuric acid reagent and subsequent heating caused it to manifest as a purple spot on TLC. Elution with the mobile phase 50% HE in EtOAc gave a R_f of 0.55 on SiGel.

The molecular formula C₁₈H₁₅O₈ was established based on the fact that the molecular ion [M-H]⁻ was indicated by the negative mode HRESI-MS spectrum at *m/z* 359.08 (figure 20). Furthermore, +36° was the optical rotation (*c* = 0.1, MeOH).

The proton spectrum of the compound (400 MHz, DMSO-d₆, figure 21, table 9) gave two sets of aromatic ABX protons between δ_H 6.55 and 7.01 ppm indicating the presence of two aromatic ring systems. It also showed trans-coupled protons on a double bond and three sets of aliphatic protons including an oxymethine proton at δ_H 4.98 ppm. The ¹³C spectrum (100 MHz) gave signals for 18 carbon atoms in the compound. These were made up of six aromatic CH, two aromatic quaternary and four phenolic carbons. The rest were two carbonyl carbons (one carboxylic acid at δ_C 172.98 and an unsaturated ester carbonyl at δ_C 166.91), two ethylenic carbons at δ_C 114.22 and 143.03 ppm, one methylene at δ_C 36.25 and one oxymethine carbon at δ_C 74.55. Analysis of its 2D NMR spectra including COSY, HMBC and HSQC confirmed the structure of the compound as follows: Correlations (³J) in the HMBC from the proton at 7.43 and 4.98 to the ester carbonyl at 166.91 indicated they had an ester linkage and other correlations to separate aromatic rings indicated they were three bonds away from the aromatic rings. Further analysis of the 2D spectra enabled

the assignments of the chemical shifts for the carbon atoms and protons in the compound. The NMR data obtained were in agreement with previous reports for rosmarinic acid (Lu and Foo, 1999).

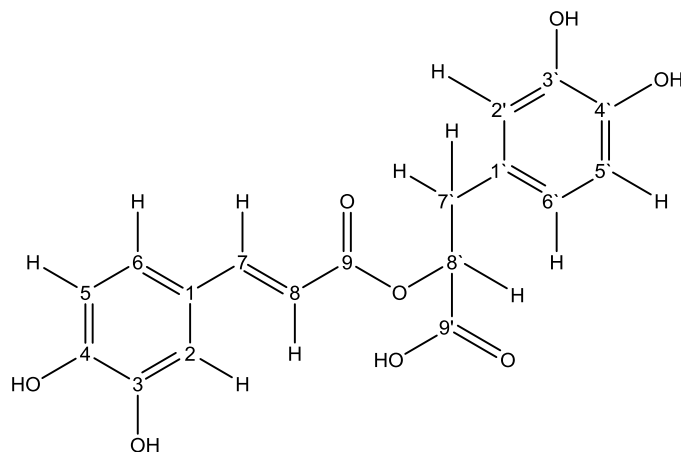


Figure 20: Structure of rosmarinic acid

Table 9: ^1H (400 MHz) and ^{13}C (100 MHz) NMR data of rosmarinic acid (M-3-21) in DMSO-d_6

Experimental Data		
Position	^1H (multiplicity), J (Hz)	^{13}C (multiplicity)
1		125.64
2	7.05 (d, $J=2.15$)	115.82
3		144.94
4		147.83
5	6.77 (d, $J=8.14$)	116.54
6	6.99 (dd, $J=8.19, 2.14$)	122.03
7	7.43 (d, $J=15.86$)	143.03
8	6.22 (d, $J=15.89$)	114.22
9		166.91
1'		128.79
2'	6.68 (d, $J=2.06$)	115.37
3'		145.5
4'		144.14
5'	6.63 (d, $J=7.71$)	113.8
6'	6.52 (dd, $J=8.06, 2.11$)	120.46
7' a	2.86 (dd, $J=14.38, 9.08$)	36.25
7' b	2.99 (d, $J=3.73$)	36.25
8'	4.98 (dd, $J=9.03, 3.84$)	74.55
9'		172.98

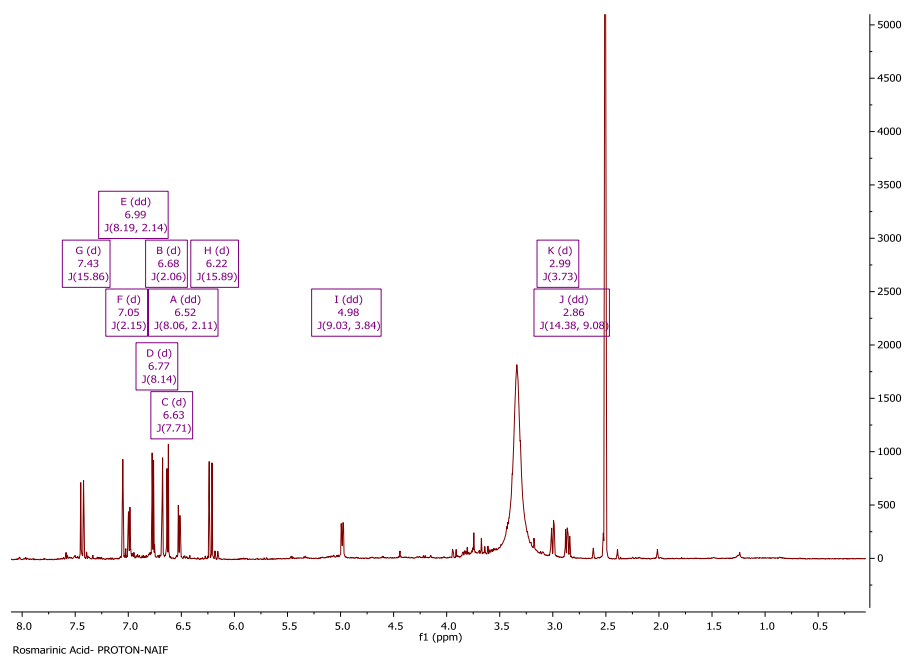


Figure 21: ¹H NMR spectrum (400 MHz) of rosmarinic acid (M-3-21) in DMSO-d₆

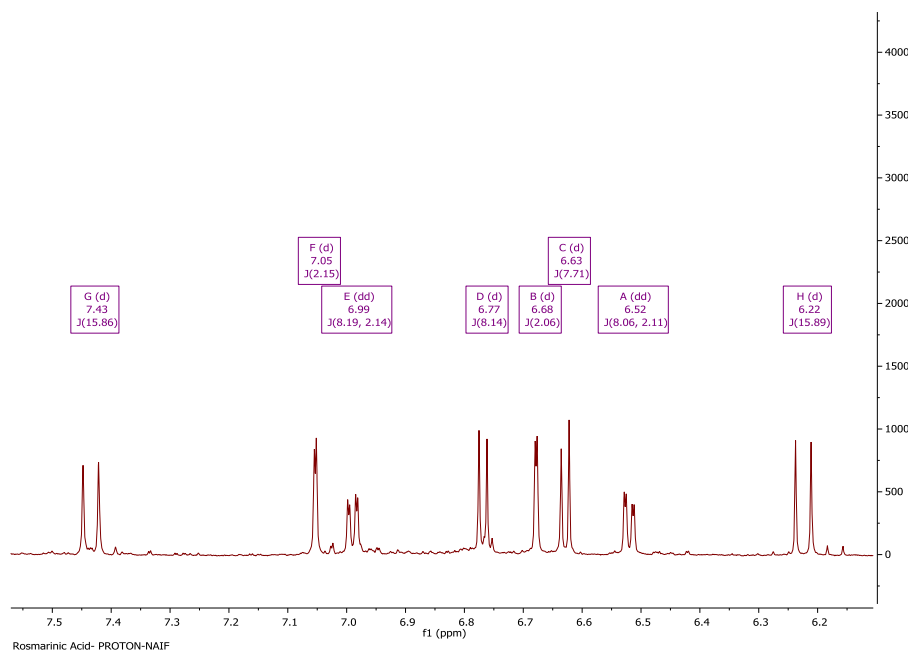


Figure 22: Selected ¹H expansion for the aromatic region of rosmarinic acid (M-3-21)

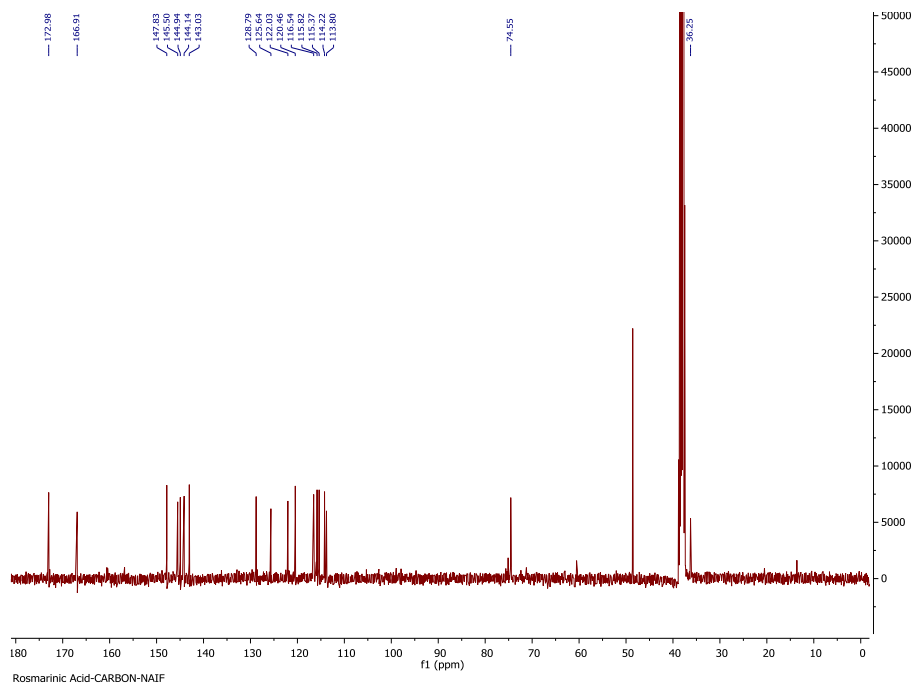


Figure 23: ^{13}C NMR spectrum (100 MHz) of rosmarinic acid (M-3-21) in DMSO-d_6

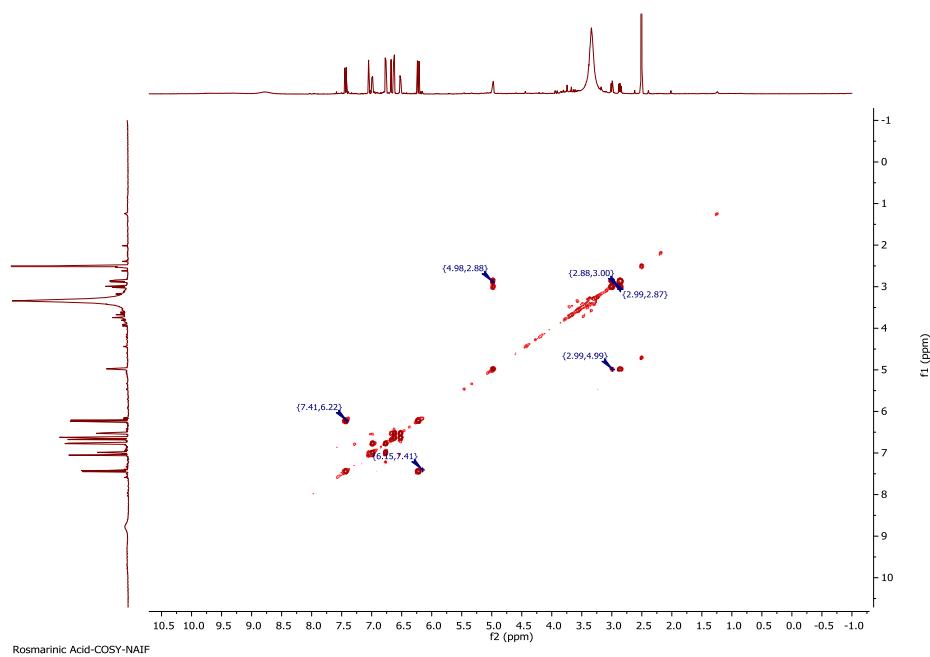


Figure 24: COSY spectrum (400 MHz) of rosmarinic acid (M-3-21) in DMSO-d_6

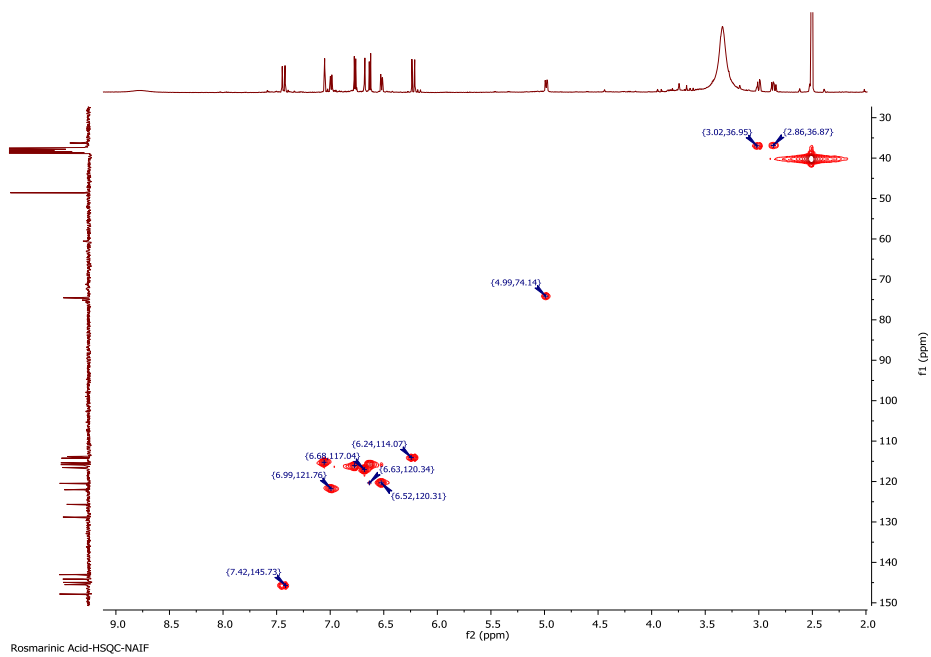


Figure 25: HSQC spectrum (400 MHz) of rosmarinic acid (M-3-21) in DMSO-d₆

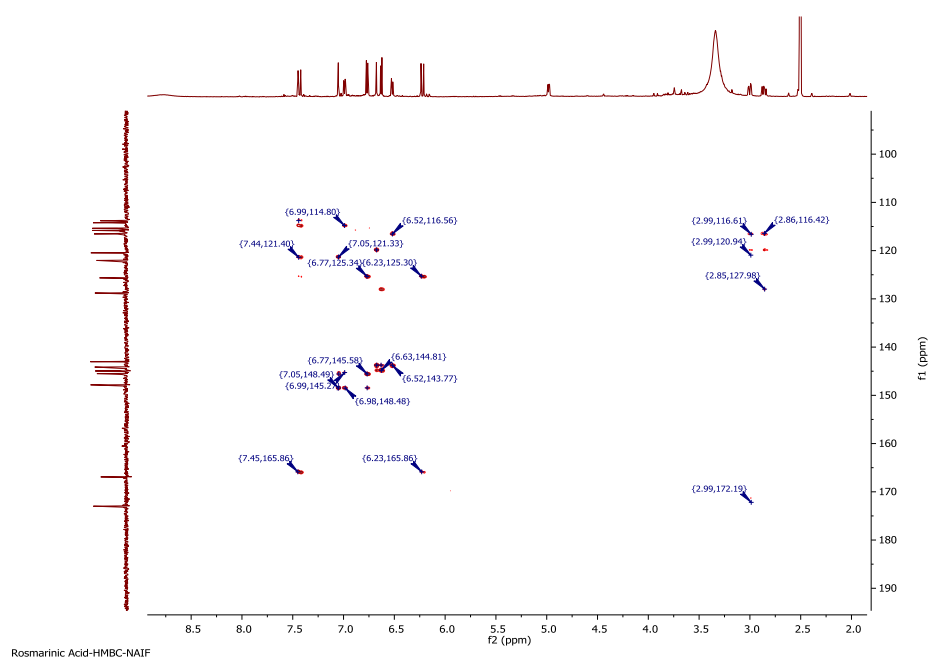


Figure 26: HMBC spectrum (400 MHz) of rosmarinic acid (M-3-21) in DMSO-d₆

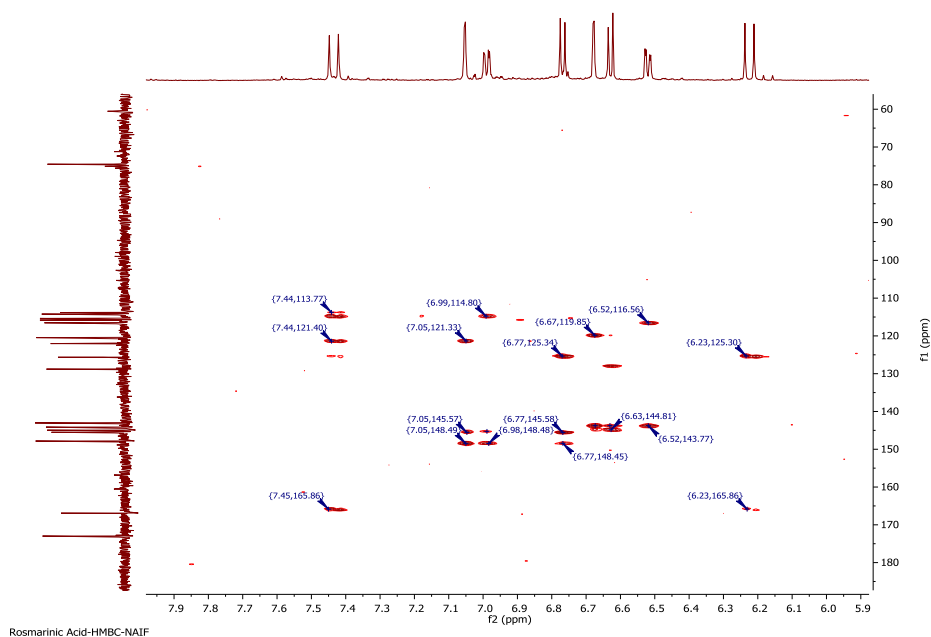


Figure 27: Selected HMBC expansion for the aromatic region of rosmarinic acid (M-3-21)

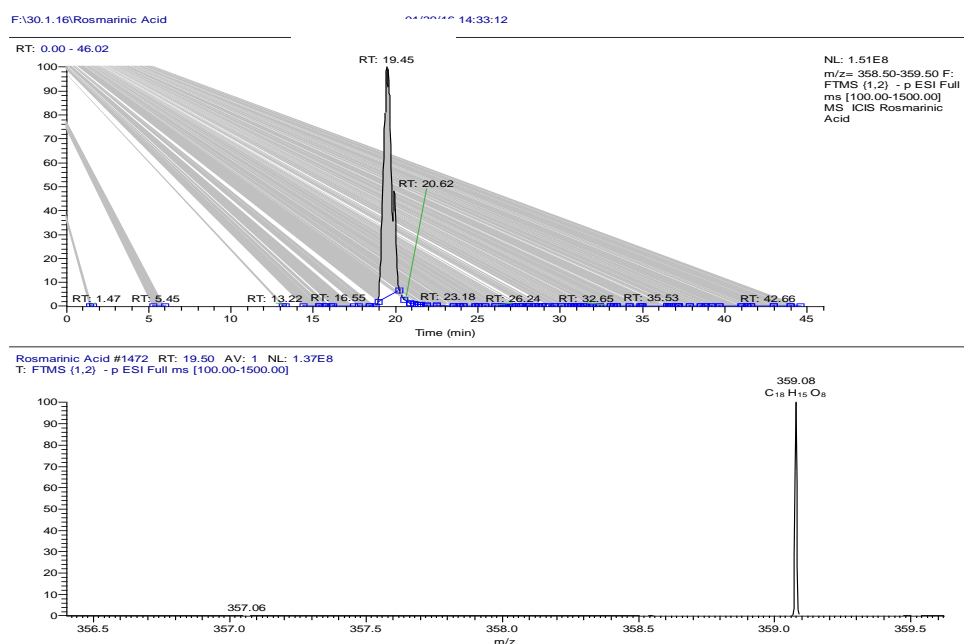


Figure 28: (A) Extracted ion chromatogram corresponding to the mass of rosmarinic acid in the negative ion mode (ve ESI) whereas (B) shows the spectrum corresponding to the rosmarinic acid chromatogram

3.4 Characterization of M-3-9 as luteolin-7-O-glucuronide

Following several chromatographic methods, including VLC and CC, SEC was applied and yielded M-3-9 from the MeOH extract of *Ocimum sanctum* L., taking the form of a yellow solid. Spraying with *p*-anisaldehyde-sulphuric acid reagent and subsequent heating caused it to manifest as a yellow spot on TLC. Elution with the mobile phase 50% HE in EtOAc gave a R_f of 0.56 on SiGel.

The molecular formula C₂₁H₁₇O₁₂ was established based on the fact that the molecular ion [M-H]⁻ was indicated by the negative mode HRESI-MS spectrum at *m/z* 461.07 (figure 29). Furthermore, the optical rotation was -69° (*c* = 0.1, MeOH).

The proton spectrum of the compound (400 MHz, DMSO-d₆, figure 30, table 10) indicated that the A- ring has two protons at δ_H 6.41 (1H, d, 2.13Hz) and 6.77 (1H, d, 2.19Hz) as H-6 and H-8 protons, respectively and ring C has just a proton singlet at δ_H 6.70 (1H, *s*). However, the B ring has three protons at δ_H 7.43 (1H, d, 2.37Hz), 6.86 (1H, d, 8.43Hz) and 7.38 (1H, dd 2.30, 8.37Hz) as H-2', H-5' and H-6' respectively. There is a glycoside sugar attached at carbon 163.39 (C-7) in ring A, this sugar (ring D) contains five protons at 5.08 (1H, d, 7.52Hz), 3.27 (1H, dd, 8.92, 7.55Hz), 3.32 (1H, t, 8.76Hz), 3.20 (1H, dd, 9.97, 8.49Hz) and 3.63 (1H, d, 9.97Hz) as H-1'', H-2'', H-3'', H-4'' and H-5'' respectively.

The ¹³C NMR spectrum gave signals for 21 carbon atoms in the compound. These were made up of six aromatic CH, seven aromatic quaternary and six phenolic carbons. The rest were two carbonyl carbons at δ_C 172.49 (C-6'') and 182.27 (C-4).

Analysis of its 2D NMR spectra including COSY, HMBC and HSQC confirmed the structure of the compound as follows: both protons at δ_H 6.41 (H-6) and δ_H 6.77 (H-8) in the ring A illustrated ³*J* correlations to the same quaternary carbon at δ_C 105.67 (C-10), (H-8) presented a ²*J* coupling to a carbon at δ_C 161.42 (C-9). The proton at δ_H 7.38 (H-6') in the ring B

indicated 3J correlations to the quaternary carbon at δ_c 151.14 (C-3') and 2J correlations to the carbon at δ_c 146.53 (C-4'). Through 3J and 2J couplings, the proton at 7.43 (1H, *d*, 2.37Hz) (H-2') correlated to the carbons at 146.53 (C-4') and 151.14 (C-3') respectively. Proton at δ_H 6.70 (H-3) presented 3J correlation to the carbon at δ_c 121.11(C-1'). 2J correlation between the signal at δ_H 6.86 (H-5') and δ_c 121.11 confirmed the assignment of this carbon signal to the C-1' of the aromatic ring B. The NMR data obtained were in agreement with previous reports (Boersma et al., 2002; Malikov and Yuldashev, 2002).

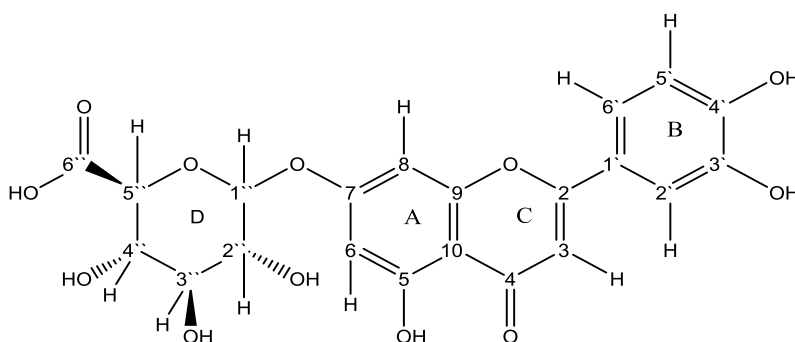


Figure 29: Structure of luteolin-7-O-glucuronide

Table 10: 1H (400 MHz) and ^{13}C (100 MHz) NMR data of luteolin-7-O-glucuronide

(M-3-9) in DMSO-d₆

Experimental Data		
Position	¹ H (multiplicity), J (Hz)	¹³ C (multiplicity)
1		
2		164.97
3	6.70 (1H, S)	103.17
4		182.27
5		157.37
5-OH	13.02 (S)	
6	6.41 (d, J= 2.13)	100
7		163.39
8	6.77 (d, J= 2.19)	94.93
9		161.42
10		105.67
1`		121.11
2`	7.43 (d, J= 2.37)	113.82
3`		151.14
4`		146.53
5`	6.86 (d, J= 8.43)	116.52
6`	7.38 (dd, J= 2.30, 8.37)	119.43
1``	5.08 (d, J= 7.52)	99.93
2``	3.27 (dd, J=8.92, 7.55)	73.37
3``	3.32 (t, J= 8.76)	76.9
4``	3.20 (dd, J= 9.97, 8.49)	72.44
5``	3.63 (d, J= 9.97)	74.2
6``		172.49

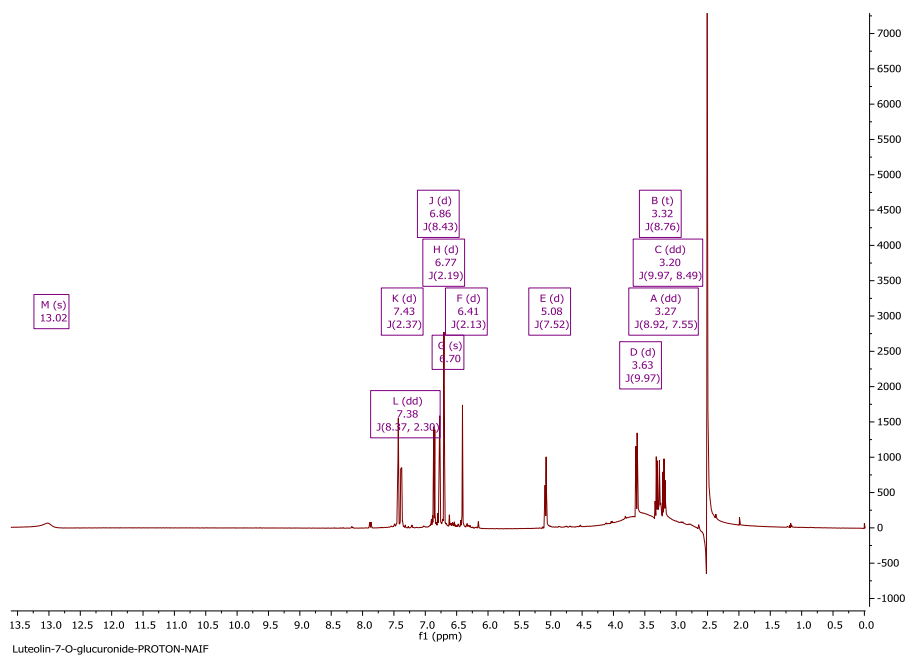


Figure 30: ¹H NMR spectrum (400 MHz) of luteolin-7-*O*-glucuronide (M-3-9) in DMSO-d₆

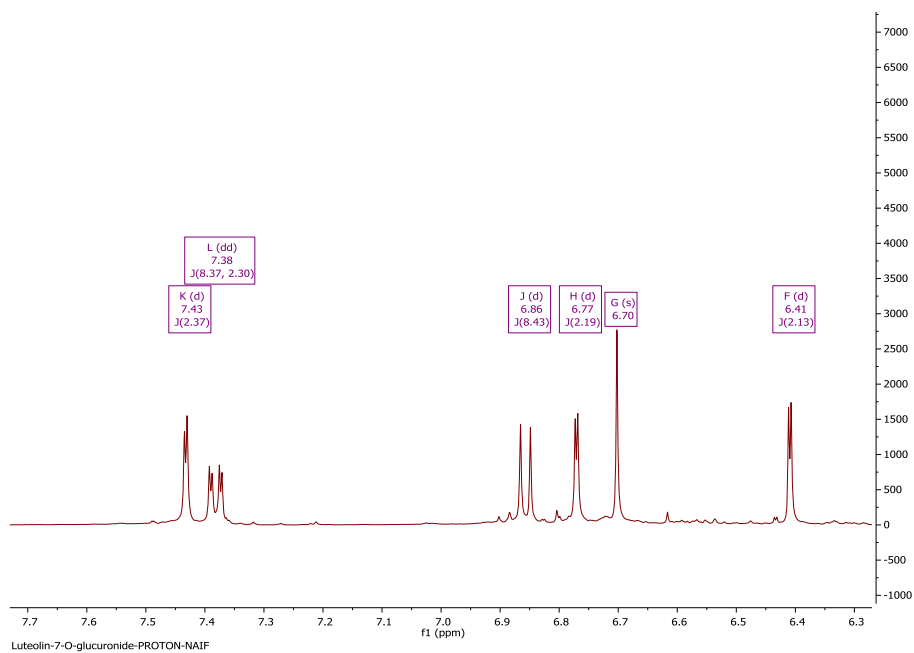


Figure 31: Selected ¹H expansion for the aromatic region of luteolin-7-*O*-glucuronide (M-3-9)

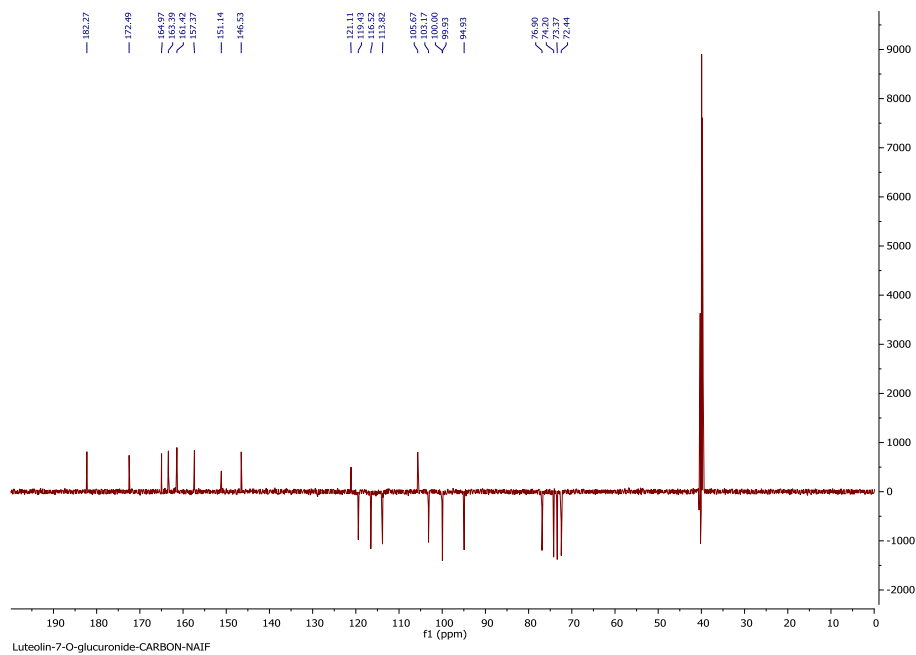


Figure 32: ^{13}C NMR spectrum (100 MHz) of luteolin-7-O-glucuronide (M-3-9) in DMSO-d_6

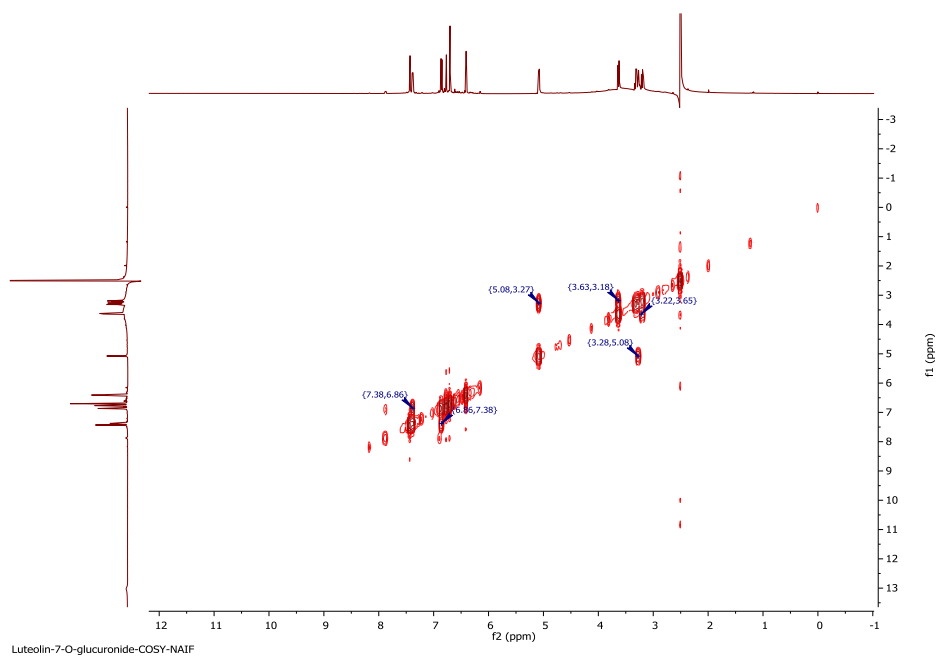


Figure 33: COSY spectrum (400 MHz) of luteolin-7-O-glucuronide (M-3-9) in DMSO-d_6

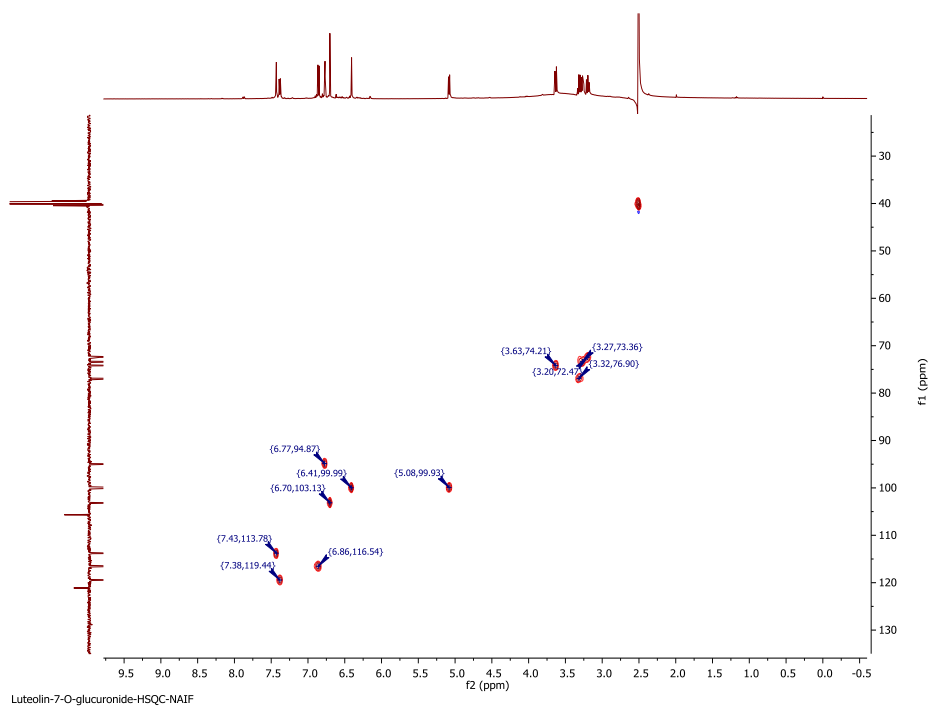


Figure 34: HSQC spectrum (400 MHz) of luteolin-7-O-glucuronide (M-3-9) in DMSO-6

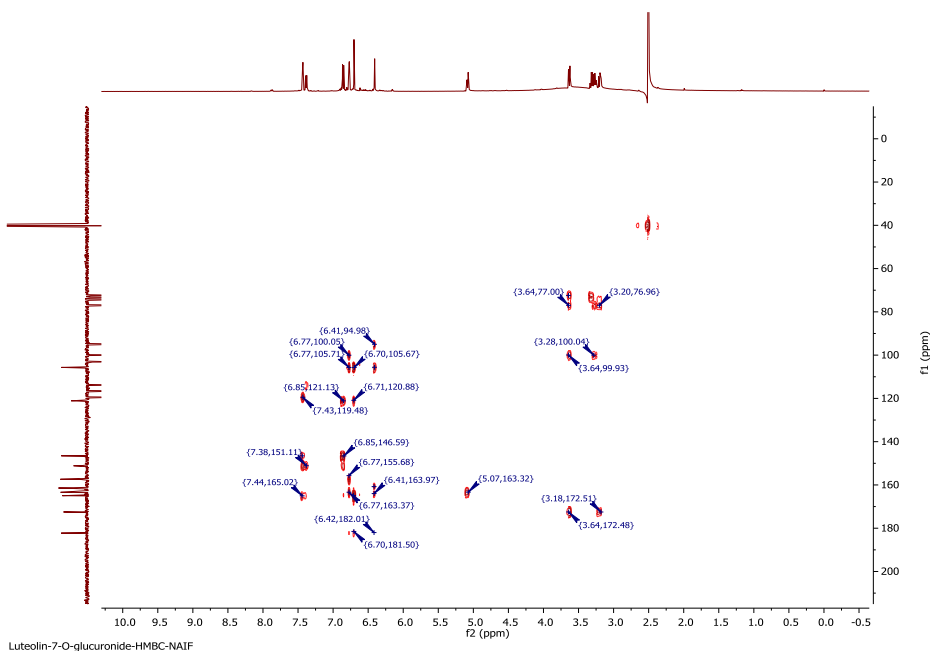


Figure 35: HMBC spectrum (400 MHz) of luteolin-7-O-glucuronide (M-3-9) in DMSO-d₆

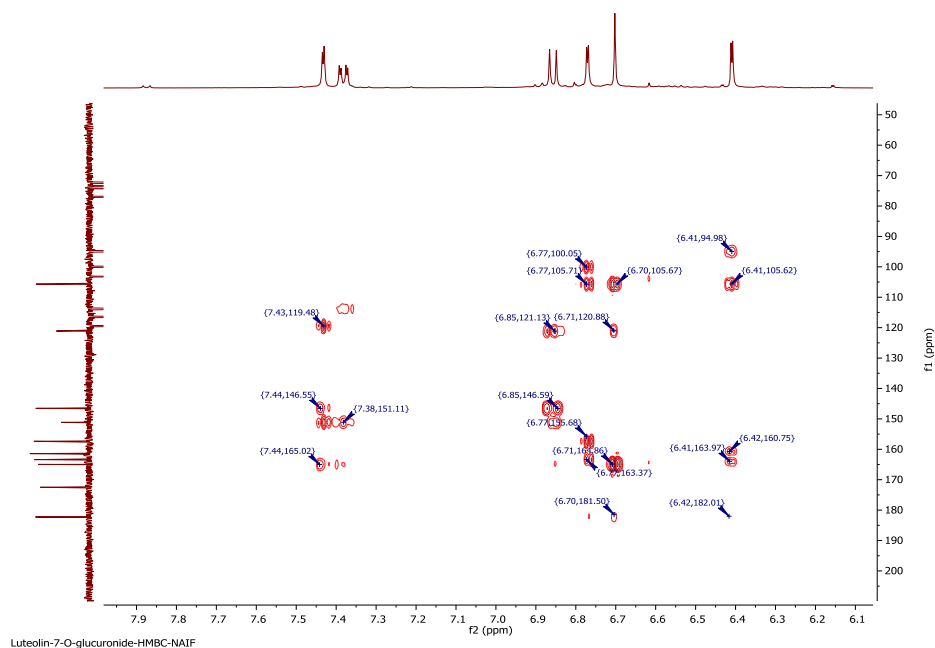


Figure 36: Selected HMBC expansion for the aromatic region of luteolin-7-O-glucuronide (M-3-9)

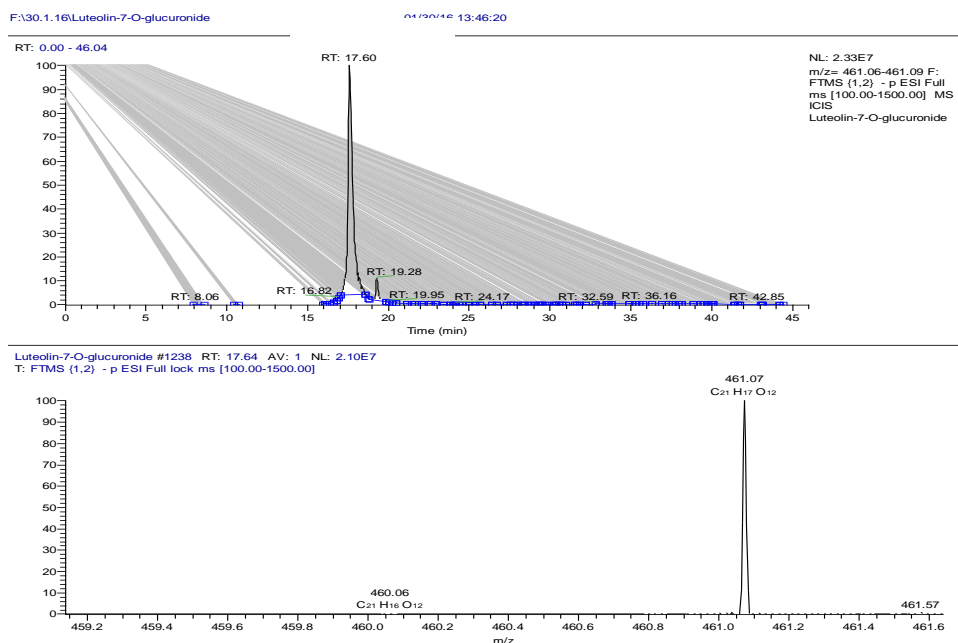


Figure 37: (A) Extracted ion chromatogram (EIC) corresponding to the mass of luteolin-7-O-glucuronide in the negative ion mode (-ve ESI) whereas (B) The mass spectrum corresponding to luteolin-7-O-glucuronide chromatogram

3.5 Characterisation of M-1-1 as ursolic acid

Following application of several chromatographic methods, including VLC, CC, SEC and PTLC, see figure 38, M-1-1 was obtained from the MeOH extract of *Ocimum sanctum* L., taking the form of a green powder. Spraying with *p*-anisaldehyde-sulphuric acid reagent and subsequent heating caused it to manifest as a purple spot on TLC. Elution with the mobile phase 80% HE in EtOAc gave an R_f of 0.76 on SiGel.

The molecular formula $C_{30}H_{47}O_3$ was established based on the fact that the molecular ion $[M-H]^-$ was indicated by the negative mode HRESI-MS spectrum at m/z 455.35 (figure 39). Furthermore, -28° was the specific optical rotation ($c = 0.025$, MeOH).

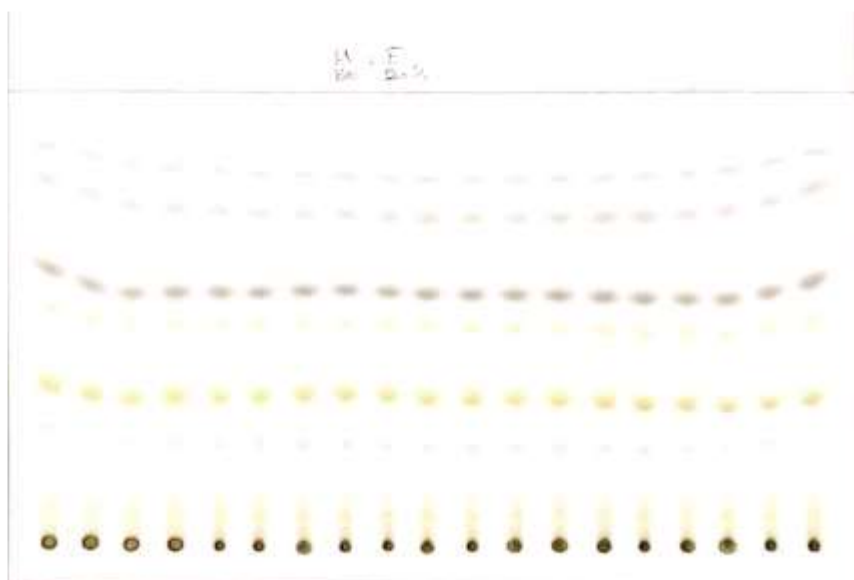


Figure 38: Separation of ursolic acid by PTLC after developing with the mobile phase HE: EtOAc (80:20%) and spraying with *p*-anisaldehyde-sulphuric acid and heating

The 1H NMR spectrum of the compound (400 MHz, DMSO- d_6 , figure 40, table 11) showed an olefinic proton signal at δ_H 5.14 ppm (H-12) a multiplet appearing as a doublet of triplet at 3.00 (d, $J = 5.53$) confirmed the presence of an oxymethine proton H-3. The spectrum also showed

seven methyl signals comprising of two methyl doublets at 0.82 (d, $J= 6.44$) and 0.88 (d, $J= 3.36$) and five methyl singlets. One broad proton singlet at 11.93 attributable to a carboxylic acid proton indicated the compound must contain a carboxylic acid group. The ^{13}C NMR spectrum displayed 30 signals made up of one carboxylic acid carbon at δ_{C} 178.55 ppm (C-28), a quaternary olefinic carbon at 138.66 (C-13) and a $-\text{CH}$ olefin at 125.04 (C-12). The oxymethine carbon signal appeared at 77.29 ppm (C-3). The rest of the carbons signals were for seven methyl signals between 15.6 and 28.8 ppm, nine methylene, five quaternary and five methine carbons. The COSY, HMQC and HMBC spectra were used to assign the chemical shifts and identified the compound as ursolic acid. The structure was further confirmed by comparing the proton and carbon NMR data with previous reports and they were found to be consistent with previous published spectral data (Blanco et al., 2007, Mahato and Kundu, 1994).

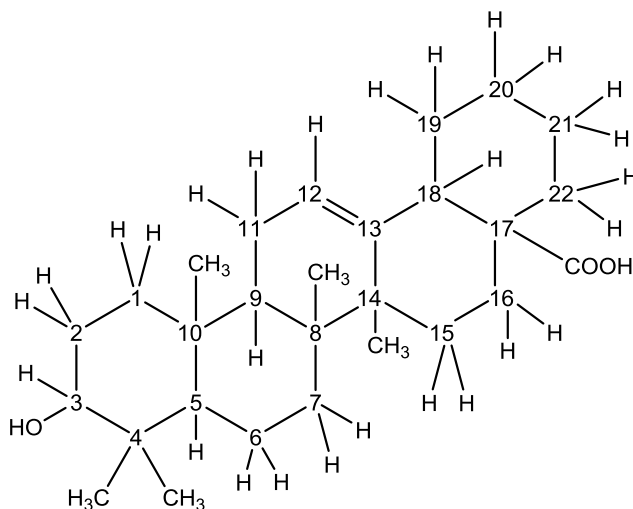


Figure 39: Structure of ursolic acid

Table 11: ^1H (400 MHz) and ^{13}C (100 MHz) NMR data of ursolic acid
(M-1-1) in DMSO-d_6

Position	¹ H (multiplicity), J (Hz)	¹³ C (multiplicity)
1	α 0.92, β 1.54	38.97
2	1.83, 1.45	28.01
3	α 3.01 (dt, J= 10.15, 5.13)	77.3
4		39.67
5	α 0.68	55.24
6	α 1.50, β 1.30	18.46
7	α 1.43, β 1.26	33.17
8		40.01
9	α 1.5	47.48
10		37
11	1.05, 0.87	23.32
12	5.14 (s)	125.04
13		138.66
14		42.12
15	α 1.45, β 0.93	27.46
16	α 1.91, β 1.52	24.27
17		47.3
18	2.11 (d, J= 10.55)	52.85
19	α 1.31	39.51
20	β 1.34	38.7
21	1.43, 1.26	30.65
22	1.56, 1.31	36.79
23	0.93	28.73
24	0.72	16.55
25	0.9	15.69
26	0.76	17.4
27	1.05	23.74
28		178.4
29	0.82 (d, J= 6.43)	17.48
30	0.91 (d, J= 9.10)	21.54

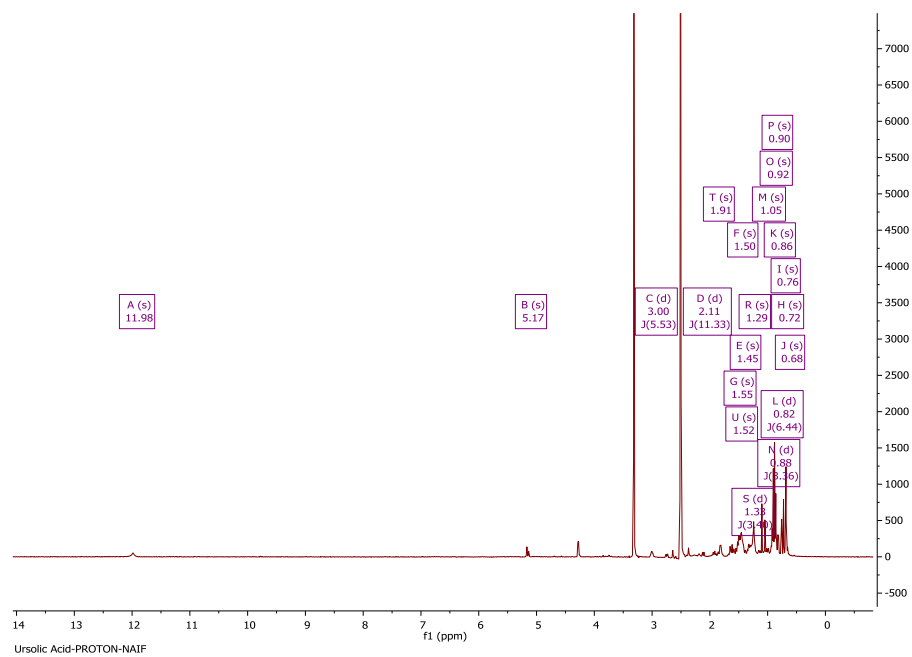


Figure 40: ^1H NMR spectrum (400 MHz) of ursolic acid(M-1-1) in DMSO-d_6

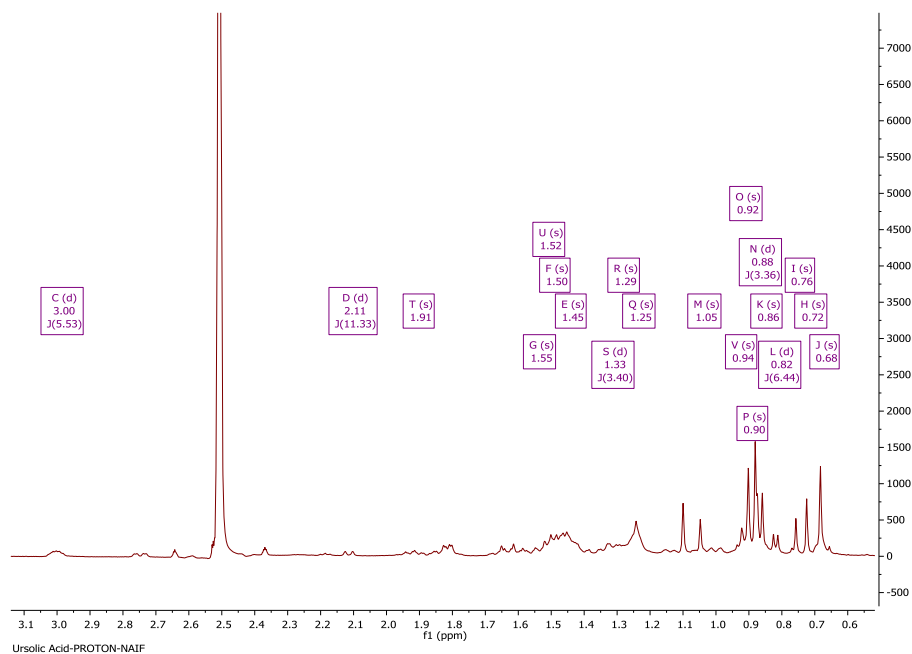


Figure 41: Selected ^1H expansion for the aliphatic region of ursolic acid (M-1-1)

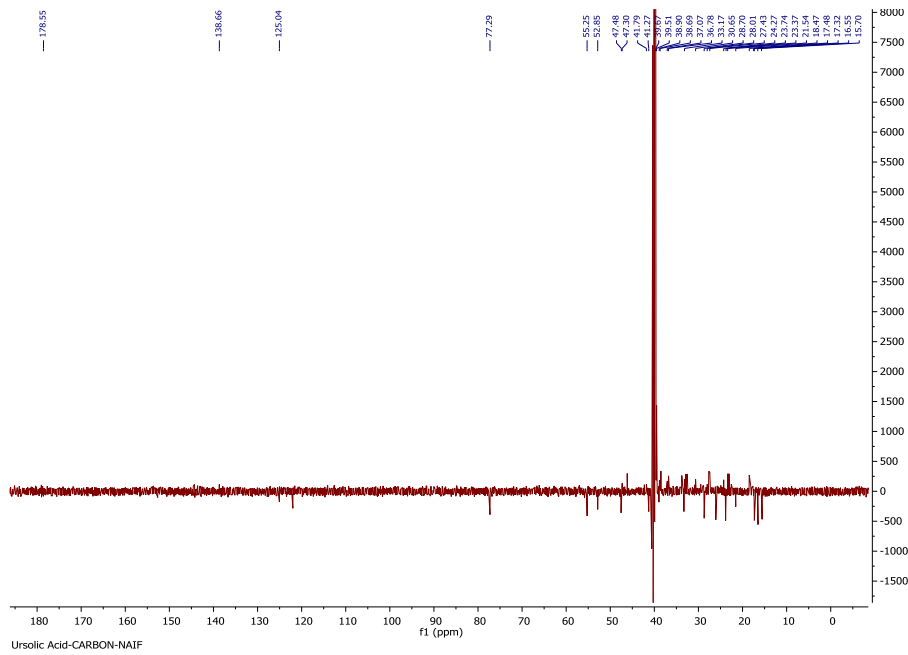


Figure 42: Full DEPTq ^{13}C NMR spectrum (100 MHz) of ursolic acid (M-1-1) in DMSO-d_6

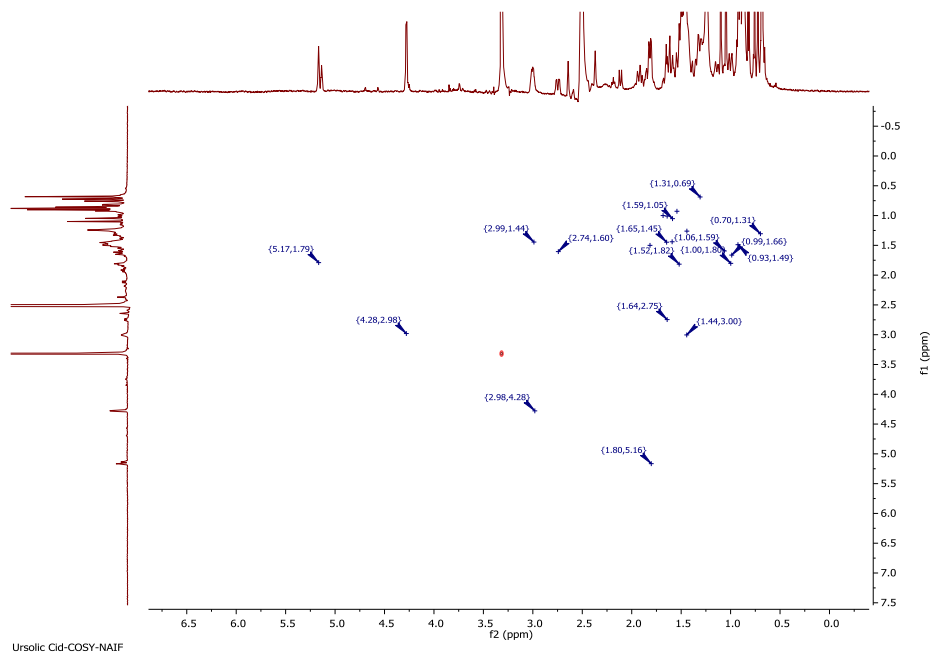


Figure 43: COSY spectrum (400 MHz) of ursolic acid (M-1-1) in DMSO-d_6

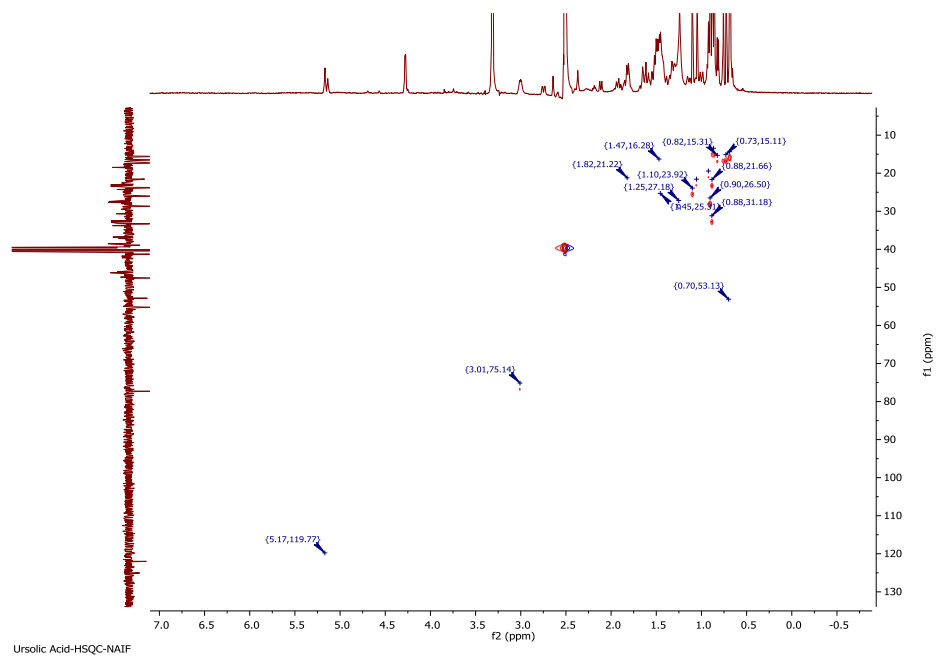


Figure 44: HSQC spectrum (400 MHz) of ursolic acid (M-1-1) in DMSO-d₆

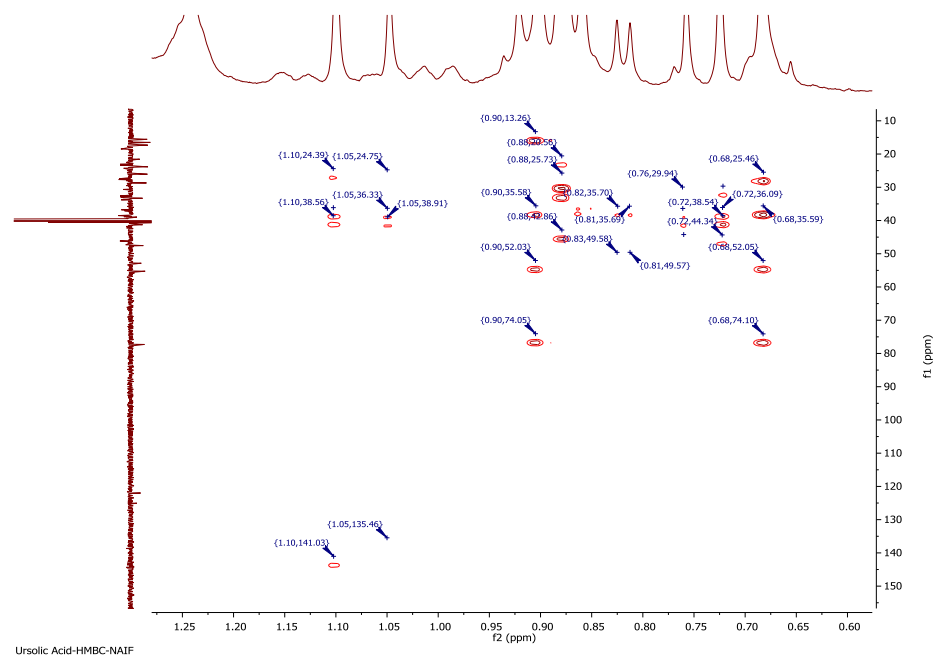


Figure 45: HMBC spectrum (400 MHz) of ursolic acid (M-1-1) in DMSO-d₆

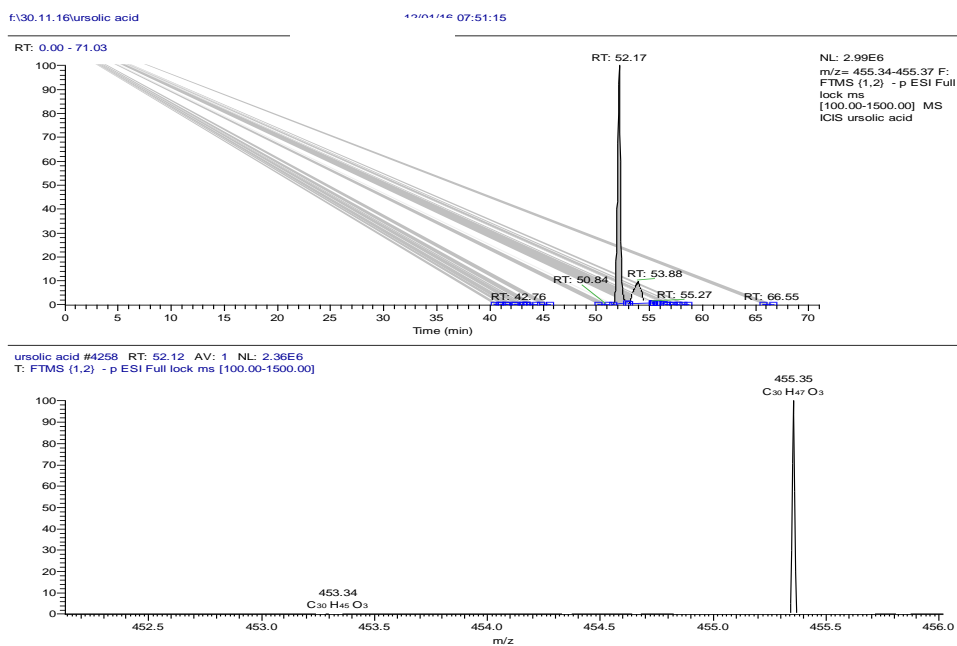


Figure 46: (A) TIC corresponding to the mass of ursolic acid in the negative ion mode (-ve ESI) whereas (B) shows the mass spectrum corresponding to the ursolic acid chromatogram

3.6 Biological activities of *Ocimum sanctum* Linn against trypanosome (*T. brucei* S427 strain)

Crude, extracted from MeOH, fractions and pure compounds (rosmarinic acid, luteolin-7-O-glucuronide and ursolic acid) collected from *Ocimum sanctum* were tested against *T. brucei*. Pentamidine and Diminazen were used as drug controls as their MIC scored 0.0045 and 0.0374 µg/ml respectively. Table 12 a and b showed the results from testing the above samples. The results showed a varying activity against *T. brucei* in between tested samples. Rosmarinic acid, 24.7 µg/ml MIC, was showing the highest activity, among tested samples, followed by ursolic acid with 49.5 µg/ml MIC whereas luteolin-7-O-glucuronide and MeOH extract crude were scored an MIC of 57.0 and 73.1 µg/ml respectively. However, none of the tested samples were considered active in comparison to tested controls and therefore these samples were not subjected for further studies. Table 12 a summarizes the biological activity of *Ocimum sanctum* samples against *T. brucei* S427 strain. It is worth to note that all tested samples were increasing cells viability (as their IC₅₀ values scored > 100 µg/ml) in contrast to Pentamidine and Diminazene which gave the lowest IC₅₀ values at 13.32 µg /mL and 29.58 µg/mL, respectively. Table 12 b shows detailed IC₅₀ values for tested samples.

Table 12 a: Drug Sensitivity assay of plant sample and its fractions on *T. brucei* S427 WT

Sample code	Exp. 1 (µg/ml)	Exp. 2 (µg/ml)	Exp. 1 (µg/ml)	Mean (µg/ml)	SD	%RSD
MeOH extract crude	75.1	73.9	70.2	73.1	2.56	3.50
Luteolin-7-O-glucuronide	57.2	57.9	55.8	57.0	1.07	1.88
Rosmarinic acid	25.3	23.9	25.0	24.7	0.72	2.92
Ursolic acid	49.4	50.8	48.3	49.5	1.22	2.46
Pentamidine(µM)	0.0044	0.0049	0.0042	0.0045	0.0004	7.9334
Diminazen(µM)	0.0377	0.0357	0.0389	0.0374	0.0017	4.4221

Table 12 b: Cytotoxicity assay of plant sample and its fractions on U937 cells

Sample code	Exp. 1 (µg/ml)	Exp. 2 (µg/ml)	Exp.3 (µg/ml)	Mean (µg/ml)	SD	%RSD
MeOH extract crude	150.7	165.8	161.3	159.3	7.75	4.87
Luteolin-7-O-glucuronide	189.3	203.5	204.1	199.0	8.38	4.21
Rosmarinic acid	94.4	92.8	106.0	97.7	7.2	7.4
Ursolic acid	177.6	172.9	163.3	171.3	7.29	4.26
Pentamidine(µM)	13.4300	14.2700	12.2500	13.3167	1.0148	7.6202
Diminazen(µM)	29.5300	31.7700	27.4300	29.5767	2.1704	7.3381

3.7 Discussion

Since they are promising rich sources of new medicines, natural products are enjoying a great deal of attention, being researched particularly in the context of drug discovery efforts. A wide range of living organisms, including plants, microbes, marine organisms, insects, and amphibians, produce secondary metabolites (Newman and Cragg, 2007), which typically have a molecular weight of less than 2,000 amu. They represent the focus of the present study.

Structure elucidation techniques enable identification or characterisation of compounds isolated from natural products. However, such techniques can generate research “bottlenecks” because they involve a lengthy process. They can pose significant challenges particularly in the case of unknown compounds. Although knowledge about chemical structures can be derived through a range of spectroscopic methods, including UV, IR, MS, X-ray crystallography and NMR, spectroscopic expertise, structure elucidation competence, comprehensive knowledge of the chemical properties of natural products, and especially a high degree of patience are needed to interpret the spectra produced by those methods (Sarker and Nahar, 2012).

Leaves of *Ocimum sanctum* were extracted successively using three different hot solvents hexane, ethyl acetate and methanol by Soxhlet extraction. Compounds with low polarity such as waxes and fatty acid esters are usually obtained from the hexane extract as hexane is non polar. Compounds with low polarity were detected, unfortunately, they were not purified and their structures were not confirmed. This was because of the complexity of the mixture and the low quantity of material obtained in the hexane extract. According to the NMR spectra, the EtOAc extract was found to have several phenolic components and flavonoids which almost share

the same polarity. Thus, isomers extraction might hinder obtaining pure, single compounds from the CC and SEC and this fraction was not worked on further.

Aromatic components were mainly in the MeOH extract. This was shown by the high level of signals in the ¹H-NMR aromatic area. This region as well showed lots of phenolic hydroxyl groups with peaks between 9 to 14 ppm in the proton NMR spectrum. The fractionation of the methanol extract of *Ocimum sanctum*, was carried out by using VLC followed by CC and SEC, and this led to the isolation of two simple phenolic compounds: rosmarinic acid and luteolin-7-o-glucuronide, whereas the triterpene ursolic acid was isolated by using PTLC.

The previous work carried out in this plant revealed the obtained compounds with numbers of active compounds such as ursolic acid, oleanolic acid, rosmarinic acid, luteolin and luteolin-7-o-glucuronide. These compounds have been investigated for several biological activities such as antibacterial, anti-anaphylactic and antihistaminic, wound healing effects (Goel et al., 2010), radio-protective effects (Devi et al., 1999), antidiabetic effects (Khan et al., 2010) and others. However, testing the obtained plant compounds by this study, see table 12 a and b, against *T. brucei* S427 WT shows relatively weak activity as well as no toxicity to U937 cells revealing another area were they are possibly not producing effects.

Mass spectroscopy was finally used in order to prove the accurate molecular weight of the isolated compounds. The mass technique (HPLC, ESI-MS) was specifically used (Joshi et al., 2011; Kumar et al., 2013; Sen, 1993; Singh et al., 2012). The mass spectrum in the negative ion mode for each compound confirmed the molecular formula for all compounds and their masses and purity within 5ppm.

Chapter 4

Chemical profiling, extraction, purification, isolation and structural elucidation of different types of propolis from various geographical areas

4 Phytochemical results for Saudi propolis

4.1 Introduction

The chemical profiling of propolis from Saudi Arabia and the detection of the main compounds underpinning its biological effects has not been extensively carried out. The few existing studies have indicated that Saudi propolis contains flavonoids, phenolics and phenolic acids such as p-coumaric acid, caffeic acid, apigenin, kaempferol, quercetin, rutin, ferruginol, totarol and terpenes such as triterpene acetate (3'-acetoxy-19(29)-taraxasten-20a-ol) (El-Mawla and Osman, 2011, Jerz et al., 2014). (Peyfoon, 2009) argued that the chemical compounds in propolis samples derived from different geographical areas would be dissimilar due to the variability of plants used by bees. In Saudi Arabia, the mountainous area in the south-west of the country, including Assir, Abha and Taif, is considered ideal for honey product collection (Jerz et al., 2014) due to the conditions that are conducive to beekeeping and benefit particularly the bee species of *Apis mellifera jemenitica* (Alqarni et al., 2011). The plants growing there also make this area stand out from other areas.

4.1.1 Extraction of sample of Saudi raw propolis

As explained by (Pietta et al., 2002), soaking, shaking, reflux and Soxhlet extraction are among the methods available for achieving the purification of raw propolis, being used together with different solvents to obtain dewaxed extracts of propolis containing numerous polyphenolic constituents. Although absolute ethanol is the solvent typically used for the preparation of propolis extracts, the use of aqueous ethanol (70-95%) can lead to acquisition of tinctures without wax and with a greater abundance of phenolic substances (Park and Ikegaki, 1998). However, the current study chose ethanol for undertaking the extraction process, and subsequently filtration was carried out to permit additional chromatographic analysis to be applied to the crude sample of propolis (table 13).

Table 13: weights of ethanolic extract of Saudi propolis

Masses	Weight (g)
Raw propolis sample (g)	18.5125 g
Empty beaker (g)	106.4607 g
Empty beaker + crude sample after cooling and drying (g)	119.3476 g
Crude sample (g)	12.8869 g

Among the instrumental methods employed for chemical profiling were high-performance liquid chromatography (HPLC) in association with a range of detectors, including evaporative light scattering detector (ELSD), ultraviolet detection (UV), and high-resolution mass spectrometry (HRMS), as well as NMR. In this way, a general understanding of the majority of constituents in the crude ethanolic extract was attained. NMR was applied to 10 mg of this extract to gain insight into the nature of the constituents (figure 47) and an LC-MS method was used for LCMS profiling (table 14, figure 48).

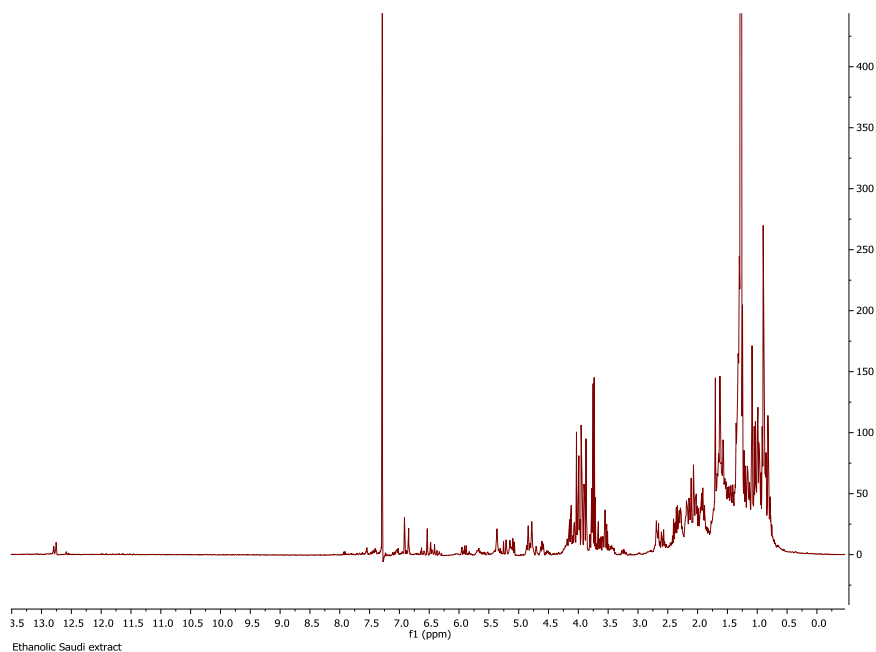


Figure 47: ¹H (400 MHz) NMR spectrum of ethanolic Saudi extract in CDCl₃. The main constituents highlighted by ¹H NMR spectrum were flavonoids and phenolics, while terpenoids and fatty acids of lesser intensity compared to flavonoids and phenolics were detected as well. MeOH extract was observed to contain aromatic compounds, this was shown by several signals from 6 to 8 ppm as well as phenolic hydroxyl group between 10-13 ppm.

Table 14: The LC-MS profiling for ethanolic Saudi propolis extract when analysed by reversed phase LC-MS in negative ion mode

Peak No.	Retention time(min)	[M-1]	Chemical formula	Delta (ppm)	Intensity
1	4.97	191.06	C ₇ H ₁₁ O ₆	0.778	E 7
2	4.97	353.09	C ₁₆ H ₁₇ O ₉	0.75	E 7
3	7.54	193.05	C ₁₀ H ₉ O ₄	-0.011	E 5
4	8.92	273.08	C ₁₅ H ₁₃ O ₅	1.989	E 8
5	9.96	545.15	C ₃₀ H ₂₅ O ₁₀	0.789	E 7
6	14.17	301.04	C ₁₅ H ₉ O ₇	-0.318	E 7
7	14.17	331.05	C ₁₆ H ₁₁ O ₈	-0.576	E 7
8	15.13	381.23	C ₂₁ H ₃₃ O ₆	1.542	E 7
9	15.6	405.08	C ₁₉ H ₁₇ O ₁₀	0.568	E 7
10	16.54	333.21	C ₂₀ H ₂₉ O ₄	2.543	E 8
11	16.84	315.05	C ₁₆ H ₁₁ O ₇	2.33	E 7
12	17.51	359.08	C ₁₈ H ₁₅ O ₈	1.363	E 7
13	19.63	335.22	C ₂₀ H ₃₁ O ₄	1.633	E 7
14	21.06	373.09	C ₁₉ H ₁₇ O ₈	1.231	E 7
15	21.06	329.07	C ₁₇ H ₁₃ O ₇	1.684	E 7
16	22.21	419.1	C ₂₀ H ₁₉ O ₁₀	1.718	E 7
17	23.08	403.1	C ₂₀ H ₁₉ O ₉	1.351	E 7
18	24.49	331.19	C ₂₀ H ₂₇ O ₄	2.619	E 7
19	27.09	361.2	C ₂₁ H ₂₉ O ₅	2.555	E 7
20	30.16	363.22	C ₂₁ H ₃₁ O ₅	2.568	E 7
21	31.12	341.14	C ²⁰ H ₂₁ O ₅	2.559	E 7
22	33.49	325.14	C ₂₀ H ₂₁ O ⁴	1.315	E 8
23	36.18	317.21	C ₂₀ H ₂₉ O ₃	3.474	E 7
24	38.85	487.34	C ₃₀ H ₄₇ O ₅	3.698	E 6
25	40.97	475.34	C ₂₉ H ₄₇ O ⁵	3.791	E 6
26	51.3	469.33	C ₃₀ H ₄₅ O ₄	2.934	E 6

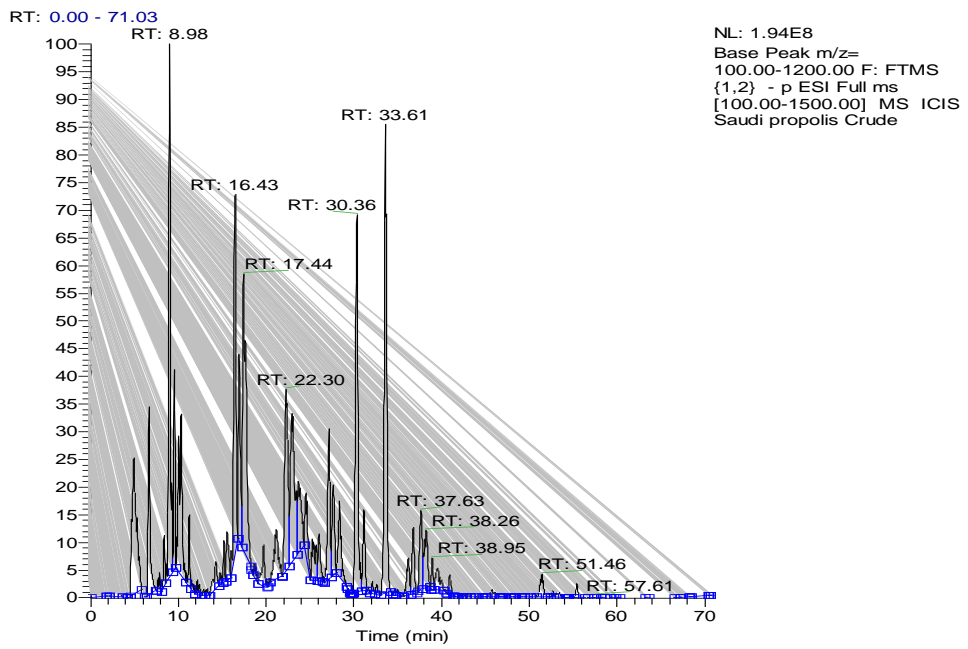
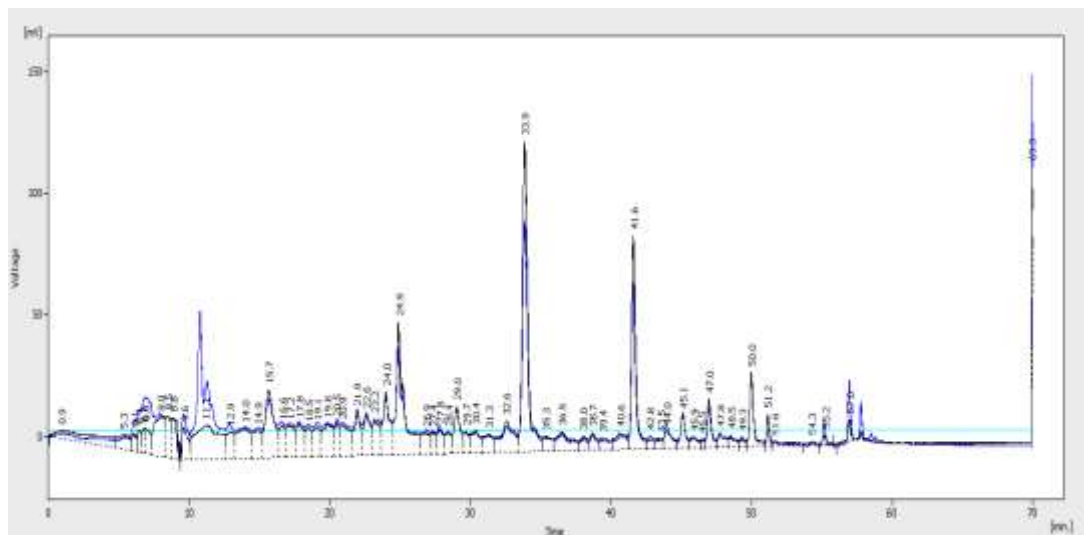


Figure 48: Chromatogram view of ethanolic Saudi crude in LC-MS negative ion mode (-ve ESI)



According to the results of HPLC-UV-ELSD, the content of the crude sample was mainly composed of compounds that could absorb UV, such as flavonoids and phenolic compounds. Although compounds lacking chromophores, like e.g. some terpenoids, were also identified, their intensities were low (figure 49). Considerable complexity was exhibited by the LC-MS chromatogram of the crude sample, revealing multiple peaks of varying intensities. As indicated in table 14 and figure 48, the crude extract of ethanolic crude consisted mainly of flavonoids and other phenolics, according to the results of LC-MS analysis. Flavonoids and phenolics were also confirmed to be the dominant constituents by the ^1H NMR spectra (figure 47). In addition, terpenoids and fatty acid compounds were highlighted by a couple of signals captured by the NMR of the crude sample, although their intensities were not as high as those of the flavonoids and phenolics.

Isolation is like extraction and due consideration must be given primarily to the nature of the compound(s) of interest in the crude extracts or fractions before the isolation procedure is selected. In particular, attention should be paid to aspects of the molecule(s) of interest demanding such as solubility (hydrophobicity or hydrophilicity), acid–base properties, charge, stability, and molecular size (Sarker et al., 2005). In order to isolate the pure compounds, several processes of separation and purification were undertaken, mostly based on CC and SEC. A quantity of the ethanolic extract of Saudi propolis (6.25g) was subjected to column chromatography and elution was sequentially performed based on a gradient profile (table 15). The total number of fractions generated was 28, and these were collected in vials with a volume of 50 ml. Chromatographic characteristics were delineated via TLC using a suitable solvent system. Application of LC-MS and NMR permitted identification of the different components and allowed combination of similar fractions. The final number of fractions was ten (table 14).

Table 15: Sequence of Column Chromatography Solvent Systems and fractions collected

No.	He %	EtOAc %	MeOH %	M.P (ml)	Fractions obtained	Weight (mg)
1	80	20	0	200	fraction S1 (M1+M2+M3+M4)	88 mg
2	60	40	0	100	fraction S2 (M5+M6)	120 mg
2	60	40	0	100	fraction S3 (M7+M8)	150 mg
3	40	60	0	50	fraction S4 (M9)	95 mg
3	40	60	0	150	fraction S5 (M10+M11+M12)	200 mg
4	20	80	0	200	fraction S6 (M13+M14+M15+M16)	475 mg
5	0	100	0	100	fraction S7 (M17+M18)	175 mg
5	0	100	0	100	fraction S8 (M19+M20)	145 mg
6	0	70	30	200	fraction S9 (M21+M22+M23+M24)	100 mg
7	0	50	50	200	fraction S10 (M25+M26+M27+M28)	45 mg

Chemical analysis is reliant to a significant extent on component fraction mass, and as such, an ample amount of the chemical component would enable performance of additional chromatographic separation. LC-MS and HPLC-UV-ELSD analysis conducted on S-6 and revealed a rich content of compounds with varied compositions, as shown in table 16 and figure 50 and 51. Based on preliminary data, the compounds were most likely to be flavonoids and phenolics. Therefore, 475 mg of fraction (S-6) from CC was subjected to SEC, yielding 23 sub-fractions (S-6-1 to S-6-23), which led to the acquisition of two pure compounds (S-6-7 and S-6-13).

Table 16: The most abundant in the Saudi's fraction (S-6) when analysed by reversed phase LC-MS in negative ion mode

Peak No.	Retention time (min)	[M-1]	Chemical formula	Delta (ppm)	Intensity
1	6.7	193.05	C ₁₀ H ₉ O ₄	-0.011	E 6
2	9.04	273.08	C ₁₅ H ₁₃ O ₅	1.33	E 7
3	9.88	545.15	C ₃₀ H ₂₅ O ₁₀	1.357	E 7
4	15.57	405.08	C ₁₉ H ₁₇ O ₁₀	0.247	E 7
5	16.31	333.21	C ₂₀ H ₂₉ O ₄	1.252	E 7
6	19.66	335.22	C ₂₀ H ₃₁ O ₄	1.185	E 7
7	20.13	373.09	C ₁₉ H ₁₇ O ₈	1.472	E 7
8	22.17	419.1	C ₂₀ H ₁₉ O ₁₀	0.334	E 8
9	33.55	325.14	C ₂₀ H ₂₁ O ₄	1.315	E 7
10	36.64	317.21	C ₂₀ H ₂₉ O ₃	1.551	E 7

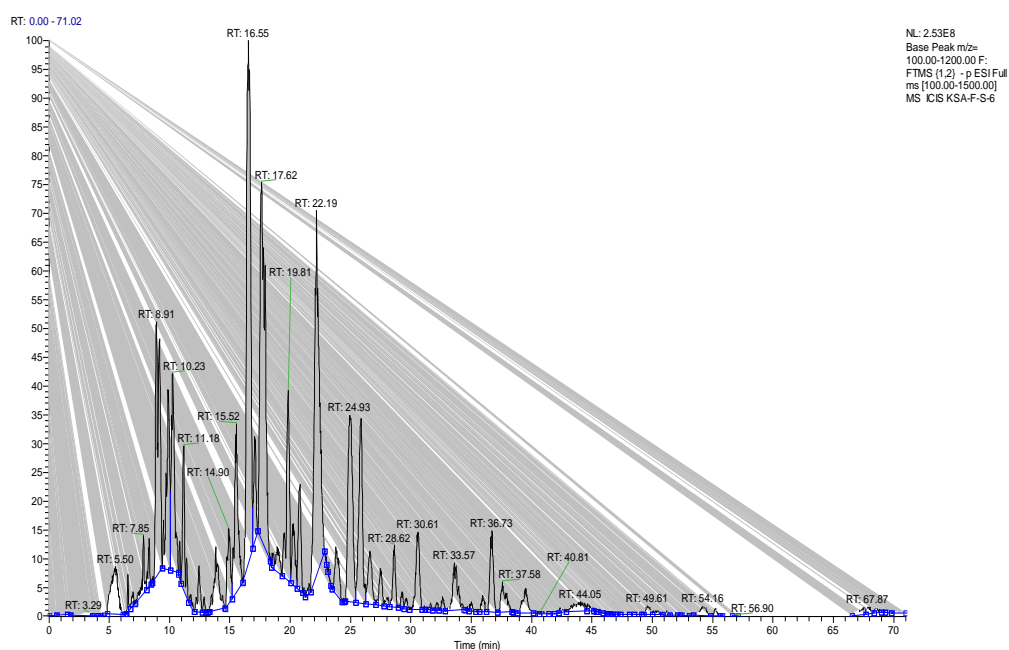


Figure 50: Chromatogram view of Saudi's fraction (S-6) using the LC-MS in negative ion mode (-ve ESI)

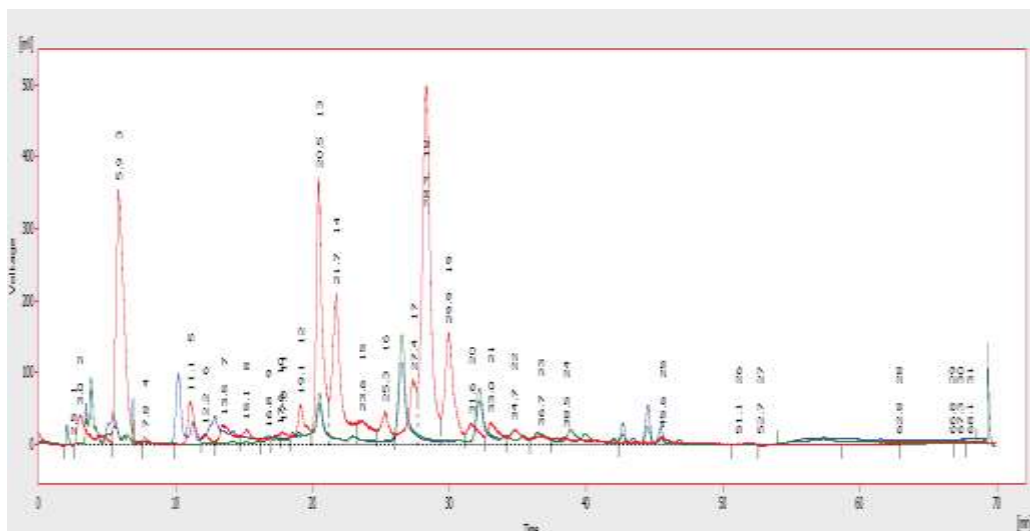


Figure 51: Chromatogram view of Saudi's fraction (S-6) on the ELSD (showed clearly that it contained mostly compounds with UV-absorbing activity (red trace), that could be flavonoids or phenolic, however, at retention times of 40 and 60 min. Terpenoids or fats or any other compounds without chromophores were detected but with low intensities (green trace).

4.1.2 Characterisation of S-6-7 as fisetinidol

CC and then SEC was performed for isolation of S-6-7 from the ethanolic extract of Saudi propolis. Spraying with *p*-anisaldehyde-sulphuric acid reagent and exposure to heat caused it to manifest as a violet spot on TLC. Elution with the mobile phase 50% HE in EtOAc gave an R_f of 0.41 on SiGel.

A molecular formula of $C_{15}H_{13}O_5$ was derived from the fact that the molecular ion $[M-H]^-$ was indicated by the negative mode HRESI-MS spectrum at m/z 273.08 (figure 52), and the optical rotation had a value of -5.9° ($c = 0.085$, MeOH).

The proton spectrum of the compound (figure 53, table 17) showed two sets of aromatic ABX spin systems. The first set were at δ_H ppm 6.83 (d, $J = 8.23$ Hz), 6.28

(dd, $J = 8.21, 2.41$) and 6.18 (d, $J = 2.34$). The second set of the aromatic ABX protons were at 6.72 (d, $J = 2.01$), 6.69 (d, $J = 8.06$) and 6.60 (dd, $J = 8.13, 2.04$). It also showed two oxymethine protons at 4.58 (d, $J = 7.17$) and 3.86 (m). There were also two methylene protons at 2.75 (dd, $J = 15.65, 4.98$) and 2.59 (dd, $J = 15.60, 8.05$). Finally, there three phenolic protons at 9.16 (s), 8.87 (s) and 8.83 (s).

The ^{13}C spectrum showed a total of 15 signals consisting of six aromatic CH carbons, two oxymethine carbons at δ_{C} ppm 81.65 and 66.79. The rest of the carbon signals were for a methylene carbon at 32.71, and four phenolic carbon atoms and two aromatic quaternary carbons at 111.52 and 131.02 ppm. The absence of a hydrogen bonded -OH proton around 12-13 ppm and a carbonyl signal between 170 and 220 ppm indicates the compound is not a flavone but a flavan derivative.

This was confirmed from its 2D NMR spectrum as long range HMBC correlations from H-2 to C-9, C-12, C-16, C-4, C-11 and C-3 were identified while correlations from H-4 to C-10, C-5 and C-9 were identified. The 7-OH gave correlations to C-6, C-7 and C-8.

Other correlations from HMQC and COSY confirmed the structure of the compound as well as the carbon and proton chemical shifts. The compound was identified as fisetinidol and its NMR spectral data were in agreement with (Almutairi et al., 2014) thus indicating that this compound is typical of Saudi propolis.

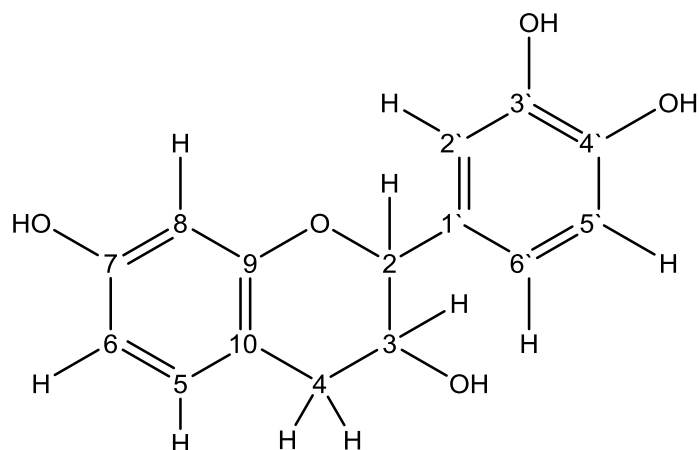


Figure 52: Structure of fisetinidol

Table 17: ^1H (400 MHz) and ^{13}C (100 MHz) NMR data of fisetinidol (S-6-7) in DMSO-d_6

Experimental Data		
Position	^1H (multiplicity), J (Hz)	^{13}C (multiplicity)
1		
2	4.58 (d, $J=7.17$)	81.65
3	3.86 (m)	66.79
3-OH	4.96 (d, $J=5.01$)	
4	2.59 (dd, $J=15.6, 8.05$)	32.71
4	2.75 (dd, $J=15.65, 4.98$)	32.71
5	6.83 (d, $J=8.23$)	130.53
6	6.28 (dd, $J=8.21, 2.41$)	108.5
7		157.03
7-OH	9.16 (s)	
8	6.18 (d, $J=2.34$)	102.67
9		155.04
10		111.52
1'		131.02
2'	6.72 (d, $J=2.01$)	114.82
3'		145.31
3'-OH	8.87 (s)	
4'		144.96
4'-OH	8.83 (s)	
5'	6.69 (d, $J=8.06$)	115.58
6'	6.6 (dd, $J=8.13, 2.04$)	118.68

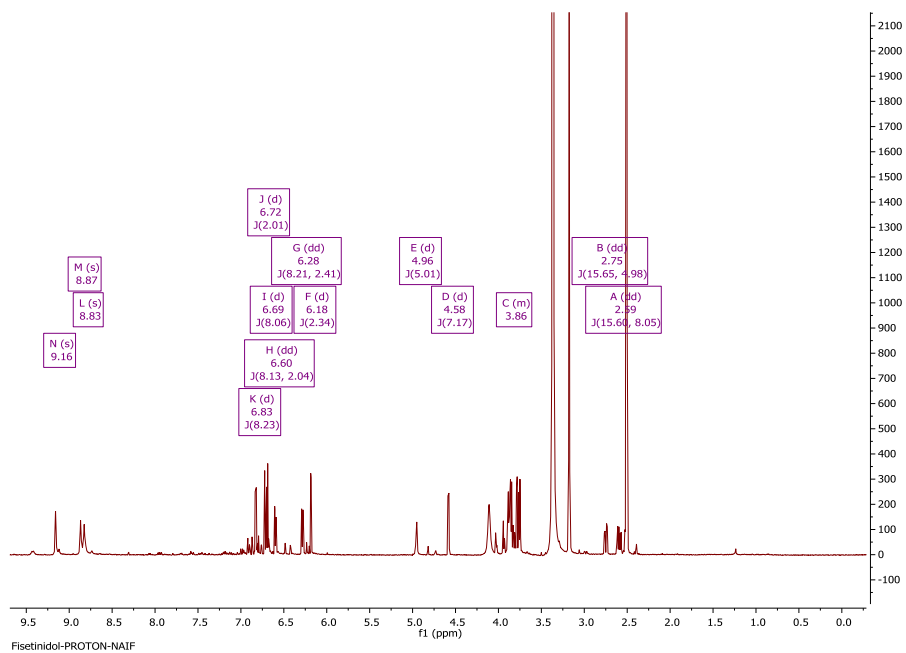


Figure 53: ¹H NMR spectrum (400 MHz) of fisetinidol (S-6-7) in DMSO-d₆

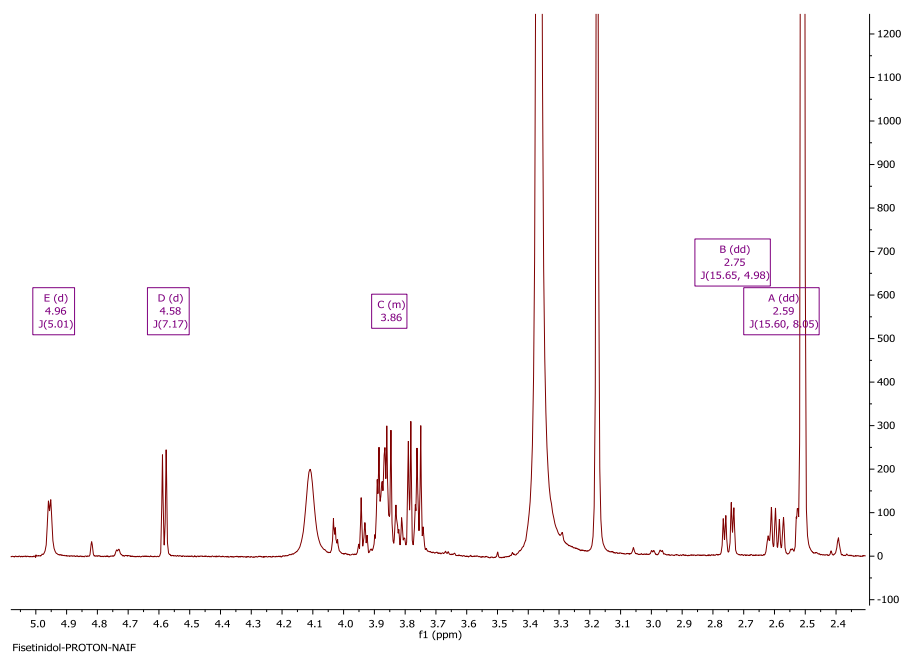


Figure 54: Selected ¹H expansion for the aliphatic region for fisetinidol (S-6-7)

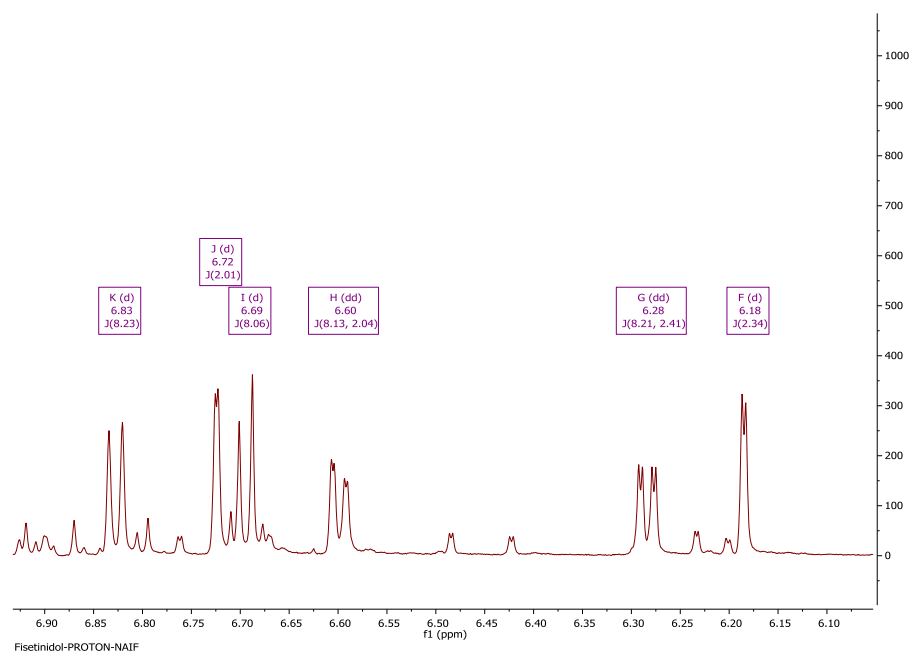


Figure 55: Selected ^1H expansion for the aromatic region for fisetinidol (S-6-7)

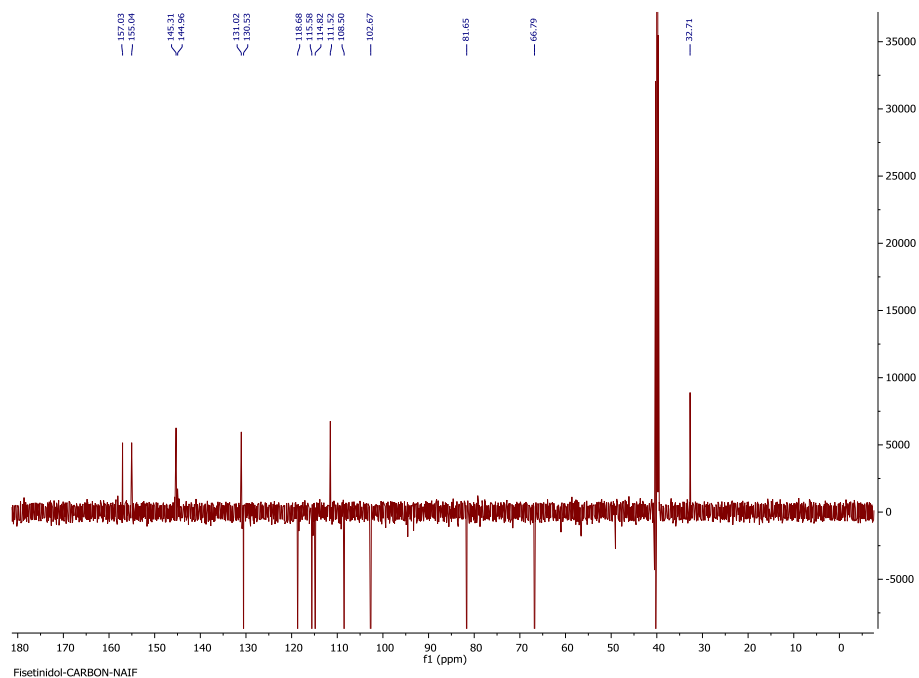


Figure 56: Full DEPTq 135 ^{13}C NMR spectrum (100 MHz) of fisetinidol (S-6-7) in DMSO-d_6

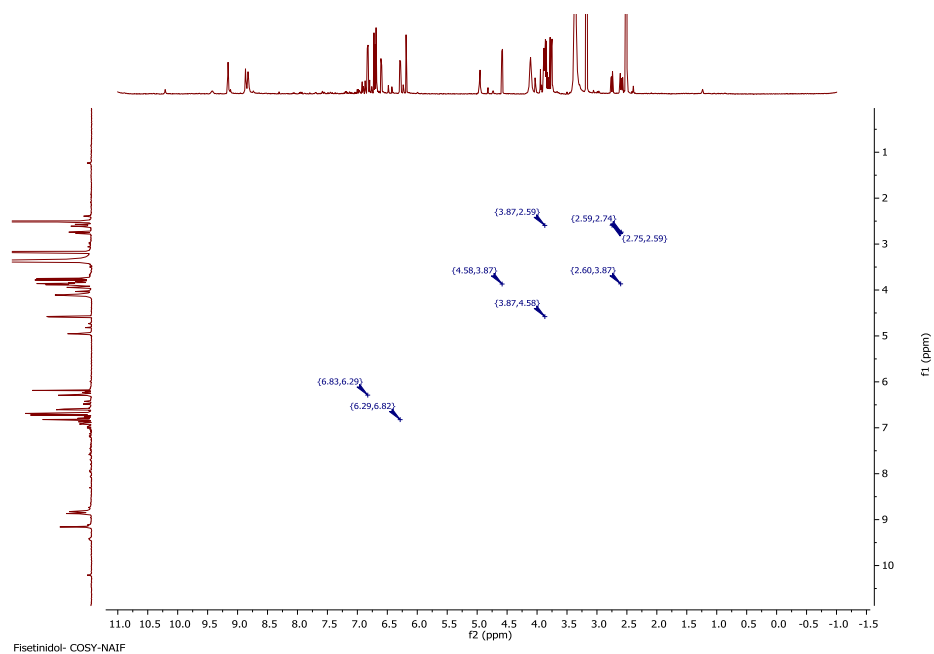


Figure 57: COSY spectrum (400 MHz) of fisetinidol (S-6-7) in DMSO-d₆

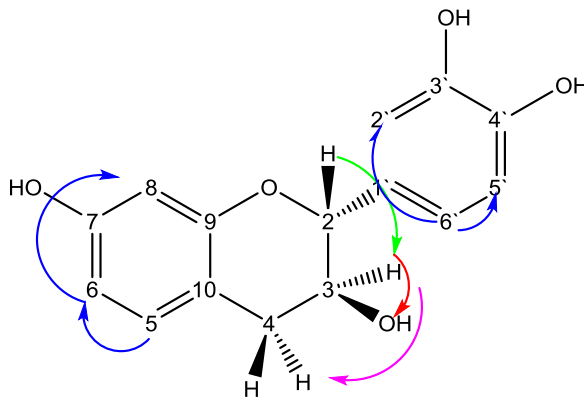


Figure 58: COSY correlations NMR spectra of fisetinidol in DMSO-d₆. The coloured arrows show the correlations corresponding COSY correlations in (figure 57)

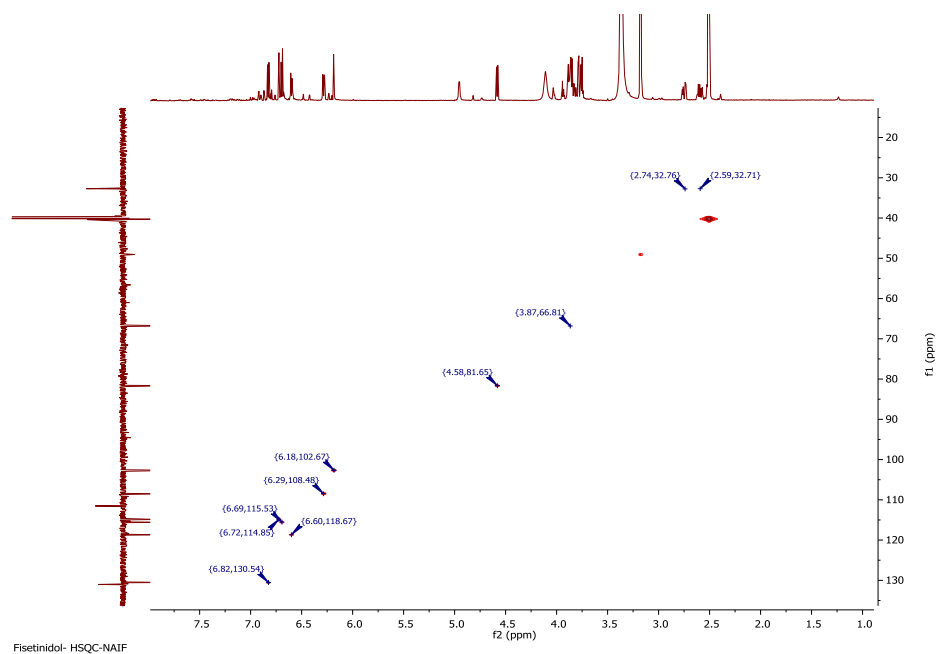


Figure 59: HSQC spectrum (400 MHz) of fisetinidol (S-6-7) in DMSO-d₆

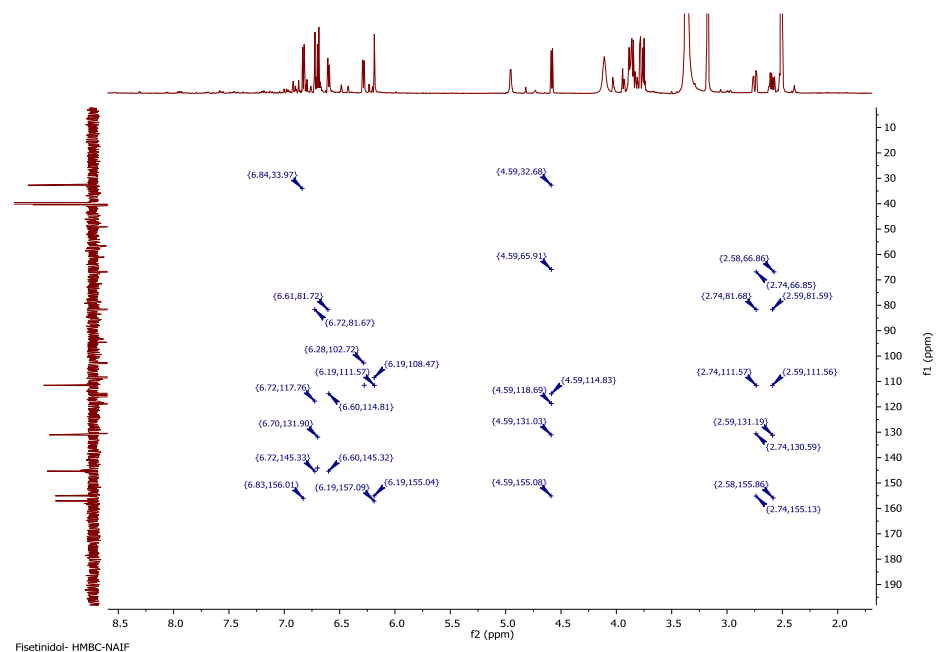


Figure 60: HMBC spectrum (400 MHz) of fisetinidol (S-6-7) in DMSO-d₆

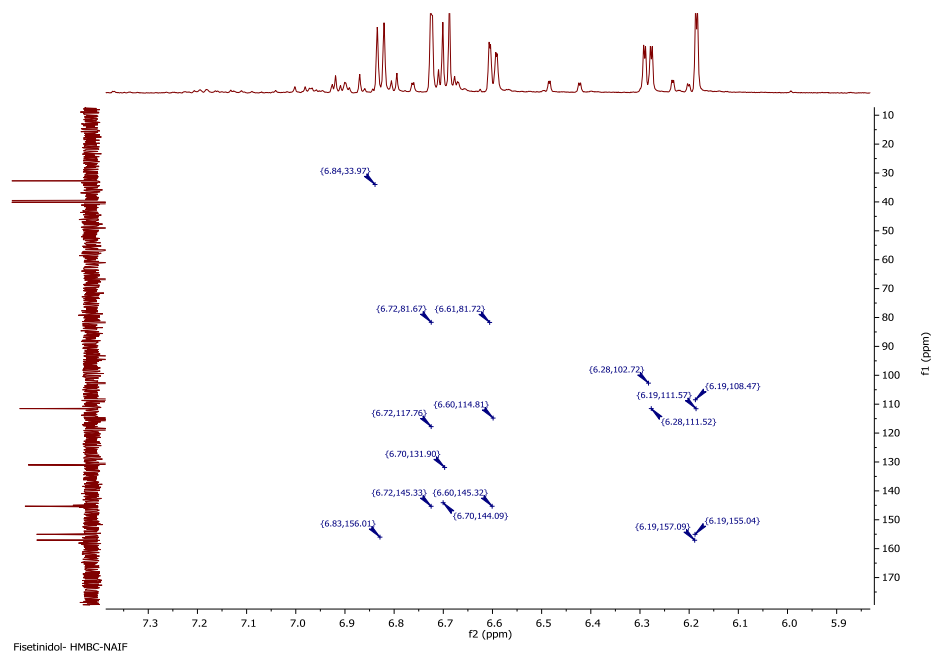


Figure 61: Selected HMBC expansion for the aromatic region for fisetinidol (S-6-7)

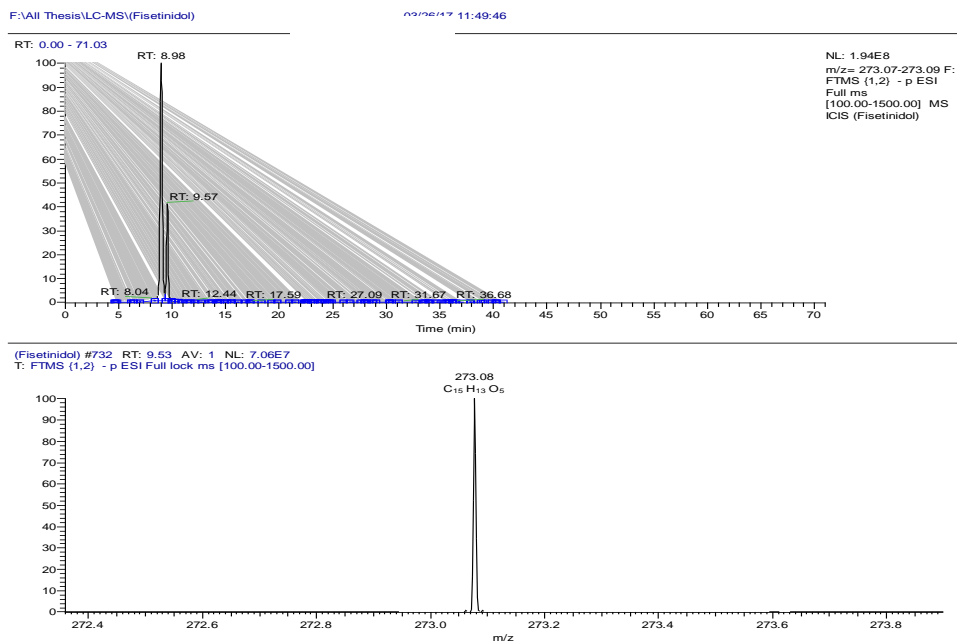


Figure 62: (A) Extracted ion chromatogram corresponding to the mass of fisetinidol in the negative ion mode (-ve ESI) (B) shows the spectrum corresponding to the fisetinidol chromatogram.

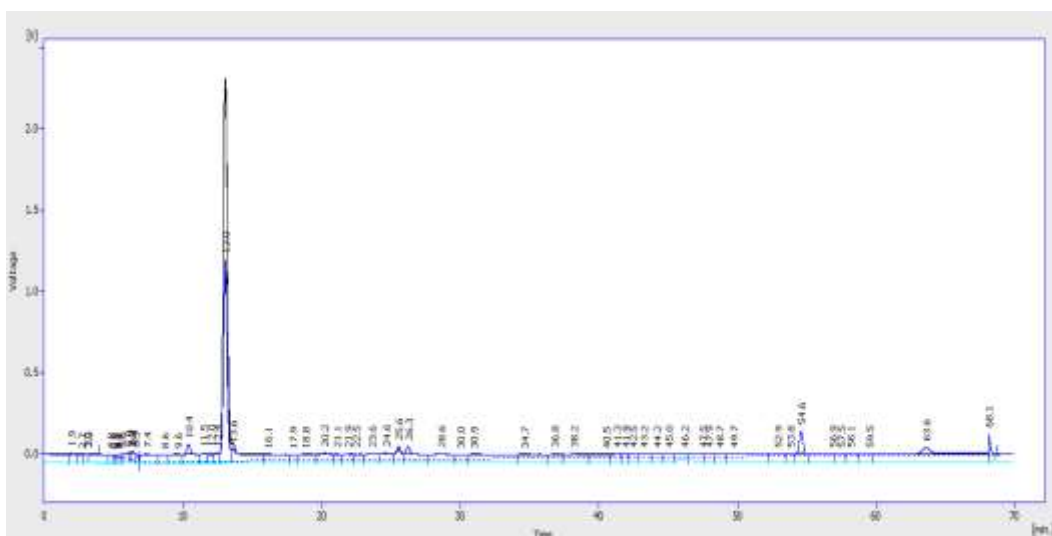


Figure 63: LC-UV-ELSD chromatogram of fisetinidol purified from SEC (Black traces ELSD and blue trace UV at 290 nm)

4.1.3 Characterization of S-6-13 as ferulic acid

CC and then SEC was performed for isolation of S-6-13 from ethanolic extract of Saudi propolis. Spraying with *p*-anisaldehyde-sulphuric acid reagent and exposure to heat caused it to manifest as a violet spot on TLC. Elution with the mobile phase 50% HE in EtOAc gave an R_f of 0.45 on SiGel.

A molecular formula of $C_{10}H_9O_4$ was derived from the fact that the molecular ion $[M-H]^-$ was indicated by the negative mode HRESI-MS spectrum at m/z 193.05 (figure 64).

The 1H -NMR (400MHz, DMSO- d_6 , table 18 and figure 65) showed two doublets at δ_H 6.21 (1H, d, $J = 15.90$, H-8) and 7.48 ppm (1H, d, $J = 15.89$, H-7). Three aromatic proton signals at 7.32 (1H, dd, $J = 8.48, 2.19$, H-6), 7.01 (1H, d, $J = 8.47$, H-5) and

7.72 (1H, d, $J = 2.17$, H-2). It also showed a methoxy signal at 3.79 (3H, s, 5-OCH₃). The ¹³C-NMR spectrum showed a deshielded signal at δ_c 168.28 ppm for a carboxylic acid carbonyl group (C-9), two olefinic CH at 116.86 and 144.36, three aromatic CH at 112.92, 119.9 and 125.11, two oxygenated aromatic carbons at 143.29 and 153.26, a quaternary carbon at 126.72 and a methoxy carbon at 56.16 ppm. This was confirmed from its 2D NMR spectrum as long range HMBC correlations from H-2 identified C-4, C-6 and C-7 while correlations from H-5 identified C-1 and C-3. Also the correlations from H-6 identified C-2, C-4 and C-7 while the correlations from H-7 identified C-2, C-6 and C-9. HMBC correlations from H-8 identified C-1 and C-9. Other correlations from HMQC and COSY confirmed the structure of the compound as well as the carbon and proton chemical shifts. The compound was identified as ferulic acid and its NMR spectral data were in agreement with (Yoshioka et al., 2004; Liao et al., 2014).

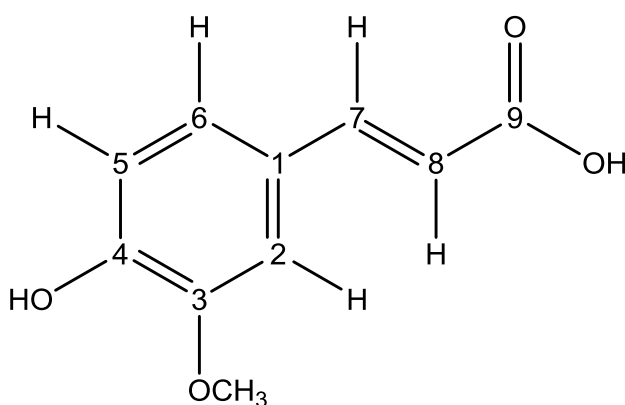


Figure 64: Structure of ferulic acid

Table 18: ^1H (400 MHz) and ^{13}C (100 MHz) NMR data of ferulic acid (S-6-13) in DMSO-d_6

Experimental Data		
Position	^1H (multiplicity), J (Hz)	^{13}C (multiplicity)
1		126.72
2	7.72 (d, $J=2.17$)	119.9
3		153.26
3-OCH ₃	3.79 (s, 3H)	56.16
4		143.29
5	7.01 (d, $J=8.47$)	112.92
6	7.32 (dd, $J=8.48, 2.19$)	125.11
7	7.48 (d, $J=15.89$)	144.36
8	6.21 (d, $J=15.90$)	116.86
9		168.28
9-OH	12.21 (s)	

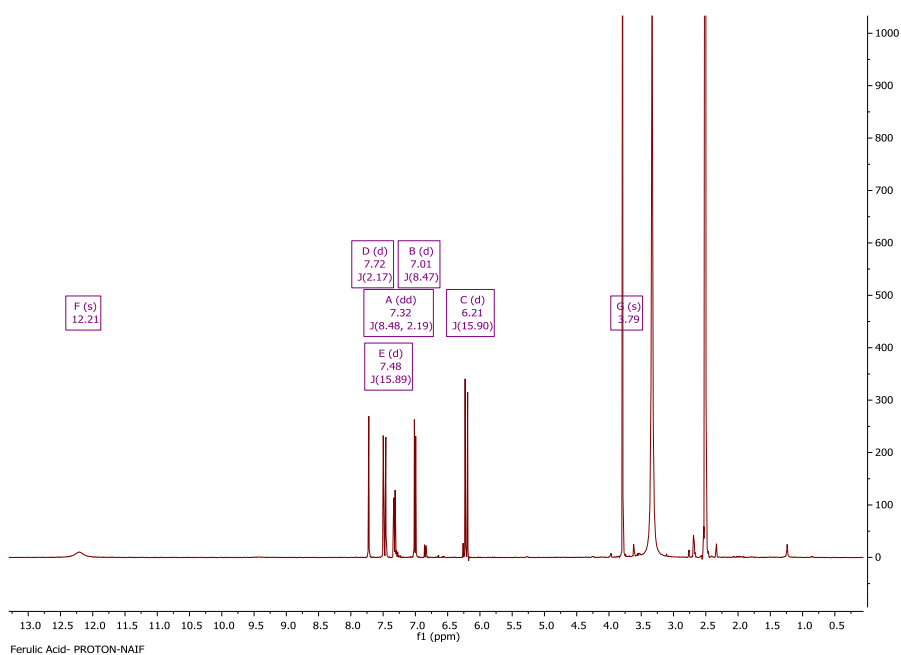


Figure 65: ^1H NMR spectrum (400 MHz) of ferulic acid (S-6-13) in DMSO-d_6

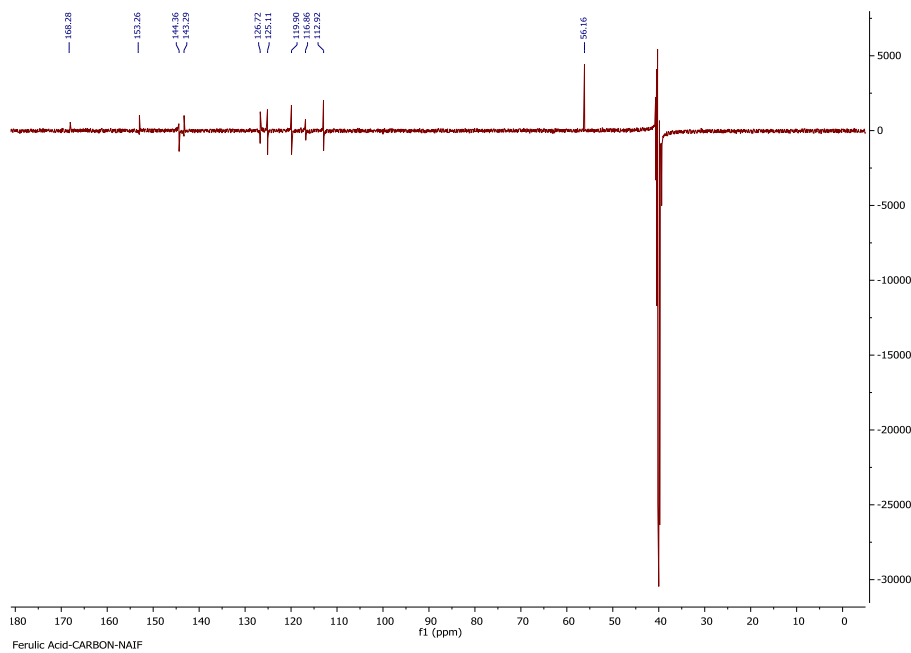


Figure 66: ^{13}C NMR spectrum (100 MHz) of ferulic acid (S-6-13) in DMSO-d_6

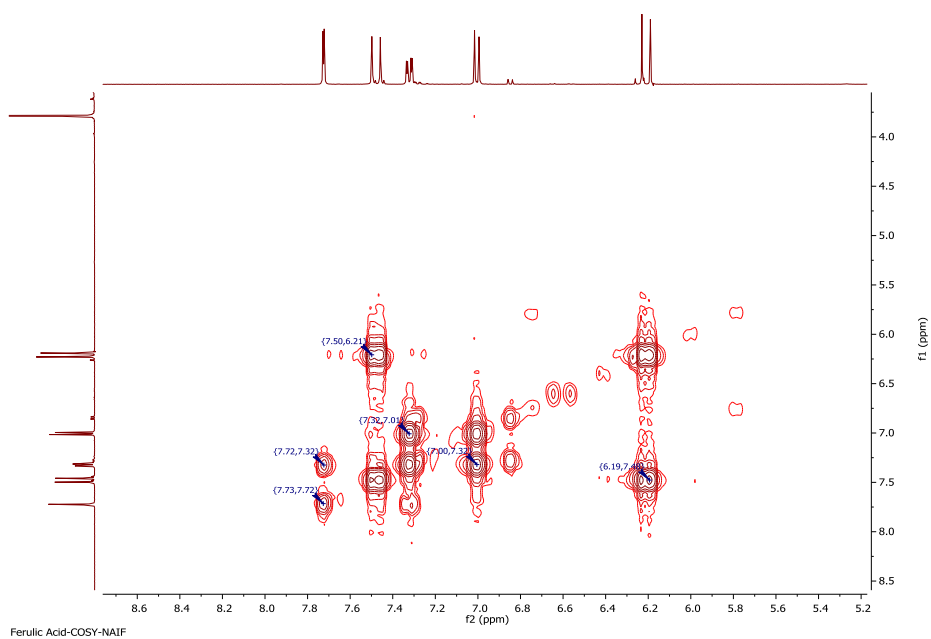


Figure 67: COSY spectrum (400 MHz) of ferulic acid (S-6-13) in DMSO-d_6

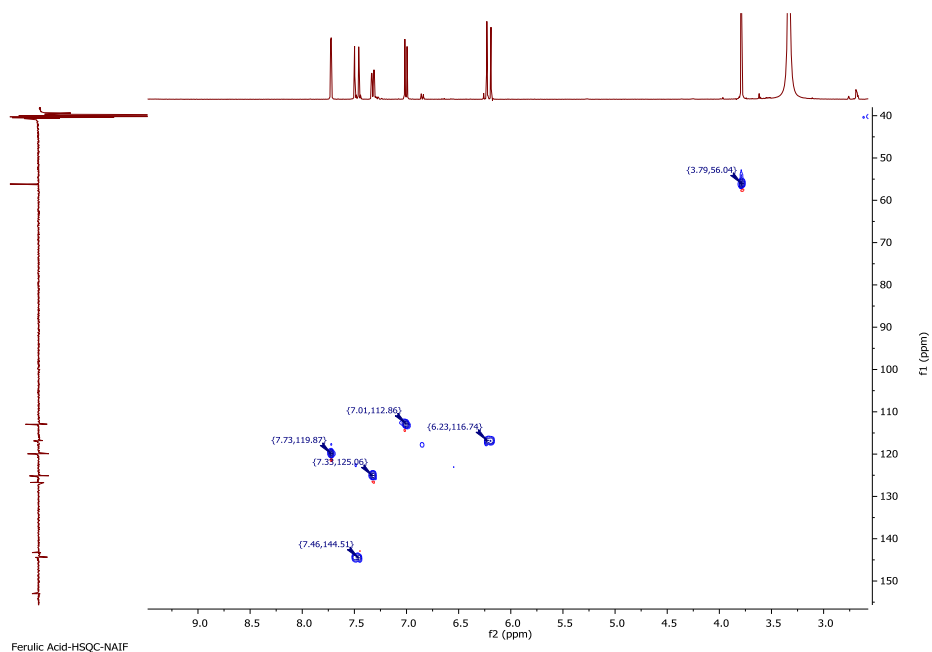


Figure 68: HSQC spectrum (400 MHz) of ferulic acid (S-6-13) in DMSO-d₆

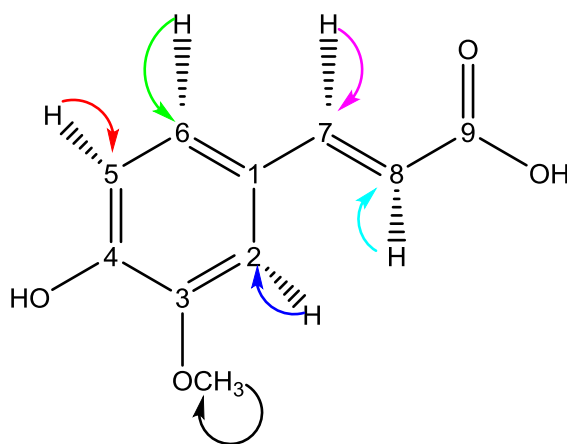


Figure 69: HSQC correlations NMR spectra of ferulic acid. The coloured arrows show the correlations corresponding HSQC correlations in figure (68)

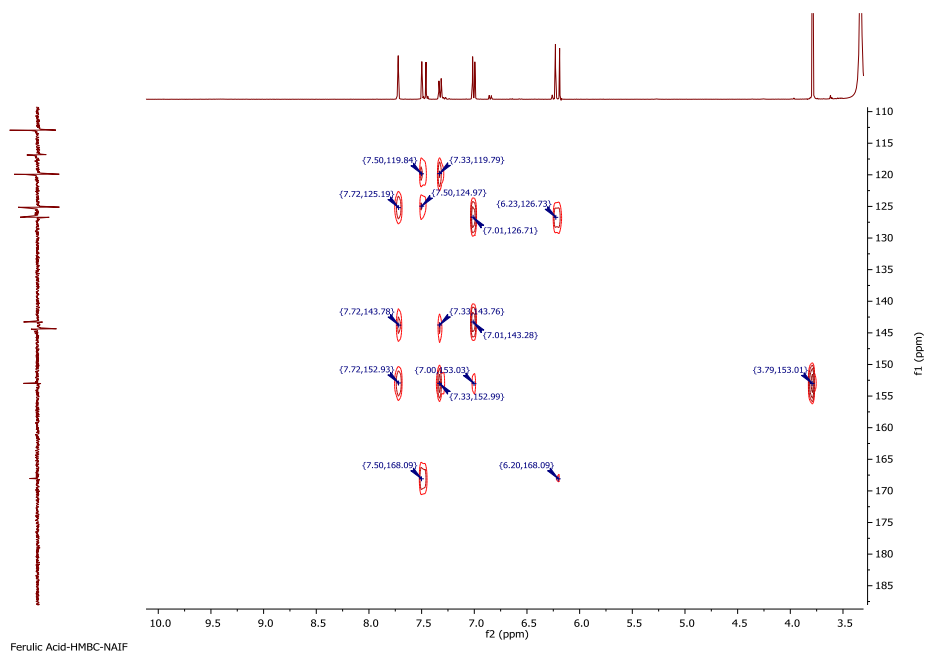


Figure 70: HMBC spectrum (400 MHz) of ferulic acid (S-6-13) in DMSO-d₆

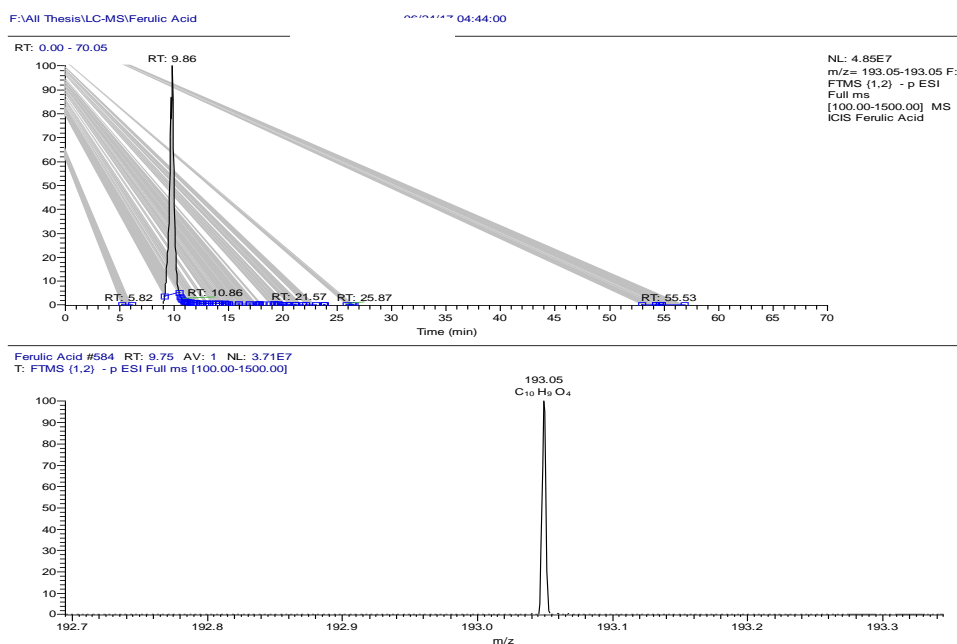


Figure 71: (A) is Extracted ionchromatogram corresponding to the mass of ferulic acid in the negative ion mode (-ve ESI) w (B) The spectrum corresponding to the ferulic acid chromatogram

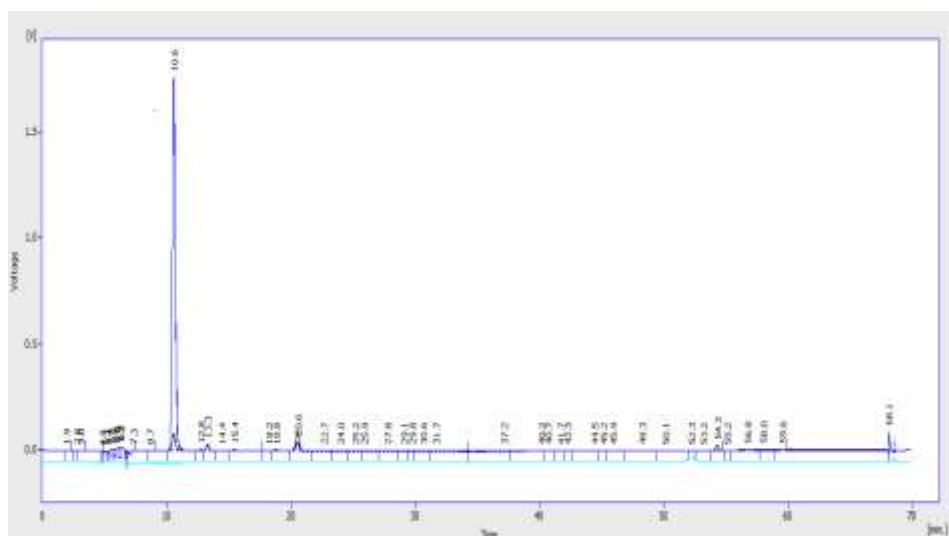


Figure 72: LC-UV-ELSD chromatogram of ferulic acid purified from SEC. (Black traces ELSD and blue trace UV at 290 nm)

4.1.4 Biological activities of Saudi propolis sample against trypanosomes (*T.brucei* S427 strain)

Crude, fractions and pure compounds (fisetinidol and ferulic acid) extracted from Saudi propolis sample were all tested against *T. brucei*. Pentamidine and Diminazene were used as drug controls as their MIC scored 0.0030 and 0.0313 $\mu\text{g/ml}$ respectively. In Table 19 a and b the results from testing the Saudi propolis and its components are shown. The results showed a varying activity against *T. brucei* between the tested samples. S-6 fraction, 2.4 $\mu\text{g/ml}$ MIC, showed the highest activity, among the tested samples, followed by Saudi crude with 4.6 $\mu\text{g/ml}$ MIC whereas fisetinidol and ferulic acid had MICs of 14.7 and 39.9 $\mu\text{g/ml}$ respectively. It is worth to note that all tested samples gave higher cell viability (as the minimum IC₅₀ value was > 60 $\mu\text{g/ml}$) than Pentamidine and Diminazene which gave the lowest IC₅₀

values at 13.32 µg /mL and 29.58 µg/mL, respectively. Table 19b shows detailed IC50 values for tested samples.

Table 19 a: Drug Sensitivity assay of Saudi propolis sample and its fractions on *T. brucei* S427 WT

Sample code	Exp. 1 (µg/ml)	Exp. 2 (µg/ml)	Exp. 3 (µg/ml)	Mean (µg/ml)	SD	%RSD
Saudi crude	4.7	4.4	4.8	4.6	0.21	4.46
S-6 fraction	2.7	2.4	2.2	2.4	0.24	9.87
Fisetinidol	15.0	14.7	14.5	14.7	0.27	1.82
Ferulic acid	38.7	41.0	40.1	39.9	1.19	2.97
Pentamidine(µM)	0.0022	0.0031	0.0036	0.0030	0.0007	23.4583
Diminazen(µM)	0.0246	0.0317	0.0377	0.0313	0.0065	20.8678

Table 19 b: Cytotoxicity assay of Saudi propolis sample and its fractions on U937 cells

Sample code	Exp. 1 (µg/ml)	Exp. 2 (µg/ml)	Exp. 3 (µg/ml)	Mean (µg/ml)	SD	%RSD
Saudi crude	129	122.3	136	129.1	6.85	5.31
S-6 fraction	57.6	56.5	62.1	58.7	2.98	5.08
Fisetinidol	275.6	273.1	222.1	256.9	30.19	11.75
Ferulic acid	86.9	93.8	82.4	87.7	5.74	6.54
Pentamidine(µM)	13.43	14.27	12.25	13.3167	1.0148	7.6202
Diminazen(µM)	29.53	31.77	27.43	29.5767	2.1704	7.3381

4.2 Phytochemical results for Philippine propolis

4.2.1 Introduction

Propolis is primarily produced by honeybees in the Philippines and is imported by other countries mostly for pharmaceutical purposes. However, anticipating a potential crisis when the demand for honeybee propolis would exceed production, the propolis produced by stingless bees of the *Trigona* species has also begun to be used. Nonetheless, the knowledge about the chemical composition and biological effects of propolis produced by stingless bees is still limited so the export of this kind of propolis is not conducted on a wide scale yet (Rabajante and Fajardo Jr, 2013).

4.2.2 Extraction of sample of Philippine raw propolis

Soaking, shaking, reflux and Soxhlet extraction can all help to achieve purification of raw propolis, and are implemented alongside various solvents in order to acquire wax-free propolis extracts with a high content of polyphenolic constituents (Pietta et al., 2002). Absolute ethanol is the most popular solvent used in the preparation of propolis extracts but, as recommended by Park and Ikegaki (1998), tinctures without wax and with a greater concentration of phenolic substances could be obtained by using aqueous ethanol (70-95%) as the solvent for extraction. Nevertheless, ethanol was used to conduct the extraction process in the present study, after which filtration was carried out in order to enable the crude sample of propolis to be subjected to additional chromatographic analysis (table 20).

Table 20: weights of ethanolic Philippine propolis extract

Masses	Weight (g)
Raw propolis sample (g)	83.1662 g
Empty beaker (g)	172.0109 g
Empty beaker + crude sample after cooling and drying (g)	199.2040 g
Crude sample (g)	27.1931 g

High-performance liquid chromatography (HPLC) in association with a number of detectors, including evaporative light scattering detector (ELSD) figure 73, ultraviolet detection (UV), and high resolution mass spectrometry (HRMS), as well as NMR were among the methods used to perform chemical profiling and gain an understanding of the majority of ethanolic crude constituents. Preliminary NMR analysis was conducted on a 10 mg sample of this extract to distinguish the main characteristics of the constituents (figure 74), after which LC-MS was applied to perform LCMS profiling, as indicated in (table 21 and figure 75).

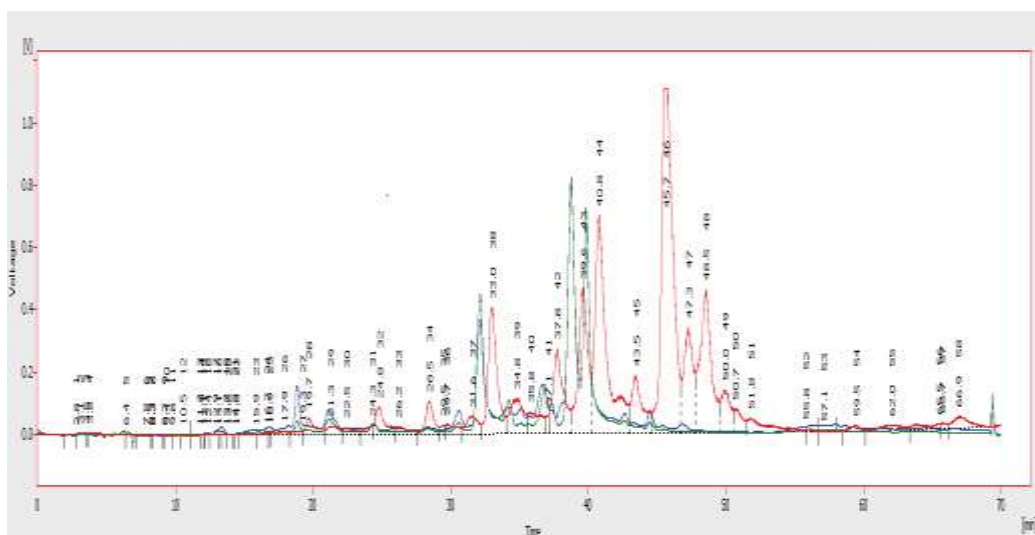


Figure 73: Chromatogram of the ethanolic extract of Philippine propolis with the ELSD (red) and UV detection (green)

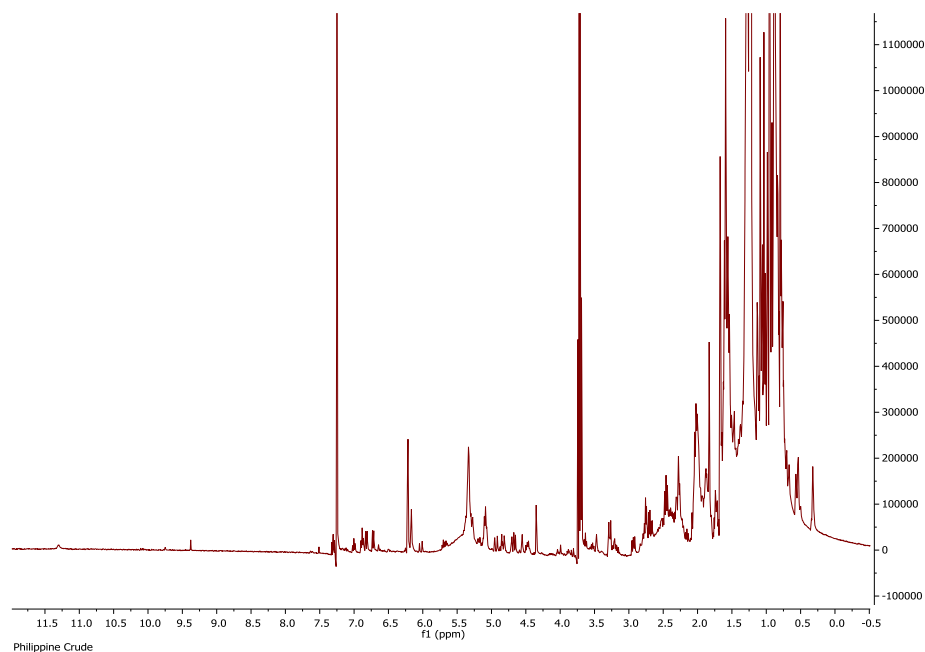


Figure 74: ¹H (400 MHz) NMR spectra of ethanolic Philippine extract in CDCl₃. The main constituents highlighted by ¹H NMR spectrum were terpenoids and fatty acids, while flavonoids and phenolics of lesser intensity compared to terpenoids and fatty acids were detected as well. MeOH extract was observed to contain aliphatic compounds, this was shown by several signals from 0.5 to 3 ppm

Table 21: The LC-MS profiling for ethanolic Philippine extract when analysed by reversed phase LC-MS in negative ion mode

Peak No.	Retention time (min)	[M-1]	Chemical formula	Delta (ppm)	Intensity
1	4.71	371.12	C ₁₃ H ₂₃ O ₁₂	1.753	E 7
2	5.37	169.01	C ₇ H ₅ O ₅	1.381	E 7
3	5.37	339.04	C ₁₄ H ₁₁ O ₁₀	2.419	E 7
4	7.13	153.02	C ₇ H ₅ O ₄	0.379	E 7
5	7.13	307.05	C ₁₄ H ₁₁ O ₈	2.441	E 7
6	7.53	567.21	C ₂₇ H ₃₅ O ₁₃	1.72	E 7
7	8.61	255.11	C ₁₂ H ₁₇ O ₄	1.322	E 6
8	8.61	463.09	C ₂₁ H ₁₉ O ₁₂	2.356	E 6
9	9.38	301	C ₁₄ H ₅ O ₈	2.025	E 7
10	9.38	906.18	C ₂₈ H ₃₃ O ₁₅	2.211	E 7
11	11.93	303.22	C ₁₆ H ₃₁ O ₅	1.658	E 6
12	12.4	261.04	C ₁₃ H ₉ O ₆	1.527	E 6
13	12.5	287.06	C ₁₅ H ₁₁ O ₆	2.155	E 6
14	12.6	309.13	C ₁₆ H ₂₁ O ₆	1.903	E 6
15	13.38	263.13	C ₁₅ H ₁₉ O ₄	1.587	E 6
16	15.24	331.25	C ₁₈ H ₃₅ O ₅	2.091	E 6
17	15.43	265.15	C ₁₅ H ₂₁ O ₄	1.952	E 6
18	15.43	311.15	C ₁₆ H ₂₃ O ₆	2.694	E 6
19	16.99	287.22	C ₁₆ H ₃₁ O ₄	1.905	E 6
20	23.86	201.15	C ₁₁ H ₂₁ O ₃	1.353	E 7
21	30.39	313.24	C ₁₈ H ₃₃ O ₄	2.354	E 6
22	31.45	503.34	C ₃₀ H ₄₇ O ₆	1.426	E 6
23	34.19	315.25	C ₁₈ H ₃₅ O ₄	1.672	E 7
24	36.15	373.24	C ₂₃ H ₃₃ O ₄	2.136	E 6
25	37.22	487.34	C ₃₀ H ₄₇ O ₅	1.995	E 7
26	39.68	359.26	C ₂₃ H ₃₅ O ₃	2.427	E 6
27	39.68	405.27	C ₂₄ H ₃₇ O ₅	1.807	E 6
28	44.17	469.33	C ₃₀ H ₄₅ O ₄	2.017	E 6
29	45.72	387.26	C ₂₄ H ₃₅ O ₄	2.704	E 6
30	45.72	471.35	C ₃₀ H ₄₇ O ₄	2.475	E 6
31	49.54	467.32	C ₃₀ H ₄₃ O ₄	2.026	E 6
32	52.3	455.35	C ₃₀ H ₄₇ O ₃	2.726	E 5
33	59.42	371.26	C ₂₄ H ₃₅ O ₃	2.348	E 6
34	64.81	373.28	C ₂₄ H ₃₇ O ₃	2.282	E 6

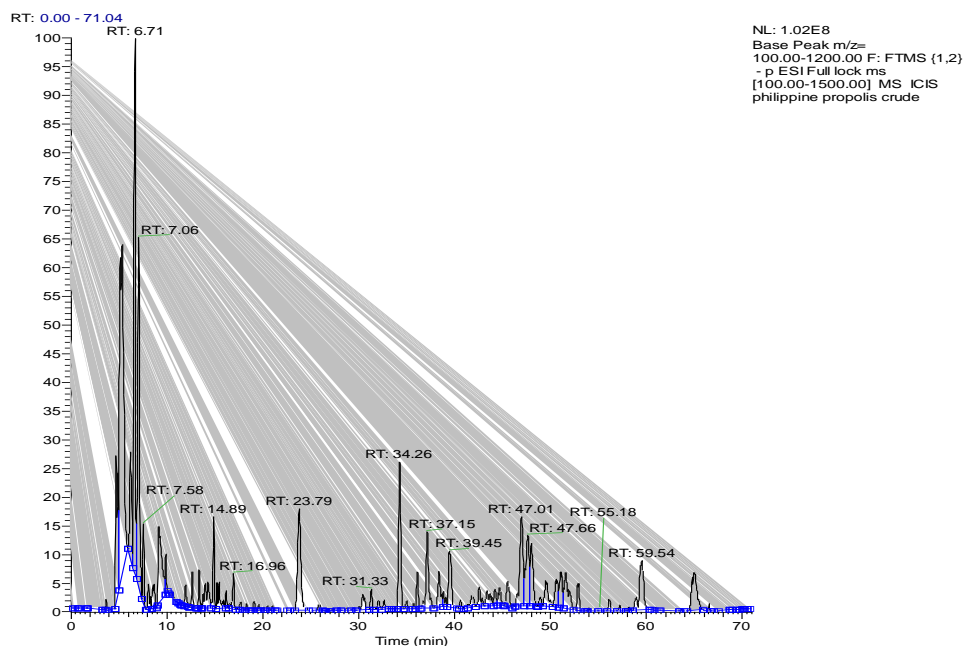


Figure 75: Chromatogram view of ethanolic Philippine crude on the LC-MS negative ion mode (-ve ESI)

According to the results of HPLC-UV-ELSD, the content of the crude sample was mainly due compounds without chromophores, such as terpenoids, fats or other compounds. Although compounds that absorbed UV were also identified, their intensities were not high (figure 73).

An overall picture of the crude sample constituents was obtained through ^1H NMR spectra (figure 74), which indicated strong responses for aliphatic protons. Alkene protons were also important and the main signals in the spectra and suggested terpenoids. Phenolic compounds were indicated by a couple of signals captured by NMR, although their intensities were not as high as those of terpenoids. Considerable complexity was exhibited by the LC-MS chromatogram of the crude sample, which was comprised of numerous peaks of varying intensities. As shown in table (21) and figure (75), terpenoids were the main constituents of the ethanolic extract, according to the results of LC-MS analysis.

A quantity of ethanolic extract of Philippine propolis (5.3 g) was subjected to column chromatography and elution was sequentially performed based on a gradient profile (table 22). The total number of fractions generated was 28, and these were collected in vials with a volume of 50 ml. Chromatographic characteristics were delineated via TLC by using a suitable solvent system. Performance of LC-MS and NMR permitted identification of the different components allowed combination of fractions. The final number of fractions was ten.

Table 22: Sequence of Column Chromatography Solvent Systems and fractions collected

No.	He %	EtOAc %	MeOH %	M.P (ml)	Fractions obtained	Weight (mg)
1	80	20	0	200	fraction Ph1 (M1+M2+M3+M4)	105 mg
2	60	40	0	200	fraction Ph2 (M5+M6+M7+M8)	877 mg
3	40	60	0	100	fraction Ph3 (M9+M10)	210 mg
3	40	60	0	100	fraction Ph4 (M11+M12)	185 mg
4	20	80	0	150	fraction Ph5 (M13+M14+M15)	113 mg
4	20	80	0	50	fraction Ph6 (M16)	80 mg
5	0	100	0	200	fraction Ph7 (M17+M18+m19+m20)	162 mg
6	0	70	30	50	fraction Ph8 (M21)	60 mg
6	0	70	30	150	fraction Ph9 (M22+M23+M24)	150 mg
7	0	50	50	200	fraction Ph10 (M25+M26+M27+M28)	160 mg

Component fraction mass is a vital aspect of chemical analysis due to the fact that, if the chemical component is available in an adequately large quantity, then additional chromatographic separation can be carried out. As indicated in table 23 and figures 76 and 77, LC-MS and HPLC-UV-ELSD analysis highlighted the richest compounds in the 877 mg of Philippine fraction (Ph-2) with a varied composition. Based on preliminary data, the compounds were most likely terpenoids. Therefore, the 877 mg of fraction (Ph-2) was subjected to SEC, yielding 61 sub-fractions (Ph-2-1 to Ph-2-

61), which led to acquisition of three pure compounds (Ph-2-11, Ph-2-14 and Ph-2-20).

Table 23: The most abundant components in the Philippine propolis fraction (PH-2) when analysed by reversed phase LC-MS in negative ion mode

Peak No.	Retention time (min)	[M-1]	Chemical formula	Delta (ppm)	Intensity
1	26.5	263.13	C ₁₅ H ₁₉ O ₄	1.473	E 6
2	39.57	405.27	C ₂₄ H ₃₇ O ₅	2.178	E 7
3	41.85	471.35	C ₃₀ H ₄₇ O ₄	2.284	E 7
4	49.64	469.33	C ₃₀ H ₄₅ O ₄	1.954	E 6
5	50.35	467.32	C ₃₀ H ₄₃ O ₄	2.155	E 7
6	53.72	455.35	C ₃₀ H ₄₇ O ₃	2.924	E 5

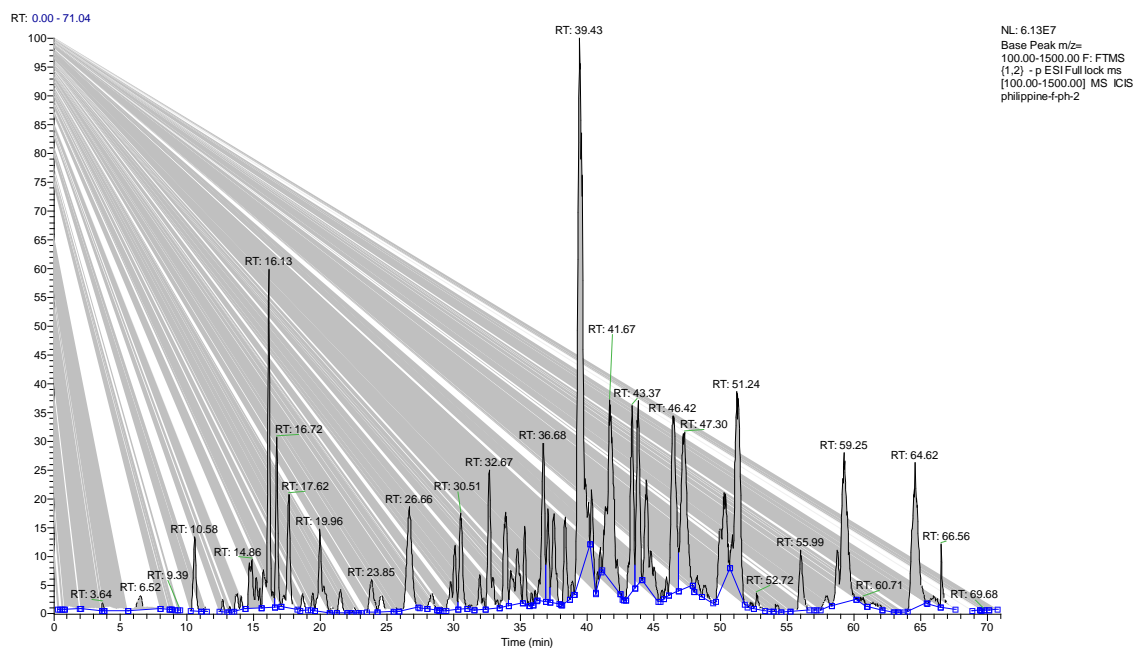


Figure 76: Chromatogram view of Philippine's fraction (Ph-2) analysed by LC-MS negative ion mode

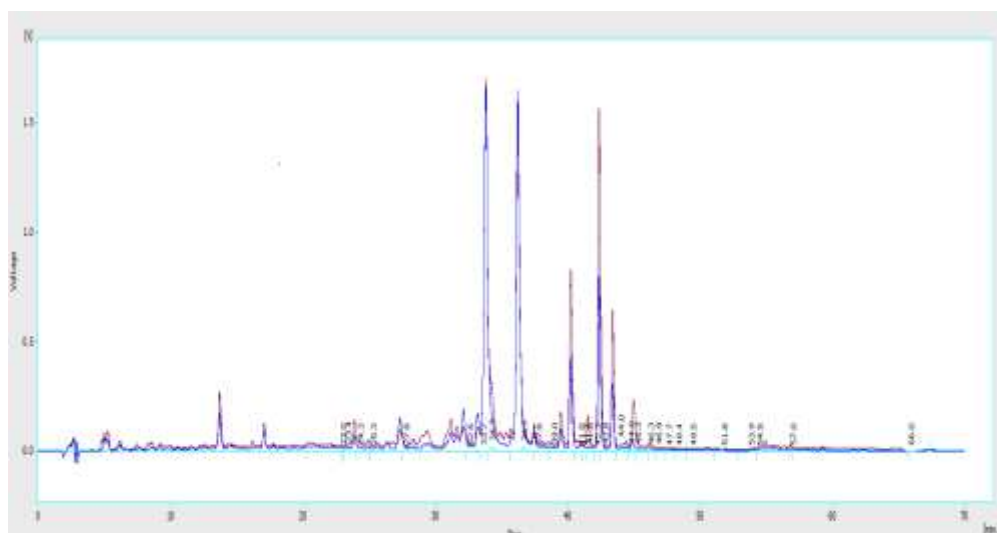


Figure 77: Chromatogram of the Philippine fraction (Ph-2) on the ELSD (blue trace); it is obvious that it consisted primarily of compounds that did not absorb UV (red trace), which could represent terpenoids, fats or other compounds without chromophores, but at retention times of 10 and 25 minutes; although compounds that absorbed UV were also identified, their intensities were not high

4.2.3 Characterisation of Ph-2-14 as 27-hydroxymangiferonic acid

Following several chromatographic methods, including CC, SEC Ph-2-14 was obtained from the ethanolic extract of Philippine propolis, taking the form of a solid of white colour. Spraying with *p*-anisaldehyde-sulphuric acid reagent and subsequent heating caused it to manifest as a single spot on TLC. Elution with the mobile phase 50% HE in EtOAc gave a R_f of 0.68 on SiGel.

The molecular formula $C_{30}H_{45}O_4$ was established based on the fact that the molecular ion $[M-H]^-$ was indicated by the negative mode HRESI-MS spectrum at m/z 469.33 (figure 78). The optical rotation was, $+34^\circ$ was the optical rotation ($c = 0.1$, MeOH).

The proton spectrum of the compound (figure 79, table 24) showed an olefinic triplet at δ_{H} 6.70 ppm, two highly shielded cyclopropane protons at 0.62 and 0.74 ppm, a methyl doublet at 1.02, a proton quartet at 1.47 ppm and an oxygenated methylene group at 4.11 ppm. Other proton signals were typical of a triterpene moiety. The carbon spectrum showed 30 carbon signals including a saturated cyclic ketone at δ_{C} 215.36 ppm, a carboxylic acid carbon at 168.83, two olefinic carbons at 145.48 (CH) and 132.85 (C), one oxygen bearing carbon at 55.23 ppm and five methyl (CH₃) signals. The protons directly bonded to carbons were obtained from the HSQC spectrum while the COSY spectrum was used to identify any neighbouring proton connectivity.

Finally the long range (³*J* and ²*J*) and one bond (¹*J*) proton-carbon correlations were used to confirm the structure and assign the chemical shifts for the compound. Correlations from the oxymethylene protons at C-27 to the carboxylic acid at C-26 indicates they were germinal. While other correlations from H-24 confirmed C-26, C-27 and C-22 and correlations from H-28 and H-29 identified C-3, C-4, C-5 and the germinal methyl carbons at C-4. The full chemical shift assignments (table 23) are in good agreement with literature reports (Escobedo-Martínez et al., 2012; Mahato and Kundu, 1994).

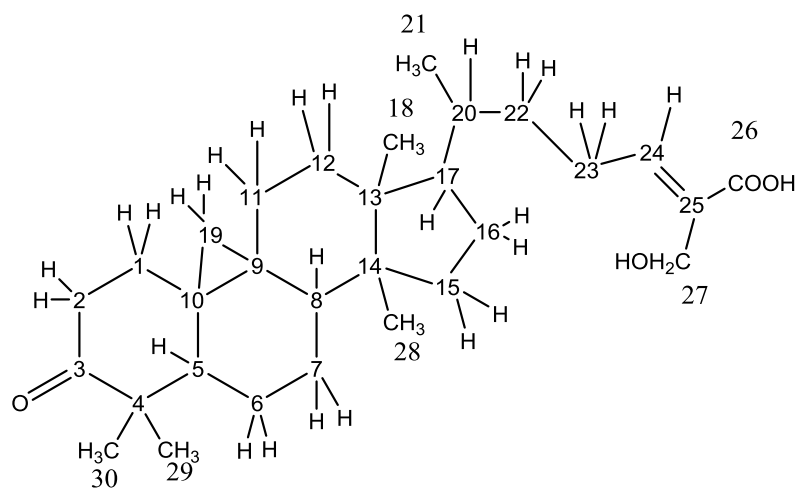


Figure 78: Structure of 27-hydroxymangiferonic acid

Table 24: ^1H (400 MHz) and ^{13}C (100 MHz) NMR data of 27-hydroxymangiferonic acid (Ph-2-14) in DMSO-d_6

Expreimental Data		
Position	^1H (multiplicity), J (Hz)	^{13}C (multiplicity)
1	1.88 (m), 1.53 (m)	33.04
2	2.70 (m), 2.32 (m)	37.4
3		215.36
4		49.95
5	1.75 (dd, $J= 13.24, 4.55$)	48.2
6	1.57 (m), 0.96 (s)	21.41
7	1.39 (s), 1.16 (m)	25.9
8	1.60 (s)	47.75
9		20.94
10		25.93
11	2.06 (s), 1.18 (s)	26.4
12	1.64 (m, 2H)	32.89
13		45.38
14		48.78
15	1.32 (m, 2H)	35.59
16	1.92 (s, 2H)	28.1
17	1.62 (s)	52.06
18	0.98 (s, 3H)	18.39
19	0.74 (d, $J= 3.97$), 0.62 (d, $J= 4.06$)	29.16
20	1.47 (s)	35.88
21	1.02 (s, 3H)	18.42
22	1.24 (s), 1.62 (s)	25.22
23	2.16 (m), 2.67 (m)	35.36
24	6.70 (t, $J= 7.65$)	145.48
25		132.85
26		168.83
27	4.11 (s, 2H)	55.23
28	0.94 (s, 3H)	22.61
29	1.02 (s,3H)	20.86
30	0.91 (s, 3H)	19.55

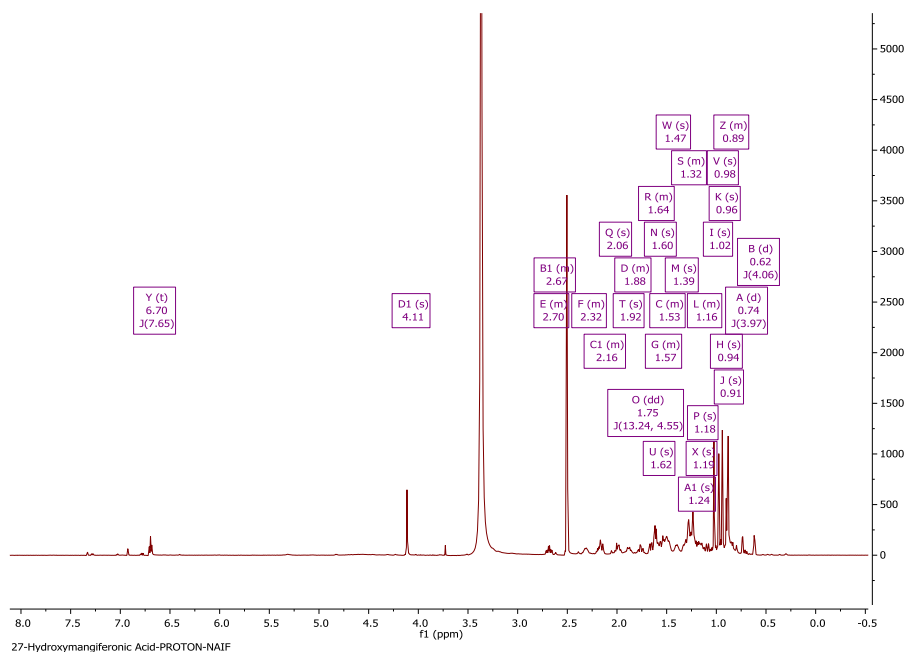


Figure 79: ^1H NMR spectrum (400 MHz) of 27-hydroxymangiferonic acid (Ph-2-14) in DMSO-d_6

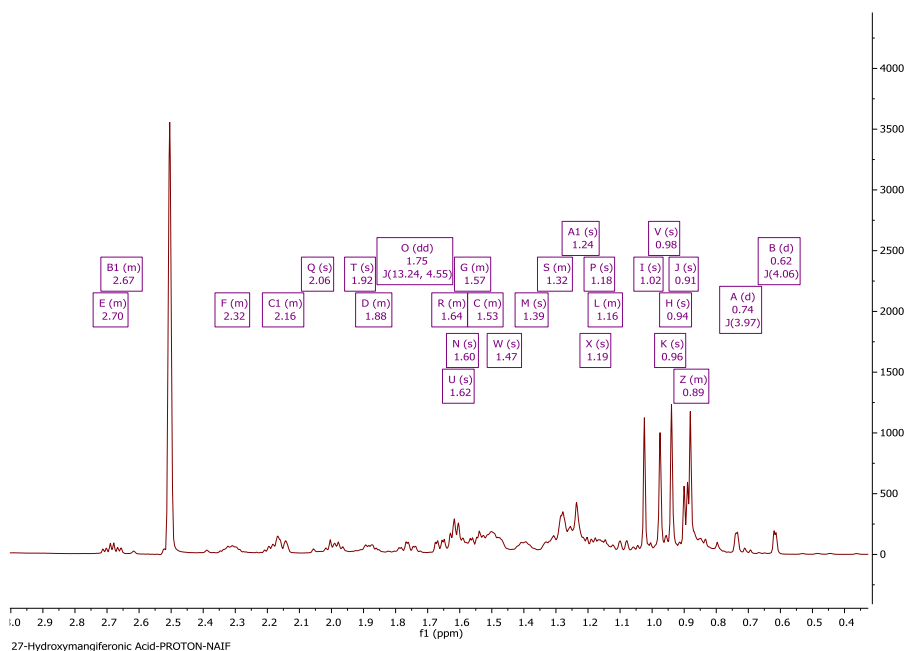


Figure 80: Selected ^1H NMR spectrum expansion for the aliphatic region of 27-hydroxymangiferonic acid (Ph-2-14)

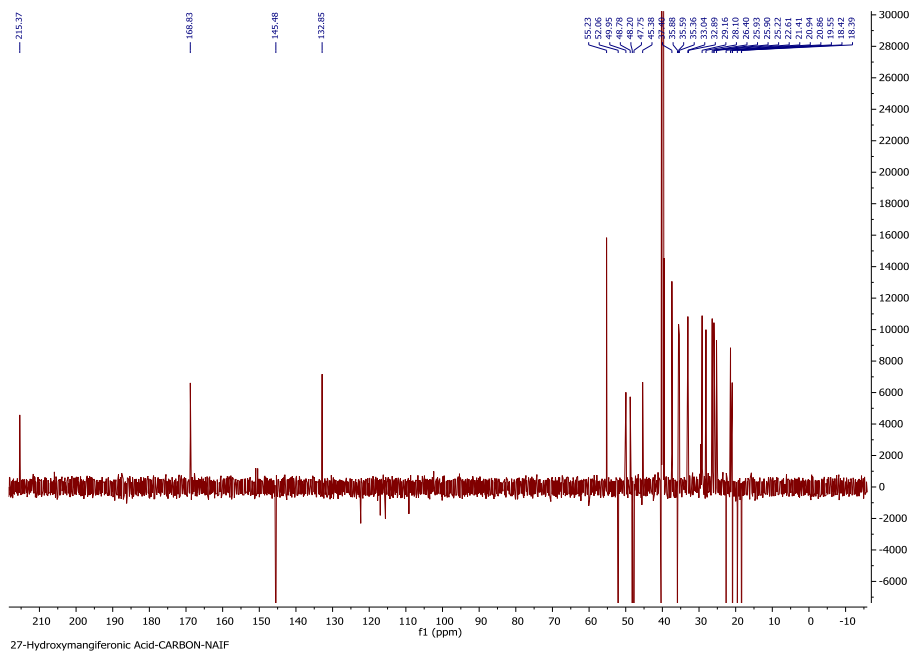


Figure 81: Full DEPTq ^{13}C NMR spectrum (100 MHz) of 27-hydroxymangiferonic acid (Ph-2-14) in DMSO-d_6

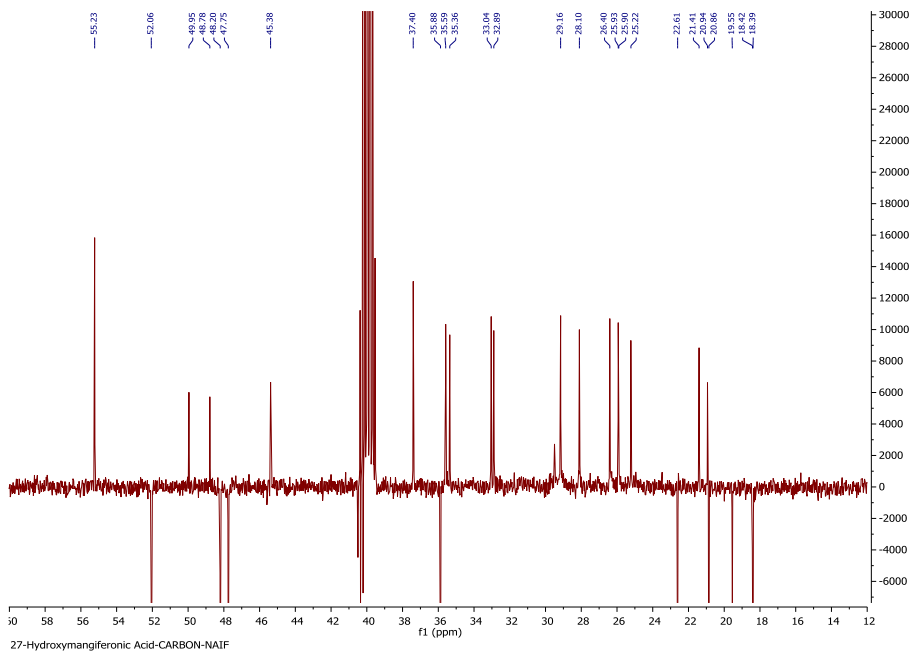


Figure 82: Selected ^{13}C NMR spectrum expansion for the aliphatic region of 27-hydroxymangiferonic acid (Ph-2-14)

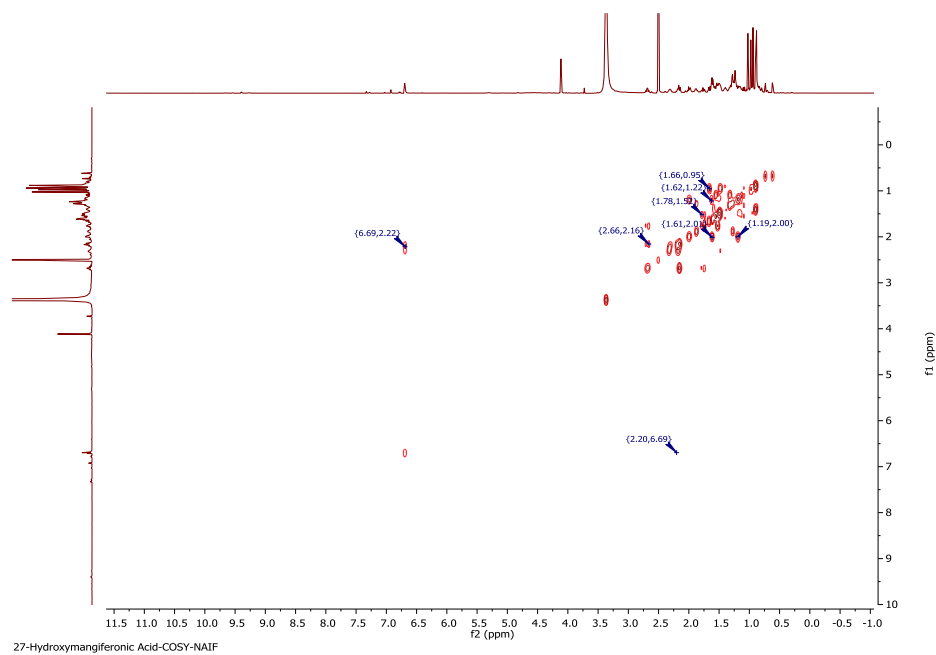


Figure 83: COSY spectrum (400 MHz) of 27-hydroxymangiferonic acid (Ph-2-14) in DMSO-d₆

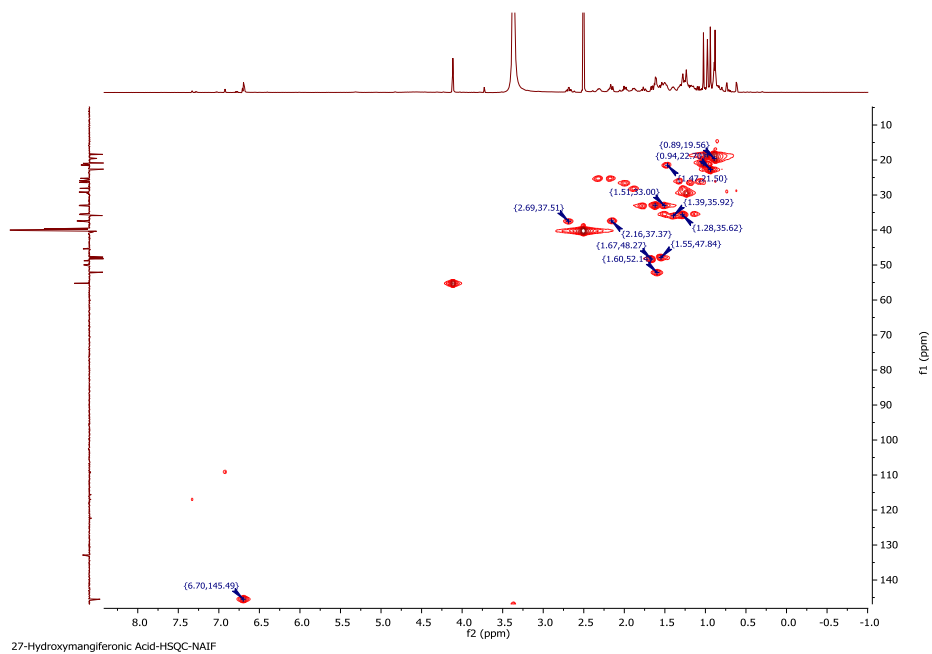


Figure 84: HSQC spectrum (400 MHz) of 27-hydroxymangiferonic acid (Ph-2-14) in DMSO-d₆

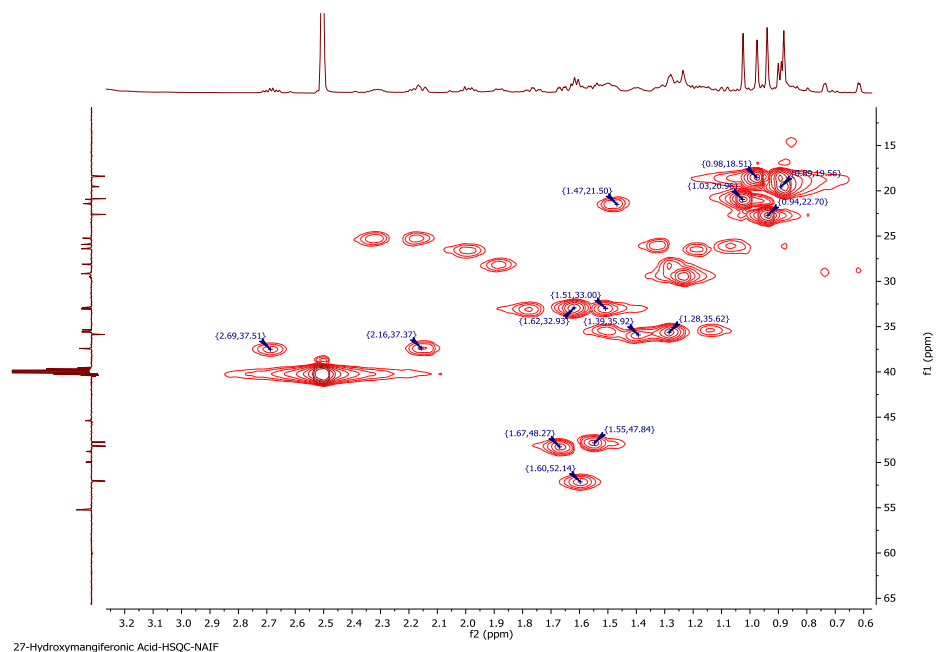


Figure 85: Selected HSQC spectrum expansion for the aliphatic region of 27-hydroxymangiferonic acid (Ph-2-14)

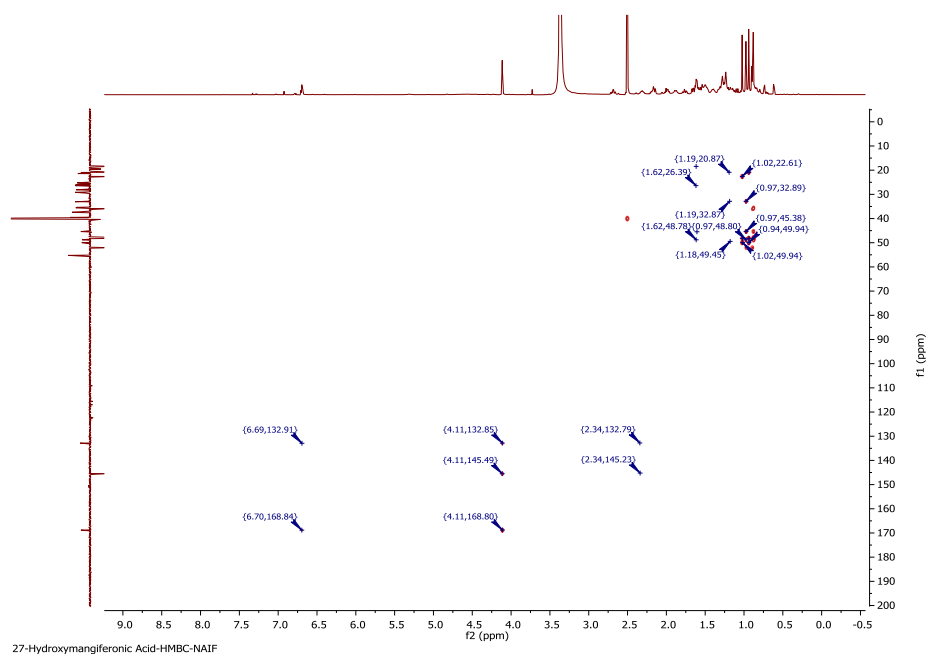


Figure 86: HMBC spectrum (400 MHz) of 27-hydroxymangiferonic acid (Ph-2-14) in DMSO-d₆

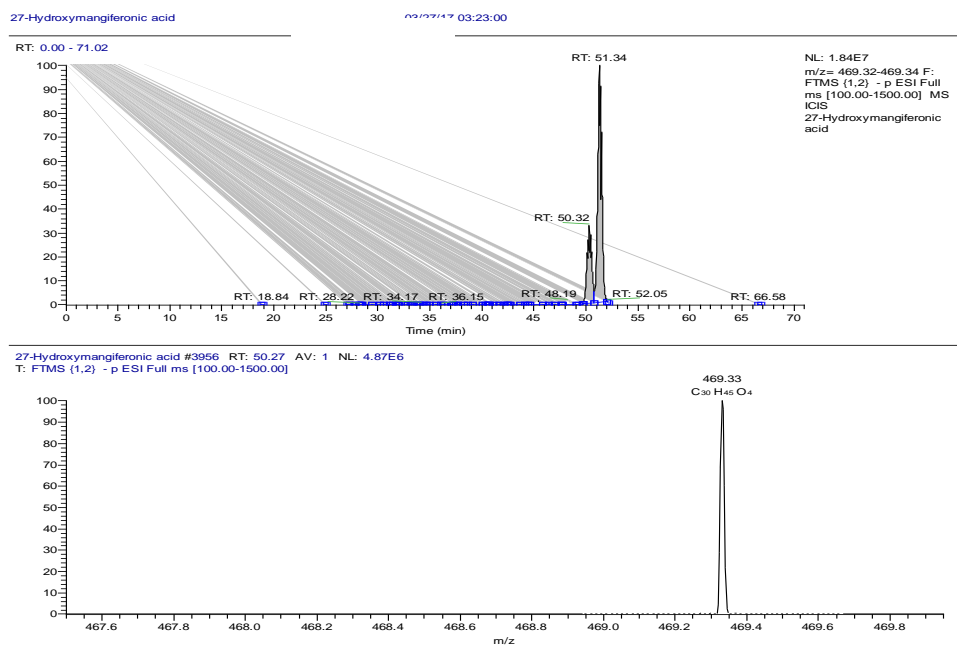


Figure 87: (A) Extracted ion chromatogram corresponding to the mass of 27-hydroxymangiferonic acid in the negative ion mode (-ve ESI) (B) The spectrum corresponding to the 27-hydroxymangiferonic acid chromatogram

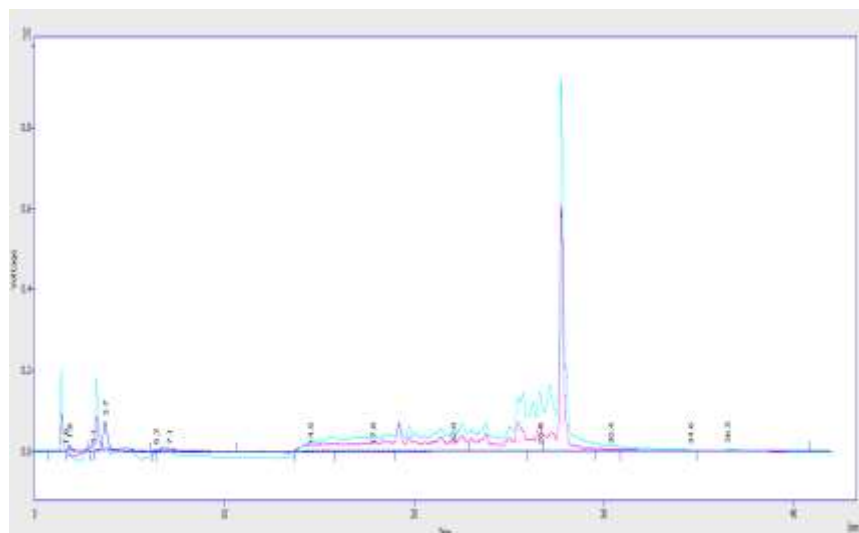


Figure 88: LC-UV-ELSD chromatogram of 27-hydroxymangiferonic acid purified from SEC

4.2.4 Characterisation of Ph-2-11 as 27-hydroxyisomangiferolic acid

CC and then SEC was performed for isolation of Ph-2-11 from the ethanolic extract of Philippine propolis. Spraying with *p*-anisaldehyde-sulphuric acid reagent and exposure to heat caused it to manifest as one spot on TLC. Elution with the mobile phase 50% HE in EtOAc gave a R_f of 0.70 on SiGel.

A molecular formula of $C_{30}H_{47}O_4$ was derived from the fact that the molecular ion $[M-H]^-$ was indicated by the negative mode HRESI-MS spectrum at m/z 471.35 (figure 89), and the optical rotation had a value of $+23.5^\circ$ ($c = 0.085$, MeOH).

Its proton spectrum (figure 90, table 25) was identical to that of Ph-2-14 except for the presence of a proton doublet of doublets at δ_H 3.06 ppm. The carbon spectrum was also identical except for the absence of the ketone carbonyl at δ_C 215.4 and the presence of an oxymethine carbon at 77.09 ppm. This supports the replacement of the ketone at C-3 and its replacement with an $-OH$ group. Examination of its 2D spectra afforded the assignment of its chemical shifts and confirmed by literature reports (Mahato and Kundu, 1994; Nguyen et al., 2016).

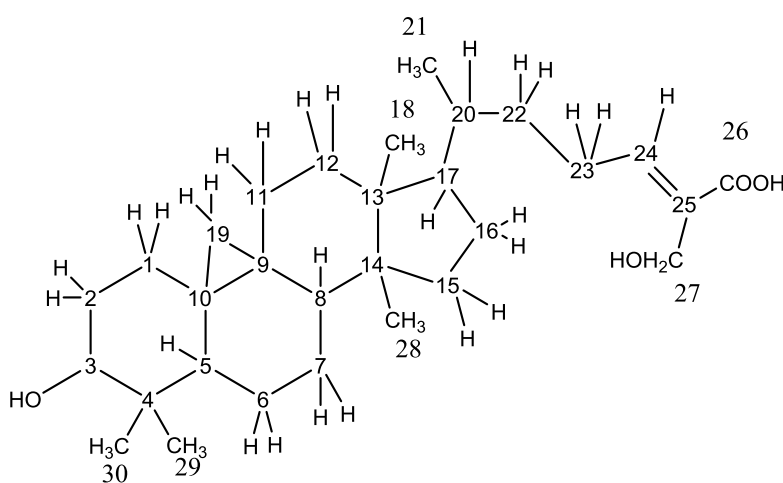


Figure 89: Structure of 27-hydroxyisomangiferolic acid

Table 25: ^1H (400 MHz) and ^{13}C (100 MHz) NMR data of 27-hydroxyisomangiferolic acid
(Ph-2-11) in DMSO-d_6

Experimental Data		
Position	^1H (multiplicity), J (Hz)	^{13}C (multiplicity)
1	1.81 (m), 1.02 (m)	28.1
2	1.93 (m), 1.62 (m)	29.09
3	3.06 (dd, $J= 4.75$)	77.09
4		39.56
5	1.84 (m)	40.56
6	1.49 (m), 0.76 (m)	21.14
7	1.24 (m), 1.09 (m)	25.04
8	1.55 (s)	47.85
9		19.55
10		26.68
11	2.01 (s), 1.14 (m)	26.33
12	1.65 (s, 2H)	32.97
13		45.33
14		48.86
15	1.26 (m, 2H)	35.55
16	1.90(s), 1.29 (s)	28.18
17	1.59 (s)	52.07
18	0.99 (s, 3H)	18.34
19	0.49 (d, $J= 3.98$), 0.30 (d, $J= 3.87$)	29.72
20	1.43 (m)	35.86
21	0.9 (d, $J= 3.56$, 3H)	18.4
22	1.57 (s), 1.18 (s)	35.48
23	2.25 (d), 2.12 (s)	26.08
24	6.62 (t, $J= 7.67$)	145.78
25		132.84
26		168.35
27	4.11 (s, 2H)	55.83
28	0.94 (s, 3H)	26.13
29	0.89 (s,3H)	21.66
30	0.98 (s, 3H)	19.76

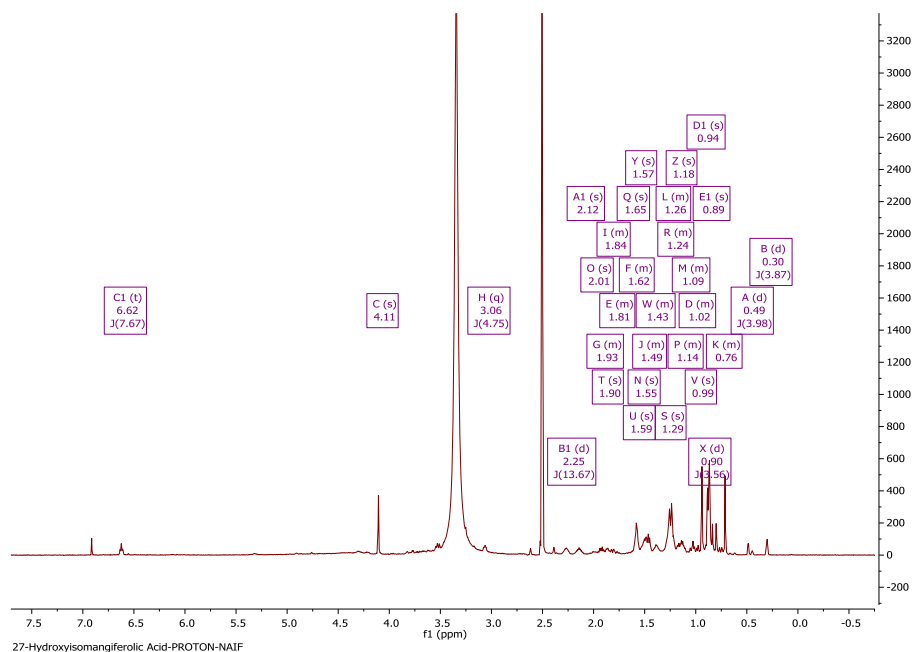


Figure 90: ^1H NMR spectrum (400 MHz) of 27-hydroxyisomangiferolic acid (Ph-2-11) in DMSO-d_6

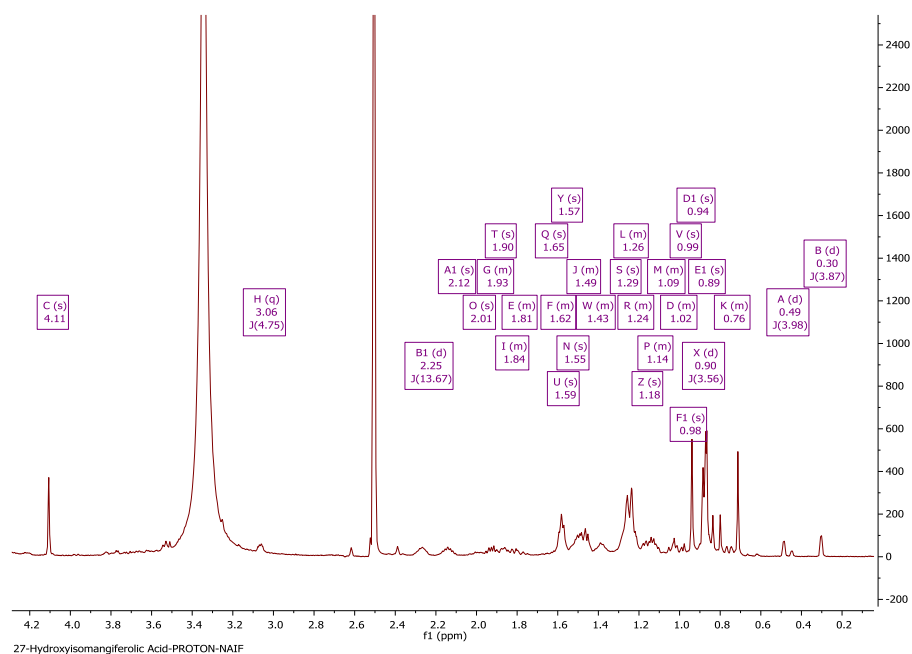


Figure 91: Selected ^1H NMR spectrum expansion for 27-hydroxyisomangiferolic acid (Ph-2-11) in the aliphatic region

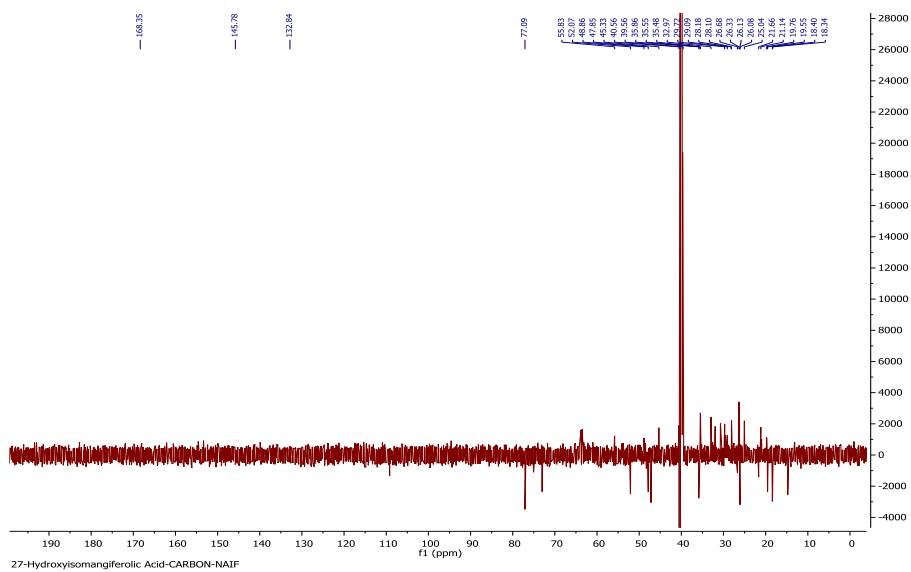


Figure 92: Full DEPTq 135 ^{13}C NMR spectrum (100 MHz) of 27-hydroxyisomangiferolic acid (Ph-2-11) in DMSO-d_6

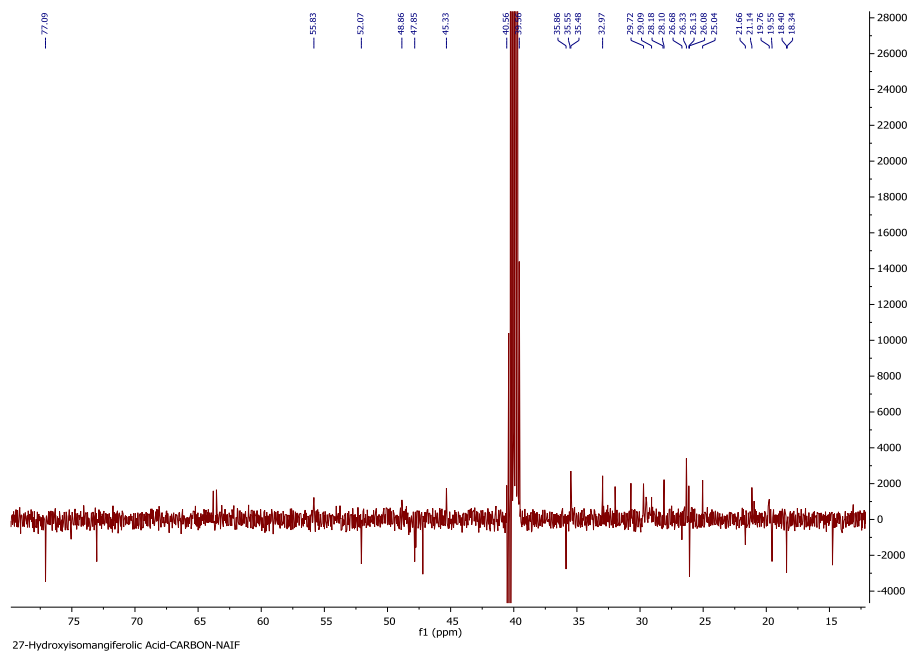


Figure 93: Selected ^{13}C NMR spectrum expansion for the aliphatic region of 27-hydroxyisomangiferolic acid (Ph-2-11)

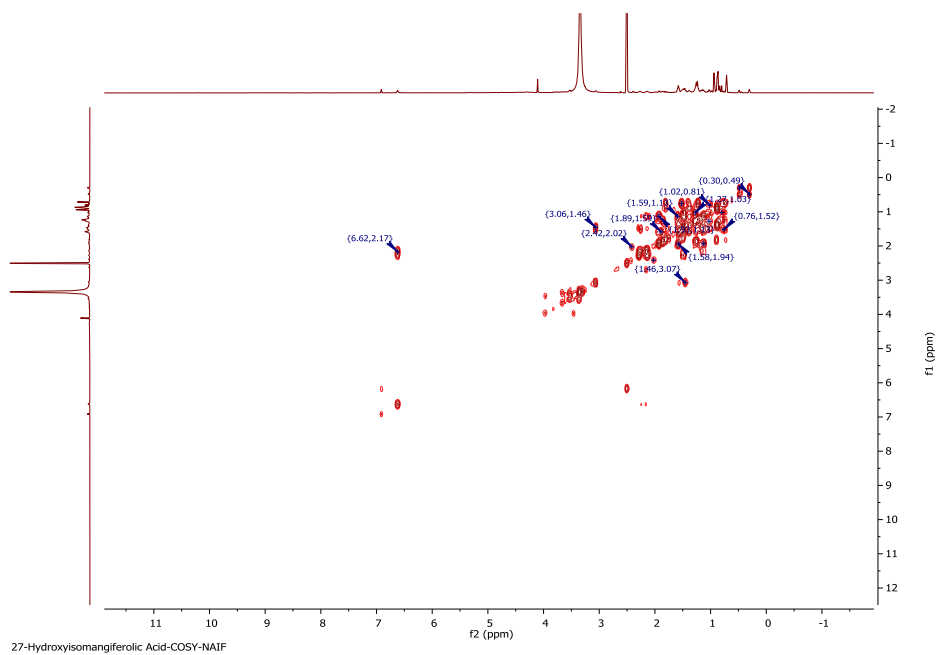


Figure 94: COSY spectrum (400 MHz) of 27-hydroxyisomangiferolic acid (Ph-2-11) in DMSO-d₆

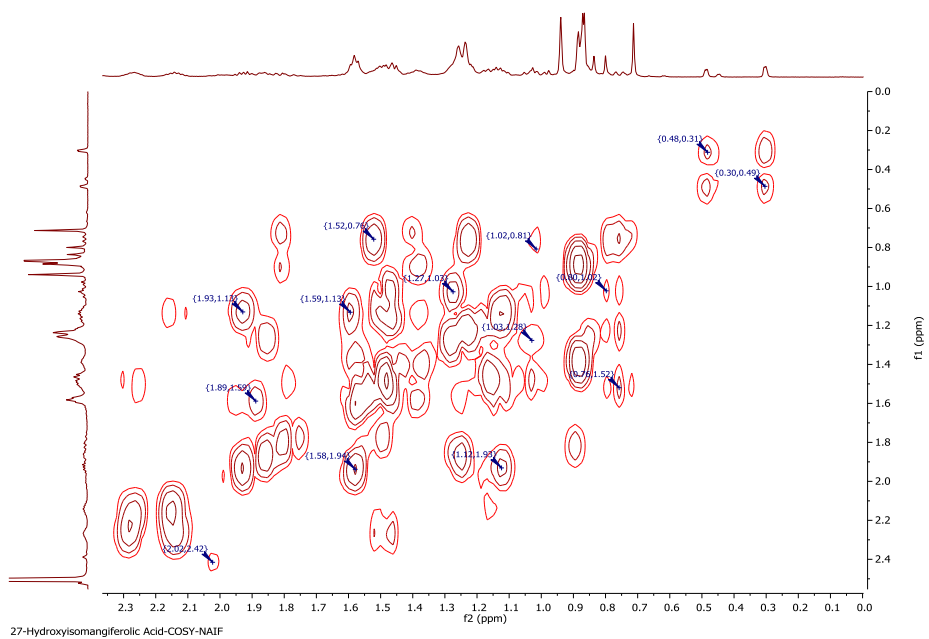


Figure 95: Selected COSY spectrum expansion for the aliphatic region of 27-hydroxyisomangiferolic acid (Ph-2-11)

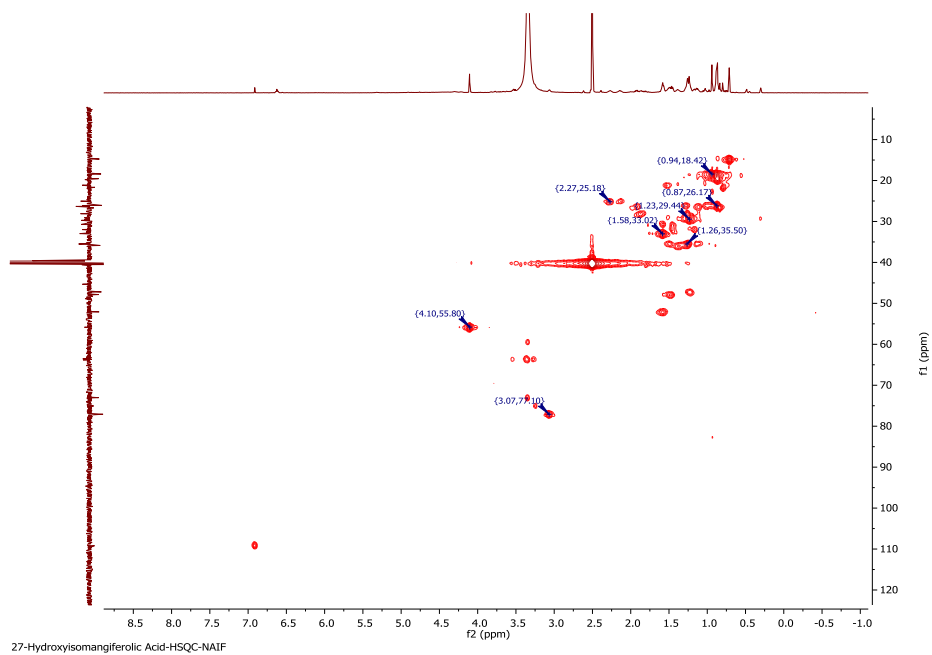


Figure 96: HSQC spectrum (400 MHz) of 27-hydroxyisomangiferolic acid (Ph-2-11) in DMSO-d₆

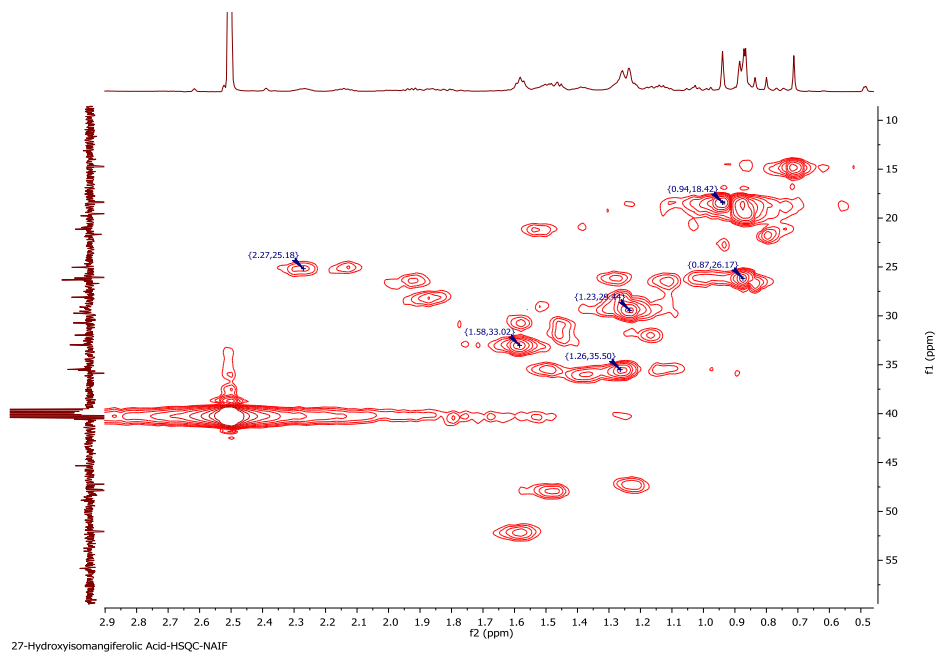


Figure 97: Selected HSQC spectrum expansion for the aliphatic region of 27-hydroxyisomangiferolic acid (Ph-2-11)

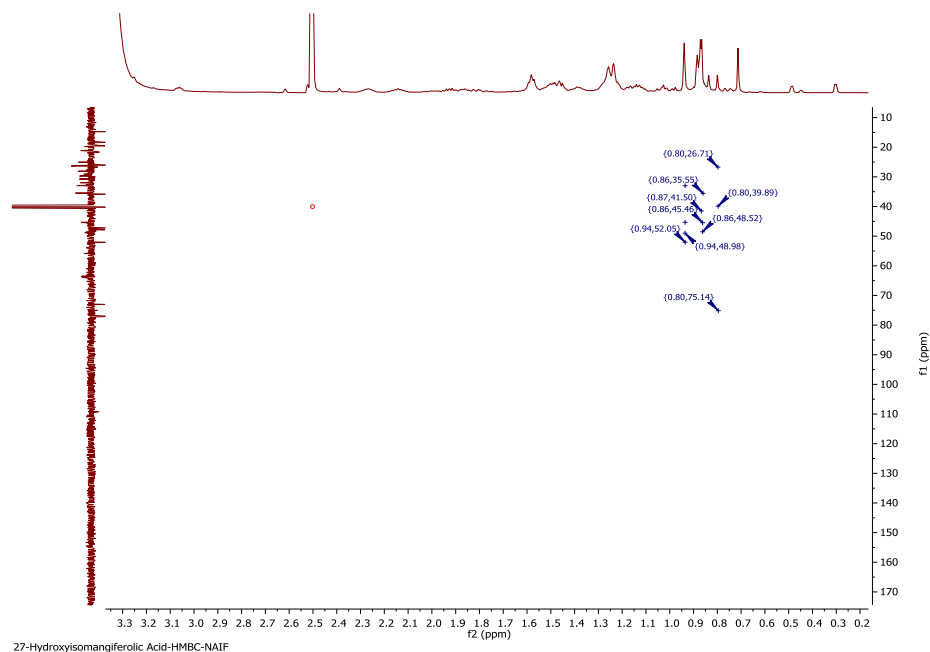


Figure 98: HMBC spectrum (400 MHz) of 27-hydroxyisomangiferolic acid (Ph-2-11) in DMSO-d₆

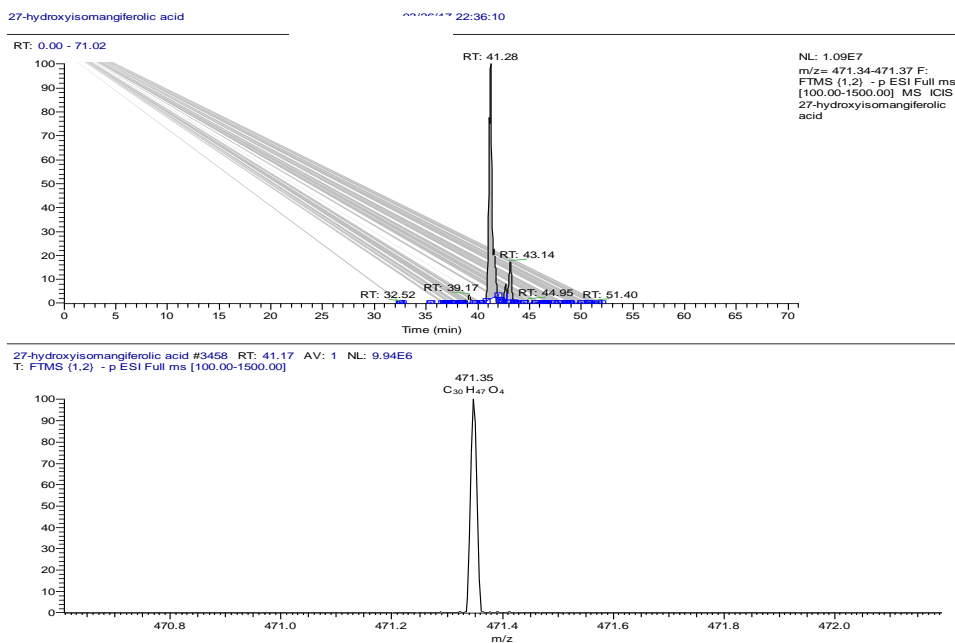


Figure 99: (A) Extracted ion chromatogram corresponding to the mass of 27-hydroxyisomangiferolic acid in the negative ion mode (-ve ESI) (B) The spectrum corresponding to 27-hydroxyisomangiferolic acid chromatogram

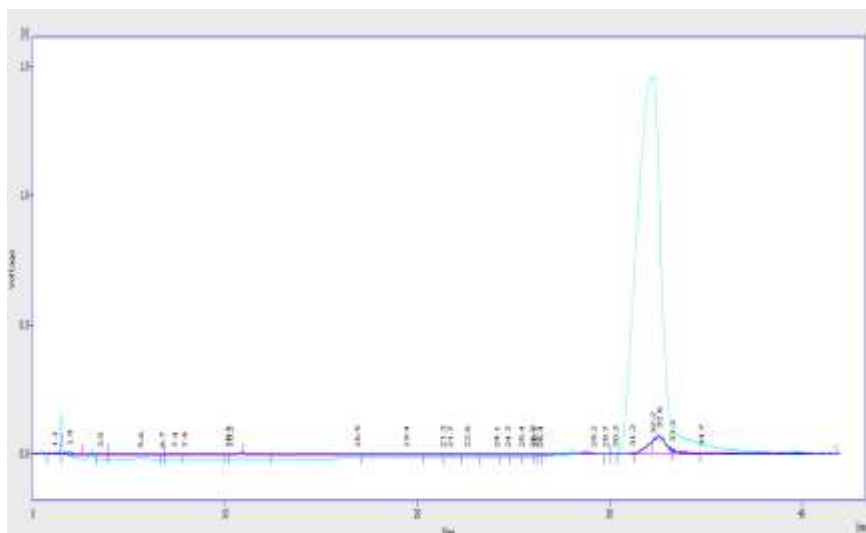


Figure 100: LC-UV-ELSD chromatogram of 27-hydroxyisomangiferolic acid purified from SEC

4.2.5 Characterisation of Ph-2-20 as isomangiferolic acid

CC and then SEC was performed for isolation of Ph-2-20 from the ethanolic extract of Philippine propolis. Spraying with *p*-anisaldehyde-sulphuric acid reagent and exposure to heat caused it to manifest as one spot on TLC. Elution with the mobile phase 50% HE in EtOAc gave a R_f of 0.70 on SiGel.

A molecular formula of $C_{30}H_{47}O_3$ was derived from the fact that the molecular ion $[M-H]^-$ was indicated by the negative mode HRESI-MS spectrum at m/z 455.35 (figure 101), and the optical rotation had a value of $+32^\circ$ ($c = 0.1$, MeOH).

The compound's proton spectrum (figure 102, table 26) was identical to that of compound Ph-2-11 except for the absence of the oxymethylene singlet at 4.11 ppm which was now replaced by a methyl singlet at 1.77 ppm(d, $J = 1.31$, 3H). All other proton signals were identical. The carbon spectrum also showed the absence of the oxymethylene carbon at 55.83 and the presence of another methyl carbon signal at 11.99 ppm. Comparing the chemical shifts and coupled with literature reports

(Mahato and Kundu, 1994, Escobedo-Martínez et al., 2012), the compound was identified as isomangiferolic acid.

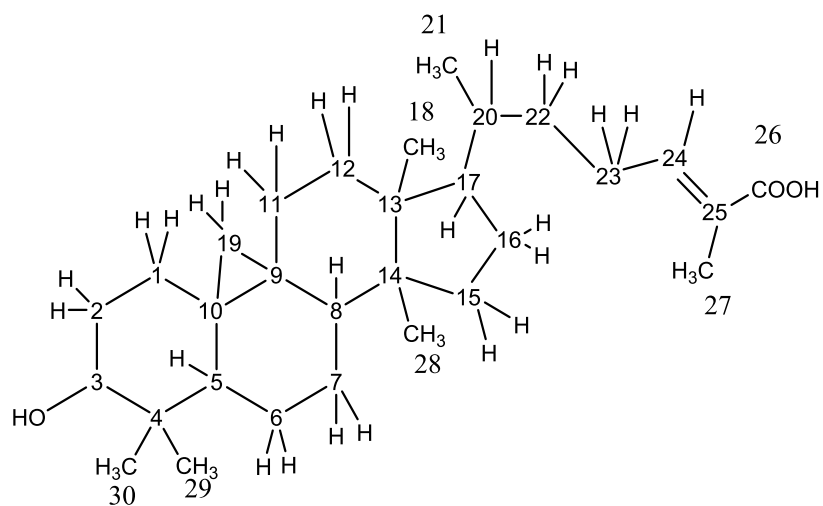


Figure 101: Structure of isomangiferolic acid

Table 26: ^1H (400 MHz) and ^{13}C (100 MHz) NMR data of isomangiferolic acid(Ph-2-200 in CDCl_3)

Expreimental Data		
Position	^1H (multiplicity), J (Hz)	^{13}C (multiplicity)
1	1.83 (m), 1.02 (s)	27.22
2	1.92 (m), 1.63 (m)	27.83
3	3.22 (m)	78.89
4		40.49
5	1.83 (m)	45.61
6	1.48 (s), 0.77 (m)	21.12
7	1.27 (m), 1.12 (m)	25.44
8	1.55 (m)	47.97
9		19.32
10		26.46
11	2.02 (m), 1.18 (m)	26.09
12	1.69 (m, 2H)	32.91
13		45.36
14		48.82
15	1.35 (m, 2H)	35.55
16	1.87 (m), 1.27 (m)	28.16
17	1.57 (s)	52.21
18	0.99 (s, 3H)	18.07
19	0.26 (d, $J=4.19$), 0.49 (d, $J=4.22$)	29.71
20	1.40 (m)	36.03
21	0.93 (s, 3H)	18.12
22	1.57 (s), 1.18 (m)	34.81
23	2.21 (m), 2.17 (m)	26.01
24	6.83 (m)	145.78
25		126.56
26		172.78
27	1.77 (d, $J=1.31$, 3H)	11.99
28	0.91 (s, 3H)	19.98
29	0.90 (s, 3H)	22.58
30	0.97 (s, 3H)	25.93

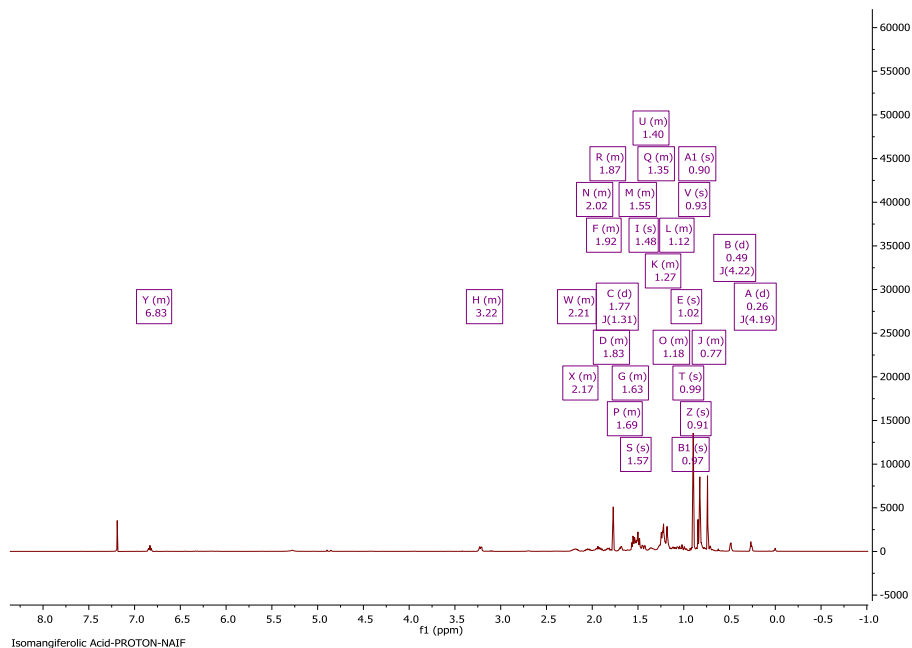


Figure 102: ^1H NMR spectrum (400 MHz) of isomangiferolic acid (Ph-2-20) in CDCl_3

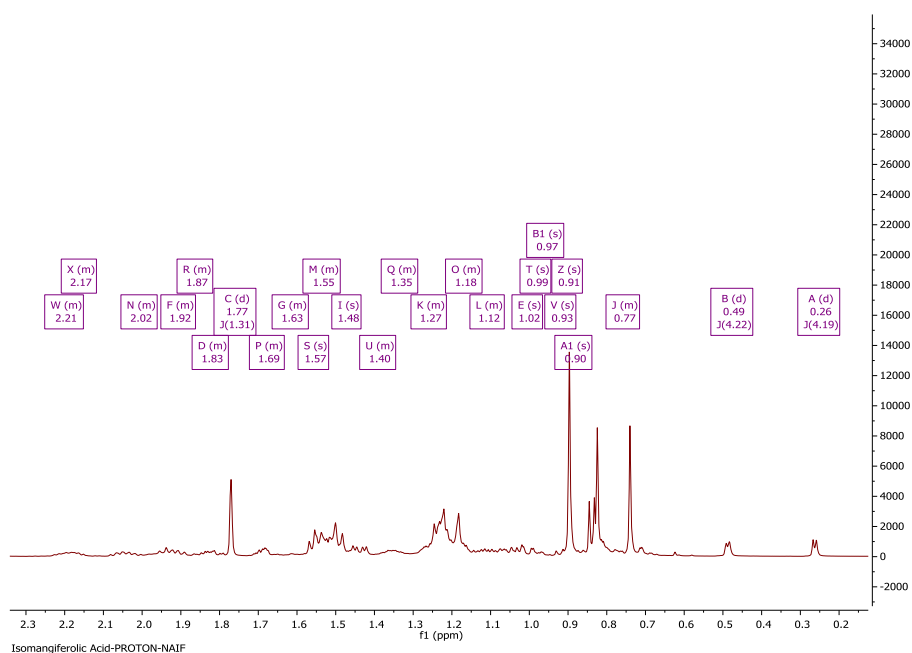


Figure 103: Selected ^1H NMR spectrum expansion of isomangiferolic acid (Ph-2-20) for the aliphatic region

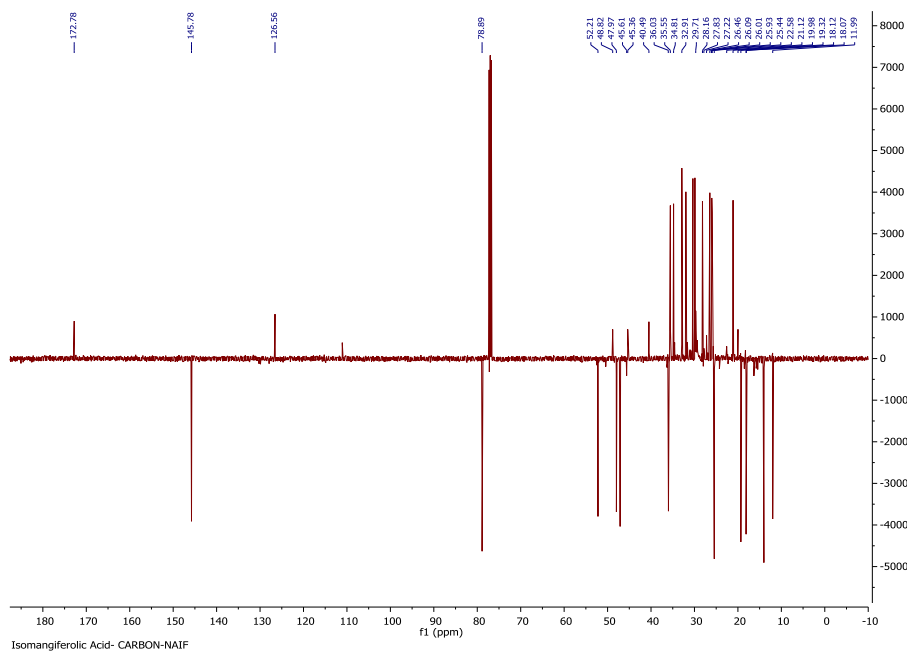


Figure 104: Full DEPTq ^{13}C NMR spectrum (100 MHz) of isomangiferolic acid (Ph-2-20) in CDCl_3

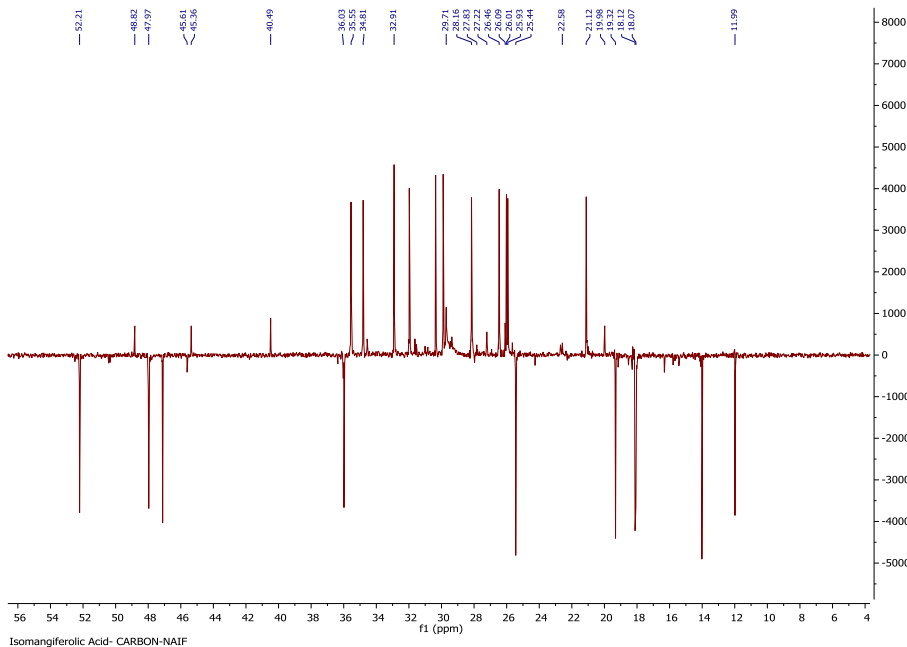


Figure 105: Selected ^{13}C NMR spectrum expansion for the aliphatic region of isomangiferolic acid (Ph-2-20)

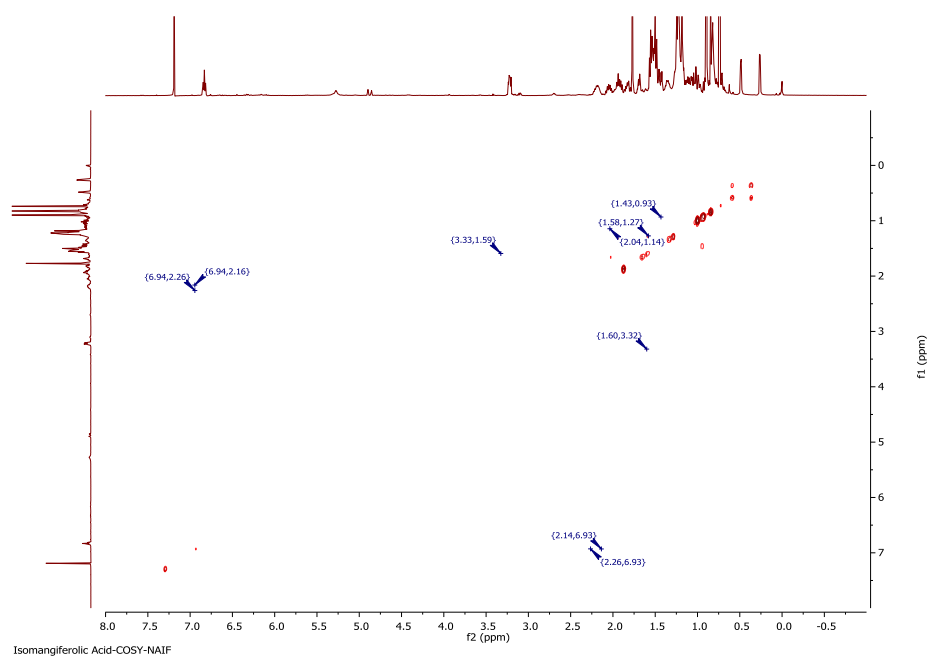


Figure 106: COSY spectrum (400 MHz) of isomangiferolic acid (Ph-2-20) in CDCl_3

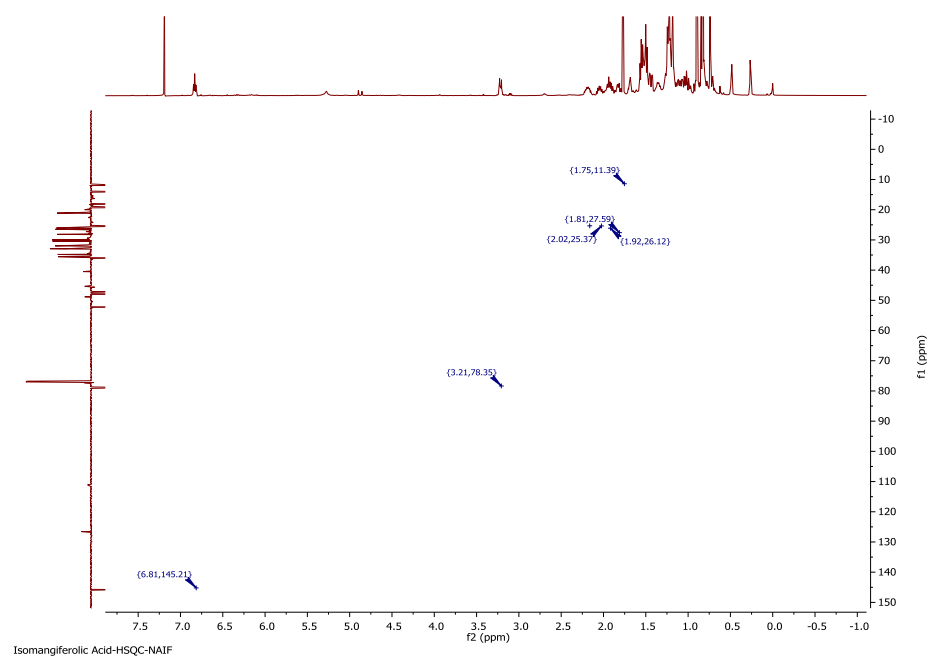


Figure 107: HSQC spectrum (400 MHz) of isomangiferolic acid (Ph-2-20) in CDCl_3

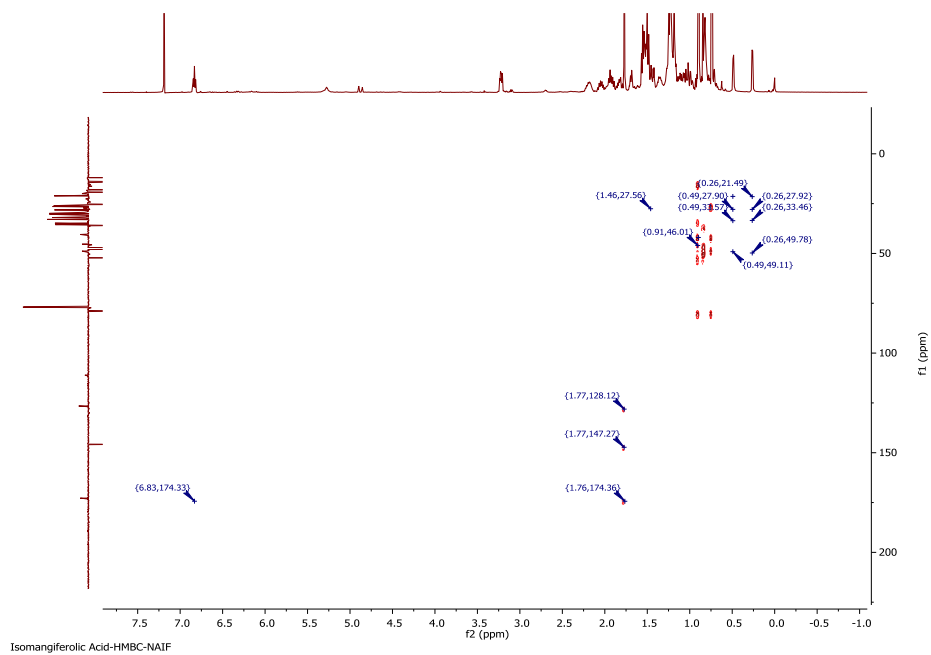


Figure 108: HMBC spectrum (400 MHz) of isomangiferolic acid (Ph-2-20) in CDCl₃

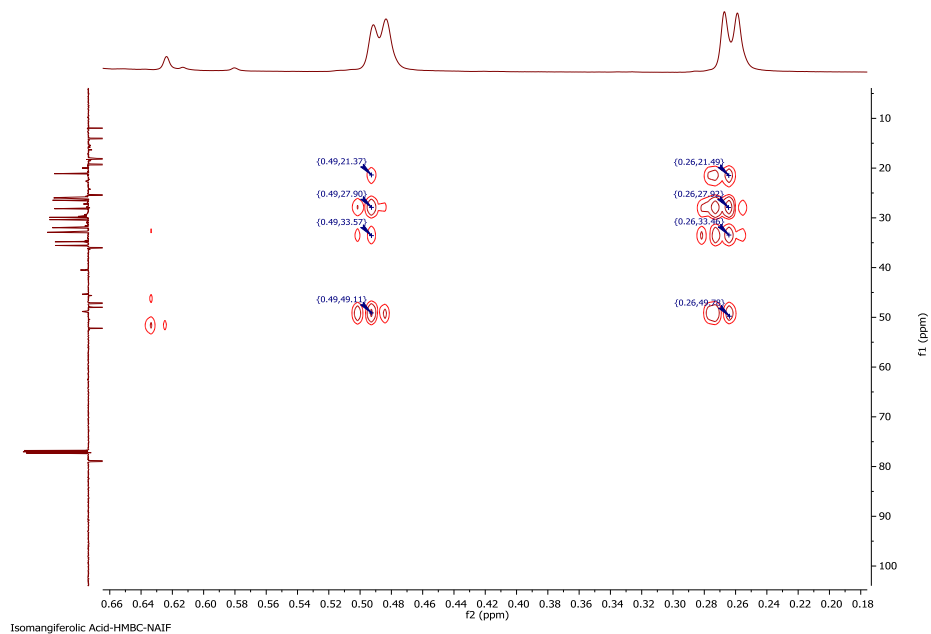


Figure 109: Selected HMBC spectrum expansion for the aliphatic region of isomangiferolic acid (Ph-2-20)

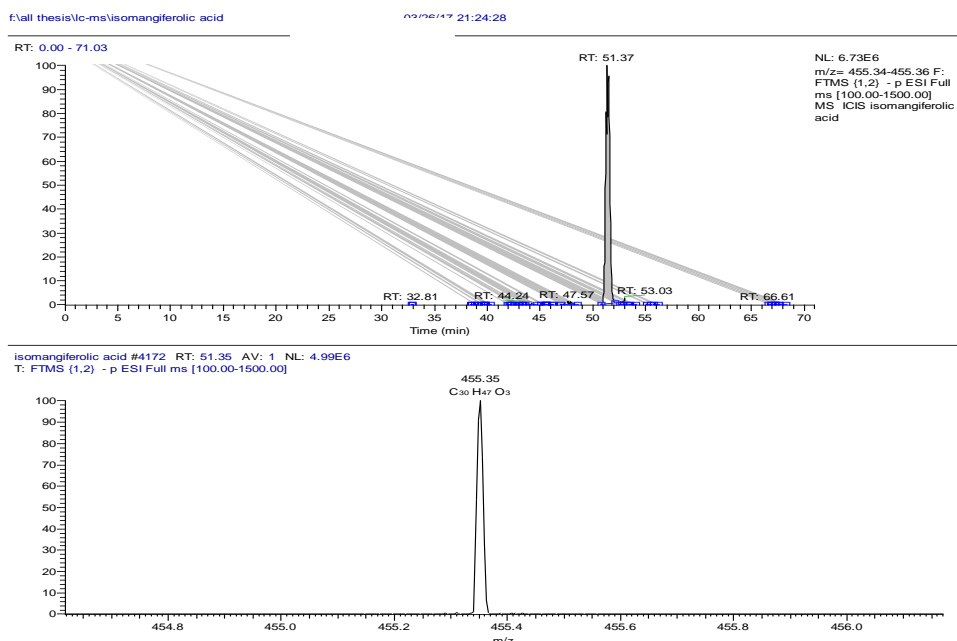


Figure 110: (A) Extracted ion chromatogram corresponding to the mass of isomangiferolic acid in the negative ion mode (-ve ESI) (B) The spectrum corresponding to isomangiferolic acid chromatogram

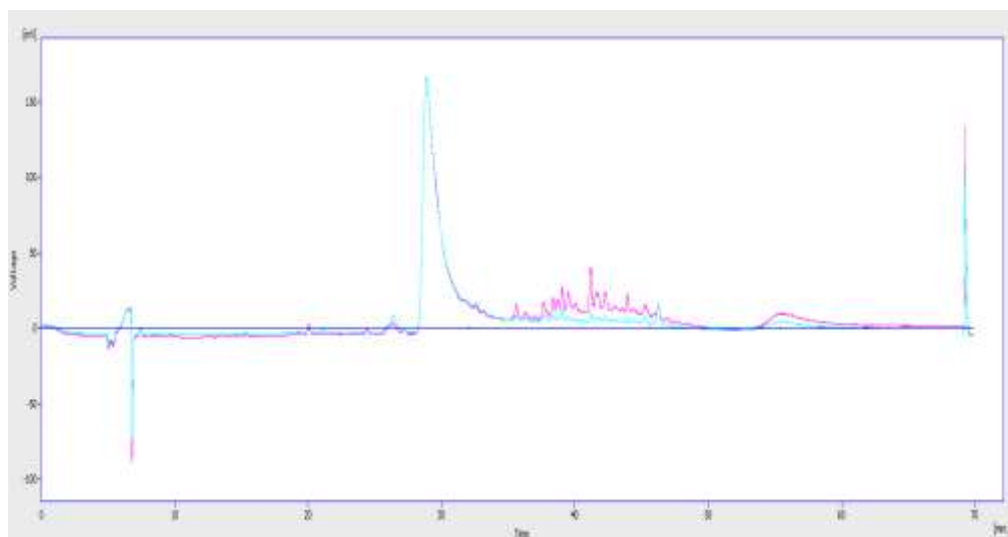


Figure 111: LC-UV-ELSD chromatogram of isomangiferolic acid purified from SEC

4.2.6 Biological activity of the Philippines propolis sample against trypanosome (*T.brucei* S427 strain)

Crude, fraction and pure compounds (Isomangiferolic acid, 27-hydroxymangiferonic acid and 27-hydroxyisomangiferolic acid) extracted from the Philippines propolis sample were tested against *T. brucei*. Pentamidine and Diminazine were used as drug controls and their MIC scores were 0.0045 and 0.0374 µg/ml respectively. Table (26a and 26b) shows the results from testing the above samples. The results showed a varying activity against *T. brucei* in between tested samples. Interestingly, 27-hydroxymangiferonic acid as well as Ph-2 fraction had a higher activity, 11.4 and 11.6 µg/ml respectively, than the crude which was 22.0 µg/ml. The other pure compounds isomangiferolic acid and 27-hydroxyisomangiferolic acid, had slightly lower activity in comparison to 27-hydroxymangiferonic acid with an MICs of 21.4 µg/ml and 13.9 µg/ml respectively. Overall, the crude extract, fractions and pure compounds had moderate activity against *T.brucei* S427 WT. Table (26a) summarizes the Philippines propolis sample biological activity against *T.brucei* S427 strain. It is worth noting that all the tested samples increased cell viability (as their IC₅₀ value > 100 µg/ml) in contrast to Pentamidine and Diminazine which gave the lowest IC₅₀ values at 13.32 µg /mL and 29.58 µg/mL, respectively. Table 26b shows detailed IC₅₀ values for the tested samples.

Table 26 a: Drug Sensitivity assay of Philippines propolis sample and its fractions on *T. brucei* S427 WT

Sample code	Exp. 1 ($\mu\text{g/ml}$)	Exp. 2 ($\mu\text{g/ml}$)	Exp. 3 ($\mu\text{g/ml}$)	Mean ($\mu\text{g/ml}$)	SD	%RSD
Philippine crude	20.3	23.7	22.2	22.0	1.71	7.78
Ph-2 fraction	10.6	11.5	12.6	11.6	0.99	8.59
Isomangiferolic acid	21.2	19.6	23.3	21.4	1.83	8.58
27-hydroxymangiferonic acid	12.6	10.5	11.0	11.4	1.07	9.46
27-hydroxyisomangiferolic acid	15.1	12.7	13.8	13.9	1.20	8.68
Pentamidine(μM)	0.0044	0.0049	0.0042	0.0045	0.0004	7.9334
Diminazen(μM)	0.0377	0.0357	0.0389	0.0374	0.0017	4.4221

Table 26 b: Cytotoxicity assay of Philippines propolis sample and its fractions on U937 cells

Sample code	Exp. 1 ($\mu\text{g/ml}$)	Exp. 2 ($\mu\text{g/ml}$)	Exp. 3 ($\mu\text{g/ml}$)	Mean ($\mu\text{g/ml}$)	SD	%RSD
Philippine crude	89.23	113.8	107.5	103.5	12.8	12.3
Ph-2 fraction	111.4	146.5	130.8	129.6	17.6	13.6
Isomangiferolic acid	154.7	189	174	172.6	17.2	10.0
27-hydroxymangiferonic acid	134.5	153.6	206	164.7	37.0	22.5
27-hydroxyisomangiferolic acid	154.5	140.6	164.9	153.3	12.2	8.0
Pentamidine(μM)	13.43	14.27	12.25	13.3	1.0	7.6
Diminazen(μM)	29.53	31.77	27.43	29.6	2.2	7.3

4.3 Phytochemical results for Red Nigerian propolis

4.3.1 Introduction

The chemistry of propolis samples from Nigeria differs depending on where they originate from geographically, as indicated by the chromatogram of crude samples subjected to analysis by HPLC-UV-ELSD. Thus, an intense ELSD only response was exhibited by the samples derived from central Nigeria and based on the fact that the UV peaks were either weak or lacking, it was deduced that the composition was dominated by terpenoids and/or fats, while compounds with chromophores (e.g. flavonoids, lignans or any other phenolic compounds) were not present. On the other hand, strong UV-ELSD responses were exhibited by samples from south Nigeria (Omar et al., 2016; Omar et al., 2017).

4.3.2 Extraction of sample of Red Nigerian raw propolis

In the present study, the extraction process was conducted with ethanol several times; afterwards, filtration was performed so that additional chromatographic analysis could be conducted on the crude extract of propolis (table 27).

Table 27: weights of ethanolic red Nigerian propolis extract

Masses	Weight (g)
Raw propolis sample (g)	86.8500 g
Empty beaker (g)	173.3100 g
Empty beaker + crude sample after cooling and drying (g)	271.00 g
Crude sample (g)	97.6900 g

Chemical profiling was carried out using many instrumental methods including: high performance liquid chromatography (HPLC) coupled to different detectors such as an evaporative light scattering detector (ELSD) figure 112, ultraviolet detection (UV), and high resolution mass spectrometry (HRMS) and also by NMR. In this way, a general understanding of ethanolic extract constituents was attained. NMR was applied to 10 mg of this extract to gain insight into the nature of the constituents (figure 113) and the LC-MS method was used for LCMS profiling (table 28) and (figure 114).

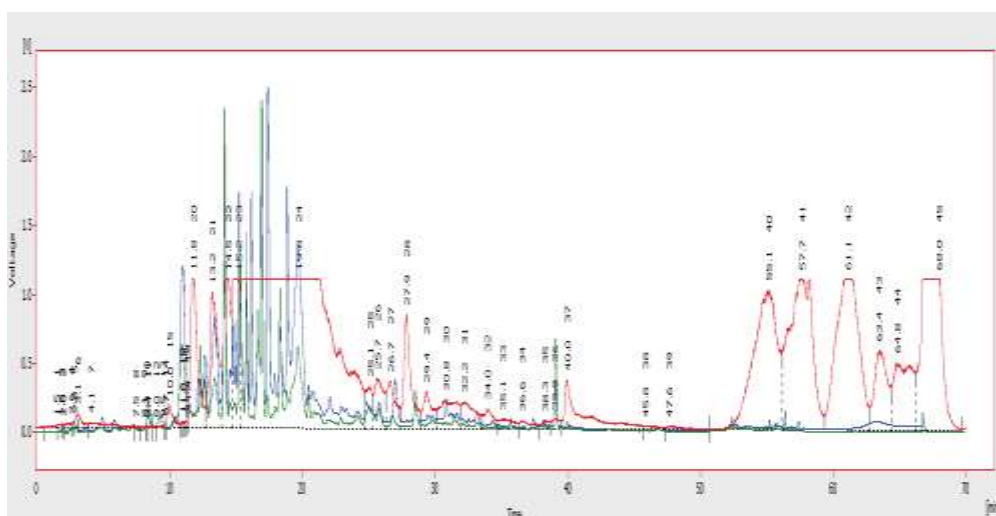


Figure 112: Chromatogram of ethanolic extract of red Nigerian on the HPLC UV (red)-ELSD (blue)

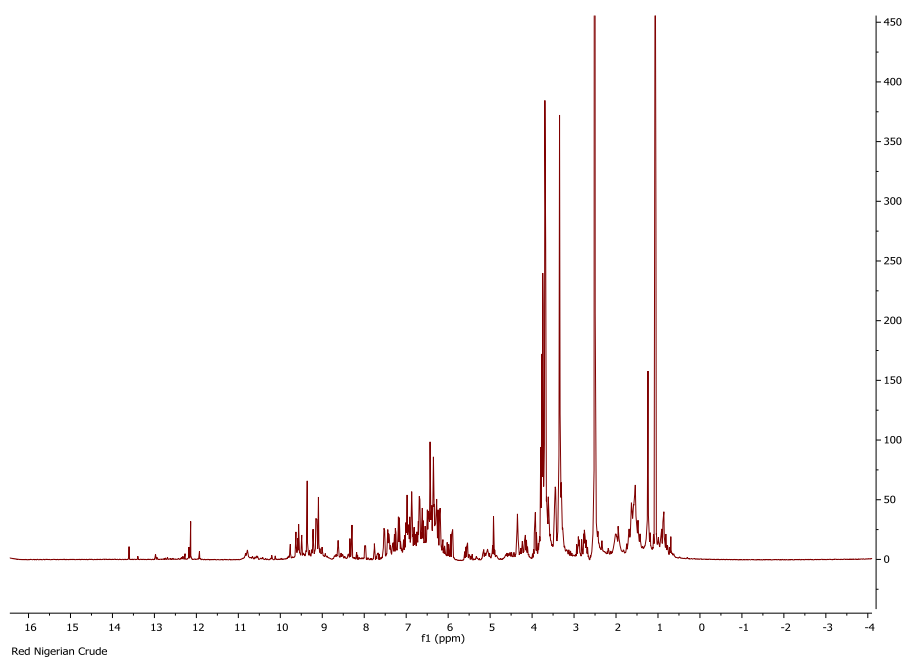


Figure 113: ^1H (400 MHz) NMR spectra of ethanolic extract of red Nigerian propolis in DMSO- d_6 . The main constituents highlighted by ^1H NMR spectrum were flavonoids and phenolics, while terpenoids and fatty acids of lesser intensity compared to flavonoids and phenolics were detected as well. MeOH extract was observed to contain aromatic compounds, this was shown by several signals from 6 to 8 ppm as well as phenolic hydroxyl group between 10-13 ppm.

Table 28: The LC-MS profiling for ethanolic extract of red Nigerian propolis when analysed by reversed phase LC-MS in negative ion mode

Peak No.	Retention time (min)	[M-1]	Chemical formula	Delta (ppm)	Intensity
1	4.8	271.06	C ₁₅ H ₁₁ O ₅	-1.0168	E 7
2	4.8	299.06	C ₁₆ H ₁₁ O ₆	-1.71	E 7
3	5.35	331.08	C ₁₇ H ₁₅ O ₇	-1.66	E 7
4	6.63	273.08	C ₁₅ H ₁₃ O ₅	-1.123	E 7
5	8.11	315.09	C ₁₇ H ₁₅ O ₆	-0.893	E 8
6	8.13	283.06	C ₁₆ H ₁₁ O ₅	-1.543	E 8
7	8.84	285.08	C ₁₆ H ₁₃ O ₅	-1.076	E 7
8	8.84	313.07	C ₁₇ H ₁₃ O ₆	-0.739	E 7
9	9.47	269.08	C ₁₆ H ₁₃ O ₄	-1.235	E 7
10	12.33	270.05	C ₁₅ H ₁₀ O ₅	-1.006	E 8
11	12.33	301.07	C ₁₆ H ₁₃ O ₆	-1.466	E 8
12	12.8	255.07	C ₁₅ H ₁₁ O ₄	-1.89	E 7
13	15.56	267.07	C ₁₆ H ₁₁ O ₄	-1.581	E 8
14	16.03	271.1	C ₁₆ H ₁₅ O ₄	-1.41	E 7
15	16.85	239.07	C ₁₅ H ₁₁ O ₃	-2.709	E 8
16	19.51	253.09	C ₁₆ H ₁₃ O ₃	-2.085	E 7
17	22.36	255.1	C ₁₆ H ₁₅ O ₃	-2.225	E 7
18	22.36	299.09	C ₁₇ H ₁₅ O ₅	-1.728	E 7
19	23.84	451.21	C ₂₇ H ₃₁ O ₆	0.417	E 7
20	24.85	241.09	C ₁₅ H ₁₃ O ₃	-0.737	E 7
21	26.69	285.11	C ₁₇ H ₁₇ O ₄	-2.077	E 7
22	30.29	339.12	C ₂₀ H ₁₉ O ₅	-0.492	E 7
23	30.29	423.18	C ₂₅ H ₂₇ O ₆	0.138	E 7
24	30.73	353.1	C ₂₀ H ₁₇ O ₆	-0.542	E 7
25	32.77	379.19	C ₂₄ H ₂₇ O ₄	-0.191	E 7
26	36.18	407.19	C ₂₅ H ₂₇ O ₅	-0.214	E 6
27	40.94	447.25	C ₂₉ H ₃₅ O ₄	-1.214	E 7
28	41.79	421.17	C ₂₅ H ₂₅ O ₆	-0.384	E 7

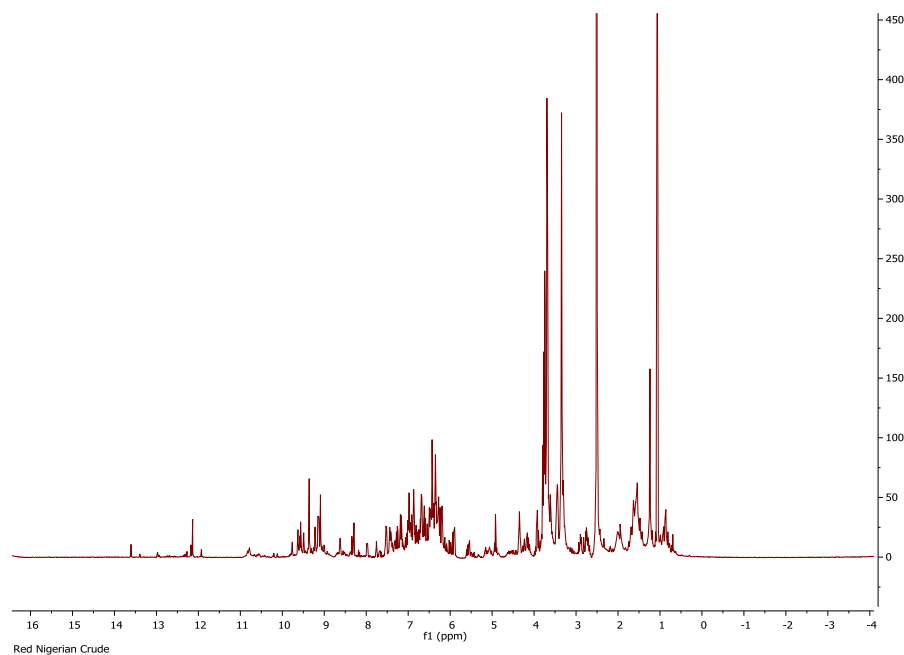


Figure 114: Chromatogram view of ethanolic extract of red Nigerian propolis obtained from LC-MS in negative ion mode (-ve ESI)

HPLC-UV-ELSD of the crude sample showed clearly that it contained mostly compounds with UV-absorbing activity, that could be flavonoids and phenolic compounds. Compounds without chromophores like terpenoids were detected but with low intensities (figure 112).

Considerable complexity was displayed by the LC-MS chromatogram of the crude sample, with numerous peaks that were more or less intense. As indicated in table 28 and Figure 114, the extract largely consisted of flavonoids and phenolics, according to the results of LC-MS analysis and this confirmed by the ^1H NMR spectra (figure 113) where there were many peaks in the aromatic region. Although terpenoids and fatty acid compounds were highlighted some signals captured by the NMR of the crude sample, they were not as intense as the flavonoids and phenolics.

A quantity of the ethanolic extract of red Nigerian propolis (8.2 g) was subjected to column chromatography and elution was sequentially performed based on a gradient

profile (table 29). The total number of fractions generated was 28, and these were collected in vials with a volume of 50 ml. Chromatographic characteristics were delineated via TLC and with selection of a suitable solvent system. Performance of LC-MS and NMR permitted identification of the different components and allowed combination of fractions. The final number of fractions was nine (table 29).

Table 29: Sequence of Column Chromatography Solvent Systems and fractions collected

No.	He %	EtOAc %	MeOH %	M.P (ml)	Fractions obtained	Weight (mg)
1	80	20	0	200	fraction RN1 (M1+M2+M3+M4)	75 mg
2	60	40	0	200	fraction RN2 (M5+M6+M7+M8)	120 mg
3	40	60	0	150	fraction RN3 (M9+M10+M11)	535 mg
4	40	60	0	50	fraction RN4 (M12)	105 mg
5	20	80	0	50	fraction RN5 (M13)	93 mg
6	20	80	0	150	fraction RN6 (M14+M15+M16)	545 mg
7	0	100	0	200	fraction RN7 (M17+M18+M19+M20)	180 mg
8	0	70	30	200	fraction RN8 (M21+M22+M23+M24)	135 mg
9	0	50	50	200	fraction RN9 (M25+M26+M27+M28)	110 mg

The process of chemical analysis relies greatly on the mass of the fraction obtained following initial separation. Therefore, additional chromatographic separation could be conducted if the chemical component was available in sufficient quantity. LC-MS and HPLC-UV-ELSD analysis conducted on fraction RN-6 revealed a rich content of compounds with varied compositions, as shown in table 30 and figure 115 and 116. Based on preliminary data, the compounds were most likely flavonoids. Therefore, 545 mg of fraction RN-6 from CC was subjected to SEC, yielding 38 sub-fractions (RN-6-1 to RN-6-38), which led to the acquisition of two pure compounds (RN-6-16 and RN-6-24).

Table 30: The most abundant components in RN-6 when analysed by reversed phase LC-MS in negative ion mode

Peak NO	Retention time (min)	[M-1]	Chemical formula	Delta (ppm)	Intensity
1	19.17	255.07	C ₁₅ H ₁₁ O ₄	-1.067	E 8
2	20.47	285.08	C ₁₆ H ₁₃ O ₅	0.292	E 8
3	20.95	271.06	C ₁₅ H ₁₁ O ₅	-1.058	E 8
4	24.54	239.07	C ₁₅ H ₁₁ O ₃	-3.252	E 8
5	31.21	283.6	C ₁₆ H ₁₁ O ₅	-0.13	E 8
6	35.85	269.08	C ₁₆ H ₁₃ O ₄	-0.305	E 7
7	36.39	285.11	C ₁₇ H ₁₇ O ₄	-0.675	E 7

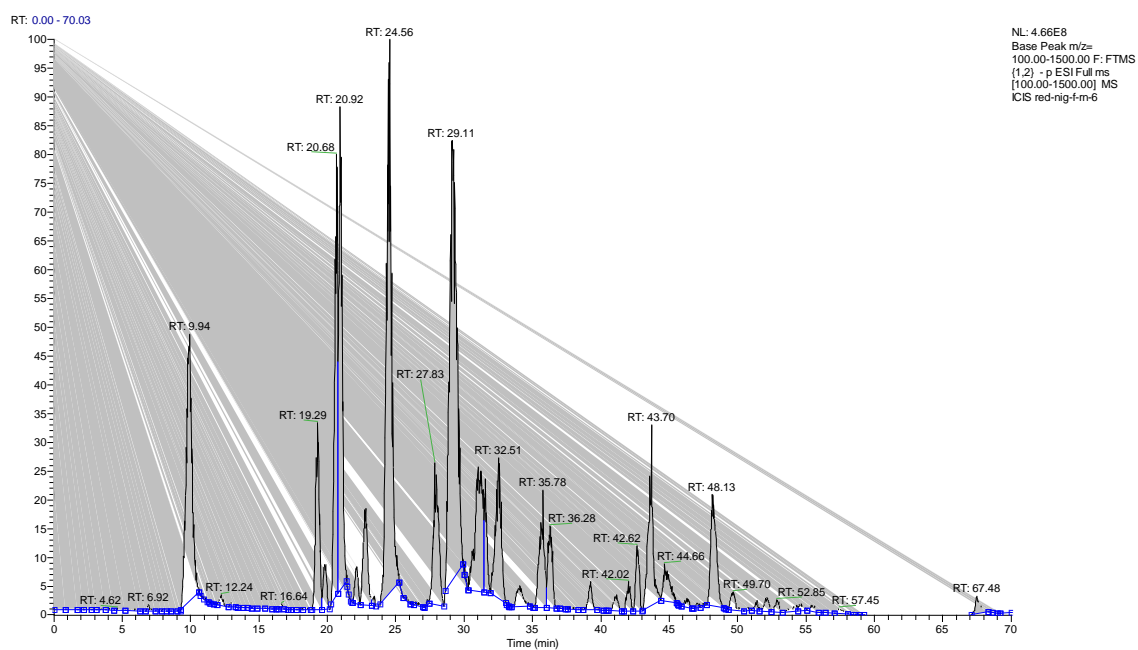


Figure 115: Chromatogram view of red Nigerian propolis fraction RN-6 on the LC-MS negative ion mode (-ve ESI)

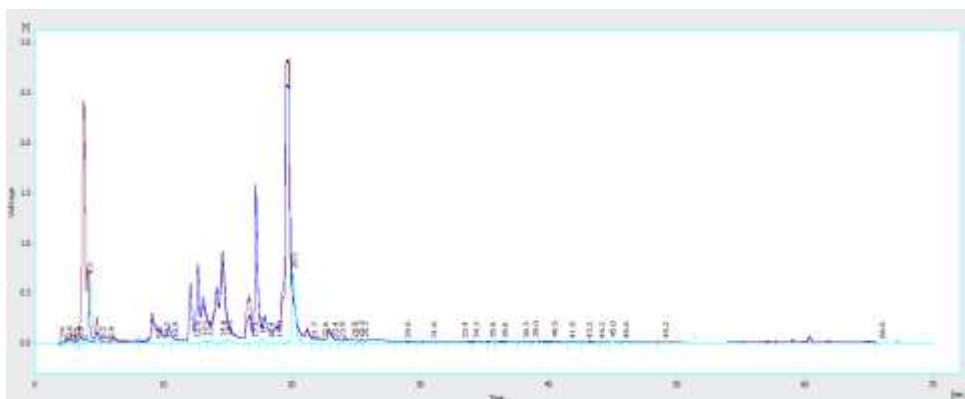


Figure 116: Chromatogram of the red Nigerian propolis fraction RN-6 HPLC UV/ELSD; it is obvious that it consisted primarily of compounds that absorbed UV (blue trace), which could represent flavonoids and phenolics. Although compounds without chromophores such as terpenoids or fats were also identified by ELSD (light blue trace) but their intensities were not high

4.3.3 Characterisation of RN-6-16 as isosativan

CC and then SEC was performed for isolation of RN-6-16 from the ethanolic extract of red Nigerian propolis, which took the form of a dark orange powder. Spraying with *p*-anisaldehyde-sulphuric acid reagent and exposure to heat caused it to manifest as a purple spot on TLC. Elution with the mobile phase 20% HE in EtOAc gave an R_f of 0.41 on SiGel.

A molecular formula of $C_{17}H_{17}O_4$ was derived from the fact that the molecular ion $[M-H]^-$ was indicated by the negative mode HRESI-MS spectrum at m/z 285.11 (figure 117), and the optical rotation had a value of $+5^\circ$ ($c = 0.1$, MeOH).

The compound in figure 118 and table 31 showed two similar sets of aromatic protons for two trisubstituted benzene rings at δ (ppm) 6.45 (d, $J = 2.87$), 6.50 (dd, $J = 8.44$,

2.48) and 7.03(d, $J = 8.48$) for one aromatic ring while the other aromatic ring protons appeared at 6.33, 6.42 and 7.01 ppm. Two oxymethylene protons, one methine and two methylene protons were observed at 4.37 (dd, $J = 3.44, 1.79$), 4.07 (d, $J = 10.10$), 3.53 (m), 3.01 (dd, $J = 15.79, 10.34$) and 2.94 (dd, $J = 5.32, 1.82$). The compound must have a saturated ring A of a flavonoid type compound and the pattern is typical of a C-3 substituted isoflavan moiety. The J modulated ^{13}C spectrum gave 17 signals made up of six aromatic CH, two aliphatic CH_2 and one CH, two methoxy and six quaternary carbons (including four phenolic ones). Analysis of its 2D spectra such as COSY, HSQC and HMBC indicated the compound to be isosativan and the structure was confirmed by literature reports (Questa-Rubio et al., 2001).

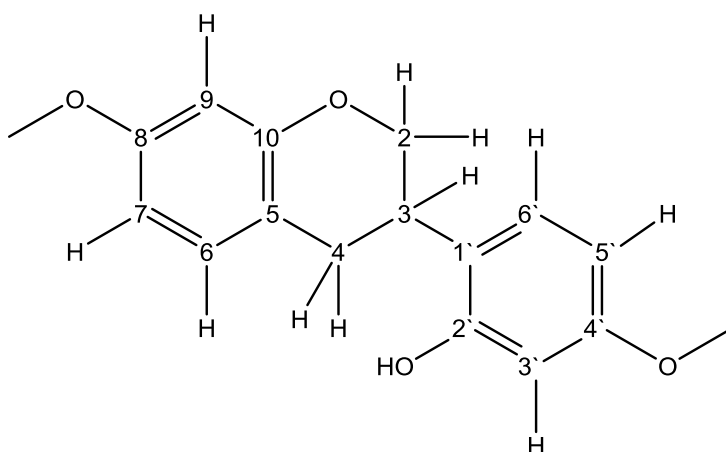


Figure 117: Structure of isosativan

Table 31: ^1H (400 MHz) and ^{13}C (100 MHz) NMR data of isosativan

(RN-6-16) in CDCl₃

Experimental Data		
Position	¹ H (multiplicity), J (Hz)	¹³ C (multiplicity)
1		
2a	4.37 (dd, J= 3.44, 1.79)	69.93
2b	4.07 (d, J=10.10)	69.93
3	3.53 (m)	31.72
4a	3.01 (dd, J= 15.79, 10.34)	30.35
4b	2.94 (dd, J= 5.32, 1.82)	30.35
5		119.99
6	7.03 (dd, J= 8.48)	130.19
7	6.50 (dd, J= 8.44, 2.48)	96.95
8		159.36
9	6.45 (d, J= 2.87)	101.43
10		155.13
1`		114.69
2`		154.44
3`	6.33 (d, J= 2.41)	102.19
4`		159.06
5`	6.42 (dd, J= 6, 2.43)	107.93
6`	7.01 (d, J= 8.33)	128.2
8-O-CH3	3.79 (s, 3H)	55.35
4`-O-CH3	3.79 (s, 3H)	55.35

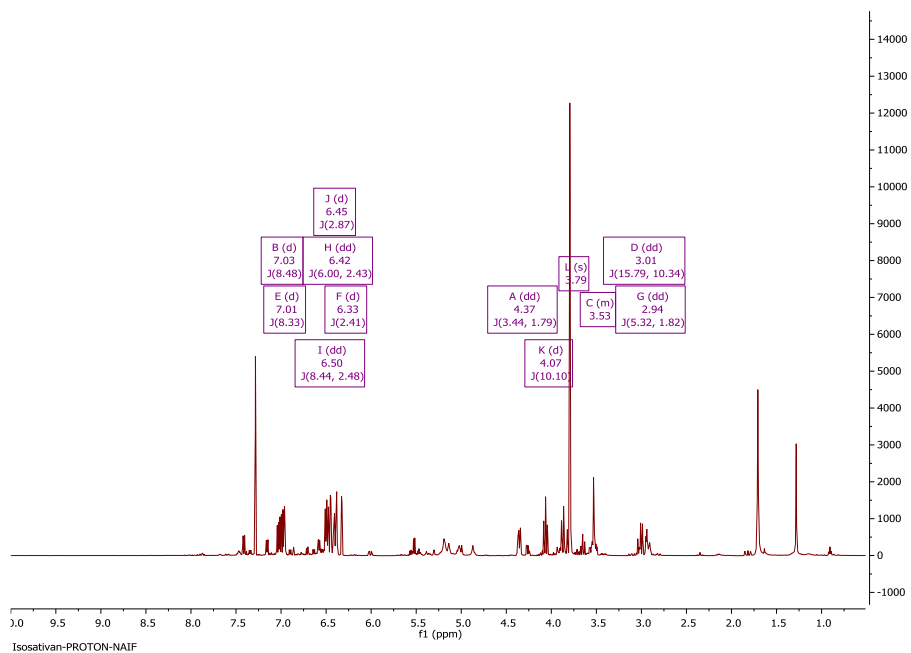


Figure 118: ^1H NMR spectrum (400 MHz) of isosativan (RN-6-16) in CDCl_3

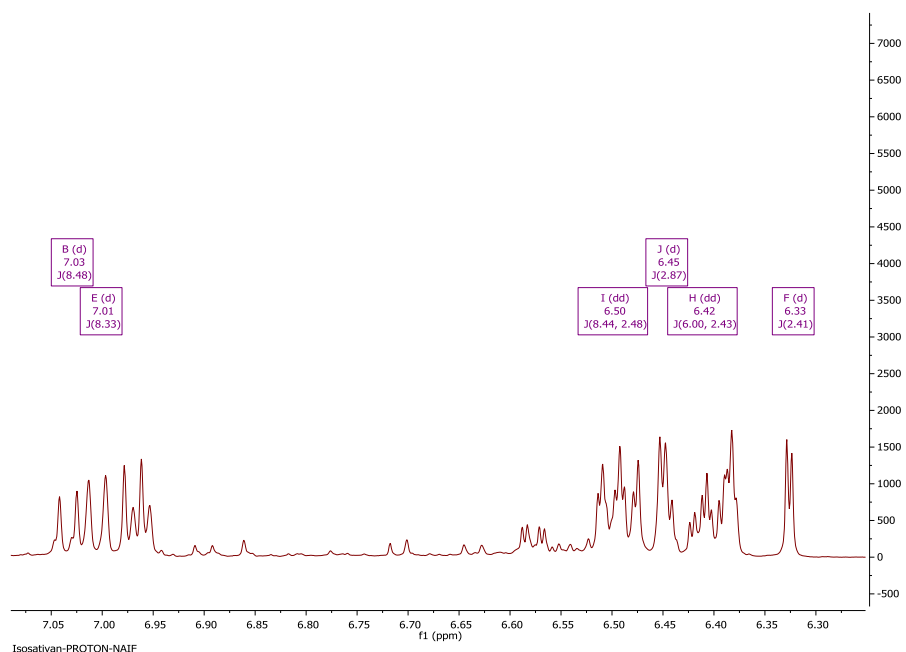


Figure 119: Selected ^1H expansion for the aromatic region of isosativan (RN-6-16)

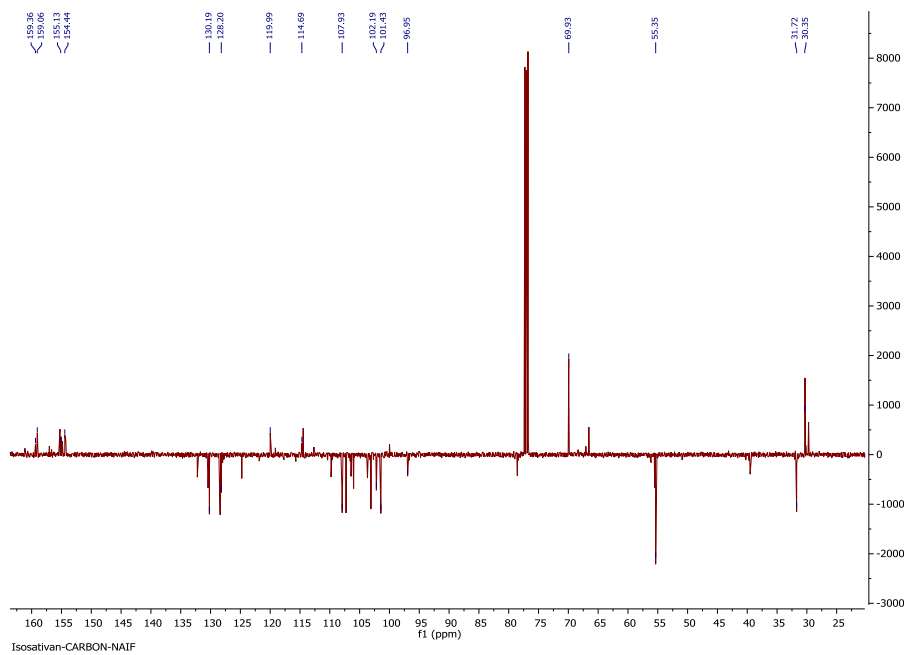


Figure 120: Full DEPTq ^{13}C NMR spectrum (100 MHz) of isosativan (RN-6-16) in CDCl_3

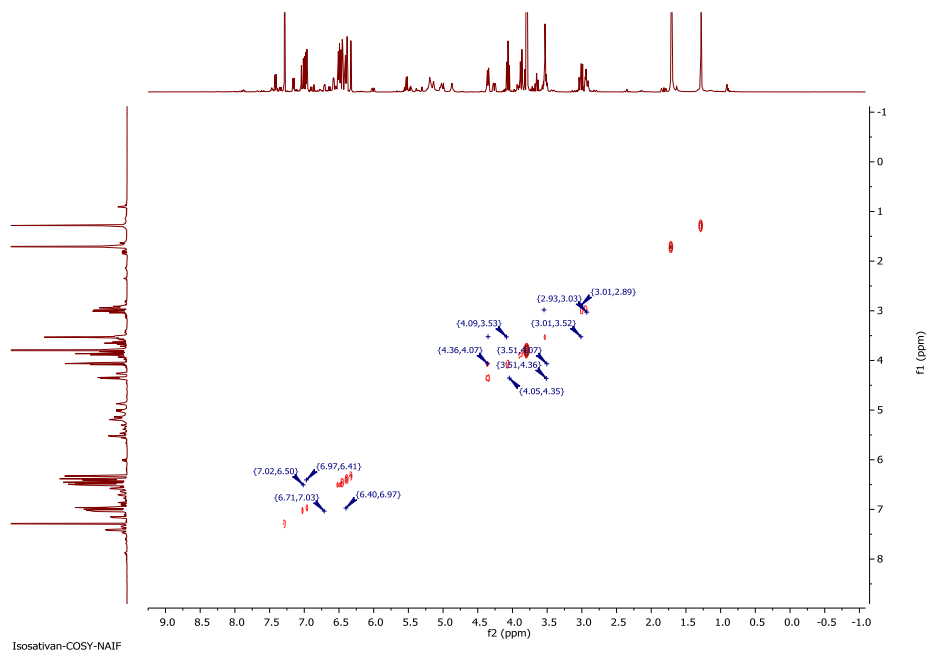


Figure 121: COSY spectrum (400 MHz) of isosativan (RN-6-16) in CDCl_3

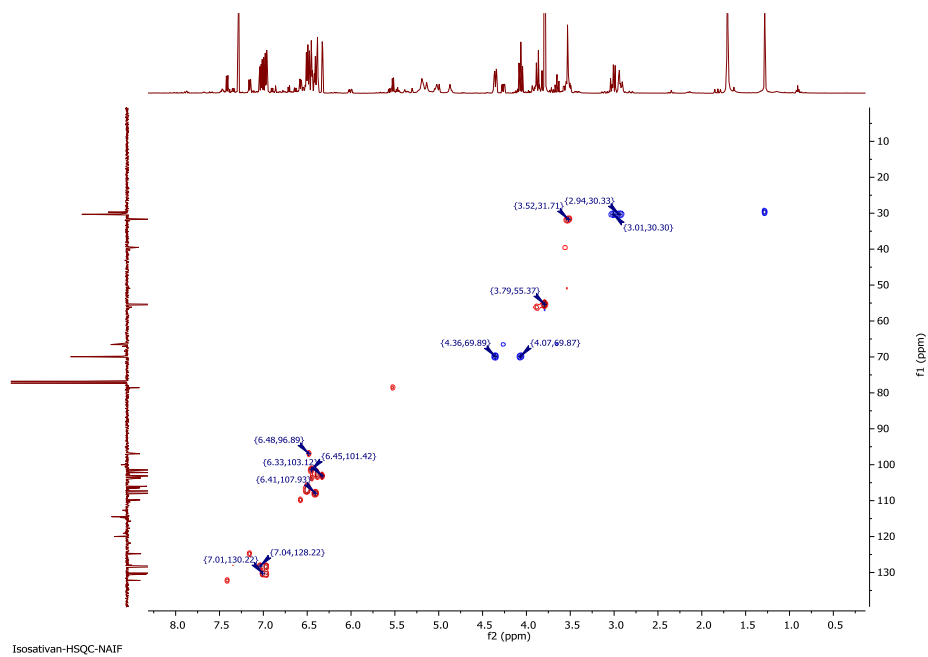


Figure 122: HSQC spectrum (400 MHz) of isosativan (RN-6-16) in CDCl_3

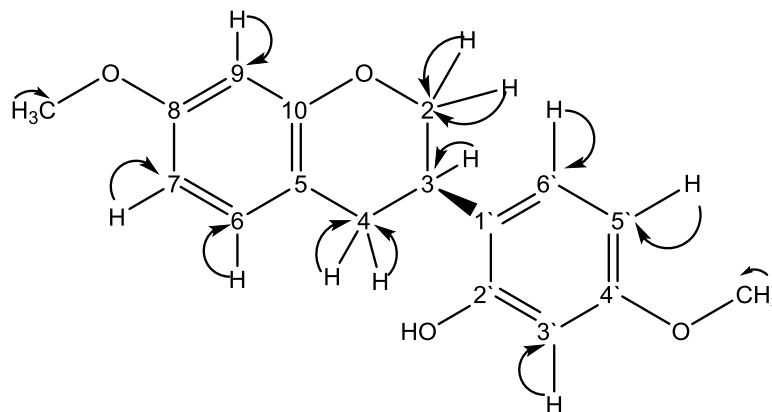


Figure 123: HSQC correlations NMR spectra of isosativan. The black arrows show the correlations corresponding HSQC correlations in figure 122.

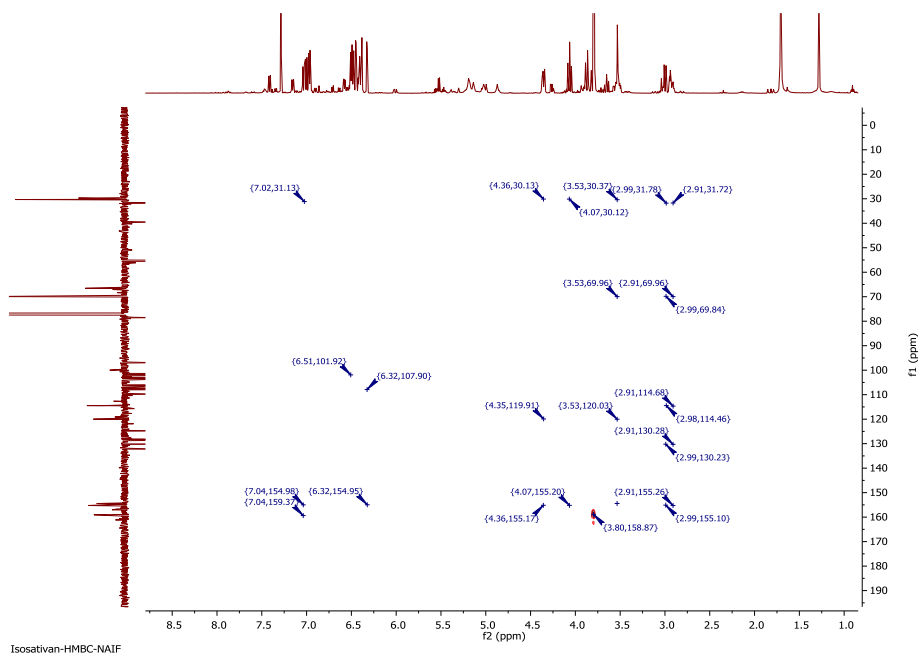


Figure 124: HMBC spectrum (400 MHz) of isosativan (RN-6-16) in $CDCl_3$

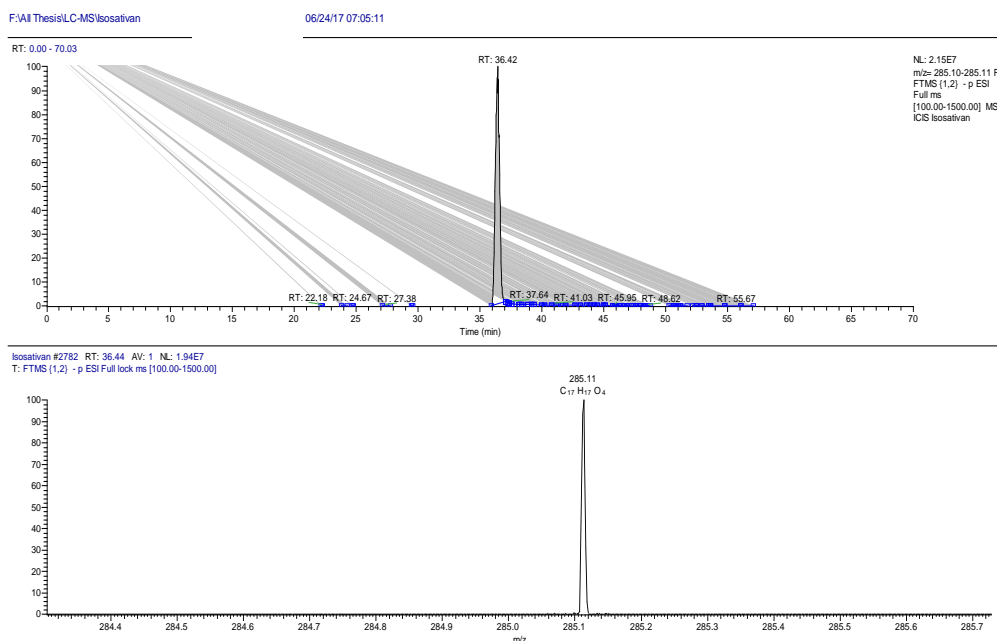


Figure 125: (A) Extracted ion chromatogram corresponding to the mass of isosativan in the negative ion mode (-ve ESI)(B) The spectrum corresponding to isosativan chromatogram

4.3.4 Characterisation of RN-6-24 as medicarpin

CC and then SEC was performed for isolation of RN-6-24 from the ethanolic extract of red Nigerian propolis, which took the form of a dark orange powder. Spraying with *p*-anisaldehyde-sulphuric acid reagent and exposure to heat caused it to manifest as a purple spot on TLC. Elution with the mobile phase 20% HE in EtOAc gave an R_f of 0.45 on SiGel.

A molecular formula of $C_{16}H_{13}O_4$ was derived from the fact that the molecular ion $[M-H]^-$ was indicated by the negative mode HRESI-MS spectrum at m/z 269.08 (figure 126), and the optical rotation had a value of $+23^\circ$ ($c = 0.1$, MeOH).

In its 1H (400 MHz) spectrum (figure 127, table 32), the compound showed signals for two oxymethylene protons at δ (ppm) 4.25 (ddd, $J = 10.91, 4.90, 0.74$) and 3.64 (t, $J = 10.87$), one methine proton at 3.54 (m) and an oxymethine proton at 5.51 (d, $J = 6.76$). The proton spectrum of the compound showed two sets of aromatic ABX spin systems and that confirmed the presence of two trisubstituted benzene rings. The first set were at δ_H ppm 7.39 (d, $J = 0.63$), 6.58 (dd, $J = 8.37, 2.5$) and 6.44 (d, $J = 2.49$). The second set of the aromatic ABX protons were at 7.16 (d, $J = 0.64$), 6.46 (dd, $J = 2.30, 0.59$) and 6.48 (d, $J = 2.27$). From the J modulated ^{13}C spectrum, 16 carbon signals were identified and were made up of six aromatic CH, one aliphatic CH_2 , two aliphatic CH, one methoxy and six quaternary carbons (including four phenolic ones). Analysis of its 2D spectra (COSY, HSQC and HMBC) indicated the compound to be medicarpin and the structure was confirmed by literature reports (Piccinelli et al., 2005).

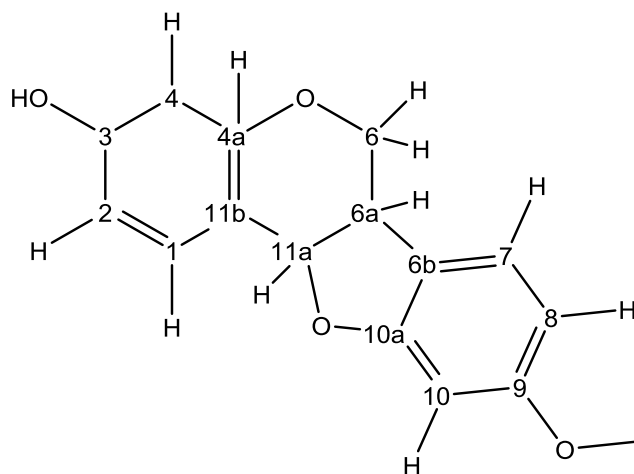


Figure 126: Structure of medicarpin

Table 32: ^1H (400 MHz) and ^{13}C (100 MHz) NMR data of medicarpin (RN-6-24) in CDCl_3

Experimental Data		
Position	^1H (multiplicity), J (Hz)	^{13}C (multiplicity)
1	7.39 (d, $J=0.63$)	132.12
2	6.58 (dd, $J=8.37, 2.5$)	109.82
3		157.34
4	6.44 (d, $J=2.49$)	103.65
4a		156.65
5		
6	Alpha 4.25 (ddd, $J=10.91, 4.90, 0.74$)	66.54
6	Beta 3.64 (t, $J=10.87$)	66.54
6a	3.54 (m)	39.53
6b		119.52
7	7.16 (d, $J=0.64$)	124.72
8	6.46 (dd, $J=2.30, 0.59$)	106.37
9		161.13
9-OCH ₃	3.79 (s, 3H)	55.5
10	6.48 (d, $J=2.27$)	96.91
10a		160.7
10b		
11a	5.51 (d, $J=6.76$)	78.59
11b		112.42

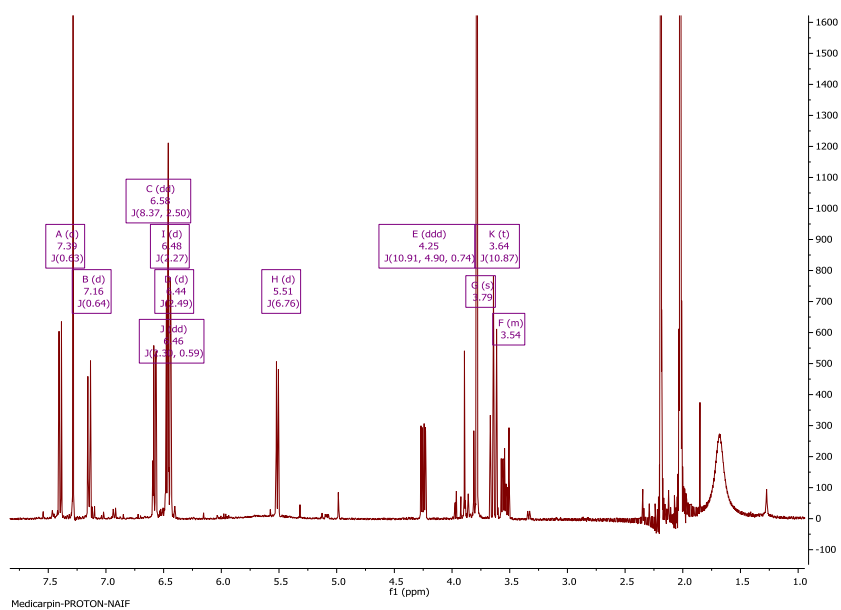


Figure 127: ^1H NMR spectrum (400 MHz) of medicarpin (RN-6-24) in CDCl_3

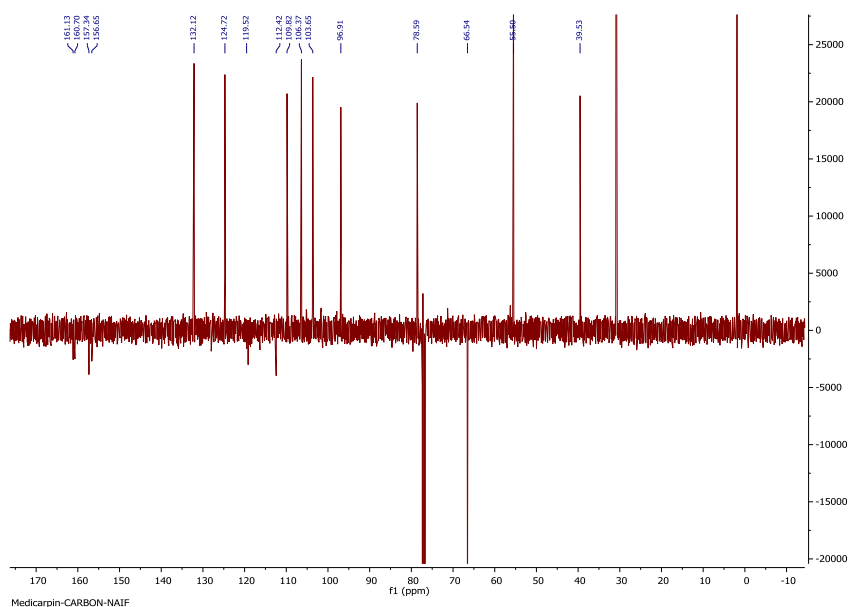


Figure 128: ^{13}C NMR spectrum (100 MHz) of medicarpin (RN-6-24) in CDCl_3

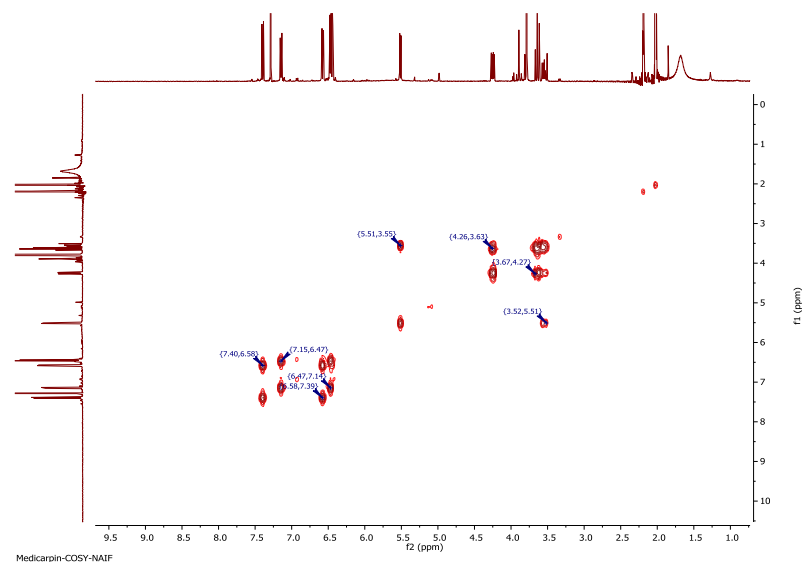


Figure 129: COSY spectrum (400 MHz) of medicarpin (RN-6-24) in CDCl₃

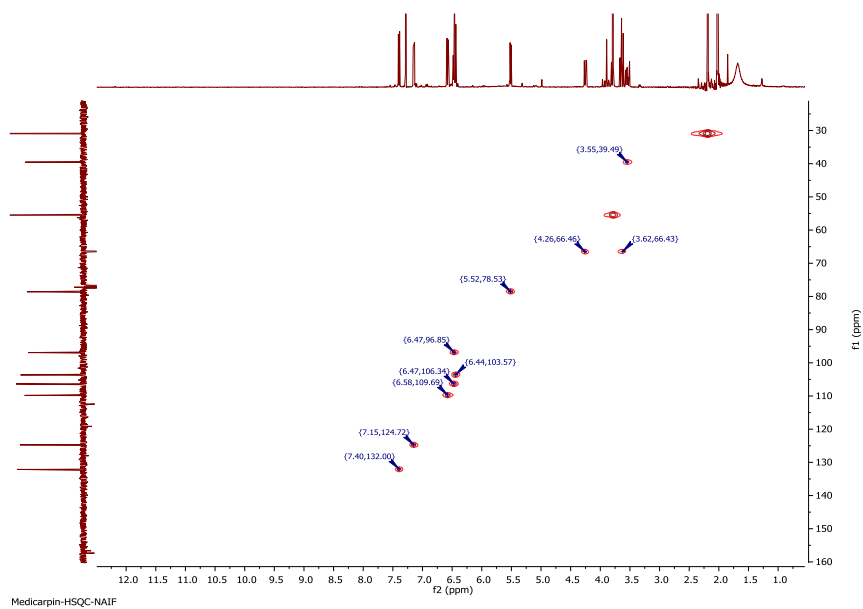


Figure 130: HSQC spectrum (400 MHz) of medicarpin (RN-6-24) in CDCl₃

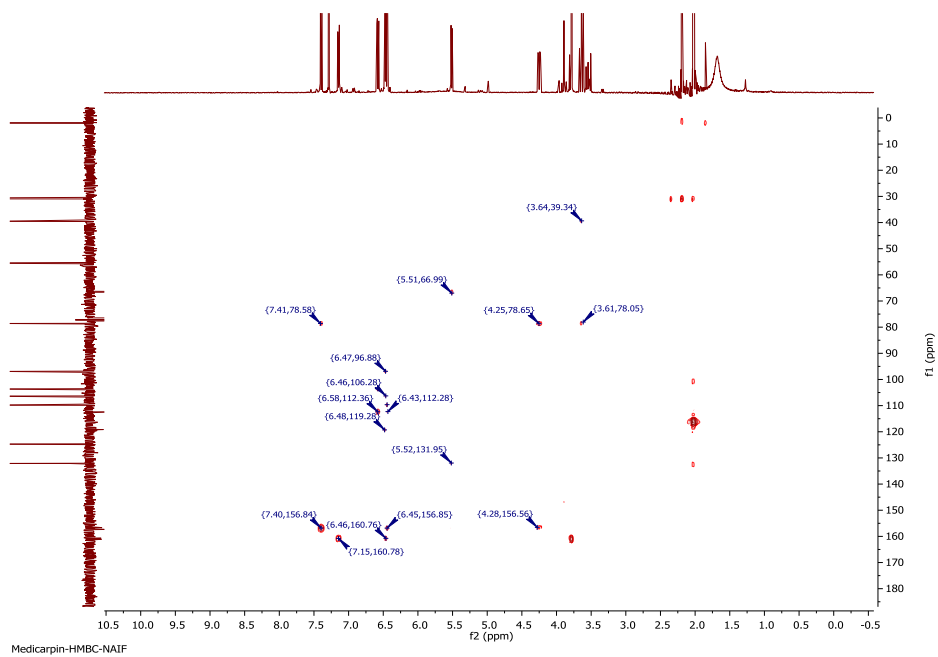


Figure 131: HMBC spectrum (400 MHz) of medicarpin (RN-6-24) in CDCl₃

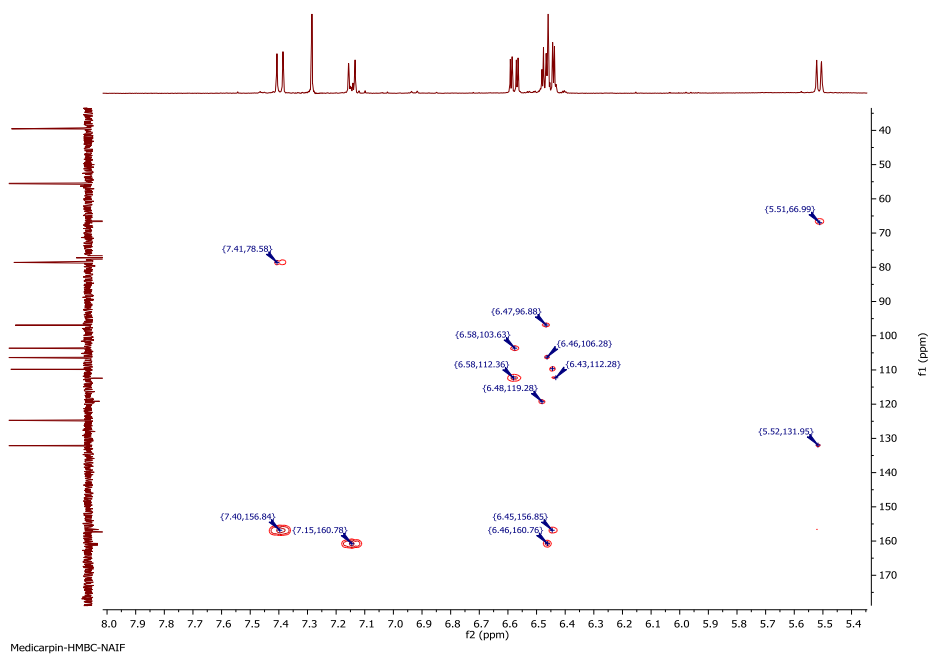


Figure 132: Selected HMBC expansion for the aromatic region of medicarpin (RN-6-24)

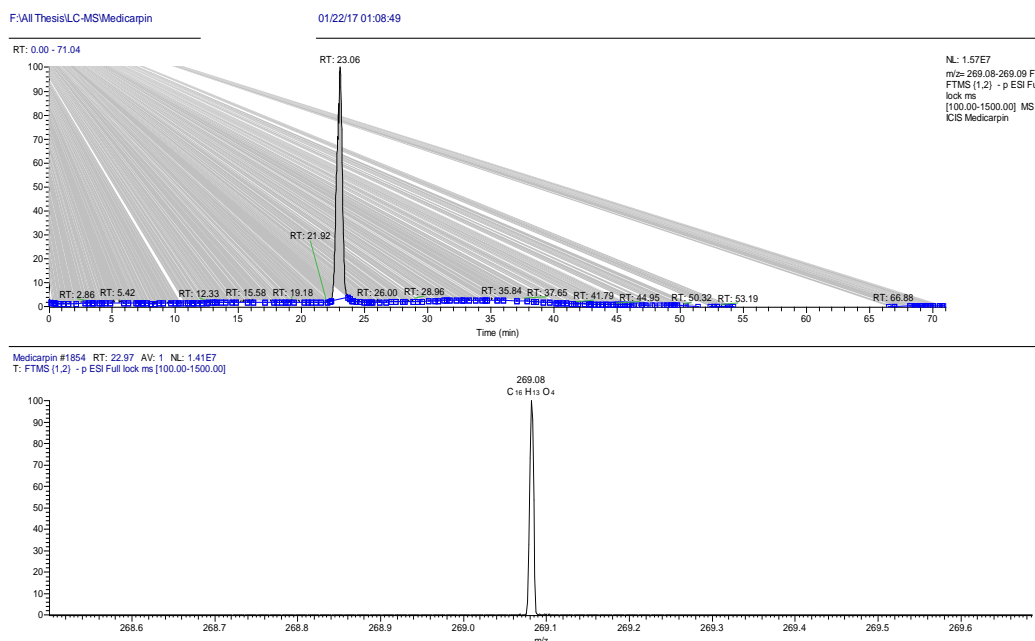


Figure 133: (A) Extracted ion chromatogram corresponding to the mass of medicarpin in the negative ion mode (-ve ESI) (B) The spectrum corresponding to the medicarpin chromatogram

4.3.5 Biological activities of Red Nigerian propolis sample against trypanosome (*T.brucei* S427 strain)

Crude, fractions and pure compounds (isosativan and medicarpin) from Red Nigerian propolis were tested against *T. brucei*. Pentamidine and Diminazene were used as drug controls and their MIC were scored 0.0030 and 0.0313 $\mu\text{g/ml}$ respectively. Tables 33a and b show the results from testing the above samples against *T. brucei*. The results showed a varying activity against *T. brucei* between tested samples. Red Nigerian crude has a higher activity, 6.5 $\mu\text{g/ml}$, than the fraction which has activity of 8.0 $\mu\text{g/ml}$. The obtained pure compounds, medicarpin and isosativan, showed moderate inhibitory activity with an MIC of 7.6 $\mu\text{g/ml}$ and 12.1 $\mu\text{g/ml}$ respectively. Overall, crude, fractions and pure compounds are moderately active against *T. brucei*

S427 WT (see table 33a). It is worth to note that all tested samples were slightly increasing cells viability except RN-6 fraction which showed a similar toxicity results to Diminazene (as its minimum IC50 value > 26 µg/ml). Pentamidine and Diminazene gave the lowest IC50 values at 13.32 µg /mL and 29.58 µg/mL, respectively. Table 33b shows detailed IC50 values for the tested samples.

Table 33 a: Drug Sensitivity assay of red Nigerian propolis sample and its fractions on *T. brucei* S427 WT

Propolis Sample Origin	Exp. 1 (µg/ml)	Exp. 2 (µg/ml)	Exp. 1 (µg/ml)	Mean (µg/ml)	SD	%RSD
Red Nigerian crude	6.6	6.3	6.5	6.5	0.15	2.28
RN-6 fraction	8.0	7.7	8.2	8.0	0.23	2.84
Isosativan	13.9	11.2	11.3	12.1	1.54	12.67
Medicarpin	7.7	7.5	7.6	7.6	0.09	1.12
Pentamidine(µM)	0.00221	0.00309	0.00358	0.0030	0.001	23.46
Diminazen(µM)	0.02461	0.03172	0.03767	0.0313	0.007	20.87

Table 33 b: Cytotoxicity assay of red Nigerian propolis sample and its fractions on U937 cells

Propolis Sample Origin	Exp. 1 (µg/ml)	Exp. 2 (µg/ml)	Exp. 1 (µg/ml)	Mean (µg/ml)	SD	%RSD
Red Nigerian crude	35.84	45.55	41.64	41.0	4.89	11.91
RN-6 fraction	27.12	27.00	25.25	26.5	1.05	3.96
Medicarpin	49.26	42.68	45.94	46.0	3.29	7.16
Isosativan	71.39	67.46	71.82	70.2	2.40	3.42
Pentamidine(µM)	13.43	14.27	12.25	13.32	1.01	7.62
Diminazen(µM)	29.53	31.77	27.43	29.58	2.17	7.34

4.4 Phytochemical results for red Brazilian propolis

4.4.1 Introduction

Following extensive study of green propolis from Brazil, a new kind of propolis has begun to attract attention, namely, red propolis from Brazil. Initially acquired in Maceio City (Alagoas state) in north-east Brazil, the product consists of compounds from the plants *Populus* sp. (poplar plant) and *Baccharis dracunculifolia* (Silva et al., 2008). The discovery and investigation of a range of types of red propolis are anticipated to provide further knowledge about the product (Salomao et al., 2008).

Compounds from the plant *Dalbergia ecastophyllum* were identified by (Daugusch et al., 2008) to be present in one type of red propolis, especially flavonoids like rutin, liquiritigenin, daidzein, pinobanksin, luteolin and isoliquiritigenin. In terms of its composition, this type of red propolis was not the same as red propolis initially established to contain materials from *Populus* sp. and *B. dracunculifolia*. It is gradually becoming clear that red Brazilian and red Nigerian propolis are very similar in composition.

4.4.2 Extraction of sample of red Brazilian raw propolis

In the current study, ethanol was employed to carry out the extraction process, which consisted of a number of steps. Subsequently, to enable additional chromatographic analysis to be undertaken on the crude sample of propolis, filtration was carried out (table 34).

Table 34: weights of ethanolic red Brazilian propolis extract

Masses	Weight (g)
Raw propolis sample (g)	125.3414 g
Empty beaker (g)	161.6152 g
Empty beaker + crude sample after cooling and drying (g)	197.4274 g
Crude sample (g)	35.8122 g

Chemical profiling was carried out using many instrumental methods including: high performance liquid chromatography (HPLC) coupled to different detectors such as an evaporative light scattering detector (ELSD) figure 134, ultraviolet detection (UV), and high resolution mass spectrometry (HRMS) and also by NMR. To discern the primary features of the constituents, preliminary NMR analysis was conducted on a 10 mg sample of the extract (figure 135), followed by application of LC-MS for the purpose of LCMS profiling, as indicated in table 35 and figure 136.

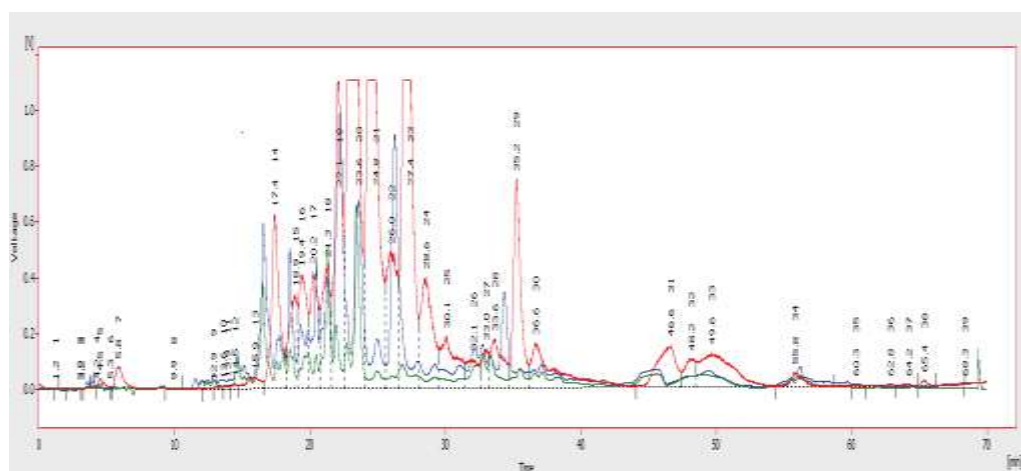


Figure 134: Chromatogram of ethanolic extract of Brazilian red propolis by using ELSD-UV

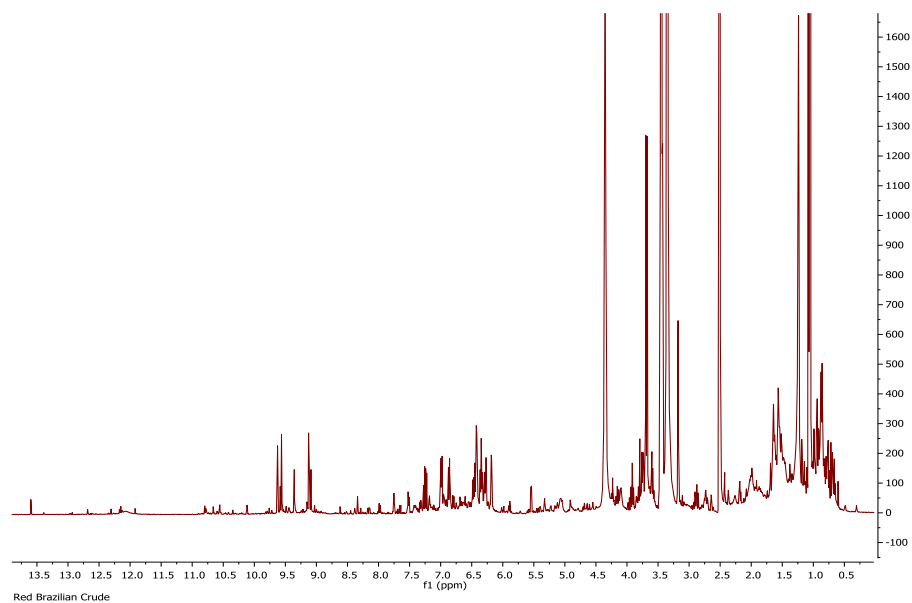


Figure 135: ^1H (400 MHz) NMR spectra of the ethanolic extract of red Brazilian propolis in DMSO-d_6 . The main constituents highlighted by ^1H NMR spectrum were flavonoids and phenolics, while terpenoids and fatty acids of lesser intensity compared to flavonoids and phenolics were detected as well. MeOH extract was observed to contain aromatic compounds, this was shown by several signals from 6 to 8 ppm as well as phenolic hydroxyl group between 10-13 ppm.

Table 35: The LC-MS profiling for the ethanolic extract of red Brazilian propolis when analysed by reversed phase LC-MS in negative ion mode

Peak No.	Retention time (min)	[M-1]	Chemical formula	Delta (ppm)	Intensity
1	5.07	173.05	C ₇ H ₉ O ₅	0.713	E 6
2	5.07	437.07	C ₂₆ H ₁₃ O ₇	3.441	E 6
3	10.26	271.06	C ₁₅ H ₁₁ O ₅	-0.578	E 6
4	10.26	121.03	C ₇ H ₅ O ₂	-1.179	E 6
5	10.26	299.06	C ₁₆ H ₁₁ O ₆	-1.409	E 6
6	10.93	331.08	C ₁₇ H ₁₅ O ₇	2.428	E 6
7	11.62	153.02	C ₇ H ₅ O ₄	1.49	E 6
8	11.62	273.08	C ₁₅ H ₁₃ O ₅	2.575	E 6
9	11.62	301.07	C ₁₆ H ₁₃ O ₆	2.387	E 6
10	13.28	253.05	C ₁₅ H ₉ O ₄	2.719	E 6
11	13.28	297.04	C ₁₆ H ₉ O ₆	2.891	E 6
12	13.57	315.09	C ₁₇ H ₁₅ O ₆	3.074	E 7
13	13.77	255.07	C ₁₅ H ₁₁ O ₄	2.697	E 7
14	14.36	283.06	C ₁₆ H ₁₁ O ₅	2.873	E 7
15	14.66	269.08	C ₁₆ H ₁₃ O ₄	3.076	E 7
16	14.94	315.05	C ₁₆ H ₁₂ O ₇	4.457	E 6
17	14.94	449.2	C ₂₇ H ₂₉ O ₆	4.003	E 6
18	15.72	285.08	C ₁₆ H ₁₃ O ₅	2.782	E 7
19	18.46	271.1	C ₁₆ H ₁₅ O ₄	2.758	E 7
20	18.75	267.07	C ₁₆ H ₁₁ O ₄	2.538	E 8
21	19.63	239.07	C ₁₅ H ₁₁ O ₃	2.604	E 7
22	21.09	401.14	C ₂₅ H ₂₁ O ₅	0.805	E 6
23	21.98	269.05	C ₁₅ H ₉ O ₅	1.648	E 6
24	27.05	299.09	C ₁₇ H ₁₅ O ₅	0.612	E 7
25	30.17	285.11	C ₁₇ H ₁₇ O ₄	1.149	E 7
26	33.21	281.05	C ₁₆ H ₉ O ₅	-0.166	E 6
27	36.23	507.24	C ₃₀ H ₃₅ O ₇	2.175	E 6
28	49.43	301.22	C ₂₀ H ₂₉ O ₂	0.951	E 6
29	51.19	469.33	C ₃₀ H ₄₅ O ₄	2.934	E 6

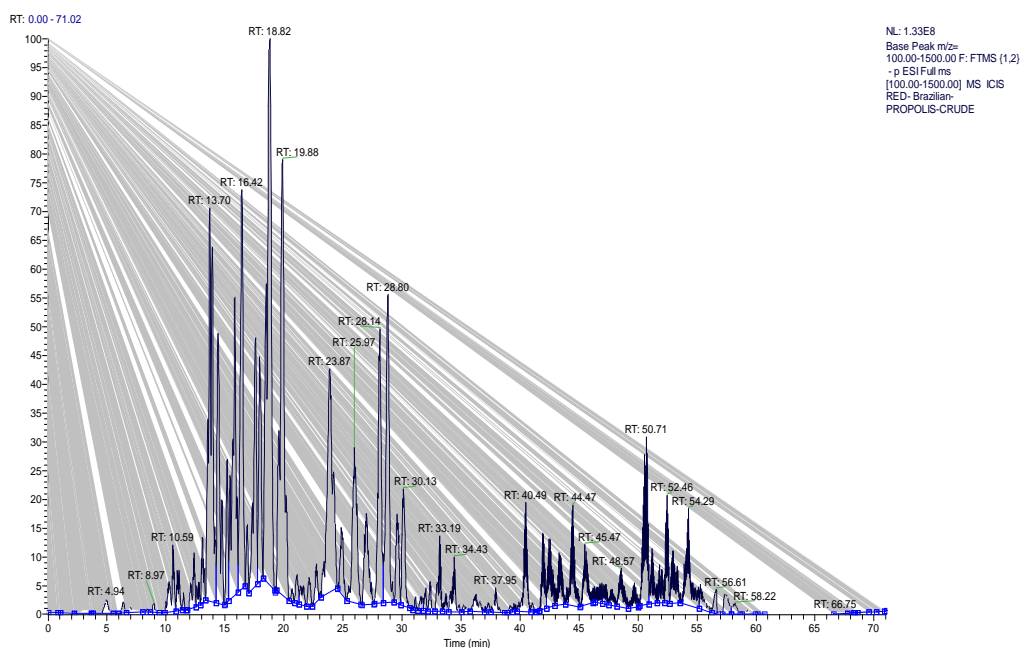


Figure 136: Chromatogram view of ethanolic extract of red Brazilian propolis by LC-MS in negative ion mode (-ve ESI)

HPLC-UV-ELSD of the crude sample showed clearly that it contained mostly compounds with UV-absorbing activity, that could be flavonoids and phenolic compounds. Compounds without chromophores like terpenoids were detected but with low intensities (figure 134).

Considerable complexity was displayed by the LC-MS chromatogram of the crude sample, with numerous peaks that were more or less intense. As indicated in table 35 and figure 136, the crude extract largely consisted of flavonoids, phenolics and terpenoids, according to the results of LC-MS analysis. The prevalence of flavonoids and phenolics was also confirmed by the ^1H NMR spectra (figure 135) which contained many signals for aromatic protons. Although terpenoids and fatty acid compounds were highlighted by the NMR of the crude sample, they were not as intense as the flavonoids and phenolics.

A quantity of the ethanolic extract of red Brazilian propolis (10.5g) was subjected to column chromatography and elution was sequentially performed based on a gradient profile (table 36). The total number of fractions generated was 28, and these were collected in vials with a volume of 50 ml. Chromatographic characteristics were delineated via TLC and using a suitable solvent system. Performance of LC-MS and NMR permitted identification of the different components and allowed combination of fractions. The final number of fractions was nine.

Table 36: Sequence of Column Chromatography Solvent Systems and fractions collected

No.	He %	EtOAc %	MeOH %	M.P (ml)	Fractions obtained	Weight (mg)
1	80	20	0	200	fraction FB1 (M1+M2+M3+M4)	55 mg
2	60	40	0	200	fraction FB2 (M5+M6+M7+M8)	215 mg
3	40	60	0	200	fraction FB3 (M9+M10+M11+M12)	470 mg
4	20	80	0	100	fraction FB4 (M13+M14)	95 mg
5	20	80	0	100	fraction FB5 (M15+M16)	102 mg
6	0	100	0	100	fraction FB6 (M17+M18)	230 mg
7	0	100	0	100	fraction FB7 (M19+M20)	140 mg
8	0	70	30	200	fraction FB8 (M21+M22+M23+M24)	80 mg
9	0	50	50	200	fraction FB9 (M25+M26+M27+M28)	105 mg

Further chemical analysis is highly dependent on weight of the fraction and additional chromatographic separation can be carried out if the quantity of the chemical component is sufficient. As indicated in table 37 and figures 137 and 138, LC-MS and HPLC-UV-ELSD analysis highlighted the richest mixture of compounds was in fraction FB-3 with a varied composition. Based on preliminary data, the compounds were most likely flavonoids, phenolics and terpenoids. Therefore, 470 mg of fraction (FB-3) from CC was subjected to size-exclusion chromatography, yielding 42 sub-

fractions (FB-3-1 to FB-3-42), which led to acquisition of two pure compounds (FB-3-10 and FB-3-14).

Table 37: The most abundant compounds in red Brazilian's fraction FB-3 when analysed by reversed phase LC-MS in negative ion mode

Peak No.	Retention time (min)	[M-1]	Chemical formula	Delta (ppm)	Intensity
1	13.05	271.06	C ₁₅ H ₁₁ O ₅	1.525	E 7
2	14.58	283.06	C ₁₆ H ₁₁ O ₅	0.824	E 7
3	16.08	255.07	C ₁₅ H ₁₁ O ₄	1.129	E 6
4	28.78	285.11	C ₁₇ H ₁₇ O ₄	0.378	E 5
5	34.95	269.08	C ₁₆ H ₁₃ O ₄	0.921	E 6
6	36.16	507.24	C ₃₀ H ₃₅ O ₇	0.677	E 7
7	41.71	271.1	C ₁₆ H ₁₅ O ₄	0.287	E 6

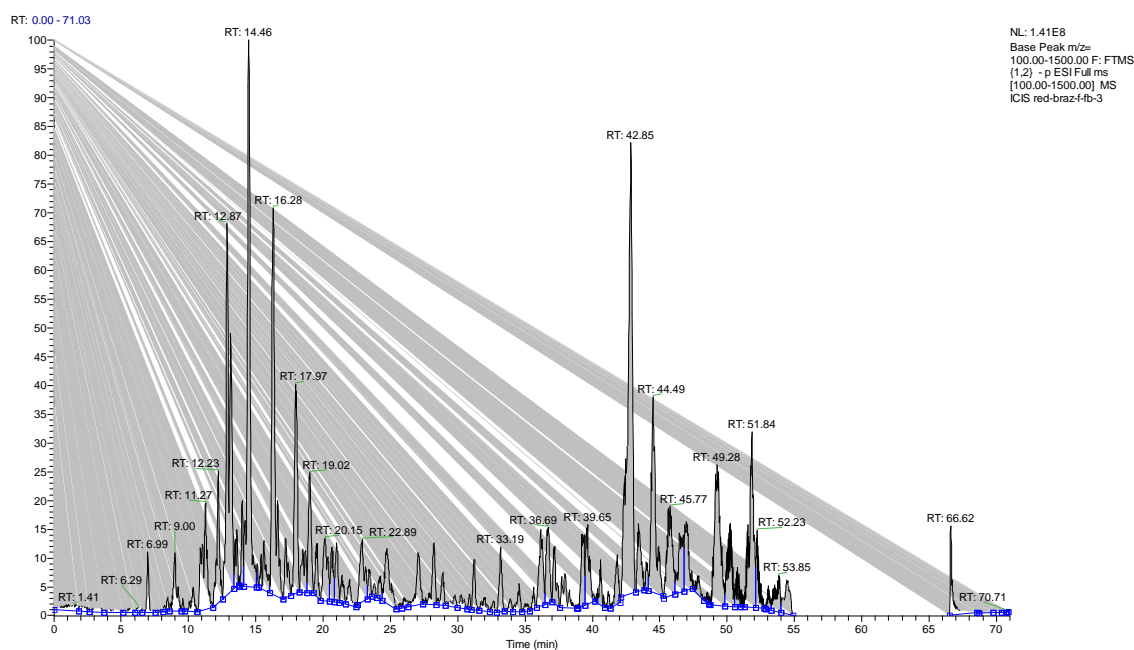


Figure 137: Chromatogram view of red Brazilian fraction FB-3 on the LC-MS in negative ion mode

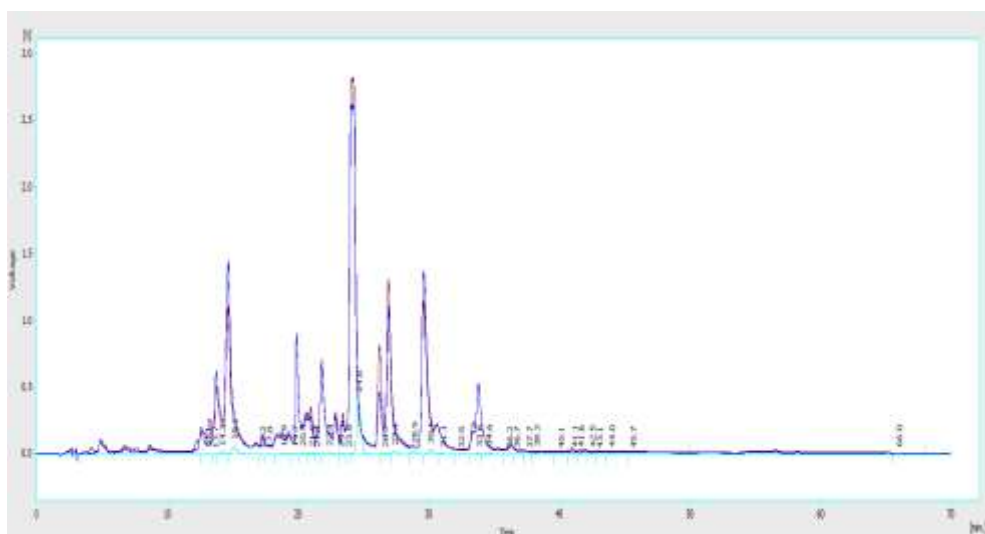


Figure 138: Chromatogram of the red Brazilian fraction (FB-3) on the ELSD-UV system; it is obvious that it consisted primarily of compounds that absorbed UV (blue trace), which could represent flavonoids and phenolics. Although compounds without chromophores such as terpenoids or fats were also identified (light blue trace) but their intensities were not high

4.4.3 Characterisation of FB-3-10 as calycosin

CC and then SEC was performed for isolation of FB-3-10 from the ethanolic extract of red Brazilian propolis, which took the form of white powder. Spraying with *p*-anisaldehyde-sulphuric acid reagent and exposure to heat caused it to manifest as a single spot on TLC. Elution with the mobile phase 40% HE in EtOAc gave a R_f of 0.40 on SiGel.

A molecular formula of $C_{16}H_{11}O_5$ was derived from the fact that the molecular ion $[M-H]^-$ was indicated by the negative mode HRESI-MS spectrum at m/z 283.06 (figure 139).

The compound in its proton NMR (figure 140, table 38) showed a deshielded proton singlet at 8.29 ppm typical of the H-2 of an isoflavone. The proton spectrum of the compound showed two sets of aromatic ABX spin systems and that confirmed the presence of two trisubstituted benzene rings. The first set were at δ_{H} ppm 7.98 (d, $J= 8.74$), 6.93 (d, $J= 2.26$) and 6.87 (d, $J= 2.24$). The second set of the aromatic ABX protons were at 7.06 (d, $J= 1.51$), 6.96 and 6.96 (d, $J= 2.01$). Finally, a methoxy group was observed at 3.80 ppm. The ^{13}C NMR showed the presence of 16 carbon atoms made up of one carbonyl, one methoxy, 12 aromatic (including a phenolic and a methoxy substituted at 146.51 and 147.97 respectively) and two olefinic carbons conjugated to a carbonyl group. From its 2D NMR spectra (COSY, HSQC and HMBC), the structure was determined to be calycosin and it was confirmed using literature reports (Du et al., 2006).

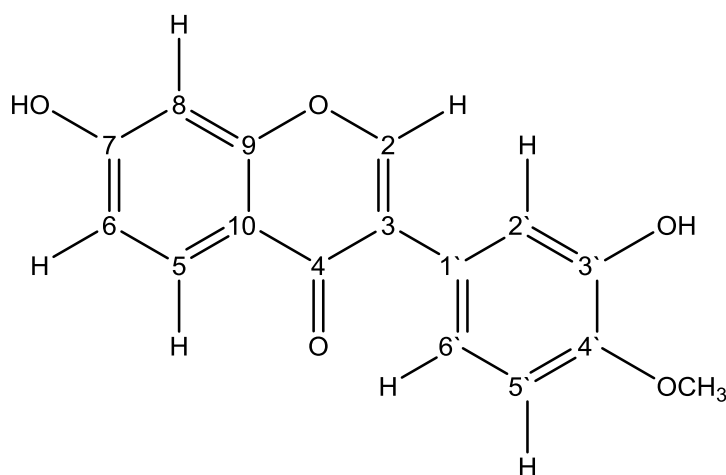


Figure 139: Structure of calycosin

Table 38: ^1H (400 MHz) and ^{13}C (100 MHz) NMR data of calycosin (FB-3-10) in DMSO-d_6

Experimental Data		
Position	^1H (multiplicity), J (Hz)	^{13}C (multiplicity)
1		
2	8.29 (s)	153.52
3		125.17
4		174.85
5	7.98 (d, $J = 8.74$)	127.76
6	6.93 (d, $J = 2.26$)	115.61
7		162.98
8	6.87 (d, $J = 2.24$)	102.57
9		157.84
10		116.37
1'		123.83
2'	7.06 (d, $J = 1.51$)	116.92
3'		146.51
4'		147.97
5'	6.96 (overlapped)	112.45
6'	6.96 (d, $J = 2.01$)	120.16
7-OH	10.78 (s)	
3'-OH	9.0 (s)	
4'-OCH ₃	3.80 (s, 3H)	56.16

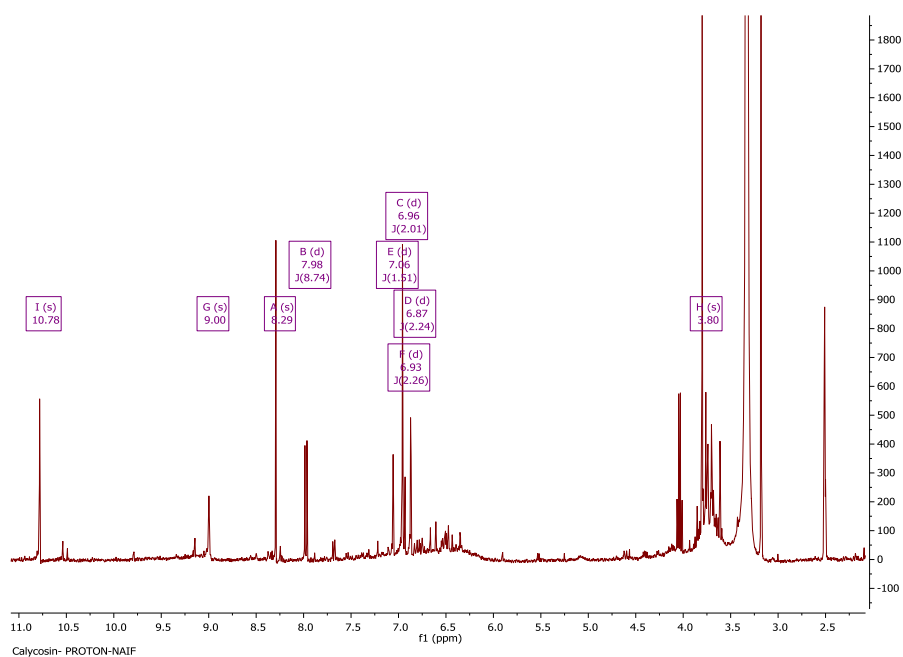


Figure 140: ^1H NMR spectrum (400 MHz) of calycosin (FB-3-10) in DMSO-d_6

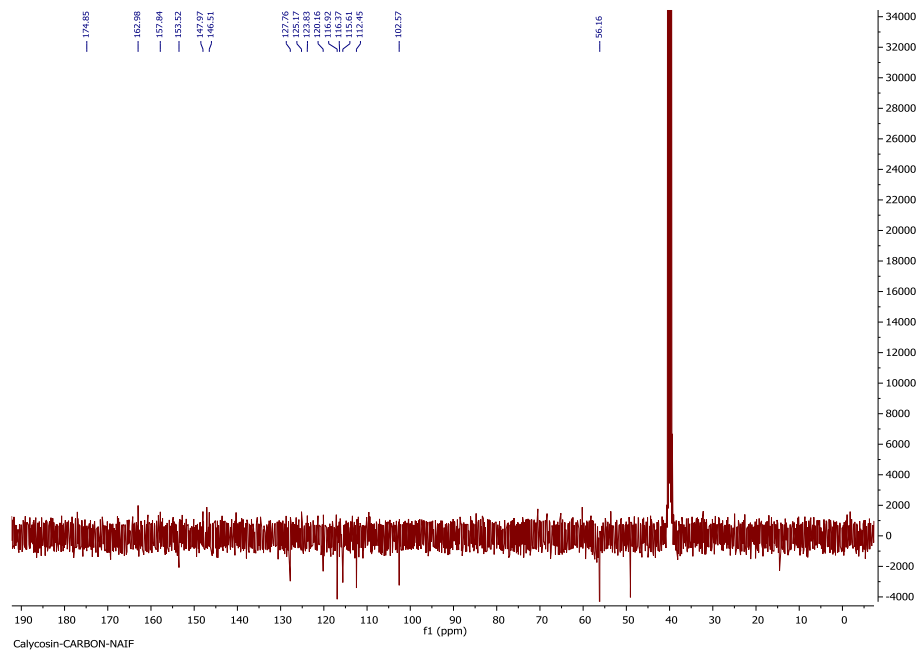


Figure 141: ^{13}C NMR spectrum (100 MHz) of calycosin (FB-3-10) in DMSO-d_6

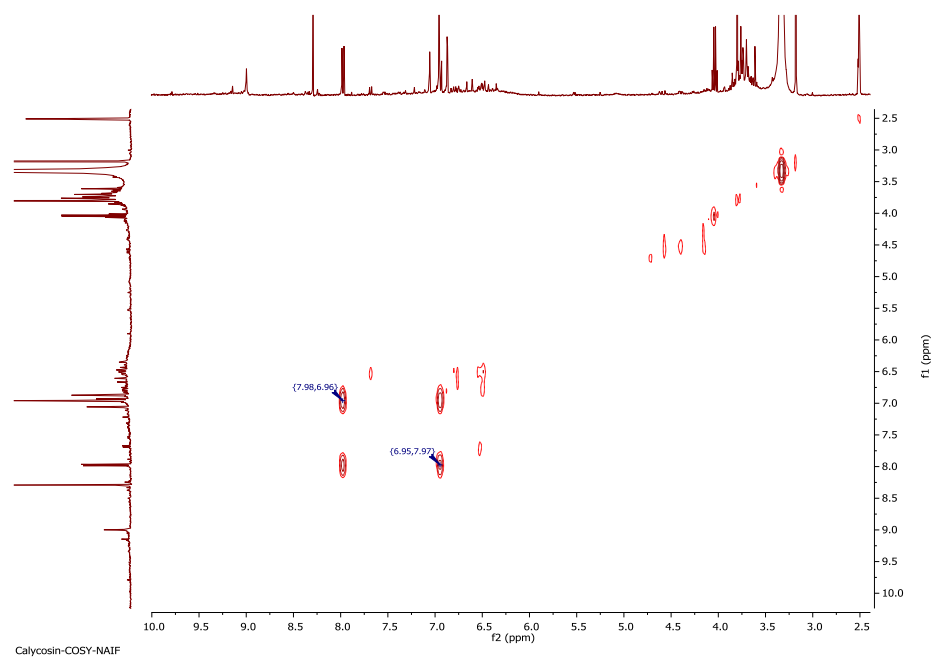


Figure 142: COSY spectrum (400 MHz) of calycosin (FB-3-10) in DMSO-d_6

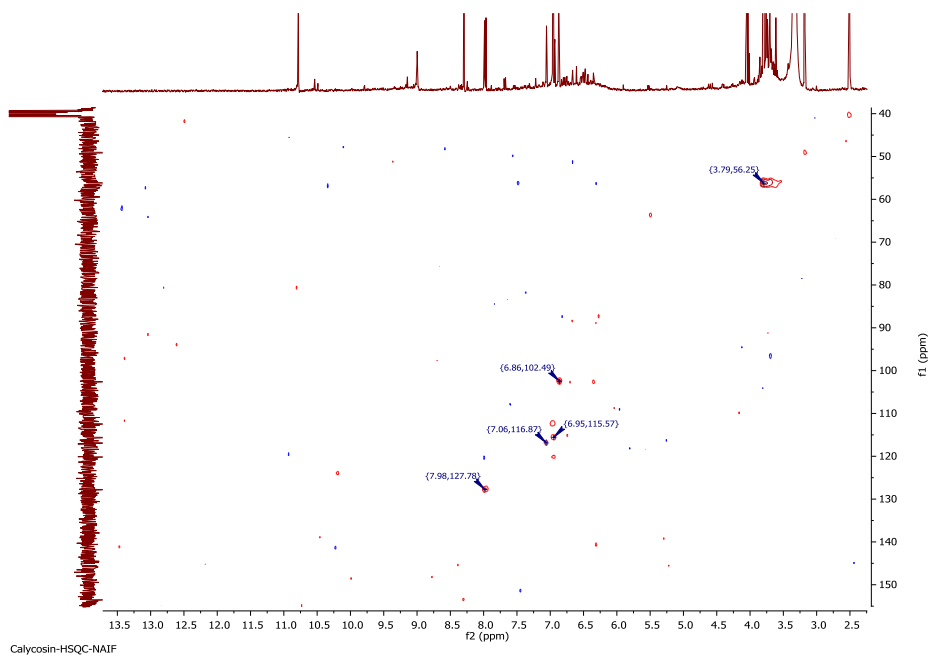


Figure 143: HSQC spectrum (400 MHz) of calycosin (FB-3-10) in DMSO-d₆

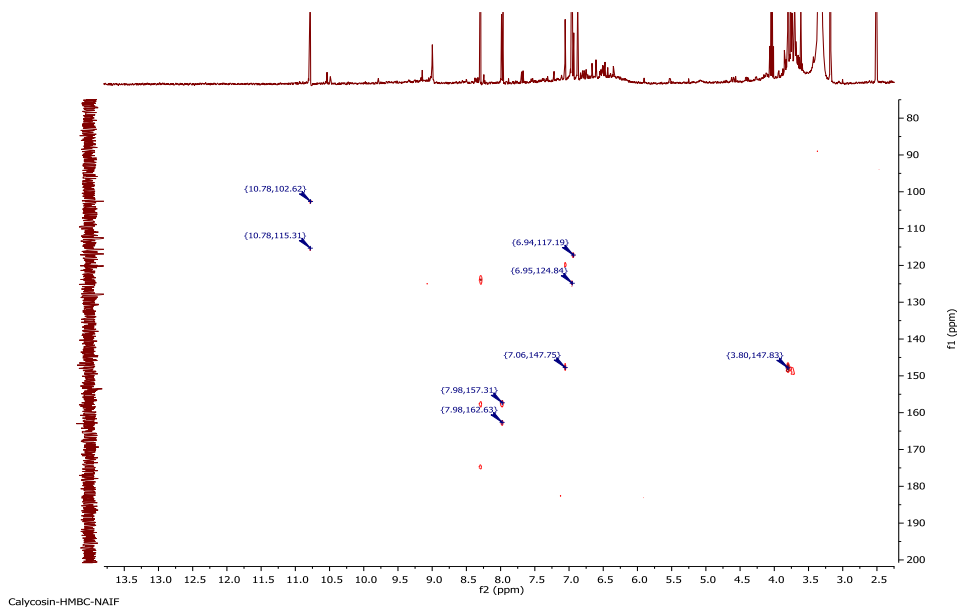


Figure 144: HMBC spectrum (400 MHz) of calycosin (FB-3-10) in DMSO-d₆

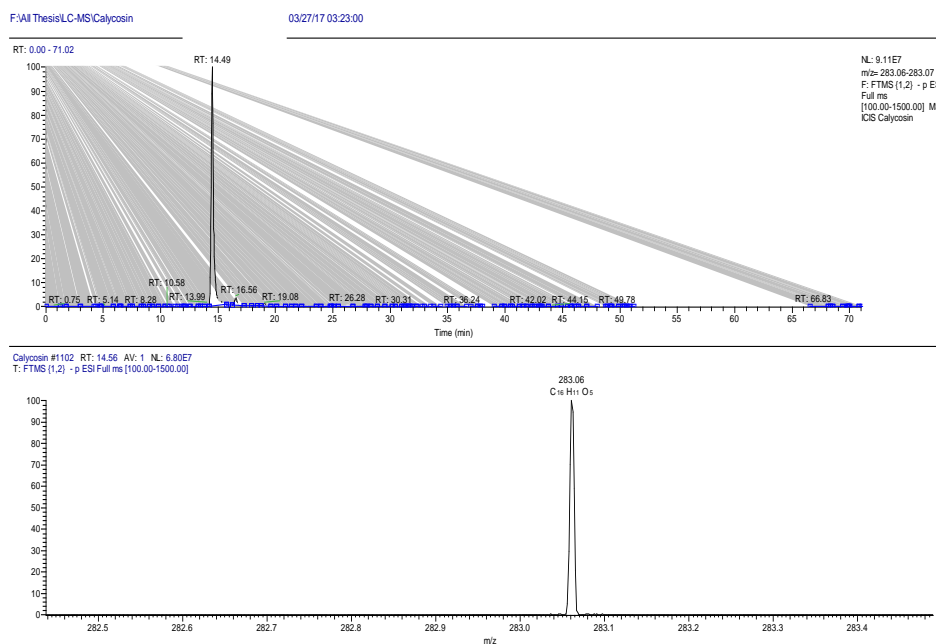


Figure 145: (A) Extracted ion chromatogram corresponding to the mass of calycosin in the negative ion mode (-ve ESI) (B) The spectrum corresponding to the calycosin chromatogram

4.4.4 Characterisation of FB-3-14 as liquiritigenin

CC and then SEC was performed for isolation of FB-3-14 from the ethanolic extract of red Brazilian propolis, which took the form of white powder. Spraying with *p*-anisaldehyde-sulphuric acid reagent and exposure to heat caused it to manifest as a single spot on TLC. Elution with the mobile phase 40% HE in EtOAc gave an R_f of 0.42 on SiGel.

A molecular formula of $C_{15}H_{11}O_4$ was derived from the fact that the molecular ion $[M-H]^-$ was indicated by the negative mode HRESI-MS spectrum at m/z 255.07 (figure 146).

In its ^1H NMR (400 MHz) spectrum the compound (figure 147, table 39) showed a set of three aromatic protons with an ABX coupling at 7.88 (d, $J= 8.65$), 6.56 (dd, $J= 8.65$, 2.37) and 6.46 (d, $J= 2.36$) for a trisubstituted benzene ring and another four aromatic protons with an AA'BB' coupling for a disubstituted benzene ring at 7.37 (d, $J= 2.13$), 7.38 (d, $J=2.11$), 6.90 (d, $J= 2.06$) and 6.92 (d, $J= 2.10$). Three coupled aliphatic protons were observed at 5.42 (dd, $J= 13.22$, 2.88), 2.82 (dd, $J= 16.86$, 2.91) and 3.06 (dd, $J= 16.85$, 13.23). Their chemical shift values were indicative of proximity to a carbonyl or electron withdrawing group such as a benzene ring. The ^{13}C spectrum showed a total of 15 carbon signals made up of one carbonyl at 175.27, 12 aromatic carbons and two aliphatic carbons at 162.64 and 159.74. Using its 2D (COSY, HMQC and HMBC), the chemical shift assignments for its proton and carbon atoms were determined and the structure was confirmed by literature reports to be liquiritigenin (Ma et al., 2005).

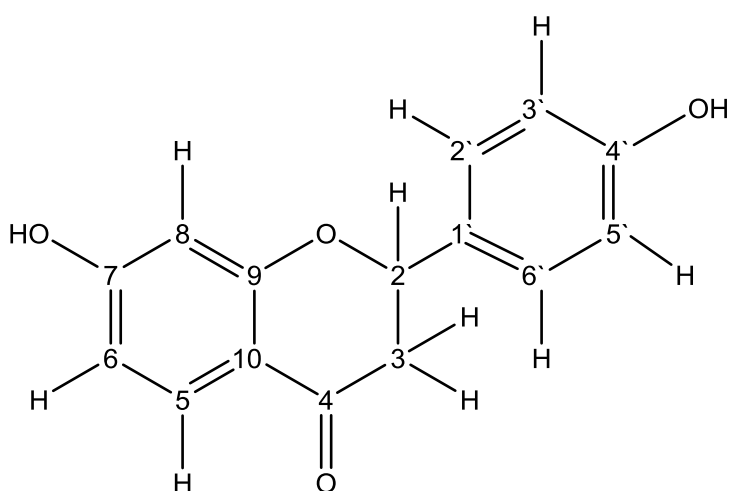


Figure 146: Structure of liquiritigenin

Table 39: ^1H (400 MHz) and ^{13}C (100 MHz) NMR data of liquiritigenin (FB-3-14) in CDCl_3

Experimental Data		
Position	^1H (multiplicity), J (Hz)	^{13}C (multiplicity)
1		
2	5.44 (dd, $J= 12.83, 2.85$)	79.42
3	2.63 (dd, $J= 16.81, 3.01$)	43.59
3	3.11 (dd, $J= 16.81, 12.91$)	43.59
4		175.04
5	7.65 (d, $J= 8.64$)	127.74
6	6.51 (dd, $J= 8.66, 2.26$)	110.99
7		163.54
8	6.33 (d, $J= 2.23$)	103.3
9		165.18
10		113.95
1`		129.74
2`	7.33 (d, $J= 8.58$)	115.59
3`	6.80 (d, $J= 8.57$)	128.7
4`		158.07
5`	6.80 (d, $J= 8.57$)	128.85
6`	7.33 (d, $J= 8.58$)	115.68

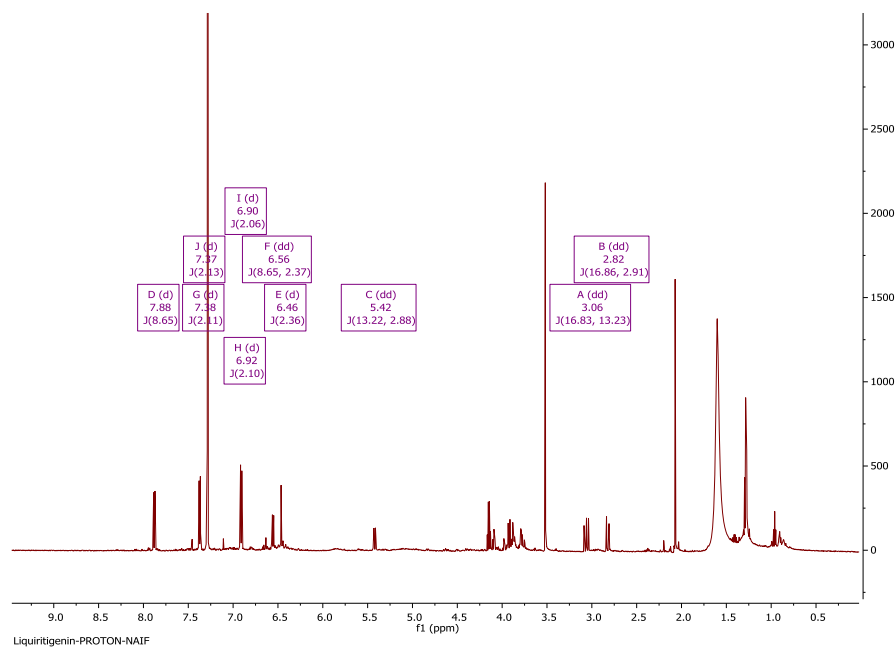


Figure 147: ^1H NMR spectrum (400 MHz) of liquiritigenin (FB-3-14) in CDCl_3

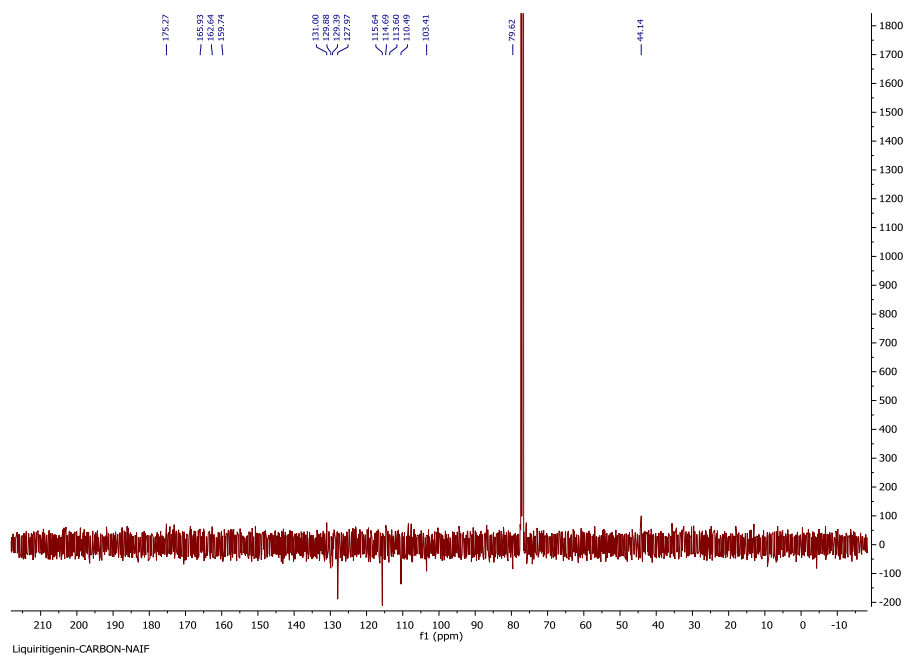


Figure 148: ^{13}C NMR spectrum (100 MHz) of liquiritigenin (FB-3-14) in CDCl_3

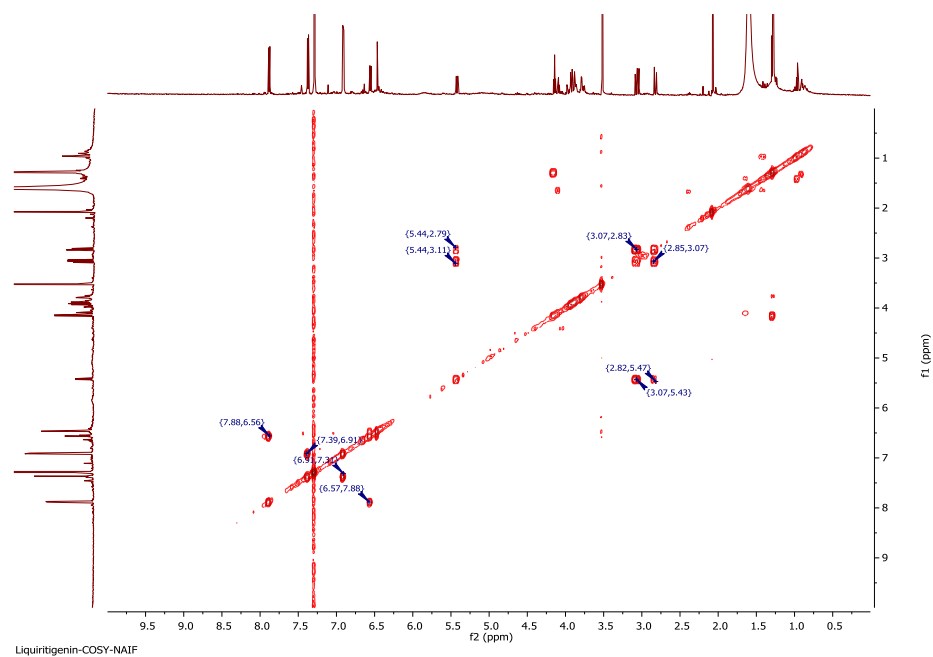


Figure 149: COSY spectrum (400 MHz) of liquiritigenin (FB-3-14) in CDCl_3

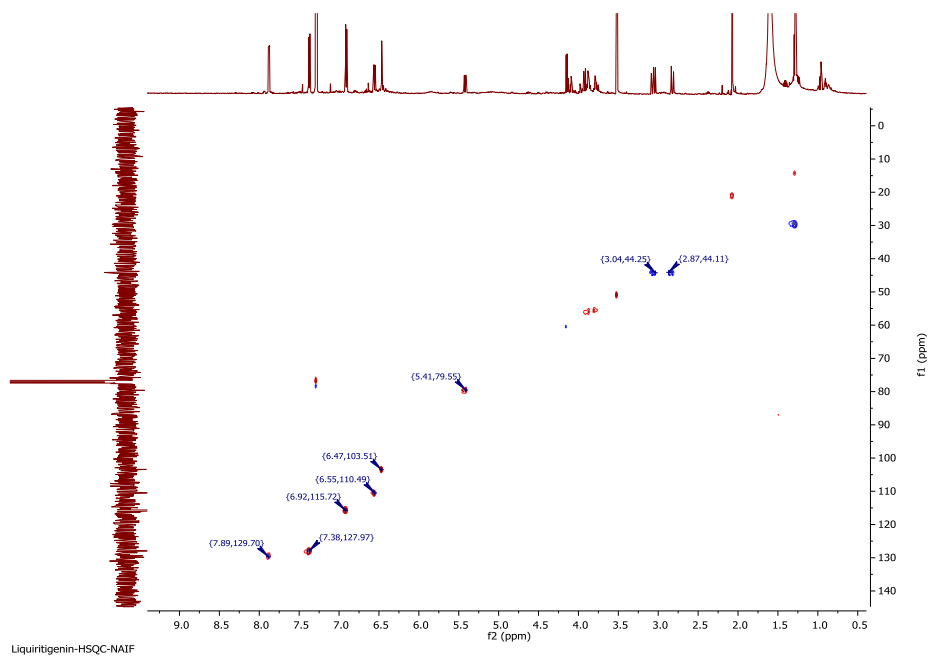


Figure 150: HSQC spectrum (400 MHz) of liquiritigenin (FB-3-14) in CDCl_3

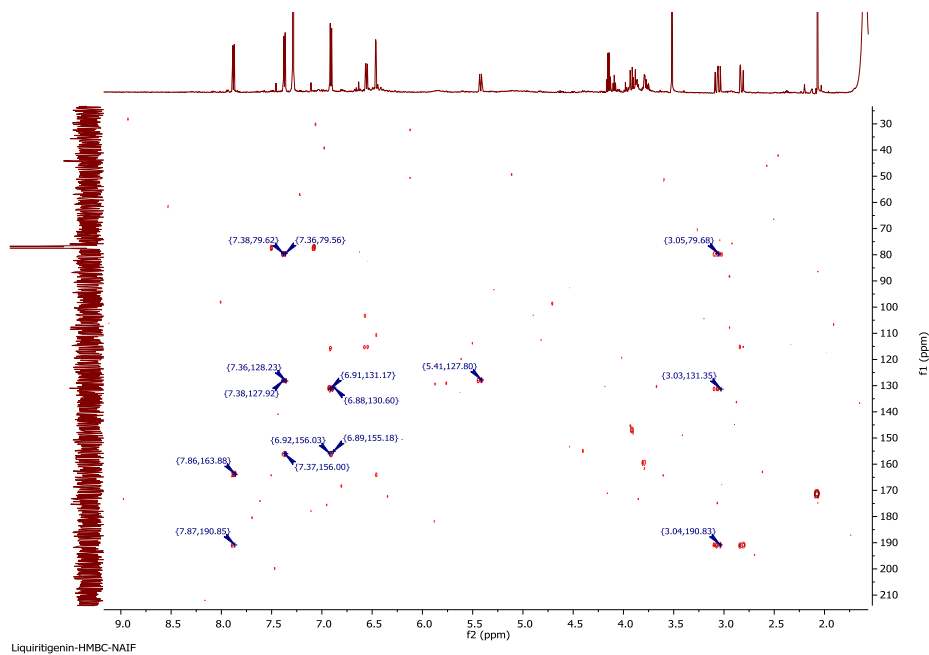


Figure 151: HMBC spectrum (400 MHz) of liquiritigenin (FB-3-14) in CDCl_3

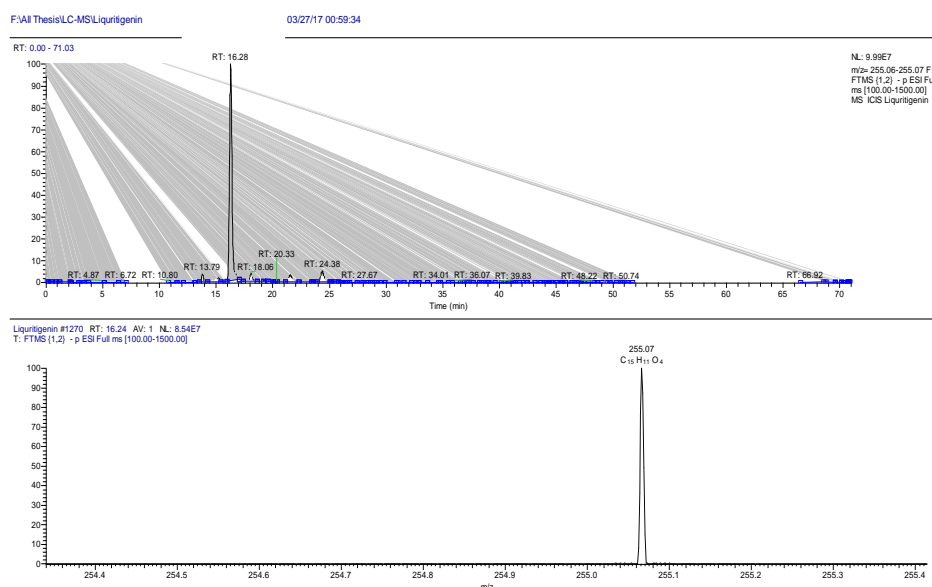


Figure 152: (A) Extracted ion chromatogram corresponding to the mass of liquiritigenin in the negative ion mode (-ve ESI) (B) The spectrum corresponding to the liquiritigenin chromatogram

4.4.5 Biological activities of the Red Brazilian propolis sample against trypanosome (*T.brucei* S427 strain)

Crude, fraction and pure compounds (liquiritigenin and calycosin) were extracted from the Red Brazilian propolis sample and all were tested against *T.brucei*. Pentamidine and Diminazen were used as drug controls and their MIC values were 0.0048 and 0.0373 µg/ml respectively. Table 40a and b below shows the results from testing red Brazilian propolis extract and its components against *T. brucei*. The results showed a varying activity against *T. brucei* between tested samples. FB-3 fraction has a higher activity, 1.6 µg/ml, than the crude which is 12.4 µg/ml and this was the most active fraction isolated in the present study. The pure compounds showed moderate activity with an MIC of 8.5 µg/ml for liquiritigenin and 8.7 µg/ml for calycosin. Overall, crude, fractions and pure compounds were mainly moderately active against

T. brucei S427 WT (see table 40 a). It is worth noting that the crude as well as liquiritigenin samples gave increased cell viability (> 100 µg /mL) while FB-3 fraction and Calycosin were showed a close toxicity result to Diminazene (as its minimum IC50 value > 30 µg/ml). Pentamidine and Diminazene gave the lowest IC50 values at 13.32 µg /mL and 29.58 µg/mL, respectively. Table 40b shows detailed IC50 values for tested samples.

Table 40 a: Drug Sensitivity assay of the red Brazilian propolis sample and its fractions on *T. brucei* S427 WT

Sample code	Exp. 1 (µg/ml)	Exp. 2 (µg/ml)	Exp. 1 (µg/ml)	Mean (µg/ml)	SD	%RSD
Red Brazilian crude	12.0	13.1	12.0	12.4	0.62	5.02
FB-3 fraction	1.7	1.7	1.5	1.6	0.11	6.50
Liquiritigenin	6.7	9.6	9.4	8.5	1.63	19.13
Calycosin	9.3	8.4	8.5	8.7	0.52	5.99
Pentamidine(µM)	0.0044	0.0049	0.0051	0.0048	0.0004	7.6110
Diminazen(µM)	0.0377	0.0357	0.0389	0.0374	0.0017	4.4221

Table 40 b: Cytotoxicity assay of red Brazilian propolis sample and its fractions on U937 cells

Sample code	Exp. 1 (µg/ml)	Exp. 2 (µg/ml)	Exp. 3 (µg/ml)	Mean (µg/ml)	SD	%RSD
Red Brazilian crude	102.3	100.6	120.8	107.9	11.20	10.38
FB-3 fraction	41.1	48.5	45.6	45.1	3.75	8.33
Liquiritigenin	86.6	97.2	93.8	92.5	5.43	5.86
Calycosin	33.9	30.1	43.6	35.8	6.99	19.50
Pentamidine(µM)	13.4300	14.2700	12.2500	13.3167	1.0148	7.6202
Diminazen(µM)	29.5300	31.7700	27.4300	29.5767	2.1704	7.3381

4.5 Discussion

The variability in the chemical composition of propolis is significant, even in the case of propolis from the same geographical area. However, besides chemical composition, biological properties are also highly important in assessing the quality of propolis and thus in standardising propolis samples. Propolis has been reported to consist of over 300 compounds, but not all compounds are related to biological effects. Under these circumstances, achievement of standardisation of propolis samples from different geographical areas with different biological effects has not been possible so far. In order to link a specific chemical type of propolis to a specific biological effect, additional study is required in order to accomplish standardisation of propolis types (Huang et al., 2014).

In recent times, ample research has been carried out on propolis derived from different geographical regions, including Europe, Asia, North America and South America, particularly Brazil (Salomao et al., 2011; da Silva Frozza et al., 2013). In the case of Asia, comprehensive investigations (Petrova et al., 2010) have focused on propolis from China (Banskota et al., 2000; Ahn et al., 2007; Yang et al., 2011), Japan (Kumazawa et al., 2007; Hamasaka et al., 2004), Taiwan (Chen et al., 2008; Lu et al., 2003), Nepal (Shrestha et al., 2007; Huang et al., 2014) and Myanmar (Li et al., 2009). Given the considerable complexity of the mixture produced by the various compounds present in propolis crude extracts, it is improbable to acquire a single pure compound from the crude extract through with just one separation method. Consequently, the crude extract frequently has to be fractionated into several different fractions with polarities or molecular sizes that do not differ much. However, attention must be paid to the fact that detection of fractions with the compound in low concentration or detection of activity in bioassays in the case of bioassay-based isolation processes may fail if the number of fractions produced is too high, as this will result in the spreading of the compound in question across too many fractions

(Sarker and Nahar, 2012). In the present study, absolute ethanol was selected as the solvent system for the extraction of different quantities of raw propolis samples from Saudi Arabia, the Philippines, Nigeria and Brazil. CC and SEC were subsequently conducted to analyse the chemistry of those samples.

The two simple compounds were isolated from Saudi propolis based on the fractionations of the ethanol extract of Saudi propolis via CC and SEC were fisetinidol and ferulic acid. Among the potential biological effects that were examined in relation to these compounds are effects against bacteria, cancer (Yoshioka et al., 2004, Liao et al., 2014, Chang et al., 2009), and leishmaniasis (Tasdemir et al., 2006).

Fisetinidol was extracted by Almutairi et al., (2014) from a sample of propolis from Saudi Arabia and found to have no activity against trypanosomes and bacteria. By contrast, Ikarashi et al., (2011) reported that fisetinidol inhibited lipase and glucosidase activity and decreased the levels of plasma triglycerides and glucose that had been heightened by lipid and carbohydrate loading. According to the findings of this second study, fisetinidol can be said to have potential anti-obesity and anti-diabetes effects.

Ferulic acid was indicated by the elemental composition $C_{10}H_9O_4$ in numerous samples of propolis from Saudi Arabia (El-Mawla and Osman, 2011) and argued that it was favourable for the histological and ultrastructural imaging of kidney that had been treated with monosodium glutamate. However, as a derivative of 3-methoxy caffeic acid, ferulic acid is 30 times less potent compared to caffeic acid. (Tasdemir et al., 2006) reported that caffeic acid effectively hindered *T. brucei rhodesiense* from growing, thanks to its ortho-dihydroxyphenyl structure that was apparently crucial for effects against trypanosomes.

From this study, table 19a, a varying activity against *T. brucei* between samples obtained from Saudi propolis was found. From table 19a, S-6 fraction, 2.4 µg/ml MIC, showed the highest activity, among tested samples, followed by Saudi crude propolis extract with 4.6 µg/ml MIC whereas fisetinidol and ferulic acid were shown to have very low to almost no activity. The inhibitory effects against *T. brucei* did not extend to toxicity against mammalian cells, table 19b, this added to the above activities indicates a potential selective anti-parasitic activity.

Three triterpenes were isolated by employing CC and then SEC for fractionation of the ethanol extract of Philippine propolis, namely, 27-hydroxymangiferonic acid, 27-hydroxyisomangiferolic acid and isomangiferolic acid. Grace et al., recently isolated these compounds from pistachio hull extracts and discovered that they exhibited some effects against oxidants (Grace et al. 2016). This is supported by the fact that the carboxylic acid and hydroxyl groups present in the chemical composition of these compounds are predisposed to produce H-donating antioxidants. Furthermore, the outcomes of a DPPH+ assay undertaken by Smina et al.,(2011) suggested that the antioxidant effects of triterpenes were due to their scavenging of superoxide radicals and strong action against lipid peroxidation *in vitro*. Campos et al.,(2014) reported that, owing to their antioxidant effects, triterpenes could suppress haemolysis in human erythrocytes.

The contribution of terpenoids to nerve function repair and improvement was highlighted by many studies e.g. Sakina and Dandiya, (1990). Moreover, the strong *in vitro* and *in vivo* activities of terpenoids was determined by Yoo and Park, (2012) who claimed that these chemical substances could be anti-Alzheimer's disease agents. Nitric oxide (NO) synthase was established to be the major determinant of CNS disorders, contributing to dopaminergic neurodegeneration and potentially encouraging production of free radicals in neuronal cells (Hunot et al., 1996; Iravani et al., 2002). Thus, due to its free radical properties, NO could adversely impact

neuronal cells and cause the destruction of dopaminergic neurons if its level were higher than normal. Along similar lines, Liberatore et al.,(1999) argued that Parkinson's disease might be treated or prevented through the use of suppressors of NO in neurons. Likewise, Honda et al., carried out an *in vivo* study and provided convincing evidence that NO production was strongly suppressed by triterpenoids. Hence, suppression of NO production could be a useful mechanism in the treatment of not only Parkinson's disease, but also any other CNS disorders (Honda et al. 1999).

In this study the biological activities of the Philippines propolis sample against trypanosome (*T. brucei* S427 strain) were tested, see table 26a. Unfortunately, of the crude, fraction and pure compounds which were tested none were toxic, table 26b, were almost inactive against *T. brucei* S427 WT and thus the further testing in this project was terminated.

The fractionation of the ethanol extract of red Nigerian propolis, using CC followed by SEC, led to the isolation of two phenolic compounds isosativan and medicarpin. Both of these compounds have been isolated from red Brazilian propolis and were tested for their antibacterial and radical scavenging activity against DPPH radicals. The results indicated that the isosativan and medicarpin are important antimicrobial components of red propolis, especially concerning activity against *C. albicans*. This is not surprising, taking into consideration that pterocarpanes are known for their antifungal activity and play a defensive role in many plants due to this activity (Trusheva et al., 2006). Isolation of these compounds further supports the fact that bees target the same plants for propolis collection in the tropical regions of Brazil and Nigeria.

Two phenolic compounds were isolated when CC and then SEC was used for fractionation of the ethanol extract of red propolis from Brazil, namely, calycosin and liquiritigenin. Red propolis from Nigeria was also found to contain these compounds

(Omar et al., 2016, Omar et al., 2017) and they exhibited moderate effects against *Trypanosoma brucei*. The moderate activity as well has been seen upon testing activities of our Red Nigerian propolis sample against trypanosome *T. brucei* S427 strain, see table 33a, which revealed that red Nigerian crude has a higher activity, 6.5 µg/ml, than one of the fractions which was 8.0 µg/ml. However, it showed a high level of cytotoxicity against mammalian cells, table 33b, which may explain these inhibitory effects.

Testing the red Brazilian propolis sample for biological activities against trypanosome, see table 40a, as well showed that the FB-3 fraction has a higher activity, 1.6 µg/ml, than the crude which was 12.4 µg/ml and can be considered a moderate to high activity against *T. brucei* S427 WT. According to the cell viability test, table 40b, the inhibitory activity of the FB-3 fraction may result from cell toxicity in contrast to the crude sample which was not cytotoxic up to 100 µg/ml.

It appears that there are many similarities between red propolis from Nigeria and red propolis from Brazil. There is an abundance of isoflavonoids in Nigerian propolis, which are not found in many plant species, being nearly completely limited to legumes (*Leguminosae* family) (Silva et al., 2008), alongside isoflavans like liquiritigenin and medicarpin. Piccinelli et al. (2005) reported that red propolis from Cuba and north Brazil, produced mainly from the resin of *Dalbergia ecastophyllum*, contained liquiritigenin and medicarpin as well.

Chapter 5

Conclusions and future work

5.1 Conclusion and further research

Numerous pharmaceutical drugs derive from plants, which constitute the basis of pharmacopoeias in traditional medicine (Farnsworth, 2007; Balick and Cox, 1996; Balunas and Kinghorn, 2005, Jones et al., 2006). An increasing number of studies point to the fact that biological and ecological activity is manifested by a wide range of secondary metabolites from organisms, including plants, and this activity primarily takes the form of mechanisms of chemical transmission and defence (Caporale, 1995, Wink, 1999). Hence, the difficult process of solvent-based extraction of plant material is a prerequisite in many scientific fields to allow isolation and identification of the compounds underpinning the biological effects of a particular plant or plant extract.

The nature of the material of origin and the compounds of interest dictate the extraction technique (Sarker et al., 2005). Hence, the purpose of extraction must be established before an extraction technique is selected. The extraction process may be geared towards obtaining a known or unknown compound, a series of compounds with similar structure, or all secondary metabolites that are generated by one specific natural source but not by another “control” source (e.g. two species belonging to the same genus or the same species with different growth conditions) in order to enable chemical fingerprinting or metabolomics studies.

The extent to which a phytochemical study can be reproduced depends significantly on the techniques used to select, gather and identify plant material. These techniques must be conducted carefully; otherwise the scientific relevance of the whole study may be compromised. In many cases, secondary metabolites concentrate in particular parts of the plants, and if these parts are not known, then several parts or

the entire plant should be collected in order to make sure that all the secondary metabolites generated by the plant are present in the prepared extracts.

Traditional chromatographic methods, such as CC, SEC, TLC, PTLC, and ion-exchange chromatography, and modern chromatographic methods, such as high-performance thin layer chromatography (HPTLC), HPLC, VLC, and several combined methods (e.g. HPLC–PDA, LC–MS, LC–NMR, LC–MS–NMR), are the major classes of chromatographic methods that can be employed for the isolation of different types of natural products (Sarker and Nahar, 2012).

Identification or description of isolated natural compounds can be achieved through structure elucidation techniques, but they may slow down research on natural products because of the long time they take to complete. This is an issue particularly in situations where the knowledge about compounds is insufficient or lacking. However, a range of spectroscopic techniques are informative about chemical structures, although the spectra generated by these techniques require detailed spectroscopic acumen, competence in structure elucidation, suitable understanding of the chemical composition of natural products, as well as patience in order to be interpreted accurately. Nevertheless, a number of helpful automated tools of structure elucidation have been developed thanks to innovations in artificial intelligence and computing (Sarker and Nahar, 2012).

There are several explanations for the loss or decrease of activity during the isolation process: retention of the active compound in the column; instability of the active compound in the conditions employed in the isolation process; incompatibility between the solvent used for preparation of the extract solution and the mobile phase, causing many active constituents to precipitate out during column loading; the distribution of the majority of active constituents over different fractions, so that the

quantity occurring in any one fraction is minimal; or synergistic interaction between several compounds may be the source of the extract effects, so that the compounds do not exhibit any activity when on their own (Sarker and Nahar, 2012).

A phytochemical analysis of *Ocimum sanctum* Labiatae was carried out during current study. To this end, solvents of growing polarity were employed to perform Soxhlet extractions of the leaf part of the plant. Isolation of triterpenoids and some flavonoids was achieved through fractionation of the obtained extracts followed by purification with different chromatographic methods. The MeOH extracts of the *Ocimum sanctum* L. yielded three known compounds. The VLC method was used to perform partial fractionation, but this did not reveal any notable constituents that could be subjected to additional separation and purification, so the phytochemical analysis on n-hexane and EtOAc extracts was not very extensive.

The resinous substance called propolis is produced by bees from plant materials to patch any gaps in the hive as well as to maintain the hive free of infection, thus ensuring the health of the community. Research has long explored the biological effects of propolis, and more recently, the substance has also begun to be investigated as a potential source of novel pharmaceuticals.

Even if derived from the same geographical area, propolis may have a different chemistry. However, propolis quality is as significant as chemical composition for standardising propolis samples. Furthermore, not all of the over 300 compounds identified in propolis have biological effects, thus hindering the achievement of standardisation of propolis samples from different geographical areas with different biological properties. More study is necessary to accomplish standardisation of the different types of propolis, and thus enable a specific chemical type of propolis to be linked to a particular biological effect.

Propolis chemistry and quality are heavily influenced by the bee species, subspecies and varieties. There are ten species in the genus *Apis*, of which nine are found in Asia, while the remaining species, *Apis mellifera* (honeybee,) is the species with the widest distribution, including Europe, Africa and Asia. Based on morphometrical, behavioural and biogeographical characteristics, there are around 25 subspecies of *A. mellifera* (Arias and Sheppard, 2005). *Meliponinae* (Brazilian stingless bee) is a key species as well, being endemic to tropical areas. Geopropolis is produced by both *Melipona scutellaris* and *Melipona fasciculata*, but it differs in composition; more specifically, in the former case, it has an abundance of benzophenones whilst lacking flavonoids, meaning that its antibacterial effects are not as potent as those of *Apis mellifera* propolis, whereas in the latter case, geopropolis is rich in polyphenols, flavonoids, triterpenoids, saponins, and even tannins (Dutra et al., 2014).

Different honeybee species do not have the same plant preferences, but even in the case of the same species, the chemical composition of the produced propolis may differ. To give an example, both green propolis and red propolis from Brazilian are produced by Africanised *A. mellifera* but their composition is dissimilar, consisting primarily of prenylated phenylpropanoids and isoflavonoids, respectively. These dissimilarities stem from the fact that green propolis is derived from the plant *B. dracunculifolia*, while red propolis is derived from *D. ecastophyllum*. Hence, the plants preferred by the bees and differences in bee species and varieties in addition to the plants growing in the vicinity of the bee hive are the factors that shape the chemical profile of propolis.

In the present study, a number of terpenoids, flavonoids and simple phenolics were isolated through fractionation of extracts followed by purification with a range of

chromatographic methods. More specifically, the ethanolic extracts of Saudi, Philippine, red Nigerian and red Brazilian propolis yielded nine known compounds.

5.2 Future Work

There is still further work to be done in order to isolate individual active compounds from the fractions which were most active against *T. brucei*. It would also be of interest to test extracts, fractions and compounds against other protozoa such as Leishmania and malaria.

Due to the need to illustrate how compounds with biological activity act or interact with specific cellular pathways, current endeavours of drug discovery have begun to use novel strategies, such as metabolomics and it would be of interest to apply metabolomics to study the effect of active compounds and fractions on cell metabolism. An important line of investigation which be followed in a future study is to assess the cytotoxic effects of extracts, fractions and pure compounds on bone marrow macrophages or other cells involved in immunity, as well as to assess non-toxic concentrations for potential involvement in triggering or suppressing IL-6, IL-10, IL-1 β and TNF- α cytokines, followed by comparison with lipopolysaccharide-induced macrophages. Preliminary results not included in the thesis indicate some very interesting activity. Further testing of the S-6 fraction from Saudi propolis may reveal important compounds. Reprogramming studies can be conducted on the pathways of interest, such as employing similar agents of activation or suppression, in order to shed more light on the potential action mechanism.

6 Bibliography

- ABU-MELLAL, A., KOOLAJI, N., DUKE, R. K., TRAN, V. H. & DUKE, C. C. 2012. Prenylated cinnamate and stilbenes from Kangaroo Island propolis and their antioxidant activity. *Phytochemistry*, 77, 251-259.
- AHN, M.-R., KUMAZAWA, S., USUI, Y., NAKAMURA, J., MATSUKA, M., ZHU, F. & NAKAYAMA, T. 2007. Antioxidant activity and constituents of propolis collected in various areas of China. *Food Chemistry*, 101, 1383-1392.
- AKINSULIRE, O. R., AIBIN, I., ADENIPEKUN, T., ADELOWOTAN, T. & ODUGBEMI, T. 2007. In vitro antimicrobial activity of crude extracts from plants *Bryophyllum pinnatum* and *Kalanchoe crenata*. *African Journal of Traditional, Complementary and Alternative Medicines*, 4, 338-344.
- ALMUTAIRI, S., EAPEN, B., CHUNDI, S. M., AKHALIL, A., SIHERI, W., CLEMENTS, C., FEARNLEY, J., WATSON, D. G. & EDRADA-EBEL, R. 2014. New anti-trypanosomal active prenylated compounds from African propolis. *Phytochemistry Letters*, 10, 35-39.
- ALMUTAIRI, S., EDRADA-EBEL, R., FEARNLEY, J., IGOLI, J. O., ALOTAIBI, W., CLEMENTS, C. J., GRAY, A. I. & WATSON, D. G. 2014. Isolation of diterpenes and flavonoids from a new type of propolis from Saudi Arabia. *Phytochemistry letters*, 10, 160-163.
- ALQARNI, A. S., HANNAN, M. A., OWAYSS, A. A. & ENGEL, M. S. 2011. The indigenous honey bees of Saudi Arabia (Hymenoptera, Apidae, *Apis mellifera jemenitica* Ruttner): Their natural history and role in beekeeping. *ZooKeys*, 83.
- AWALE, S., SHRESTHA, S. P., TEZUKA, Y., UEDA, J.-Y., MATSUSHIGE, K. & KADOTA, S. 2005. Neoflavonoids and related constituents from Nepalese propolis and their nitric oxide production inhibitory activity. *Journal of natural products*, 68, 858-864.
- BAGAG, A., GIULIANI, A. & LAPRÉVOTE, O. 2008. Atmospheric pressure photoionization mass spectrometry of oligodeoxyribonucleotides. *European Journal of Mass Spectrometry*, 14, 71-80.
- BALICK, M. J. & COX, P. A. 1996. *Plants, people, and culture: the science of ethnobotany*, Scientific American Library.
- BALUNAS, M. J. & KINGHORN, A. D. 2005. Drug discovery from medicinal plants. *Life sciences*, 78, 431-441.
- BANERJEE, S. & MAZUMDAR, S. 2012. Electrospray ionization mass spectrometry: a technique to access the information beyond the molecular weight of the analyte. *International journal of analytical chemistry*, 2012.
- BANKOVA, V. 2005. Recent trends and important developments in propolis research. *Evidence-based complementary and alternative medicine*, 2, 29-32.
- BANKOVA, V. 2009. Chemical diversity of propolis makes it a valuable source of new biologically active compounds. *Journal of ApiProduct and ApiMedical Science*, 1, 23-28.
- BANKOVA, V. S., DE CASTRO, S. L. & MARCUCCI, M. C. 2000. Propolis: recent advances in chemistry and plant origin. *Apidologie*, 31, 3-15.
- BANSKOTA, A. H., TEZUKA, Y., ADNYANA, I. K., MIDORIKAWA, K., MATSUSHIGE, K., HUERTAS, A. A. & KADOTA, S. 2000. Cytotoxic, hepatoprotective and free radical scavenging effects of propolis from Brazil, Peru, the Netherlands and China. *Journal of Ethnopharmacology*, 72, 239-246.
- BANSKOTA, A. H., TEZUKA, Y. & KADOTA, S. 2001. Recent progress in pharmacological research of propolis. *Phytotherapy research*, 15, 561-571.
- BANSKOTA, A. H., TEZUKA, Y., PRASAIN, J. K., MATSUSHIGE, K., SAIKI, I. & KADOTA, S. 1998. Chemical constituents of Brazilian propolis and their cytotoxic activities. *Journal of Natural Products*, 61, 896-900.
- BARRETT, M. P., BOYKIN, D. W., BRUN, R. & TIDWELL, R. R. 2007. Human African trypanosomiasis: pharmacological re-engagement with a neglected disease. *British journal of pharmacology*, 152, 1155-1171.

- BARRETT, M. P., BURCHMORE, R. J., STICH, A., LAZZARI, J. O., FRASCH, A. C., CAZZULO, J. J. & KRISHNA, S. 2003. The trypanosomiasis. *The Lancet*, 362, 1469-1480.
- BEN-YEHOSHUA, S., BOROWITZ, C. & HANUŠ, L. O. 2012. Frankincense, myrrh, and balm of Gilead: ancient spices of Southern Arabia and Judea. *Horticultural Reviews, Volume 39*, 1-76.
- BESSEN, H. A. 1986. Therapeutic and toxic effects of digitalis: William Withering, 1785. *Journal of Emergency Medicine*, 4, 243-248.
- BISI-JOHNSON, M. A., OBI, C. L., HATTORI, T., OSHIMA, Y., LI, S., KAMBIZI, L., ELOFF, J. N. & VASAIKAR, S. D. 2011. Evaluation of the antibacterial and anticancer activities of some South African medicinal plants. *BMC complementary and alternative medicine*, 11, 14.
- BLANCO, F., ALKORTA, I. & ELGUERO, J. 2007. Spectral assignments and reference data. *Magn. Reson. Chem*, 45, 797-800.
- BLAYLOCK, R. L. & MAROON, J. 2012. Natural plant products and extracts that reduce immunoexcitotoxicity-associated neurodegeneration and promote repair within the central nervous system. *Surgical neurology international*, 3.
- BOERSMA, M. G., VAN DER WOUDE, H., BOGAARDS, J., BOEREN, S., VERVOORT, J., CNUBBEN, N. H., VAN IERSEL, M. L., VAN BLADEREN, P. J. & RIETJENS, I. M. 2002. Regioselectivity of phase II metabolism of luteolin and quercetin by UDP-glucuronosyl transferases. *Chemical research in toxicology*, 15, 662-670.
- BOGDANOV, S. & BANKOVA, V. 2012. The Propolis Book. *Bee hexagon*.
- BOGDANOV, S. 2012. Propolis: composition, health, medicine: a review. *Bee Product Science*, [www. Bee-hexagon. Net](http://www.bee-hexagon.net).
- BOUTEILLE, B., OUKEM, O., BISSER, S. & DUMAS, M. 2003. Treatment perspectives for human African trypanosomiasis. *Fundamental & clinical pharmacology*, 17, 171-181.
- BREITMAIER, E. & SINNEMA, A. 1993. *Structures Elucidation by NMR in Organicchemistry*, Wiley Chichester New York Brisbane Toronto Singapore.
- BROADHURST, C. 1996. Benefits of bee propolis. *Health Supplement Retailer*, 46-48.
- BURDOCK, G. 1998. Review of the biological properties and toxicity of bee propolis (propolis). *Food and Chemical toxicology*, 36, 347-363.
- CAMPOS, J. F., DOS SANTOS, U. P., MACORINI, L. F. B., DE MELO, A. M. M. F., BALESTIERI, J. B. P., PAREDES-GAMERO, E. J., CARDOSO, C. A. L., DE PICOLI SOUZA, K. & DOS SANTOS, E. L. 2014. Antimicrobial, antioxidant and cytotoxic activities of propolis from *Melipona orbignyi* (Hymenoptera, Apidae). *Food and Chemical Toxicology*, 65, 374-380.
- CANTARELLI, M. Á., CAMIÑA, J. M., PETTENATI, E. M., MARCHEVSKY, E. J. & PELLERANO, R. G. 2011. Trace mineral content of Argentinean raw propolis by neutron activation analysis (NAA): Assessment of geographical provenance by chemometrics. *LWT-Food Science and Technology*, 44, 256-260.
- CAPORALE, L. H. 1995. Chemical ecology: a view from the pharmaceutical industry. *Proceedings of the National Academy of Sciences*, 92, 75-82.
- CHANG, S. W., KIM, K. H., LEE, I. K., CHOI, S. U., RYU, S. Y. & LEE, K. R. 2009. Phytochemical constituents of *Bistorta manshuriensis*. *Nat Prod Sci*, 15, 234-240.
- CHEN, Y. W., WU, S. W., HO, K. K., LIN, S. B., HUANG, C. Y. & CHEN, C. N. 2008. Characterisation of Taiwanese propolis collected from different locations and seasons. *Journal of the Science of Food and Agriculture*, 88, 412-419.
- CHIN, Y.-W., BALUNAS, M. J., CHAI, H. B. & KINGHORN, A. D. 2006. Drug discovery from natural sources. *The AAPS journal*, 8, E239-E253.
- CLARIDGE, T. D. 2016. *High-resolution NMR techniques in organic chemistry*, Elsevier.

- COGGSHALL, W. L. & MORSE, R. A. 1984. Beeswax: production, harvesting, processing and products. *Beeswax: production, harvesting, processing and products*.
- COLL, J. C. & BOWDEN, B. F. 1986. The application of vacuum liquid chromatography to the separation of terpene mixtures. *Journal of Natural Products*, 49, 934-936.
- CRAGG, G. M. & NEWMAN, D. J. 2005. Plants as a source of anti-cancer agents. *Journal of ethnopharmacology*, 100, 72-79.
- CRAGG, G. M., NEWMAN, D. J. & SNADER, K. M. 1997. Natural products in drug discovery and development. *Journal of natural products*, 60, 52-60.
- CRANE, E. 1988. Beekeeping: Science. *Practice and World Recourses*, Heinemann, London.
- DANTAS, A. P., OLIVIERI, B. P., GOMES, F. H. & DE CASTRO, S. L. 2006a. Treatment of *Trypanosoma cruzi*-infected mice with propolis promotes changes in the immune response. *Journal of ethnopharmacology*, 103, 187-193.
- DANTAS, A. P., SALOMÃO, K., BARBOSA, H. S. & DE CASTRO, S. L. 2006b. The effect of Bulgarian propolis against *Trypanosoma cruzi* and during its interaction with host cells. *Memorias do Instituto Oswaldo Cruz*, 101, 207-211.
- DA SILVA FROZZA, C. O., GARCIA, C. S. C., GAMBATO, G., DE SOUZA, M. D. O., SALVADOR, M., MOURA, S., PADILHA, F. F., SEIXAS, F. K., COLLARES, T. & BORSUK, S. 2013. Chemical characterization, antioxidant and cytotoxic activities of Brazilian red propolis. *Food and chemical toxicology*, 52, 137-142.
- DAUGSCH, A., MORAES, C. S., FORT, P. & PARK, Y. K. 2008. Brazilian red propolis—chemical composition and botanical origin. *Evidence-Based Complementary and Alternative Medicine*, 5, 435-441.
- DE CASTRO, S. & HIGASHI, K. 1995. Effect of different formulations of propolis on mice infected with *Trypanosoma cruzi*. *Journal of ethnopharmacology*, 46, 55-58.
- DEREVICI, A., POPESCO, A. & POPESCO, N. 1965. Biological properties of propolis. *Revue de Pathologie Comparee*, 2, 21-24.
- DEVI, P. U., GANASOUNDARI, A., RAO, B. & SRINIVASAN, K. 1999. In vivo radioprotection by ocimum flavonoids: survival of mice. *Radiation Research*, 151, 74-78.
- DOUGLAS, N. M., ANSTEY, N. M., ANGUS, B. J., NOSTEN, F. & PRICE, R. N. 2010. Artemisinin combination therapy for vivax malaria. *The Lancet infectious diseases*, 10, 405-416.
- DU, X., BAI, Y., LIANG, H., WANG, Z., ZHAO, Y., ZHANG, Q. & HUANG, L. 2006. Solvent effect in 1H NMR spectra of 3'-hydroxy-4'-methoxy isoflavonoids from *Astragalus membranaceus* var. *mongholicus*. *Magnetic Resonance in Chemistry*, 44, 708-712.
- DUTRA, R. P., ABREU, B. V. D. B., CUNHA, M. S., BATISTA, M. C. A., TORRES, L. M. B. O., NASCIMENTO, F. R. F., RIBEIRO, M. N. S. & GUERRA, R. N. M. 2014. Phenolic acids, hydrolyzable tannins, and antioxidant activity of geopropolis from the stingless bee *Melipona fasciculata* Smith. *Journal of Agricultural and Food Chemistry*, 62, 2549-2557.
- EL-ANEED, A., COHEN, A. & BANOUB, J. 2009. Mass spectrometry, review of the basics: electrospray, MALDI, and commonly used mass analyzers. *Applied Spectroscopy Reviews*, 44, 210-230.
- EL-MAWLA, A. M. A. & OSMAN, H. E. H. 2011. HPLC analysis and role of the Saudi Arabian propolis in improving the pathological changes of kidney treated with monosodium glutamate. *J. Complement. Med. Drug Discov*, 1, 119-127.
- EL HADY, F. K. A. & HEGAZI, A. G. 2002. Egyptian propolis: 2. Chemical composition, antiviral and antimicrobial activities of East Nile Delta propolis. *Zeitschrift für Naturforschung C*, 57, 386-394.
- ESCOBEDO-MARTÍNEZ, C., CONCEPCIÓN LOZADA, M., HERNÁNDEZ-ORTEGA, S., VILLARREAL, M. L., GNECCO, D., ENRÍQUEZ, R. G. & REYNOLDS, W. 2012. 1H and 13C NMR characterization of new cycloartane triterpenes from *Mangifera indica*. *Magnetic Resonance in Chemistry*, 50, 52-57.

- EVANS, W. C. 2009. *Trease and Evans' Pharmacognosy E-Book*, Elsevier Health Sciences.
- FAIRLAMB, A. H. 2003. Chemotherapy of human African trypanosomiasis: current and future prospects. *Trends in parasitology*, 19, 488-494.
- FALCÃO, S. I., VALE, N., COS, P., GOMES, P., FREIRE, C., MAES, L. & VILAS-BOAS, M. 2014. In vitro evaluation of Portuguese propolis and floral sources for antiprotozoal, antibacterial and antifungal activity. *Phytotherapy research*, 28, 437-443.
- FARNSWORTH, N. R. Ethnopharmacology and drug development. Ciba Foundation Symposium 185-Ethnobotany and the Search for New Drugs, 2007. Wiley Online Library, 42-59.
- FEARNLEY, J. 2001. *Bee propolis: natural healing from the hive*, Souvenir Press.
- FREITAS, S., SHINOHARA, L., SFORCIN, J. & GUIMARÃES, S. 2006. In vitro effects of propolis on *Giardia duodenalis* trophozoites. *Phytomedicine*, 13, 170-175.
- FRIEBOLIN, H. & BECCONSALL, J. K. 1993. *Basic one-and two-dimensional NMR spectroscopy*, VCH Weinheim.
- GANESAN, A. 2008. The impact of natural products upon modern drug discovery. *Current opinion in chemical biology*, 12, 306-317.
- GAVAGHAN, C., WILSON, I. & NICHOLSON, J. 2002. Physiological variation in metabolic phenotyping and functional genomic studies: use of orthogonal signal correction and PLS-DA. *FEBS letters*, 530, 191-196.
- GOEL, A., KUMAR, S., SINGH, D. K. & BHATIA, A. K. 2010. Wound healing potential of *Ocimum sanctum* linn. With induction of tumor necrosis factor.
- GOTTLIEB, H. E., KOTLYAR, V. & NUDELMAN, A. 1997. NMR chemical shifts of common laboratory solvents as trace impurities. *The Journal of organic chemistry*, 62, 7512-7515.
- GRACE, M. H., ESPOSITO, D., TIMMERS, M. A., XIONG, J., YOUSEF, G., KOMARNYTSKY, S. & LILA, M. A. 2016. Chemical composition, antioxidant and anti-inflammatory properties of pistachio hull extracts. *Food chemistry*, 210, 85-95.
- GUPTA, S., PRAKASH, J. & SRIVASTAVA, S. 2002. Validation of traditional claim of Tulsi, *Ocimum sanctum* Linn. As a medicinal plant.
- HADDAD, P. R. 1996. *Chromatographic methods: A. Braithwaite and FJ Smith*; Blackie Academic & Professional, London, Glasgow, Weinheim (1996); Price (paperback version) £ 32.50; ISBN 0-7514-0158-7, XIV+ 559 pp. Elsevier
- HAMASAKA, T., KUMAZAWA, S., FUJIMOTO, T. & NAKAYAMA, T. 2004. Antioxidant activity and constituents of propolis collected in various areas of Japan. *Food Science and Technology Research*, 10, 86-92.
- HARVEY, A. L. 2008. Natural products in drug discovery. *Drug discovery today*, 13, 894-901.
- HAVSTEEN, B. 1983. Flavonoids, a class of natural products of high pharmacological potency. *Biochemical pharmacology*, 32, 1141-1148.
- HEFTMANN, E. 2004. *Chromatography: Fundamentals and applications of chromatography and related differential migration methods-Part B: Applications*, Elsevier.
- HERNÁNDEZ, I. M., FERNANDEZ, M. C., CUESTA-RUBIO, O., PICCINELLI, A. L. & RASTRELLI, L. 2005. Polyprenylated benzophenone derivatives from Cuban propolis. *Journal of natural products*, 68, 931-934.
- HIDAYATHULLA, S., CHANDRA, K. K. & CHANDRASHEKAR, K. 2011. Phytochemical evaluation and antibacterial activity of *Pterospermum diversifolium* Blume. *International Journal of Pharmacy and Pharmaceutical Sciences*, 3, 165-167.
- HIGASHI, K. & DE CASTRO, S. 1994. Propolis extracts are effective against *Trypanosoma cruzi* and have an impact on its interaction with host cells. *Journal of ethnopharmacology*, 43, 149-155.
- HOET, S., OPPERDOES, F., BRUN, R. & QUETIN-LECLERCQ, J. 2004. Natural products active against African trypanosomes: a step towards new drugs. *Natural product reports*, 21, 353-364.

- HONDA, T.-I., ROUNDS, B. V., BORE, L., FAVALORO JR, F. G., GRIBBLE, G. W., SUH, N., WANG, Y. & SPORN, M. B. 1999. Novel synthetic oleanane triterpenoids: a series of highly active inhibitors of nitric oxide production in mouse macrophages. *Bioorganic & medicinal chemistry letters*, 9, 3429-3434.
- HOUGHTON, P. 1998. Propolis as a medicine. Are there scientific reasons for its reputation? *Beeswax and Propolis for Pleasure and Profit*, 10.
- HUANG, S., ZHANG, C.-P., WANG, K., LI, G. Q. & HU, F.-L. 2014. Recent advances in the chemical composition of propolis. *Molecules*, 19, 19610-19632.
- HUNOT, S., BOISSIERE, F., FAUCHEUX, B., BRUGG, B., MOUATT-PRIGENT, A., AGID, Y. & HIRSCH, E. 1996. Nitric oxide synthase and neuronal vulnerability in Parkinson's disease. *Neuroscience*, 72, 355-363.
- IKARASHI, N., TAKEDA, R., ITO, K., OCHIAI, W. & SUGIYAMA, K. 2011. The inhibition of lipase and glucosidase activities by acacia polyphenol. *Evidence-Based Complementary and Alternative Medicine*, 2011.
- IRAVANI, M. M., KASHEFI, K., MANDER, P., ROSE, S. & JENNER, P. 2002. Involvement of inducible nitric oxide synthase in inflammation-induced dopaminergic neurodegeneration. *Neuroscience*, 110, 49-58.
- JAGGI, R. K., MADAAN, R. & SINGH, B. 2003. Anticonvulsant potential of holy basil, *Ocimum sanctum* Linn. and its culture s.
- JERZ, G., ELNAKADY, Y. A., BRAUN, A., JÄCKEL, K., SASSE, F., AL GHAMDI, A. A., OMAR, M. O. & WINTERHALTER, P. 2014. Preparative mass-spectrometry profiling of bioactive metabolites in Saudi-Arabian propolis fractionated by high-speed countercurrent chromatography and off-line atmospheric pressure chemical ionization mass-spectrometry injection. *Journal of Chromatography A*, 1347, 17-29.
- JONES, W. P., CHIN, Y.-W. & KINGHORN, A. D. 2006. The role of pharmacognosy in modern medicine and pharmacy. *Current drug targets*, 7, 247-264.
- JOSHI, B., SAH, G. P., BASNET, B. B., BHATT, M. R., SHARMA, D., SUBEDI, K., JANARDHAN, P. & MALLA, R. 2011. Phytochemical extraction and antimicrobial properties of different medicinal plants: *Ocimum sanctum* (Tulsi), *Eugenia caryophyllata* (Clove), *Achyranthes bidentata* (Datiwan) and *Azadirachta indica* (Neem). *Journal of Microbiology and Antimicrobials*, 3, 1-7.
- KAROU, D., DICKO, M. H., SIMPORE, J. & TRAORE, A. S. 2005. Antioxidant and antibacterial activities of polyphenols from ethnomedicinal plants of Burkina Faso. *African Journal of Biotechnology*, 4, 823-828.
- KASOTE, D., SULEMAN, T., CHEN, W., SANDASI, M., VILJOEN, A. & VAN VUUREN, S. 2014. Chemical profiling and chemometric analysis of South African propolis. *Biochemical Systematics and Ecology*, 55, 156-163.
- KELM, M., NAIR, M., STRASBURG, G. & DEWITT, D. 2000. Antioxidant and cyclooxygenase inhibitory phenolic compounds from *Ocimum sanctum* Linn. *Phytomedicine*, 7, 7-13.
- KHAN, M., ISLAM, M., HOSSAIN, M., ASADUJJAMAN, M., WAHED, M., RAHMAN, B., ANISUZZAMAN, A., SHAHEEN, S. & AHMED, M. 2010. Antidiabetic effects of the different fractions of ethanolic extracts of *Ocimum sanctum* in normal and alloxan induced diabetic rats. *Journal of Scientific Research*, 2, 158-168.
- KITANI, Y., ZHU, S., OMOTE, T., TANAKA, K., BATKHUU, J., SANCHIR, C., FUSHIMI, H., MIKAGE, M. & KOMATSU, K. 2009. Molecular analysis and chemical evaluation of Ephedra plants in Mongolia. *Biological and pharmaceutical bulletin*, 32, 1235-1243.
- KRELL, R. 1996. *Value-added products from beekeeping*, Food & Agriculture Org.
- KREMMER, T. & BOROSS, L. 1979. *Gel chromatography: theory, methodology, applications*, John Wiley & Sons.
- KUMAR, A., RAHAL, A., CHAKRABORTY, S., TIWARI, R., LATHEEF, S. K. & DHAMA, K. 2013. *Ocimum sanctum* (Tulsi): a miracle herb and boon to medical science—A Review. *Int J Agron Plant Prod*, 4, 1580-9.

- KUMAZAWA, S., UEDA, R., HAMASAKA, T., FUKUMOTO, S., FUJIMOTO, T. & NAKAYAMA, T. 2007. Antioxidant prenylated flavonoids from propolis collected in Okinawa, Japan. *J. of Agricultural and Food Chemistry*, 55, 7722-7725.
- LAM, K. S. 2007. New aspects of natural products in drug discovery. *Trends in microbiology*, 15, 279-289.
- LANGENHEIM, J. H. 2003. *Plant resins: chemistry, evolution, ecology, and ethnobotany*, Timber Press.
- LEE, C. & MAURICE, J. 1983. *The African trypanosomiases: methods and concepts of control and eradication in relation to development*, The World Bank.
- LEE, Y. S., KIM, W. S., KIM, K. H., YOON, M. J., CHO, H. J., SHEN, Y., YE, J.-M., LEE, C. H., OH, W. K. & KIM, C. T. 2006. Berberine, a natural plant product, activates AMP-activated protein kinase with beneficial metabolic effects in diabetic and insulin-resistant states. *Diabetes*, 55, 2256-2264.
- LEGROS, D., OLLIVIER, G., GASTELLU-ETCHEGORRY, M., PAQUET, C., BURRI, C., JANNIN, J. & BÜSCHER, P. 2002. Treatment of human African trypanosomiasis—present situation and needs for research and development. *The Lancet infectious diseases*, 2, 437-440.
- LI, F., AWALE, S., TEZUKA, Y. & KADOTA, S. 2008. Cytotoxic constituents from Brazilian red propolis and their structure–activity relationship. *Bioorganic & medicinal chemistry*, 16, 5434-5440.
- LI, F., AWALE, S., ZHANG, H., TEZUKA, Y., ESUMI, H. & KADOTA, S. 2009. Chemical constituents of propolis from Myanmar and their preferential cytotoxicity against a human pancreatic cancer cell line. *Journal of natural products*, 72, 1283-1287.
- LIAO, C.-R., KUO, Y.-H., HO, Y.-L., WANG, C.-Y., YANG, C.-S., LIN, C.-W. & CHANG, Y.-S. 2014. Studies on cytotoxic constituents from the leaves of *Elaeagnus oldhamii* Maxim. in non-small cell lung cancer A549 cells. *Molecules*, 19, 9515-9534.
- LIBERATORE, G. T., JACKSON-LEWIS, V., VUKOSAVIC, S., MANDIR, A. S., VILA, M., MCAULIFFE, W. G., DAWSON, V. L., DAWSON, T. M. & PRZEDBORSKI, S. 1999. Inducible nitric oxide synthase stimulates dopaminergic neurodegeneration in the MPTP model of Parkinson disease. *Nature medicine*, 5, 1403.
- LIDDELL, H. G. & SCOTT, R. 1897. *A greek-english lexicon*, New York: American Book Company.
- LOTFY, M. 2006. Biological activity of bee propolis in health and disease. *Asian Pac J Cancer Prev*, 7, 22-31.
- LU, L.-C., CHEN, Y.-W. & CHOU, C.-C. 2003. Antibacterial and DPPH free radical-scavenging activities of the ethanol extract of propolis collected in Taiwan. *Journal of Food and Drug Analysis*, 11, 277-282.
- LU, L.-C., CHEN, Y.-W. & CHOU, C.-C. 2005. Antibacterial activity of propolis against *Staphylococcus aureus*. *International Journal of Food Microbiology*, 102, 213-220.
- LU, Y. & FOO, L. Y. 1999. Rosmarinic acid derivatives from *Salvia officinalis*. *Phytochemistry*, 51, 91-94.
- MA, C.-J., LI, G.-S., ZHANG, D.-L., LIU, K. & FAN, X. 2005. One step isolation and purification of liquiritigenin and isoliquiritigenin from *Glycyrrhiza uralensis* Risch. using high-speed counter-current chromatography. *Journal of Chromatography A*, 1078, 188-192.
- MAHATO, S. B. & KUNDU, A. P. 1994. ¹³C NMR spectra of pentacyclic triterpenoids—a compilation and some salient features. *Phytochemistry*, 37, 1517-1575.
- MAIKAI, V. 2010. Antitrypanosomal activity of flavonoid extracted from *Ximenia Americana* stem bark. *International Journal of Biology*, 3, 115.
- MAKAROV, A. & SCIGELOVA, M. 2010. Coupling liquid chromatography to Orbitrap mass spectrometry. *Journal of Chromatography A*, 1217, 3938-3945.

- MALIKOV, V. & YULDASHEV, M. 2002. Phenolic compounds of plants of the *Scutellaria* L. genus. Distribution, structure, and properties. *Chemistry of natural compounds*, 38, 358-406.
- MARCUCCI, M. C. 1995. Propolis: chemical composition, biological properties and therapeutic activity. *Apidologie*, 26, 83-99.
- MARCUCCI, M., FERRERES, F., GARCÍA-VIGUERA, C., BANKOVA, V., DE CASTRO, S., DANTAS, A., VALENTE, P. & PAULINO, N. 2001. Phenolic compounds from Brazilian propolis with pharmacological activities. *Journal of ethnopharmacology*, 74, 105-112.
- MARTOS, I., COSENTINI, M., FERRERES, F. & TOMÁS-BARBERÁN, F. A. 1997. Flavonoid composition of Tunisian honeys and propolis. *Journal of Agricultural and Food Chemistry*, 45, 2824-2829.
- MATYSIAK, J., SCHMELZER, C. E., NEUBERT, R. H. & KOKOT, Z. J. 2011. Characterization of honeybee venom by MALDI-TOF and nanoESI-QqTOF mass spectrometry. *Journal of pharmaceutical and biomedical analysis*, 54, 273-278.
- MEGALLA, S. E. 1983. Rapid, economical qualitative method for separation of aflatoxins B-1, B-2 & G-1, G-2 by dry column chromatography. *Mycopathologia*, 84, 45-47.
- MULHOLLAND, D. A., LANGAT, M. K., CROUCH, N. R., COLEY, H. M., MUTAMBI, E. M. & NUZILLARD, J.-M. 2010. Cembranolides from the stem bark of the southern African medicinal plant, *Croton gratissimus* (Euphorbiaceae). *Phytochemistry*, 71, 1381-1386.
- NEGRI, G., MARCUCCI, M. C., SALATINO, A. & SALATINO, M. L. F. 1998. Hydrocarbons and monoesters of propolis waxes from Brazil. *Apidologie*, 29, 305-314.
- NEWMAN, D. J. & CRAGG, G. M. 2007. Natural products as sources of new drugs over the last 25 years. *Journal of natural products*, 70, 461-477.
- NEWMAN, D. J. & CRAGG, G. M. 2012. Natural products as sources of new drugs over the 30 years from 1981 to 2010. *Journal of natural products*, 75, 311-335.
- NEWMAN, D. J., CRAGG, G. M. & SNADER, K. M. 2000. The influence of natural products upon drug discovery. *Natural product reports*, 17, 215-234.
- NGURE, R. M., ONGERI, B., KARORI, S. M., WACHIRA, W., MAATHAI, R. G., KIBUGI, J. & WACHIRA, F. N. 2009. Anti-trypanosomal effects of *Azadiracta indica* (neem) extract on *Trypanosoma brucei rhodesiense*-infected mice. *Eastern Journal of Medicine*, 14, 2.
- NGUYEN, H. X., DO, T. N. V., LE, T. H., NGUYEN, M. T. T., NGUYEN, N. T., ESUMI, H. & AWALE, S. 2016. Chemical Constituents of *Mangifera indica* and Their Antiausterity Activity against the PANC-1 Human Pancreatic Cancer Cell Line. *Journal of natural products*, 79, 2053-2059.
- NICODEMO, D., DE JONG, D., COUTO, R. & MALHEIROS, B. 2013. Honey bee lines selected for high propolis production also have superior hygienic behavior and increased honey and pollen stores. *Genetics and Molecular Research*, 6931-6938.
- NICODEMO, D., MALHEIROS, E. B., DE JONG, D. & COUTO, R. H. N. 2014. Increased brood viability and longer lifespan of honeybees selected for propolis production. *Apidologie*, 45, 269-275.
- NICOLAS, A. 1947. *Cire d'abeilles et propolis*. Nancy, France: Thomas, 141-142.
- OMAR, R., IGOLI, J. O., ZHANG, T., GRAY, A. I., EBILOMA, G. U., CLEMENTS, C. J., FEARNLEY, J., EBEL, R. E., PAGET, T. & DE KONING, H. P. 2017. The chemical characterization of Nigerian propolis samples and their activity against *Trypanosoma brucei*. *Scientific reports*, 7, 923.
- OMAR, R. M., IGOLI, J., GRAY, A. I., EBILOMA, G. U., CLEMENTS, C., FEARNLEY, J., EBEL, E., ANGELI, R., ZHANG, T. & DE KONING, H. P. 2016. Chemical characterisation of Nigerian red propolis and its biological activity against *Trypanosoma Brucei*. *Phytochemical Analysis*, 27, 107-115.
- ORGANIZATION, W. H. WHO traditional medicine strategy 2014-2023. WHO Geneva Switzerland. 2013.

- ORGANIZATION, W. H. 2002. WHO Traditional Medicine Strategy 2002–2005. Geneva: World Health Organization.
- PALOMBO, E. A. 2011. Traditional medicinal plant extracts and natural products with activity against oral bacteria: potential application in the prevention and treatment of oral diseases. *Evidence-Based Complementary and Alternative Medicine*, 2011.
- PARK, Y. K. & IKEGAKI, M. 1998. Preparation of water and ethanolic extracts of propolis and evaluation of the preparations. *Bioscience, biotechnology, and biochemistry*, 62, 2230-2232.
- PARREIRA, N. A., MAGALHÃES, L. G., MORAIS, D. R., CAIXETA, S. C., DE SOUSA, J. P., BASTOS, J. K., CUNHA, W. R., SILVA, M. L., NANAYAKKARA, N. & RODRIGUES, V. 2010. Antiprotozoal, schistosomicidal, and antimicrobial activities of the essential oil from the leaves of *Baccharis dracunculifolia*. *Chemistry & biodiversity*, 7, 993-1001.
- PATTANAYAK, P., BEHERA, P., DAS, D. & PANDA, S. K. 2010. *Ocimum sanctum* Linn. A reservoir plant for therapeutic applications: An overview. *Pharmacognosy reviews*, 4, 95.
- PETROVA, A., POPOVA, M., KUZMANOVA, C., TSVETKOVA, I., NAYDENSKI, H., MULI, E. & BANKOVA, V. 2010. New biologically active compounds from Kenyan propolis. *Fitoterapia*, 81, 509-514.
- PEYFOON, E. 2009. *Chemical and biological properties of propolis*. The University of Strathclyde.
- PFUNDSTEIN, B., EL DESOUKY, S. K., HULL, W. E., HAUBNER, R., ERBEN, G. & OWEN, R. W. 2010. Polyphenolic compounds in the fruits of Egyptian medicinal plants (*Terminalia bellerica*, *Terminalia chebula* and *Terminalia horrida*): characterization, quantitation and determination of antioxidant capacities. *Phytochemistry*, 71, 1132-1148.
- PICCINELLI, A. L., CAMPO FERNANDEZ, M., CUESTA-RUBIO, O., MARQUEZ HERNANDEZ, I., DE SIMONE, F. & RASTRELLI, L. 2005. Isoflavonoids isolated from Cuban propolis. *Journal of Agricultural and Food Chemistry*, 53, 9010-9016.
- PIETTA, P., GARDANA, C. & PIETTA, A. 2002. Analytical methods for quality control of propolis. *Fitoterapia*, 73, S7-S20.
- POPOVA, M. P., CHINOU, I. B., MAREKOV, I. N. & BANKOVA, V. S. 2009. Terpenes with antimicrobial activity from Cretan propolis. *Phytochemistry*, 70, 1262-1271.
- POPOVA, M. P., GRAIKOU, K., CHINOU, I. & BANKOVA, V. S. 2010. GC-MS profiling of diterpene compounds in Mediterranean propolis from Greece. *Journal of agricultural and food chemistry*, 58, 3167-3176.
- PRAKASH, P. & GUPTA, N. 2005. Therapeutic uses of *Ocimum sanctum* Linn (Tulsi) with a note on eugenol and its pharmacological actions: a short review. *Indian journal of physiology and pharmacology*, 49, 125.
- QUESTA-RUBIO, O., FRONTANA-URIBA, B. & PEREZ, J. 2001. Isoflavonoides en propoleos Cubanos. *Rev Cubana Farm*, 35, 58-61.
- RABAJANTE, J. F. & FAJARDO JR, A. C. FORAGING BEHAVIOR OF STINGLESS BEES (*Tetragonula biroi* Friese): DISTANCE, DIRECTION AND HEIGHT OF PREFERRED FOOD SOURCE.
- RAGHUKUMAR, R., VALI, L., WATSON, D., FEARNLEY, J. & SEIDEL, V. 2010. Antimethicillin-resistant *Staphylococcus aureus* (MRSA) activity of 'pacific propolis' and isolated prenylflavanones. *Phytotherapy research*, 24, 1181-1187.
- RAI, M., CORDELL, G. A., MARTINEZ, J. L., MARINOFF, M. & RASTRELLI, L. 2012. *Medicinal plants: biodiversity and drugs*, CRC Press.
- RASSI, A. & DE REZENDE, J. M. 2012. American trypanosomiasis (Chagas disease). *Infectious Disease Clinics*, 26, 275-291.
- REID, R. G. & SARKER, S. D. 2006. Isolation of natural products by low-pressure column chromatography. *Natural Products Isolation*. Springer.

- RIGHI, A. A., ALVES, T. R., NEGRI, G., MARQUES, L. M., BREYER, H. & SALATINO, A. 2011. Brazilian red propolis: unreported substances, antioxidant and antimicrobial activities. *Journal of the Science of Food and Agriculture*, 91, 2363-2370.
- SAKINA, M. & DANDIYA, P. 1990. A psycho-neuropharmacological profile of Centella asiatica extract. *Fitoterapia*, 61, 291-296.
- SALATINO, A., TEIXEIRA, É. W. & NEGRI, G. 2005. Origin and chemical variation of Brazilian propolis. *Evidence-Based Complementary and Alternative Medicine*, 2, 33-38.
- SALITURO, G. M. & DUFRESNE, C. 1998. Isolation by low-pressure column chromatography. *Natural Products Isolation*. Springer.
- SALOMÃO, K., DE SOUZA, E., BARBOSA, H. & DE CASTRO, S. 2010. Propolis and derivatives of megazol: In vitro and in vivo activity on Trypanosoma cruzi, mechanism of action and selectivity. *International Journal of Infectious Diseases*, 14, e441-e442.
- SALOMAO, K., DE SOUZA, E. M., HENRIQUES-PONS, A., BARBOSA, H. S. & DE CASTRO, S. L. 2011. Brazilian green propolis: effects in vitro and in vivo on Trypanosoma cruzi. *Evidence-Based Complementary and Alternative Medicine*, 2011.
- SALOMAO, K., PEREIRA, P. R. S., CAMPOS, L. C., BORBA, C. M., CABELLO, P. H., MARCUCCI, M. C. & DE CASTRO, S. L. 2008. Brazilian propolis: correlation between chemical composition and antimicrobial activity. *Evidence-Based Complementary and Alternative Medicine*, 5, 317-324.
- SAMUELSON, G. 1999. Drugs of natural origin: a textbook of pharmacognosy. Taylor & Francis Group.
- SARKER, S. D., LATIF, Z. & GRAY, A. I. 2005. *Natural products isolation*, Springer Science & Business Media.
- SARKER, S. D. & NAHAR, L. 2012. An introduction to natural products isolation. *Natural products isolation*. Springer.
- SATYAVATI, G., RAINA, M. & SHARMA, M. 1987. *Medicinal plants of India*, Indian Council of Medical Research.
- SCIGELOVA, M., HORNSHAW, M., GIANNAKOPOULOS, A. & MAKAROV, A. 2011. Fourier transform mass spectrometry. *Molecular & Cellular Proteomics*, 10, M111. 009431.
- SEIDEL, V. 2012. Initial and bulk extraction of natural products isolation. *Natural Products Isolation*. Springer.
- SEN, P. 1993. Therapeutic potentials of Tulsi: from experience to facts. *Drugs News & Views*, 1, 15-21.
- SFORCIN, J. M. & BANKOVA, V. 2011. Propolis: is there a potential for the development of new drugs? *Journal of ethnopharmacology*, 133, 253-260.
- SHAW, D., LEON, C., KOLEV, S. & MURRAY, V. 1997. Traditional remedies and food supplements. *Drug safety*, 17, 342-356.
- SHISHODIA, S., MAJUMDAR, S., BANERJEE, S. & AGGARWAL, B. B. 2003. Ursolic acid inhibits nuclear factor- κ B activation induced by carcinogenic agents through suppression of I κ B α kinase and p65 phosphorylation: correlation with down-regulation of cyclooxygenase 2, matrix metalloproteinase 9, and cyclin D1. *Cancer research*, 63, 4375-4383.
- SHOEB, M. 2006. Anti-cancer agents from medicinal plants. *Bangladesh journal of Pharmacology*, 1, 35-41.
- SHRESTHA, S. P., NARUKAWA, Y. & TAKEDA, T. 2007. Chemical constituents of Nepalese propolis (II). *Chemical and pharmaceutical bulletin*, 55, 926-929.
- SHUBHARANI, R., SIVARAM, V. & KISHORE, B. 2014. In-vitro cytotoxicity of Indian bee propolis on cancer cell lines. *Int J Pharm Bio Sci*, 5, 698-706.
- SIHERI, W., ALENEZI, S., TUSIIMIRE, J. & WATSON, D. G. 2017. The Chemical and Biological Properties of Propolis. *Bee Products-Chemical and Biological Properties*. Springer.
- SIHERI, W., IGOLI, J. O., GRAY, A. I., NASCIEMENTO, T. G., ZHANG, T., FEARNLEY, J., CLEMENTS, C. J., CARTER, K. C., CARRUTHERS, J. & EDRADA-EBEL, R. 2014.

- The isolation of antiprotozoal compounds from Libyan propolis. *Phytotherapy research*, 28, 1756-1760.
- SIHERI, W., ZHANG, T., EBILOMA, G. U., BIDDAU, M., WOODS, N., HUSSAIN, M. Y., CLEMENTS, C. J., FEARNLEY, J., EBEL, R. E. & PAGET, T. 2016. Chemical and antimicrobial profiling of propolis from different regions within Libya. *PLoS One*, 11, e0155355.
- SILVA, B. B., ROSALEN, P. L., CURY, J. A., IKEGAKI, M., SOUZA, V. C., ESTEVES, A. & ALENCAR, S. M. 2008. Chemical composition and botanical origin of red propolis, a new type of Brazilian propolis. *Evidence-based complementary and alternative medicine*, 5, 313-316.
- SINGH, E., SHARMA, S., DWIVEDI, J. & SHARMA, S. 2012. Diversified potentials of *Ocimum sanctum* Linn (Tulsi): An exhaustive survey. *J Nat Prod Plant Resour*, 2, 39-48.
- SIRIPATRAWAN, U., VITCHAYAKITTI, W. & SANGUANDEEKUL, R. 2013. Antioxidant and antimicrobial properties of Thai propolis extracted using ethanol aqueous solution. *International Journal of Food Science & Technology*, 48, 22-27.
- SMINA, T., MATHEW, J., JANARDHANAN, K. & DEVASAGAYAM, T. 2011. Antioxidant activity and toxicity profile of total triterpenes isolated from *Ganoderma lucidum* (Fr.) P. Karst occurring in South India. *Environmental toxicology and pharmacology*, 32, 438-446.
- SOLECKI, R. S. 1975. Shanidar IV, a Neanderthal flower burial in northern Iraq. *Science*, 190, 880-881.
- STOYANOVA, R. & BROWN, T. 2001. NMR spectral quantitation by principal component analysis. *NMR in Biomedicine*, 14, 271-277.
- TASDEMIR, D., KAISER, M., BRUN, R., YARDLEY, V., SCHMIDT, T. J., TOSUN, F. & RÜEDI, P. 2006. Antitrypanosomal and antileishmanial activities of flavonoids and their analogues: in vitro, in vivo, structure-activity relationship, and quantitative structure-activity relationship studies. *Antimicrobial agents and chemotherapy*, 50, 1352-1364.
- TORETI, V. C., SATO, H. H., PASTORE, G. M. & PARK, Y. K. 2013. Recent progress of propolis for its biological and chemical compositions and its botanical origin. *Evidence-based complementary and alternative medicine*, 2013.
- TROUBLESHOOTING, L. 2004. Success with evaporative light-scattering detection. *LC• GC Europe*, 17, 192-199.
- TRUSHEVA, B., POPOVA, M., BANKOVA, V., SIMOVA, S., MARCUCCI, M. C., MIORIN, P. L., PASIN, F. D. R. & TSVETKOVA, I. 2006. Bioactive constituents of Brazilian red propolis. *Evidence-Based Complementary and Alternative Medicine*, 3, 249-254.
- WAGH, V. D. 2013. Propolis: a wonder bee's product and its pharmacological potentials. *Advances in pharmacological sciences*, 2013.
- WALDI, D. 1965. Spray reagents for thin-layer chromatography. *Thin-layer chromatography*. Springer.
- WATSON, D. G. 2015. *Pharmaceutical Analysis E-Book: A Textbook for Pharmacy Students and Pharmaceutical Chemists*, Elsevier Health Sciences.
- WATSON, J. T. & SPARKMAN, O. D. 2007. *Introduction to mass spectrometry: instrumentation, applications, and strategies for data interpretation*, John Wiley & Sons.
- WILM, M. 2011. Principles of electrospray ionization. *Molecular & Cellular Proteomics*, 10, M111. 009407.
- WINK, M. 1999. *Functions of plant secondary metabolites and their exploitation in biotechnology*, Taylor & Francis.
- WOJTYCZKA, R. D., KEPA, M., IDZIK, D., KUBINA, R., KABAŁA-DZIK, A., DZIEDZIC, A. & WAŚNIK, T. J. 2013. In vitro antimicrobial activity of ethanolic extract of Polish propolis

- against biofilm forming *Staphylococcus epidermidis* strains. *Evidence-Based Complementary and Alternative Medicine*, 2013.
- WOLLENWEBER, E. & BUCHMANN, S. L. 1997. Feral honey bees in the Sonoran Desert: Propolis sources other than poplars (*Populus* spp.). *Zeitschrift für Naturforschung C*, 52, 530-535.
- YANG, H., DONG, Y., DU, H., SHI, H., PENG, Y. & LI, X. 2011. Antioxidant compounds from propolis collected in Anhui, China. *Molecules*, 16, 3444-3455.
- YOO, K.-Y. & PARK, S.-Y. 2012. Terpenoids as potential anti-Alzheimer's disease therapeutics. *Molecules*, 17, 3524-3538.
- YOSHIOKA, T., INOKUCHI, T., FUJIOKA, S. & KIMURA, Y. 2004. Phenolic compounds and flavonoids as plant growth regulators from fruit and leaf of *Vitex rotundifolia*. *Zeitschrift für Naturforschung C*, 59, 509-514.
- YOUNG, C. S. & DOLAN, J. W. 2003. Success with evaporative light-scattering detection. *LCGC North America*, 21, 120-128.